

**Application of circadian biology to behavioural
and physiological assessments in mice**

by

Lindsay Anne Benson BVSc

**Thesis submitted to the University of Nottingham for the
Degree of Doctor of Veterinary Medicine**

December 2016

Abstract

Circadian rhythms are present in all living organisms; daily oscillations of biological process from the expression of a gene to the number of times that an animal displays a given behaviour. The light/dark cycle is the primary cue that entrains these rhythms and the suprachiasmatic nuclei, within the hypothalamus are the central pacemaker which synchronises peripheral body clocks. Mice are useful circadian biology models and two peripheral circadian outputs were studied, locomotor activity and the rhythm of body temperature in a common inbred strain, the C57BL/6 mouse.

The use of individually ventilated cages to house mice increases biocontainment, enabling the maintenance of high health status colonies and reducing the risk of allergies for laboratory personnel. The effect of these sealed units on ambient light levels was examined, using locomotor activity as a marker of entrainment to the light/dark cycle. Mice housed closer to the overhead light source experienced greater levels of illumination than those at the lower levels, yet all entrained to the light/dark cycle. Mice housed lower on the rack showed more activity during light hours when they normally rest and the onset of activity was advanced in relation to the time the lights turned off. Individually ventilated cages do not therefore compromise circadian entrainment but cage position may alter the distribution of rest and activity in relation to the light cycle.

Measuring the rhythm of body temperature of animals is often confounded by the stress associated with immobilisation and restraint. A novel non-invasive method, a thermal imaging camera was trialled against an indwelling intraperitoneal implant, to compare the

relationship between peripheral and core body temperature under different light cycles. A stable relationship was found between the two methods (average R^2 value = 0.92) and this persisted in conditions of constant darkness, where lack of light cues resulted in free-running of the rhythm, assuming a shorter period length of oscillation. This novel method has potential for use in circadian phenotyping studies and to improve welfare, following experimental interventions where the mouse, a small, metabolically active animal is at risk of hypothermia.

Acknowledgements

I would like to thank all the people at the former Veterinary Services, University of Oxford who guided me through the first year of laboratory animal work; Paul West, Janet Rodgers, Maggie Lloyd, Caroline Bergmann, Paul Honess, Manuel Berdoy and Marc Martin- I hope I was able to contribute something useful to the department. Also to Paul Schroeder, my DVM colleague who started alongside me.

Sincere thanks to Stuart Peirson who supervised my research and generated some great ideas of what exactly to study within the vast field of circadian biology, also for the purchase of the first thermal camera and continued encouragement to write followed by efficient and instructive proof-reading. Thanks also to Sibah, Carrie, Violetta and Eric who are mentioned specifically in the Chapter Acknowledgements.

Thank you to Alison, Andrew and Jonathan, plus occasional others in the animal unit for looking after the mice after surgery, including my requests for extra weekend checks for my first non-clinical patients.

Finally, thanks to my husband Sean for providing computing advice, teaching a former large animal vet who wrote appointments in a diary to process extensive spreadsheets was just the beginning and I wouldn't have got this far without his patience and support.

Preface

This thesis includes research work completed during the final two years of a Wellcome Trust sponsored programme in Laboratory Animal Medicine, organised and examined by the School of Veterinary Medicine and Science, University of Nottingham. The first year was spent gaining clinical laboratory animal veterinary experience in the Department of Biomedical Services, University of Oxford and the subsequent research was undertaken in the Foster lab, Nuffield Laboratory of Ophthalmology (Nuffield Department of Clinical Neurosciences), University of Oxford. The completion of this research has given the author valuable experience of the use of animals in academic research and this enhances ongoing work as a laboratory animal vet.

Declaration

I declare that the work in this thesis was carried out in accordance with the Regulations of the University of Nottingham. The work is original, except where indicated by special references in the text, and no part of the thesis has been submitted for any other academic award. Any views expressed in the thesis are those of the author.

L. A. Benson

September 2014

Circadian Terminology and Abbreviations

Amplitude	Distance between maximum and minimum values for a rhythmic parameter
AVP	Arginine vasopressin
BAT	Brown adipose tissue
Circadian	From Latin “circa diem”, around a day, describes biological rhythms with a period of approximately 24 hours
Circadian time	Refers to the subjective time in a circadian cycle under constant conditions
Clock genes	Genes which are rhythmically expressed as part of the molecular clock and drive circadian rhythms, include <i>Clock</i> , <i>Bmal 1</i> , <i>Rev-Erb α</i> , <i>Per</i> , <i>Cry</i>
Clock proteins	Translational product of the Clock genes- <i>CLOCK</i> , <i>BMAL 1</i> , <i>REV-ERB α</i> , <i>PER</i> , <i>CRY</i>
DD	Constant darkness
Diurnal	A day active animal, or rhythm with a period of approximately 24 hours under a light dark cycle
ECG	Electrocardiogram
EEG	Electroencephalogram- in mice surgically prepared for EEG, electromyogram (EMG) biopotentials are collected simultaneously

Entrainment	Alignment of the endogenous biological clock with external (environmental) stimuli
GABA	γ aminobutyric acid, a neurotransmitter
Infradian	Biological rhythms with a period of more than 24 hours
LD	Light Dark- refers to a photoperiod made up of light and dark phases, may be preceded by a numerical ratio i.e. 12:12 LD
LED	Light emitting diode
LP	Light pulse
LL	Constant light
LTC	Light tight cabinet- a large cupboard with interior lighting and ventilation in which mouse cages can be kept
Masking	An acute effect of a change in the <i>zeitgeber</i> , does not require SCN input
Nocturnal	An animal which is naturally active at night
Period (<i>Tau</i>)	The duration of one cycle of a rhythm
Phase angle	Angle on onset of a rhythm relative to the <i>zeitgeber</i> , can be measured as the time difference in minutes
Phase response curve	The variation in sensitivity to a given stimulus over the period of a rhythm

PK 2	Prokineticin 2, a neurotransmitter
PLR	Pupillary light reflex
POAH	Pre-optic anterior hypothalamus, site of thermoregulation
pRGC	Photosensitive retinal ganglion cell, contains melanopsin
PVN	Paraventricular nucleus
RHT	Retinohypothalamic tract
SCN	Suprachiasmatic nuclei, the circadian pacemaker
TGF α	Transforming growth factor α , a polypeptide neurotransmitter
Ultradian	Biological rhythms with a period of less than 24 hours
VIP	Vasoactive intestinal peptide, a neurotransmitter
<i>Zeitgeber</i>	Cue which entrains circadian rhythms, primarily this is light
<i>Zeitgeber</i> time	Refers to the time in a entrained cycle where ZT0 is the onset of the <i>Zeitgeber</i> , i.e. ZT 0 = lights on

Table of Contents

Chapter 1 Introduction and Background.....	21
1.1 The circadian system	22
1.1.1 The input pathway.....	23
1.1.2 The central circadian pacemaker.....	26
1.1.3 The molecular basis of circadian rhythms	27
1.1.4 Peripheral clocks.....	31
1.2 Outputs of the circadian clock.....	32
1.2.1 Locomotor activity	33
1.2.1.1 Photoperiod.....	33
1.2.1.2 Photoentrainment and free-running.....	34
1.2.1.3 Masking	35
1.2.1.4 Phase shifts	37
1.2.2 Sleep	37
1.2.3 Endocrine outputs	41
1.2.3.1 Melatonin	42
1.2.3.2 Corticosterone	43
1.2.4 Body temperature	45
1.2.4.1 Deviations from normothermia.....	48
1.2.4.2 The circadian rhythm of body temperature	50

1.3 Conclusion and Aims.....	53
Chapter 2 General methods.....	55
2.1 Licence authority and ethical review.....	55
2.2 Source and health status of animals.....	55
2.3 Housing and husbandry of mice.....	56
2.4 Health checking and distress scoring of mice.....	57
Chapter 3 Wheel running activity at different positions in an individually ventilated cage rack.....	58
3.1 Introduction.....	59
3.1.1 Properties of light	59
3.1.2 Light and photoreception	60
3.1.3 Non-image forming responses relevant to locomotor activity studies	62
3.1.3.1 Photoentrainment	62
3.1.3.2 Masking	64
3.1.4 Effects of photoperiod on activity	65
3.1.5 Individually ventilated cages	67
3.1.5.1 Advantages of IVCs	67
3.1.5.2 Disadvantages of IVCs.....	69
3.1.6 Wheel running activity of mice.....	71
3.2 Methods.....	74
3.2.1 General methods	75

3.2.2 Husbandry and care of mice	76
3.2.3 Adaptation of IVCs to include a running wheel	76
3.2.4 Experimental design and scheduling	79
3.2.5 Recording the activity data	85
3.2.6 Processing the activity data	89
3.3 Statistical analysis	96
3.4 Results	96
3.4.1 Average hourly activity across all rack positions	98
3.4.2 Activity during the light phase	99
3.4.3 Activity during the dark phase	101
3.4.4 Activity during the light/dark transition	103
3.4.5 Activity during the hour before lights off	104
3.4.6 Activity at lights off	107
3.4.7 Summary of Results	110
3.5 Discussion and Conclusion	112
3.5.1 Evaluation of the methods	112
3.5.2 Evaluation of the results	116
3.5.3 Conclusion	120
Chapter 4 Validation of infrared thermography with radiotelemetry as a method of assessing body temperature in mice.....	121
4.1 Introduction.....	122

4.1.1 Thermoregulation in mice.....	122
4.1.2 Methods of measuring body temperature.....	124
4.1.2.1 Contact methods.....	124
4.1.2.2 Non-contact methods; infrared thermography or thermal imaging.....	126
4.1.3 Thermal imaging in human medicine.....	126
4.1.4 Thermal imaging in veterinary medicine and biomedical research.....	127
4.1.5 Relationship between core and peripheral temperature in mammals.....	128
4.2 Methods.....	130
4.2.1 General methods.....	131
4.2.2 Experimental design.....	132
4.2.3 Surgical preparation of mice.....	133
4.2.3.1 Pre-surgical assessment.....	133
4.2.3.2 Surgery and anaesthesia.....	135
4.2.3.3 Post-op recovery.....	136
4.2.4 Recording the temperature data.....	137
4.2.5 Processing the temperature data.....	144
4.2.5.1 Peripheral temperature data.....	144
4.2.5.2 Core temperature data.....	145
4.3 Statistical Analysis.....	148
4.4 Results.....	149

4.4.1 Three Temperature mice in 12:12 LD.....	150
4.4.2 Five EEG mice in 12:12 LD.....	154
4.4.3 Two Temperature mice in transition from 12:12 LD into DD.....	156
4.4.4 Three Temperature mice in DD	157
4.4.5 Three Temperature mice in transition from DD to LL	159
4.4.6 Three Temperature mice in LL.....	161
4.4.7 Activity and body temperature rhythms	163
4.4.8 Cosinor analysis for assessment of period length	164
4.4.9 Summary of results.....	167
4.5 Discussion and Conclusion.....	170
4.5.1 Discussion of the methods.....	170
4.5.2 Discussion of the results	172
4.5.3 Conclusion	177
Chapter 5 Effect of implantation surgery on the post-operative core and peripheral body temperature of mice.....	179
5.1 Introduction	180
5.1.1 Anaesthesia of laboratory mice	180
5.1.2 Thermoregulation under anaesthesia	181
5.1.2.1 Consequences of hypothermia during surgery.....	183
5.1.2.2 Preventing hypothermia under anaesthesia	183
5.1.3 The effect of anaesthesia and surgery on the circadian system	184

5.2 Methods.....	186
5.2.1 General methods	186
5.2.2 Experimental design	187
5.2.3 Surgical preparation of mice.....	188
5.2.3.1 Pre-surgical assessment and transmitter detail	188
5.2.3.2 Surgery and anaesthesia.....	189
5.2.3.3 Post-op recovery and temperature data recording.....	190
5.3 Results	191
5.3.1 Two Temperature mice	192
5.3.2 EEG and ECG mice.....	197
5.3.3 Summary of temperature variation for all mice	198
5.3.4 Summary of results.....	199
5.4 Discussion and Conclusion.....	201
5.4.1 Discussion of methods.....	201
5.4.2 Discussion of results	202
5.4.3 Conclusion	204
Chapter 6 General Summary and Perspectives	205
Bibliography.....	212

List of Figures and Tables

Chapter 1 Introduction and Background

Figure 1.1 The circadian waveform	21
Figure 1.2 The circadian system	23
Figure 1.3 Detail of retinal structure	24
Figure 1.4 Spectral sensitivity of the 4 mouse photoreceptors.....	25
Figure 1.5 The molecular clock oscillator	29
Table 1.1 Circadian locomotor phenotypes of clock mutant mice	30
Figure 1.6 Sample double-plotted actogram showing entrainment and free-running	34
Figure 1.7 Phase shift in response to a light pulse	36
Figure 1.8 Generation of a phase response curve	37
Figure 1.9 Homeostatic and circadian control of sleep	38
Figure 1.10 The hypothalamic- pituitary-adrenal axis	44

Chapter 3 Wheel running activity at different positions in an individually ventilated cage rack

Figure 3.1 Light as part of the electromagnetic spectrum	59
Figure 3.2 Irradiance response curve	62
Figure 3.3 Light intensity within the colony room.....	76
Figure 3.4 Seal-safe Green Line IVC rack and two views of an IVC.....	77
Figure 3.5 Photos of the Igloo, baseplate, wheel and magnet within an IVC	79
Figure 3.6 Plan of the colony room	81

Figure 3.7 Representation of cage rack with lux values	82
Table 3.1 Rotation patterns through top, middle and bottom rack positions.....	83
Table 3.2 Summary table of 18 mice and days analysed for each rack position	85
Figure 3.8 Two views of the cage docked on the rack.....	87
Figure 3.9 Detail of the reed switch relays wiring	88
Figure 3.10 Junction box on top of cage rack	88
Figure 3.11 Example of an Activity Profile output	90
Figure 3.12 Example of a Timeseries output	91
Figure 3.13 Example of an Actogram output.....	92
Figure 3.14 Hourly average plots for Mouse 17 and Mouse 15- raw data	94
Figure 3.15 Hourly average plots for Mouse 17 and Mouse 15- normalised data	94
Figure 3.16 Ten minute average activity plots for Mouse 17 and Mouse 15	95
Figure 3.17 Actograms from 6 mice.....	96
Figure 3.18 Average hourly counts of 18 mice across 3 rack positions	98
Figure 3.19 Average total activity during the light phase.....	99
Table 3.3 Mean light counts per rack position for the light phase	99
Figure 3.20 Average total activity during the dark phase.....	101
Table 3.4 Mean dark counts per rack position for the dark phase.....	101
Figure 3.21 Average counts per 10 minutes at the light/dark transition	103
Figure 3.22 Average counts during the hour before lights off	104

Table 3.5 Mean counts per position during the hour before lights off	104
Figure 3.23 Average counts at the time of lights off	107
Table 3.6 Mean counts per position at lights off	107
Table 3.7 Summary of sphericity in the data.....	110
Table 3.8 Summary of significant and non-significant differences between rack levels.....	111
 Chapter 4 Validation of infrared thermography with radiotelemetry as a method of assessing body temperature in mice	
Figure 4.1 Photo of a Light Tight Chamber.....	131
Table 4.1 Duration of temperature recordings for Temperature mice.....	132
Table 4.2 Duration of temperature recordings for EEG mice.....	133
Figure 4.2 The Physiotel TA-F10 transmitter.....	134
Figure 4.3 The Physiotel F20-EET transmitter.....	134
Figure 4.4 Thermal image of a mouse from above, showing hotspot Area 1.....	138
Figure 4.5 The Optris PI 160 thermal camera.....	139
Figure 4.6 Schematic diagram of the thermal cabinet.....	141
Figure 4.7 Schematic diagram of the cabinet air vent.....	141
Figure 4.8 Photograph of the thermal cabinet and laptop.....	142
Figure 4.9 Photograph of the interior of the thermal cabinet.....	143
Figure 4.10 Raw, 5 minute max and smoothed data plots.....	147
Figure 4.11 Peripheral and core temperature data for M1T, M2T and M3T in 12:12 LD.....	150
Table 4.3 R ² values for the three Temperature mice in 12:12 LD.....	151

Figure 4.12 Individual Bland Altman plots for M1T, M2T, M3T in 12:12 LD.....	151
Figure 4.13 Combined Bland Altman plot for three Temperature mice in 12:12 LD.....	152
Figure 4.14 Plots of core and peripheral temperature with 2.5-3° added for M1T, M2T, M3T.....	153
Figure 4.15 Peripheral and core data for five EEG mice in 12:12 LD.....	154
Table 4.4 R ² values for the five EEG mice in 12:12 LD.....	155
Figure 4.16 Combined Bland Altman plot for five EEG mice in 12:12 LD.....	155
Figure 4.17 Peripheral and core data for two Temperature mice in transition from LD to DD.....	156
Figure 4.18 Combined Bland Altman plot for M1T and M3T in transition from LD to DD.....	156
Figure 4.19 Peripheral and core data for three Temperature mice in DD.....	157
Table 4.5 R ² values for three Temperature mice in transition from LD to DD and in DD.....	158
Figure 4.20 Combined Bland Altman plot of M1T, M2T and M3T in DD.....	158
Figure 4.21 Peripheral and core data for three Temperature mice in transition from DD to LL.....	159
Figure 4.22 Combined Bland Altman plot for three Temperature mice in transition from DD to LL.....	160
Figure 4.23 Peripheral and core data for three Temperature mice in LL.....	161
Table 4.6 R ² values for three Temperature mice in transition from DD to LL and in LL.....	162
Figure 4.24 Combined Bland Altman plot for M1T, M2T and M3T in LL.....	162
Figure 4.25 Activity and core temperature for M1T in LD, M2T in DD and M3T in LL.....	163
Figure 4.26 Cosinor analysis by non-linear regression for M1T in LD, M2T in DD and M3T in LL.....	164
Table 4.7 <i>Tau</i> values for peripheral and core datasets in LD, DD and LL.....	165
Figure 4.27 Average <i>Tau</i> values for M1T, M2T and M3T in LD, DD and LL.....	166

Figure 4.28 Average amplitude values for M1T, M2T and M3T in LD, DD and LL.....	166
Table 4.8 Average values per group for R^2 and Bland Altman temperature difference.....	167
 Chapter 5 Effect of implantation surgery on the post-operative core and peripheral body temperature of mice	
Table 5.1 Overview of mice per experimental group, implant and anaesthetic time.....	188
Figure 5.1 Baseline peripheral temperature recordings for M1T and M2T in 12:12 LD.....	192
Figure 5.2 Post-implantation peripheral and core recordings for M1T and M2T in 12:12 LD.....	193
Figure 5.3 Pre- and post-op recordings for M1T with curve fitting by non-linear regression.....	194
Figure 5.4 Pre- and post-op recordings for M2T with curve fitting by non-linear regression.....	195
Table 5.2 <i>Tau</i> values for two Temperature mice through baseline and post-op recordings.....	196
Figure 5.5 Post-operative peripheral and core recordings for M3ECG and M2EEG.....	196
Table 5.3 Temperature values through the perioperative period for all mice.....	198

Chapter 1 Introduction and Background

Biological rhythms may be classified as infradian, circadian or ultradian in nature. Circadian rhythms are regular oscillations that occur in behavioural and physiological variables on a daily basis, from the Latin “*circa diem*” – about a day. Examples of infradian (less frequent) and ultradian (more frequent) rhythms include the reproductive cycle in species such as sheep (seasonal breeders in response to shortened daylength) and the distribution of rapid eye movement stages during sleep (which occur several times during a typical rest phase) respectively. Due to their oscillatory nature, circadian rhythms may be considered as a wave. Several parameters can be measured, see Figure 1.1 (Refinetti, 2006a);

Period- the time taken to complete one full cycle, the inverse of frequency, denoted τ

Mean or mesor- the average value, the midpoint of the oscillation

Amplitude- the maximum displacement from the mean value

Phase- the phase of the cycle relative to a fixed point

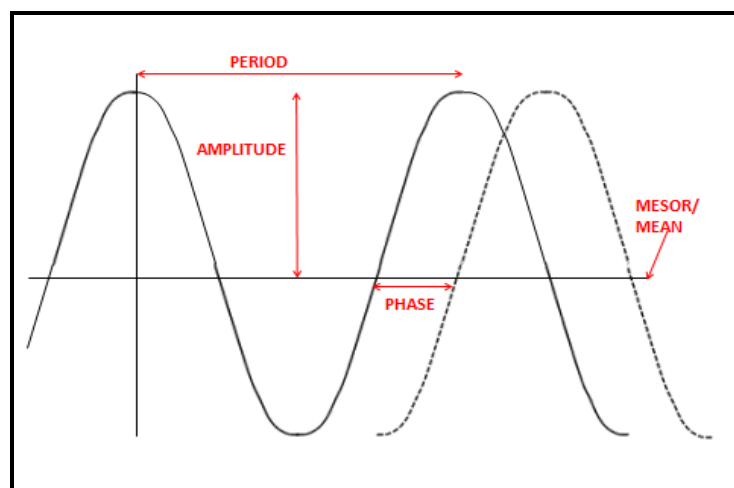


Figure 1.1 The circadian waveform

All circadian rhythms share several features; they can be aligned with or entrained by external periodic signals, termed *zeitgebers* or “time-givers” (Aschoff 1954), they free-run or assume a period length intrinsic to the host organism when external cues are absent (Pittendrigh and Daan, 1976) and they are temperature-compensated (Ruby et al., 1999). The light/dark cycle is the main influence on all circadian rhythms and animal behaviour has evolved as diurnal (active during daylight), nocturnal (active during darkness) or crepuscular (active during twilight). Humans, as a diurnal species, can also be recognised as late- or early-chronotype, depending on their natural propensity to be active in the morning or evening. Jet-lag, which follows air travel across different timezones is an example of when the stable relationship between endogenous period and the environment is disturbed and a phase shift is necessary to allow re-entrainment (Benloucif et al., 1997a).

1.1 The circadian system

The circadian system can be considered in three parts; the input pathway for the detection of light, the master clock or pacemaker within the central nervous system and the downstream effector pathways which manifest the rhythms of behaviour and physiology (Edery, 2000). The mammalian pacemaker, the suprachiasmatic nuclei (SCN) located within the hypothalamic area of the brain, are insensitive to light, so ocular photoreceptors supply this input information, in addition to normal vision (Daan, 2010, Van Gelder, 2003). Photoentrainment may therefore be compromised in blind individuals (depending on the ocular lesion) and is lacking in those who have undergone enucleation (Nelson and Zucker, 1981).

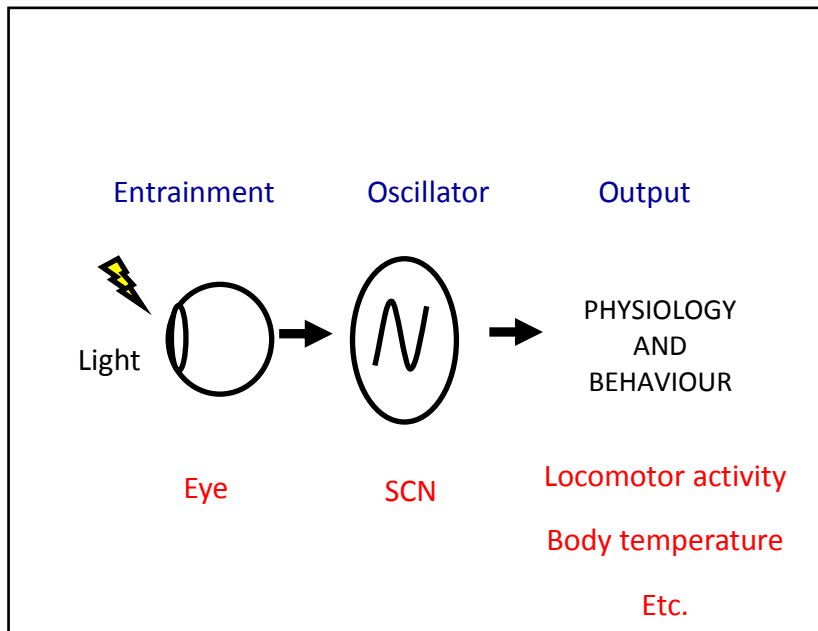


Figure 1.2 The circadian system as a simple input-oscillator-output system which drives rhythms in response to photoperiodic clues.

1.1.1 The input pathway

Retinal photoreceptors convey light signals to the visual centre of the brain, via the optic nerve and also to the circadian pacemaker in the hypothalamus via a monosynaptic pathway, the retinohypothalamic tract, or RHT (Moore and Lenn, 1972). Each photoreceptor contains a photopigment, integral to its function, consisting of an opsin protein linked to a chromophore (11 *cis*-retinal, a form of vitamin A). Rods and cones, considered the classical, visual photoreceptors are found at the back of the eye in the outer nuclear layer, adjacent to the retinal pigment epithelium and a third photoreceptor, photosensitive retinal ganglion cells (pRGCs) are located remotely, in the inner retina, adjacent to the innervation of the optic nerve (Hankins et al., 2008).

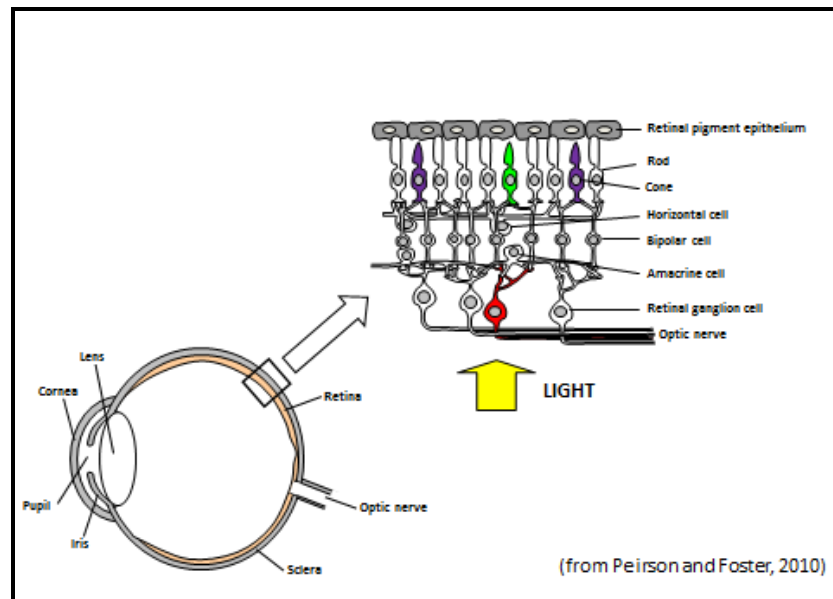


Figure 1.3 Detail of retinal structure showing the distribution of rods, cones and retinal ganglion cells, from Peirson and Foster (2010).

Jeon et al.(1998) found that the retina of the C57BL/6 mouse was composed mostly of rods, with a rod to cone ratio of 35:1, as expected in a nocturnal animal which is active in (scotopic) dim lighting conditions (requiring rods) and has low visual acuity (requiring cones). Mouse photoreceptor cells may be classified as green cones (medium wavelength sensitive), UV cones (short wavelength sensitive), rods and pRGCs (Thompson et al., 2008) and their four associated photopigments show maximum sensitivity to particular wavelengths of light, see Figure 1.4.

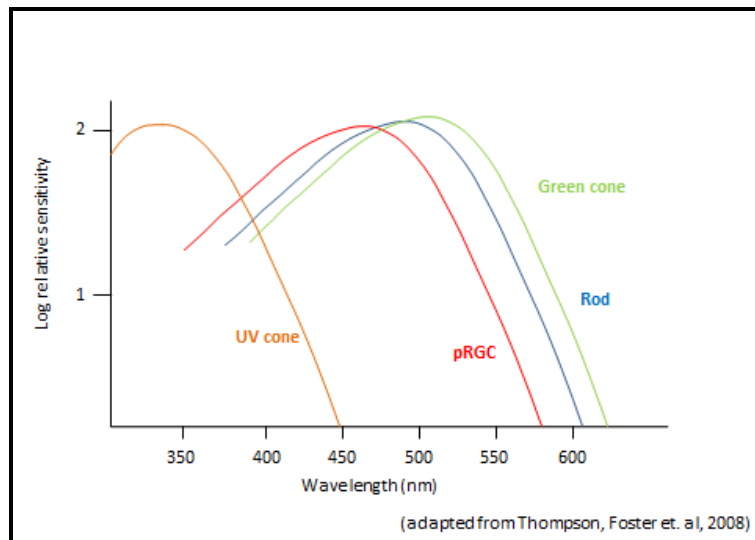


Figure 1.4 Spectral sensitivity of the 4 mouse photoreceptors, showing the wavelengths at which maximal absorbance occurs. Adapted from Thompson et al. (2008).

Temporally-relevant light signals are detected by the pRGCs which contain the recently discovered photopigment melanopsin, or *Opn4* (Berson et al., 2002a, Hattar et al., 2003, Panda et al., 2002b, Lucas et al., 2001b). The pRGCs have little involvement in visual responses (Berson et al., 2002a, Provencio et al., 2002) and melanopsin requires bright light stimuli of relatively long duration (Peirson and Foster, 2010). The pRGCs can be activated either via their own “melanopsin pathway” phototransduction cascade or with support from the rods and cones (Lall et al., 2010, Hattar et al., 2003, Mrosovsky and Hattar, 2003). Through-signalling of information from the classical photoreceptors occurs via bipolar, horizontal and amacrine cells in the inner nuclear layer (Güler et al., 2008, Wong et al., 2007, Van Gelder, 2003). The relative contribution of the photoreceptors to photoentrainment has been advanced by studies using various mutant mice, lacking one or more photoreceptors. A naturally occurring mutant, where the rods decline as the mice age

is the *rd/rd* (retinal degenerate) mouse (Farber et al., 1994) and prior to the discovery of melanopsin, Foster et al. (1991) found that this mouse successfully entrained to a light/dark cycle. To establish if cones were responsible for transmitting light signals to the SCN the *rd/rdcl* (rodless, coneless) mouse, with no functional photoreceptors in the outer retina was evaluated and still found to entrain (Freedman et al., 1999). Deletion of melanopsin resulted in a loss of photosensitivity in the pupillary light response, another non-image forming response to light (Lucas et al., 2003), yet mice could still entrain and maintained free-running rhythms under constant darkness (Panda et al., 2002b). Hattar et al (2003) showed that a mouse model lacking all three photoreceptors failed to entrain, confirming the roles that rods and cones play in circadian phototransduction.

1.1.2 The central circadian pacemaker

The RHT terminates in the ventrolateral aspect of the SCN. The pacemaker derives its name from its anatomical position dorsal to the optic chiasm, with which it communicates, although it remains functionally distinct from the visual system (Altimus et al., 2008). Immunohistochemistry studies of *Fos* (an intermediate early gene) expression within the RHT demonstrate the link between the pRGCs and the circadian pacemaker and analysis of tissues from neonatal mice showed that a functional connection exists from birth (Sekaran et al., 2005). *Fos* induction in the retinorecipient areas of the circadian pacemaker depends upon the phase of the daily cycle when the light pulse is given (Masana et al., 1996, Colwell and Foster, 1992) and De la Iglesia and Schwartz (2002) also demonstrated that some efferent neurons travelling from the SCN to other brain areas were *Fos* positive following light stimulation.

The SCN are two pear-shaped nuclei, each containing about 10,500 neurons. They can be divided into a ventrolateral inner core and a dorsomedial outer shell, characterised by their cellular expression of the neuropeptides VIP (vasoactive intestinal peptide) and AVP (arginine vasopressin) respectively (Abrahamson and Moore, 2001). The pacemaker signals other neural tissues and the rest of the body via neural and endocrine mechanisms, confirmed by the presence of genetic transcripts within SCN tissues (Panda et al., 2002a). The principal neurotransmitter within the SCN is GABA (Moore and Lenn, 1972) and other significant neuropeptides have been identified in direct signalling pathways between the SCN and other brain areas, such as PK2 (Li et al., 2006) and TGF α (Kalsbeek et al., 2008). AVP-based neural innervations project to the basal forebrain, thalamus, paraventricular nucleus and the dorso- and ventro-medial hypothalamic nuclei. SCN recruitment of parts of the pituitary gland results in peripheral tissue rhythms of gonadal hormones, glucocorticoids, mineralocorticoids, thyroid stimulating hormone and other metabolic substances (Yang, 2010, Abrahamson and Moore, 2001, Van der Zee et al., 2005, Kalsbeek et al., 2010).

1.1.3 The molecular basis of circadian rhythms

The core mechanism underlying the oscillatory behaviour of the SCN is a molecular clock. This involves the production of several different clock genes which participate in two separate feedback loops involving intracellular transcription of genetic material and translation into proteins (Yang, 2010), as shown in Figure 1.5. At the heart of the mechanism are *Clock* (circadian locomotor output cycles kaput) and *Bmal 1* genes, which initiate the transcription of other clock genes within the cell's nucleus. *CLOCK* and *BMAL 1* proteins form a heterodimer and bind to specific promoter sites (E box enhancers) on *Period*

(*Per*), *Cryptochrome (Cry)* and *Rev-Erb α* genes (King et al., 1997, Gekakis et al., 1998, Lee et al., 2001). *PER* and *CRY* proteins then move into the cytoplasm where post-translational modification occurs. Translocation of these proteins back into the nucleus results in *CRY 1*- and *CRY 2*-mediated inhibition of the *CLOCK/BMAL 1* heterodimer, and therefore their own transcription (Vitaterna et al., 1999, Kondratov et al., 2006). Nuclear entry of this *CRY* and *PER* “timesome” is regulated (Lee et al., 2001, Reppert and Weaver, 2002) and *CRY*-mediated repression is integral to the maintenance of circadian rhythms (Sato et al., 2006).

BMAL 1 is also repressed by the *REV-ERB α* protein which competes with *ROR α* (an activator) for binding sites, forming a second feedback loop (Reppert and Weaver, 2002). The two-sided autorepression of the initiating clock genes causes oscillatory behaviour and the interlocked nature of the two loops makes the oscillator robust and tunable (Ripperger and Brown, 2010, Yang, 2010). Post-translational modification of clock proteins (most frequently by phosphorylation) is essential for establishing and maintaining circadian rhythms (Gallego and Virshup, 2007). Other clock-associated genes encode for kinases and phosphatases which catalyse these reactions (Ripperger and Brown, 2010). Casein kinase 1 (CK1) is an important enzyme and has seven known isoforms which promote degradation of *PER* proteins (Vanselow and Kramer, 2010).

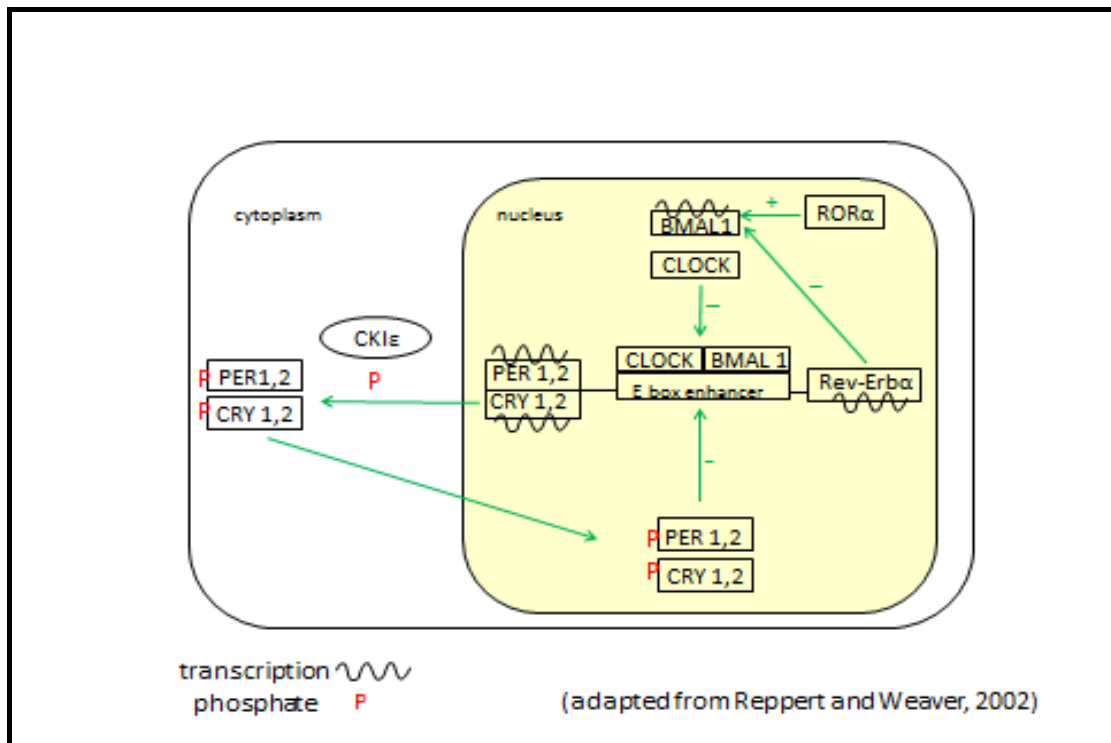


Figure 1.5 The molecular clock oscillator- showing interplay between clock genes inside the nucleus and movement of *PER* and *CRY* proteins. Adapted from Reppert and Weaver (2002).

Two large scale mouse mutagenesis projects exist to elucidate the exact role of the clock proteins. Distinctive circadian phenotypes, usually detected by aberrations in locomotor activity rhythms can be generated by forward genetics approaches such as ENU mutagenesis programmes (Takahashi et al., 1994, Takahashi et al., 2008b, Ripperger et al., 2011) or by targeted mutagenesis methods which cause deletion mutations and give rise to mice which lack one or more clock genes (Reppert and Weaver, 2002). The *Clock* gene was discovered first as the mutant mouse showed a different circadian period and loss of locomotor activity rhythms in constant darkness compared to wild types (Vitaterna et al., 1994, King et al., 1997, Redlin et al., 2005). The mutation followed a Mendelian inheritance pattern, therefore could be attributed to one gene (Daan, 2010). Other circadian mutant mice show abnormalities of their locomotor phenotype (see Table 1.1) and these are often

accompanied by altered physiological output rhythms as clock genes have a housekeeping role (Takahashi et al., 2008a).

Table 1.1 Circadian locomotor phenotypes of clock-mutant mice; effect of deletion of clock genes on period length and entrainment.

Clock gene missing	Effect upon phenotype (locomotor activity)
CLOCK	Increased Tau > arrhythmic
BMAL1	Arrhythmic
PER 1	Decreased Tau > arrhythmic
PER 2	Decreased Tau > arrhythmic
PER 1 and 2	Arrhythmic
CRY 1	Decreased Tau
CRY 2	Increased Tau
CRY 1 and 2	Arrhythmic
Casein kinase 1 ϵ	Decreased Tau
Rev-Erb α	Decreased Tau

Incorporating reporter genes coding for fluorescent proteins into the mouse genome allows the relationship between the SCN and the peripheral tissues to be explored (Cheng et al., 2009, Yoo et al., 2004), these proteins have short degradation half- lives so are suitable for dynamic rhythm monitoring in imaging studies (Ripperger et al., 2011).

1.1.4 Peripheral clocks

Clock genes are also expressed in many other cells and tissues throughout the body. These “peripheral clocks” exhibit rhythmic gene expression which can be sustained *ex-vivo*, as seen in cultured mouse fibroblast cells containing a fluorescent reporter gene (Nagoshi et al., 2004). SCN master control is biologically advantageous, allowing recruitment of tissues at an appropriate temporal phase and prevents damping of rhythms (Holzberg and Albrecht, 2003, Stratmann and Schibler, 2006, Takahashi et al., 2008b, Froy, 2011). SCN control is also necessary as mammalian peripheral oscillators cannot be directly entrained by light (Takeda and Maemura, 2010). Panda, Morse et al. (2002) demonstrated SCN signalling to the periphery when fibroblasts harvested from a *PER 1* deficient mouse (with an abnormally shortened *Tau* of 20 hours) implanted into a wild type animal assumed the rhythmic expression period of the host.

In contrast to SCN neurons, peripheral clocks don't communicate with each other, there is no locally-generated phase coherence within tissues or organs (Asher and Schibler, 2011). Levels and timing of gene expression seem to be tissue-specific (Holzberg and Albrecht, 2003, Panda et al., 2002a) and Peirson, Butler et al. (2006) noted differences in the phasing, waveform and amplitude between the SCN and the periphery in free-running (non-*zeitgeber* entrained) mice. The central oscillator directly targets only 10% of the mammalian transcriptome (Panda et al., 2002a, Yang, 2010) yet 50% of the 49 murine nuclear receptors show rhythmic expression over time (Yang et al., 2006) and approximately 6/7^{ths} of the mRNA generated in mouse liver cells is under local clock control (Kornmann et al., 2007) indicating a widespread influence of the SCN.

Light is the primary *zeitgeber* although other cues such as locomotor activity (Hughes and Piggins, 2012), ambient temperature (Refinetti, 2010), feeding (Mendoza, 2007), arousal (Mrosovsky, 1996) and social interaction (Mistlberger and Skene, 2004, Meerlo et al., 1996, Keeney et al., 2001, Tornatzky and Miczek, 1993, Paul and Schwartz, 2007) can entrain peripheral clocks. Daily rhythms are evident in critical physiological outputs such as blood pressure and heart rate (Witte et al., 2004, Arraj and Lemmer, 2006b, Lemmer, 2007, Bastianini et al., 2012) and in circulating levels of immune cells and cytokines which resist infection (Coogan and Wyse, 2008). Mice show diurnal variation in lipopolysaccharide-induced endotoxic shock (Marpegan et al., 2009) and increased mortality rates were recorded when phase-shifted (jet-lagged) mice were challenged (Castanon-Cervantes et al., 2010). The phase of the peripheral clock affects response to drug and treatment interventions and this has been recognised and considered within the emerging field of chronopharmacology and chronotherapeutics in human medicine (De Giorgi et al., 2013, Dallmann et al., 2014, Scully et al., 2011, Chassard et al., 2007).

1.2 Outputs of the circadian clock

Peripheral outputs more complex than rhythms evident at cellular and tissue levels can be broadly divided into behavioural and physiological responses, although some overlap occurs. Photoentrainment, which manifests most simply as modulation of locomotor activity under altered light/dark cycles has been the most experimentally useful (described in detail below) but there are a few other noteworthy non-image forming responses to light; suppression of pineal melatonin, induction of sleep and the pupillary light response. The PLR is mediated through pRGC projections to the olivary pretectal nucleus (Trejo and Cicerone, 1984) and cone activation plays a significant role (Lall et al., 2010, Lucas et al., 2001a)

although it still occurs via melanopsin pathway phototransduction in *rd/rdcl* mice (Semo et al., 2003).

Behavioural outputs

1.2.1 Locomotor activity

The primary zeitgeber for mammals is light (Daan, 2010) and the locomotor activity of laboratory mice is rhythmic, with most activity occurring during darkness in this nocturnal species. The most common and convenient method of measuring rodent activity is via wheel running studies, alternatives include the use of passive infrared movement sensors or videotracking followed by scoring of variations in the behavioural repertoire.

1.2.1.1 Photoperiod

The photoperiod is easy to control within the laboratory and various permutations of light and dark can be applied in circadian research. The Code of Practice for the Housing and Care of Animals used in Scientific Procedures, issued under the United Kingdom Animals (Scientific Procedures) Act 1986 suggests that experimental rodents should be housed under a 12 hour light/12 hour dark cycle, denoted as 12:12 LD. Consequently, circadian experiments that require alteration of the LD cycle may require authorisation in research project licences. Chronobiologists divide the daily cycle into *alpha* (activity) and *rho* (rest) phases and some activity inevitably occurs during the *rho* phase in mice as they do not sleep for extended periods of time. In diurnal species the *alpha* phase occurs during daylight and the *rho* phase during darkness. The photoperiod can be described in units of “zeitgeber time” where, under a 12:12 LD cycle ZT 0 is lights on and ZT 12 is lights off (Jud et al., 2005).

1.2.1.2 Photoentrainment and free-running

Synchronisation of the internal clock to the external photoperiod occurs, providing the effective *zeitgeber* is within the oscillator's range of entrainment (Casiraghi et al., 2012, Jud et al., 2005). Refinetti (2006b) summarises the work of several authors, showing that photoentrainment of mice occurs under a variety of different light/dark cycles, ranging in duration from 21.3 to 26.5 hours. The endogenous circadian period can be seen when mice free-run under conditions of constant darkness, denoted as DD (Takahashi et al., 2008b). *Tau* is precise- it is 23.7 hours in C57BL/6 mice with a standard deviation of 10 minutes (Vitaterna et al., 1994).

Circadian activity rhythms are often represented as actograms, where each horizontal line represents one day (Jud et al., 2005). Actograms may be double-plotted with 48 hours along the time axis, enabling easy assessment of the degree of synchronisation. Entrained mice will commence their activity around the onset of darkness and free-running mice will start slightly earlier each day as *Tau* is < 24 hours (see Figure 1.6). The time difference between the entraining external and the displayed internal rhythm, here the onset of activity is called the phase angle difference (Ψ) and a stable phase angle indicates true entrainment (Jud et al., 2005, Refinetti, 2006c). The lack of a *zeitgeber* under constant conditions such as DD means that ZT terminology is not applicable and CT "circadian time" is used, where one daily cycle is divided into 24 units- for C57BL/6 mice 1 CT equals 59.25 minutes (Jud et al., 2005, Verwey et al., 2013).



Figure 1.6 Sample double-plotted actogram showing entrainment to a 12:12 LD cycle and free-running during constant darkness over several successive days.

1.2.1.3 Masking

Masking effects also shape the activity rhythm generated by the LD cycle. Masking is an acute, direct response to light (Redlin et al., 2005) and does not involve environmental synchronisation of the endogenous pacemaker, unlike photoentrainment (Mrosovsky, 1999). Negative masking of mice occurs when a light pulse applied during the dark phase reduces locomotor activity (Mrosovsky et al., 2001), positive masking is increased activity in response to dim light (Aschoff and Von Goetz, 1988). The masking response varies with the irradiance (intensity) of the incident light (Mrosovsky, 1994).

1.2.1.4 Phase shifts

Phase shifts occur (see Figure 1.7) with changes in photic cues resulting in adjustment of internal physiology to the new environment. Chronic jet lag can be induced in experimental mice by significantly altering the LD cycle and the resulting change in activity rhythm represents resetting of the endogenous pacemaker (Casiraghi et al., 2012, Benloucif et al.,

1997b). Dark adaptation of mice for 10-21 days will establish a steady free-running state before *zeitgeber* changes (light pulses) to induce phase shifts are applied, see Figure 1.7 (Refinetti, 2001, Albrecht and Oster, 2001). Following adaptation, increased sensitivity to light occurs and phase shifts can cause changes in period length indicating considerable after-effects on the internal clock (Refinetti, 2001). The speed of onset of a photic *zeitgeber*-induced shift also varies between inbred strains of laboratory mice (Kopp et al., 1998).

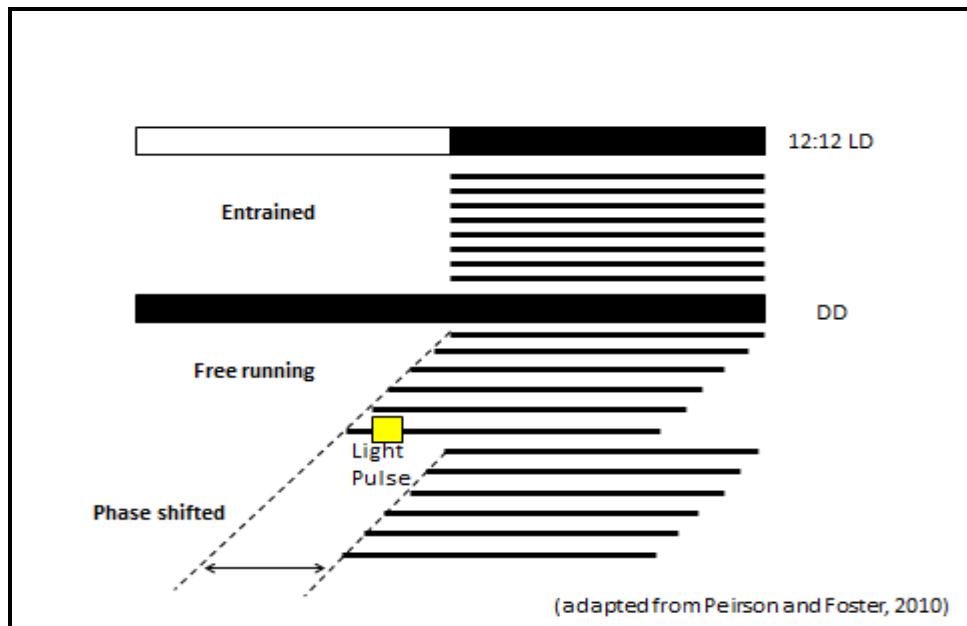


Figure 1.7 Phase shift in response to a light pulse; photoentrainment to 12:12 LD followed by dark adaptation prior to the delivery of a light pulse which resulted in a delay in the onset of the activity rhythm. Adapted from Peirson and Foster (2010).

A phase response curve (PRC) can be generated by delivering timed light pulses to a free-running, dark-adapted mouse (see Figure 1.8). The evoked shift depends upon the phase in which the stimulus was given- pulses delivered early in the *alpha* phase cause delays and

those given later result in advancement of the rhythm (Refinetti, 2006c). The size of the shift varies with the intensity and wavelength of the light stimulus in a dose dependant manner (Peirson and Foster, 2010) and also depends upon the endogenous circadian period of the mouse (Daan and Pittendrigh, 1976). The PRC gave circadian biologists the first clearly defined experimental tool for probing the physiology of circadian systems (Daan, 2000).

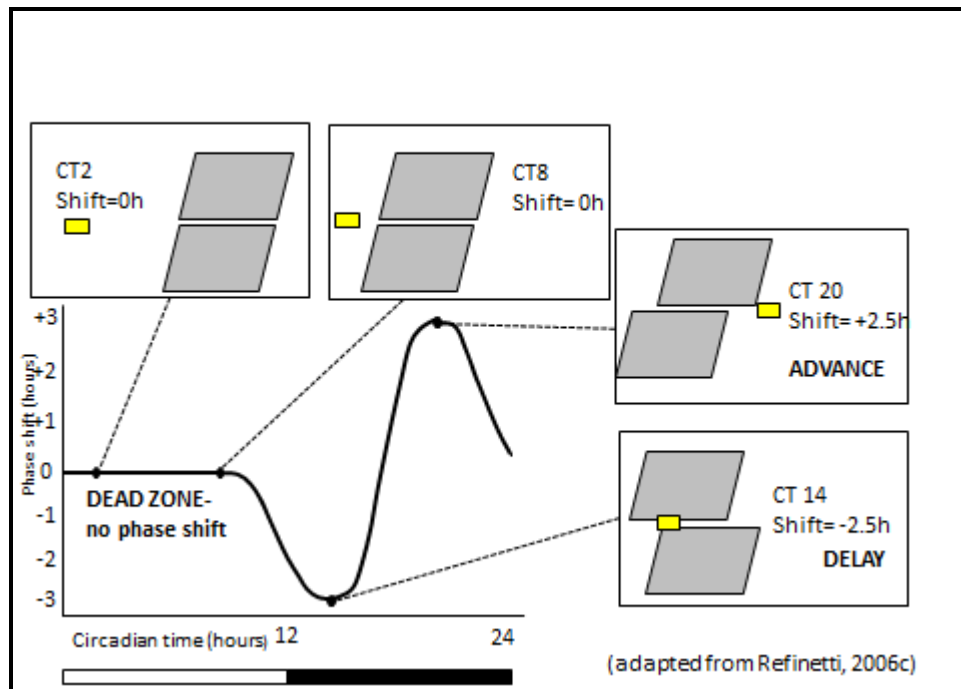


Figure 1.8 Generation of a phase response curve- light pulses delivered during the inactive phase do not affect the activity rhythm – this is the “dead zone”. Pulses given early in the active phase delay the onset of activity and those given later advance it. Adapted from Refinetti (2006c).

1.2.2 Sleep

The sleep wake cycle is an example of an outwardly expressed behaviour which has an appreciable daily rhythm. Sleep is not, however considered to be a simple output of the circadian clock, as a “sleep homeostat” or relaxation oscillator also exerts an effect (Franken

and Dijk, 2009, Lupi et al., 2008, Borbély, 1998). The circadian control is a self-sustained oscillatory process and the sleep homeostat is described as an “hourglass” oscillator as it is driven by the sleep/wake distribution. Pressure for sleep accrued during the active phase increases sleep propensity, this decreases once the animal enters sleep and propensity for the wake state rises (Borbély et al., 1989). The circadian sleep/wake process opposes the homeostatic changes in sleep drive (Franken and Dijk, 2009), as shown in Figure 1.9.

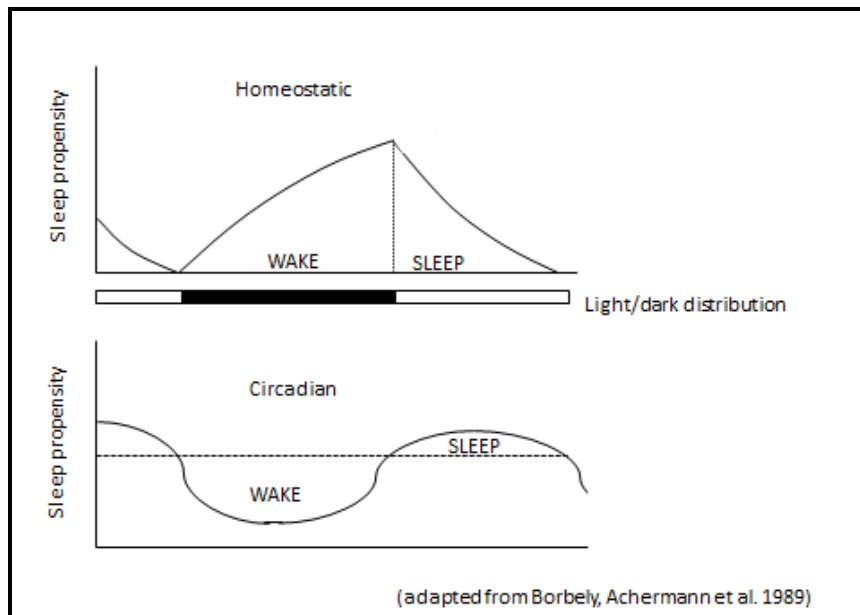


Figure 1.9 Homeostatic and circadian control of sleep in a nocturnal animal; sleep propensity rises during darkness when the animal is active and falls during the light phase when the animal is resting. Adapted from Borbély et al. (1989).

Rodents are commonly used in biomedical sleep studies; the underlying homeostatic, circadian and neural mechanisms are similar to humans but rodent sleep is polyphasic and physiologically fragmented, with shorter rapid eye movement (REM) and non-REM (NREM) cycles (Revel et al., 2009). However, delta power, the amplitude of the slow electrical oscillations seen in NREM sleep are predictable and mathematical modelling of these

dynamics allows detailed sleep assessment (Franken and Dijk, 2009). Electroencephalographic (EEG) and electromyogram (EMG) telemetry methods are well established in mice (Weiergräber et al., 2005) and differences in sleep architecture have been seen between inbred strains (Huber et al., 2000, Franken et al., 1998). Physiological correlates of NREM sleep include high amplitude, slow frequency electrical activity and reduced muscle tone, blood pressure and heart rate under vagotonic influence. Conversely, REM sleep is characterised by low amplitude, fast frequency waves and increased blood pressure, heart rate and muscle tone and obviously, ocular movement under sympathetic tone (Pick et al., 2011, Kushikata et al., 2012). Recently, a non-invasive method of determining sleep duration, latency and fragmentation was detailed (Fisher et al., 2012) where video tracking methods were used to record periods of immobility when the mouse was asleep. This method provided a high correlation (>0.94) with EEG/ EMG assessment and following administration of a sedative and caffeine.

Sleep/wake control occurs via a “flip/flop” switch mechanism found in the hypothalamus (Saper et al., 2001). The GABAergic ventrolateral preoptic area (VLPO) signals to inhibit basal brain structures at the onset of sleep (Franks and Zecharia, 2011), there are also GABA neurons which project long distances across the cortex (Gerashchenko and Shiromani, 2004). Conversely, the ascending arousal system, a collection of nuclei in the caudal midbrain and rostral pons promote wakefulness by secreting aminergic substances such as noradrenaline, serotonin and histamine. The addition of orexinergic projections from the lateral hypothalamus stimulates the basal forebrain and cerebral cortex (Franks and Zecharia, 2011, Saper et al., 2001). The SCN, which are in proximity to the VLPO and other hypothalamic nuclei, receive information about the sleep/wake state and signal to these

structures via intermediary neurons (Deboer et al., 2003). It is possible that the SCN may have a sleep- and a wake-promoting action (Dijk and Duffy, 1999). Mice which have been SCN-lesioned show increased (8.1%) total sleep time compared to controls (Easton et al., 2004).

The effect of the circadian clock on the sleep wake cycle can be seen from studies using clock mutant mice. *Bmal 1* knockout mice sleep more, have increased fragmentation and delta power (Laposky et al., 2005) and *Clock* mutant mice showed decreased levels of NREM sleep and overall consolidation (Naylor et al., 2000). *Cry* double knockout mice (which lack a functional clock) show more consolidated NREM sleep, spending longer in this phase and displaying higher delta power (Wisor et al., 2002). This mouse was intended as a homeostatic sleep model but genetic deletion of the clock's influence resulted in sleep abnormalities, suggesting a regulatory role for *Cry* genes (Foster and Peirson, 2012).

Canonical circadian clock genes are therefore implicated in sleep homeostasis. Sleep phenotypes seem to match *Per* expression, which is considered to be a state variable of the molecular clock. NREM sleep deprivation increases *Per* expression although this varies with genetic background (Franken et al., 2007). *Per* is upregulated under a strong sleep pressure in the brain of *Cry* knockouts and downregulated in *Clock* mutant mice (Franken and Dijk, 2009). *Per* expression within the forebrain reverts to control levels within two hours of the onset of sleep (Franken et al., 2007, Wisor et al., 2002). The sleep/wake homeostat seems to influence clock gene expression outside the SCN as normal levels of *Per* expression were seen in the forebrain of sleep- deprived, SCN-lesioned mice (Bourgin et al., 2008). This homeostatic control is likely mediated by *NPAS 2* (neuronal PAS domain containing protein 2) as studies of *NPAS 2* knockout mice did not reveal a sleep wake pattern (Reick et al.,

2001). *Npas 2* expression also overlaps with *Per* expression sites following sleep deprivation (Franken et al., 2007). Interestingly, all the clock proteins contain a PAS signal sensor domain (Franken and Dijk, 2009).

Further evidence of circadian involvement is the acute modulation of sleep by environmental light. Lupi, Oster et al. (2008) compared the response of rodless, coneless, melanopsin (*Opn4*^{-/-}) knockout and wildtype mice to a light pulse given four hours after the onset of the dark phase. Sleep was rapidly induced in *rd/rdcl* and wildtype mice but *Opn4*^{-/-} mice were resistant, even at high irradiances. There was no evidence of *Fos* induction in the SCN or in the VLPO in these mice, suggesting melanopsin is necessary for input to the sleep/wake cycle and rods and cones are not. Other authors have found that the classical photoreceptors do contribute to the induction of sleep during the light phase (Altimus et al., 2008, Tsai et al., 2009) whereas only melanopsin is required in dark conditions.

Physiological outputs

1.2.3 Endocrine outputs

The endocrine system produces many hormones from central and peripheral glands which circulate and exert effects at various body sites. These humoral cues may be considered as internal *zeitgebers* as the SCN regulates their production and release (Mutoh et al., 2003, Ishida et al., 2005). Two hormones, important in the circadian cycle are melatonin and corticosterone.

1.2.3.1 Melatonin

Melatonin is known as the darkness hormone as levels rise at night in vertebrates (Roseboom et al., 1998). It is produced by the pineal gland which receives SCN input via the paraventricular nucleus of the hypothalamus (PVN). Melatonin influences food intake, reproduction and pelage moult (Barrett et al., 2003) and administration can cause phase shifts or reduce the effects of jet lag (Zisapel et al., 2005). Noradrenaline, a catecholamine hormone activates arylalkylamine-N-acetyltransferase (AANAT) which catalyses conversion of serotonin, (a monoamine neurotransmitter also known as 5-hydroxytryptamine) first into N-acetyl serotonin, then into melatonin, which enters the bloodstream and the cerebrospinal fluid (Korf and von Gall, 2006). Many mouse strains don't produce melatonin due to a natural mutation resulting in deficiency of the AANAT gene (Vivien-Roels et al., 1998, Roseboom et al., 1998). Daily rhythms of melatonin are present in proficient strains such as C3H and CBA mice and absent in BALB/c, DBA, 129Sv and C57BL/6 (Goto and Ebihara, 1990). Selective breeding pressure may have caused deficiency- as melatonin has an inhibitory effect upon reproduction as it signals for decreasing day length (Bronson, 1979). A study of C3H and C57BL/6 mice showed that *Tau* and *Per 1* expression were identical, suggesting that circadian rhythms are generated independently of melatonin, despite its effects upon phase. A light pulse given early in the dark phase caused the same delay in both of these strains (von Gall et al., 1998).

Application of light attenuates melatonin levels, as mediated via the RHT (Goto and Ebihara, 1990). Two proficient strains were compared- C3H with hereditary retinal degeneration (*rd*) and CBA with normal vision. Low, medium and high light intensities caused melatonin suppression in CBA mice, whereas only high light levels resulted in reduction in C3H *rd* mice.

Functional rods and cones therefore seem to be required to relay photic information to the pineal gland.

Melatonin acts within the central nervous system, recruiting the SCN to excite the sympathetic nervous system following administration to anaesthetised BALB/c mice (Mutoh et al., 2003). Light pulsing during anaesthesia resulted in SCN activation, increased cardiovascular parameters and renal sympathetic activity. Intra-cerebroventricular administration of melatonin attenuated these responses without increasing peripheral circulating levels, indicating mediation through central receptors. Melatonin receptors are found within the SCN and pars tuberalis of the pituitary gland (Mutoh et al., 2003, Ono et al., 2008). Pinealectomised C3H mice with a targeted deletion of melatonin receptors showed an absence of clock gene expression in the pars tuberalis compared to wildtype controls (Von Gall et al., 2002, Von Gall et al., 2005).

Thyroxine, a metabolic hormone produced from the thyroid gland also appears to be involved in photoperiodic signal transduction. Expression of genes coding for thyroid stimulating hormone and its breakdown enzymes are seen in the pituitary and hypothalamus of CBA mice and administration of melatonin to deficient C57BL/6 mice induces the same genes (Ono et al., 2008).

1.2.3.2 Corticosterone

The adrenal cortex secretes corticosterone, or cortisol, a glucocorticoid hormone which is the end product of the hypothalamic-pituitary-adrenal (HPA) axis (Lightman, 2008). Diurnal variation of corticosterone is well-characterised in many species and levels also rise following physiological or psychological stress (Moberg, 1987). The circadian rhythm of

cortisol is formed from many shorter ultradian rhythms as pulses occur approximately once hourly (Windle et al., 1998). The duration or severity of the stressor affects the ratio of corticotropin releasing hormone (CRH) to AVP, the peptide outputs of the PVN, as shown in Figure 1.10;

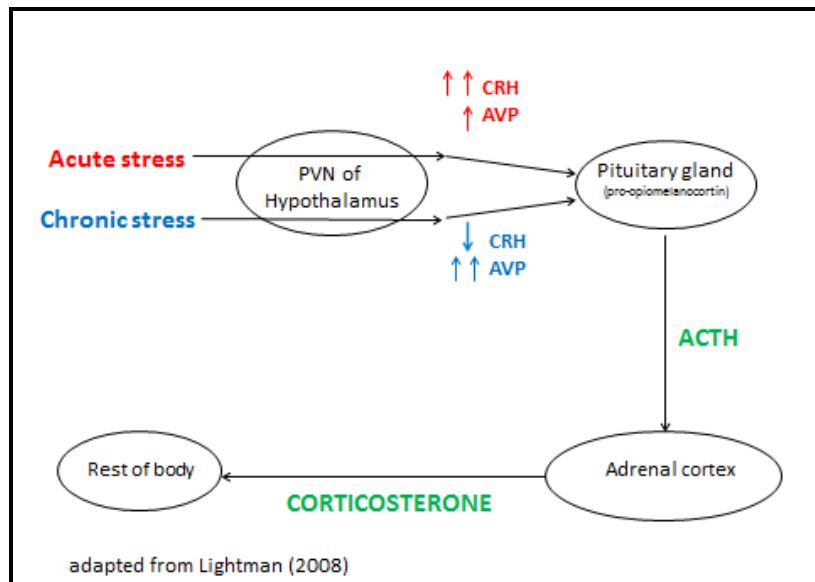


Figure 1.10 The hypothalamic-pituitary-adrenal axis; showing the neural structures and organs involved and the effect of acute and chronic stress on the proportions of the neurotransmitters released from the PVN. Adapted from Lightman (2008).

Adrenocorticotrophic hormone (ACTH) is released from the pituitary gland and signals for glucocorticoid production from the *zona fasciculata* of the adrenal cortex where clock gene rhythms are apparent (Korf and von Gall, 2006, Bittman et al., 2003). Corticosterone acts widely within the body, affecting memory and cognition, glucose, protein and fat metabolism and the cardiovascular system to name but a few (Lightman, 2008).

Circulating corticosterone concentrations vary between mouse strains and C57BL/6 do not show negative feedback suppression following exogenous administration of ACTH, unlike C3H mice (Oster et al., 2006, Ishida et al., 2005). The HPA axis is defective in clock mutant mice (Oster et al., 2006). Light induces *Per 1* and *Per 2* expression in the adrenal gland *in vivo*, but not in the kidney or liver (Ishida et al., 2005). This occurs under SCN control via the splanchnic nerve which innervates the adrenal medulla, the site of adrenaline production. Early adrenocortical gene activation results in glucocorticoid release into the circulation. This alternative pathway to the HPA shows that glucocorticoids provide time cues to cell autonomous peripheral oscillators as they are produced in response to light (Schibler and Brown, 2005). Ishida, Mutoh et al. (2005) confirmed SCN involvement by showing that corticosterone was not released in SCN-lesioned mice in response to a light pulse.

1.2.4 Body temperature

Animals can be categorised as endotherms or ectotherms in terms of how they regulate body temperature. The endotherms (mammals and birds) maintain body temperature around an internal set point, regardless of ambient temperature (Gordon, 2012) which enables them to inhabit many different environments. Endotherms can be further classified as homeotherms, who regulate temperature tightly within narrow limits and heterotherms, who allow body temperature to drop significantly during periods of hibernation or torpor. Body temperatures of ectotherms (fish, reptiles and amphibians) fluctuate with external ambient temperature, therefore environmental selection and behaviour are critical for these animals.

Mammalian body temperature varies 1-4°C throughout the day (Brown et al., 2002) and is affected by eating, drinking, local insulation and level of activity among other factors (van

den Heuvel et al., 2004). The temperature waveform is sinusoidal with peaks and troughs corresponding to active and sleeping phases (Hasselberg et al., 2013) and both circadian temporal organisation and primary temperature homeostasis shape the rhythm (Aschoff, 1980). The rat has been the primary rodent thermoregulatory model (Bicego et al., 2007) but random ultradian oscillations of up to 0.7 °C per hour have been seen in the temperature rhythms of mice (Gordon, 2009). There is heterogeneity of absolute temperatures within the body and the brain, core and shell are recognised as functionally discrete areas (Gordon, 1993).

The shell represents the thermal interaction of the body with the environment and as mammals are usually warmer than their surroundings heat is lost by convection, conduction and radiation along the gradient across the skin's surface (Gordon, 1993). Thermal conductance rates are inversely proportional to body weight and also display circadian rhythmicity, which supports heat loss during activity (Aschoff, 1980). The rate of loss is controlled by the cutaneous vasomotor response (Gordon, 1993) and Phillips and Heath (1995) found that vasomotive index across 29 animal species (the ability to regulate temperature via the skin) is positively correlated with body size and decreasing surface area to body volume ratio. Small animals such as rodents are tachymetabolic or "metabolic specialists", altering metabolic rate in preference to skin temperature to thermoregulate (Phillips and Heath, 1995, Gordon, 1993). Thermal capacitance also increases with body mass; the absolute temperature differential of mice compared to rats shows that rats thermoregulate more efficiently and limit within a smaller range (Gordon, 2009). Minimal values within daily temperature rhythm are lower in smaller animals and the range of

oscillation can be 2.5-5 times greater for a 10g animal compared to one weighing 1kg (Aschoff, 1980).

The physiological seat of thermoregulation is in the pre-optic anterior hypothalamus (POAH) which is composed of warm and cold sensitive neurons, with integral thermoreceptors which monitor local blood flow (Oka et al., 2001). Deviations from a set point initiate a sympathetic response which drives alterations in physiological and behavioural effector mechanisms through various neural networks (Adler et al., 1988). The hypothalamus controls many autonomic functions and temperature information is integrated with other processes such as those controlling water balance and food intake (Gordon, 1993). Body core and brain temperature are maintained within narrow limits, the latter via carotid retes (a network of anastomosing arteries) in some species, although these are not present in rodents (Gordon, 1993).

The primary peripheral response to warm environments is to alter the vasomotor response by sympathetic neuromodulation of the smooth muscle in vessel walls, as seen in the tails of rodents and the ears of rabbits (Brown and Pham-Le, 2011). Some species, like dogs, pant and an increased respiratory rate can be seen in rodents under extreme thermal load. Rodents are more prone to cold stress and metabolic thermogenesis mechanisms are well-developed to cope with cool environments. Shivering, asynchronous muscle contractions (Berne and Levy, 1996) are an early response to cold and produce heat peripherally (Gordon, 1993). Non shivering thermogenesis involves noradrenergic activation of brown adipose tissue (BAT), the principal deposit is found in the interscapular space in mice. BAT is not found in all mammals, it declines in many species as they mature from neonates (Bicego

et al., 2007). It differs from white fat, having a multilocular structure which contains many more mitochondria; the site of heat production via uncoupling of electron transport during ATP production on the inner membrane (Bartelt et al., 2011, Cannon and Nedergaard, 2004). An increased amount of NST is seen in mice in environments of 22°C compared to 29°C (Talan et al., 1996). In cold-acclimated animals increased uncoupling protein and lipase levels, mitochondrial density and generalised tissue hypertrophy are seen in response to persistent noradrenaline stimulation (Gordon, 1993) and uncoupling protein genes are upregulated by elevated concentrations of the thyroid hormone, T3 (Bicego et al., 2007). Non-shivering thermogenesis is ecologically significant as rodents can use it to raise body temperature before the onset of activity, as it is effective within minutes (Haim and Izhaki, 1993).

Animals also change their behaviour to maintain thermal comfort. They may make a conscious choice to move towards or away from a heat source (positive or negative thermotaxis). When ambient temperature is high reduced activity is seen and wallowing or changes in posture may occur in larger animals (Gaskill et al., 2011). Rodents do possess eccrine sweat glands but they are non-functional so they groom, spreading saliva onto their paws, scrotum and tail, to increase heat loss by evaporation (Gordon, 1993). In cool environments they huddle together, hoard food and build nests, described further in Chapter 3.

1.2.4.1 Deviations from normothermia

Temperature is widely used as a marker of health and it may increase or decrease from normal levels in a variety of circumstances;

Following infection, the body releases inflammatory cytokines in response to the presence of microbes in the bloodstream (Leon, 2002). These cytokines are endogenous pyrogens

which cross the blood brain barrier and are detected by the thermosensitive neurons of the POA, causing prostaglandin release which results in inflammation. The fever, or rise in the body's set point temperature which follows is advantageous as it facilitates the cellular immune response and the cytokines released are thought to inhibit microbial growth (Oka et al., 2001). Pyrexia also occurs during psychological stress, where BAT is activated, in addition to the hypothalamic-pituitary-adrenal axis (Gordon, 1993). The magnitude of the temperature rise is constant across warm or cold environments, suggesting that it is centrally regulated (Oka et al., 2001). Aydin et al. (2011) found that the ambient temperature limits between which rats can maintain normothermia are reduced when they are restrained. Iatrogenic administration of substances can also change body temperature- lipopolysaccharides and bacterial endotoxins are used in research for their pyrogenic effects (Newsom et al., 2004) and opioids increase temperature in many species (Adler et al., 1988). Stimulants such as caffeine and cocaine raise body temperature and somnogenic substances like melatonin and benzodiazepines reduce it (van den Heuvel et al., 2004).

Body temperature falls under general anaesthesia, as thermoregulatory mechanisms are impaired (Gordon, 1993), a significant problem facing biomedical researchers who use mice in surgical procedures (Bagis et al., 2004, Rembert et al., 2004). Ambient temperature was found to increase the sleep time of mice intoxicated with alcohol, as recovery times were negatively correlated with their rectal temperatures (Wenger and Alkana, 1984). All dosing in regulatory toxicology studies should therefore be conducted at suitably controlled ambient temperatures (Gordon et al., 2008).

Although mice do not hibernate, they are facultative daily heterotherms which enter a state of torpor if energy resources are low (Cannon and Nedergaard, 2004). Fasting leads to

reduced body temp (Jensen et al., 2013) and mice in torpor can reduce below 20°C and still recover by recruiting brown adipose tissue at the time of arousal (Oelkrug et al., 2011). During torpor rodents tend to reduce temperature rather than altering metabolic rate (Geiser, 2004) although Brown et al. (2010) found that the respiratory rate within mitochondria dropped by up to 24% and cardiovascular parameters were depressed, indicating increased total peripheral resistance (Swoap and Gutilla, 2009). PK2 expression (a neurotransmitter associated with the SCN) was upregulated in the paraventricular nucleus of fasted mice, an area linked with thermoregulatory control although the exact connection between thermoregulation and the circadian pacemaker is not known (Zhou et al., 2012).

1.2.4.2 The circadian rhythm of body temperature

The circadian rhythm of temperature is well established in mice with an acrophase during darkness (Weinert and Waterhouse, 1998), the exact timing of which varies between strains (Tankersley et al., 2002). Higher temperatures under darkness is not due to increased activity as a clear rhythm persists when activity is limited, although amplitude is slightly decreased (Gordon, 1993) and temperature rhythms persist in very old mice when their locomotor activity rhythms subside (Weinert et al., 2002, Weinert and Waterhouse, 2007). The circadian rhythm of temperature is usually phase-advanced with respect to activity in mammals, as temperature always rises before waking (Refinetti and Menaker, 1992, Tokura and Aschoff, 1983). Skin conductance values show a temporal variation, being higher during the active phase, resulting in more efficient dissipation of heat (Aschoff, 1981).

Light is a *zeitgeber* for body temperature, just like any other circadian output. Temperature rhythm changes following exposure to long and short daylengths (Haim and Zisapel, 1995)

and the spectral composition seems to be significant with rats showing greater phase shifts to changes in longer wavelength cycles (McGuire et al., 1973). Light pulses during darkness decrease temperature (Studholme et al., 2013) and shifted temperature rhythms retrain faster than those of locomotor activity (Sato et al., 2006). Timed food restriction, a common experimental manipulation is associated with phase-advances of the rhythms of locomotor activity, temperature and melatonin release (Challet et al., 1997). Social interactions also have an impact as the stress associated with conflicts between rodents resulted in loss of temperature rhythms for up to eight days and an associated reduction in amplitude persisted for weeks (Meerlo et al., 1996, Tornatzky and Miczek, 1993, Harper et al., 1996).

Environmental temperatures exert a weak, indirect *zeitgeber* effect (Tokura and Aschoff, 1983, Refinetti, 2010, Francis and Coleman, 1990), with cool ambient temperatures advancing locomotor activity rhythms and thus increasing body temperature (Mistlberger et al., 1996) and Francis and Coleman (1990) found that a warm environment caused negative masking of activity in marsupial mice. There is a temporal variation of how mice cope with cold and the Rev-Erb α receptor has been suggested as a potential link between the thermogenic and circadian networks (Gerhart-Hines et al., 2013). The mammalian SCN is “decoupled” and resists entrainment by either endogenous or environmental temperatures, allowing it to drive other core rhythms appropriately and SCN lesions do not appear to impair body temperature rhythm (Fuller et al., 1981). Ambient temperatures have profound effects on harvested mammalian cells maintained *ex-vivo*, as temperature cycles can propagate and even change natural genetic oscillations (Tsuchiya et al., 2003, Buhr et al.,

2010, Brown et al., 2002, Saini et al., 2012), suggesting that endogenous temperature may contribute to entraining peripheral tissues.

Sleep has a bradymetabolic effect and the polyphasic sleep/wake pattern of rodents affects the thermoregulatory process (Gordon, 1993). These two rhythms can, however, persist independently of each other (Aschoff, 1983), seen during forced short light cycles in rats, where sleep followed the photoperiod and temperature free-ran (Cambras et al., 2007). Sleepiness and changes in body temperature are temporally associated and there is evidence that human insomnia may be caused by impaired heat loss capacity (van den Heuvel et al., 2003). The onset of sleep correlates with increased peripheral and decreased core temperature (VanSomeren, 2000) and elevations in core temperature once asleep increase the likelihood of waking up (Hasselberg et al., 2013).

1.3 Conclusion and Aims

Circadian rhythms occur in all living organisms and they benefit health and function by entraining body clocks to the environment to maximise the efficiency of internal processes. Within animals, circadian rhythms can be evaluated at the genetic, cellular, tissue, organ or whole body level and the study of peripheral clock outputs enables evaluation of rhythms in a holistic context, as multiple factors interplay in the production of rhythms of physiology and behaviour. In general, whole animal outputs reduce invasive experimental techniques and reduce the cost to experimental models, thereby improving welfare.

The aims and hypotheses of this project are;

1. To study one behavioural output- locomotor activity and the level of entrainment that mice experience within the context of current laboratory animal housing practices, living in an individually ventilated cage (IVC). Light is the primary *zeitgeber* and the level of ambient light that mice receive within these closed cages, and therefore the effect that IVCs have upon circadian rhythms is largely unknown.

Hypothesis: cage position (relative to overhead light sources) within an individually ventilated cage rack will affect the voluntary wheel running activity of singly-housed mice.

2. To study one physiological output- the body temperature rhythm of mice, a species in which conventional methods of measurement are difficult due to their small size and confounded by the stress associated with handling and restraint. A novel non-invasive method of measuring peripheral temperature will be trialled simultaneously

with an established implant, measuring core temperature in the hope that it will provide reliable data on both fluctuations in the rhythm of body temperature and absolute values. Longitudinal recording of both core and peripheral temperature in standard 12:12 LD, then in constant darkness (DD) and finally under constant light conditions (LL) should reveal if the ambient light cycle affects the rhythm of body temperature.

Hypothesis: Using infrared thermography/thermal imaging to measure peripheral surface radiation is a valid method of assessing the body temperature of mice.

Hypothesis: the circadian rhythm of body temperature, as seen when mice are entrained to a regular light/dark cycle alters under conditions of constant light or constant darkness.

Chapter 2 General Methods

2.1 Licence authority and ethical review

All experiments conducted during the generation of this thesis were carried out under the authority of the Project Licence (PPL) no. 30/2812 “Non-image forming responses to light” and the author’s personal licence (PiL) 30/9509 with primary availability at the Registered Medical and Scientific Departments of the University of Oxford. The PPL was reviewed by the Clinical Medicine Ethical Review Committee (now known as the Clinical Medicine Animal Welfare and Ethical Review Body) prior to being granted by the Secretary of State. A Research Projects Concept Note and Ethical Review document was also submitted to and checked by the Research Directorate at the University of Nottingham.

2.2 Source and health status of animals

All animals used were laboratory mice (*mus musculus*) sourced from Harlan Laboratories, a commercial breeder and supplier with facilities within the United Kingdom. A commonly used inbred strain was selected, the C57BL/6 J0laHsd mouse, see http://www.harlan.com/products_and_services/research_models_and_services/research_models/c57bl6_inbred_mice.hi

Mice were bred within a barrier unit to achieve specified pathogen free (SPF) health status and maintained within same sex groups in individually ventilated cages (IVCs) until the point of sale. After arrival, micro-organisms detected on health screening of sentinel mice from the experimental colony were *Entamoeba muris* (an amoeba which inhabits the large intestine, considered commensal/non-pathogenic) and *Helicobacter hepaticus* (a bacteria

commonly found in the large intestine of laboratory mice which does not appear to cause disease in non-susceptible or immune-compromised mouse strains). Routine health screening of sentinel mice was carried out at quarterly intervals and no new microbes were detected.

2.3 Housing and husbandry of mice

All mice were singly housed, to control for the effect of social housing on circadian rhythms. Mice were maintained on ad-libitum RM3(E) irradiated diet (SDS) and chlorinated water (2x Instachlor Rapid chlorine tablets 0.35mg in 50 litres). Mice used in Chapter 3 were housed in Tecniplast Green Line individually ventilated cages on autoclaved woodchip bedding. Mice used in Chapters 4 and 5 were housed in open top cages inside light tight chambers (LTCs), horizontally aligned cupboards with built in ventilation and overhead lights, so the ambient light cycle can be varied independently of the holding room. The cages of the “Temperature” and “ECG” implanted mice had conventional wire lids into which the food supply and water bottle were placed, the “EEG” implanted mice were kept in high-sided open top (no lid) cages to reduce the risk of damage to the cranial implant when rearing or climbing. All mice remained in their home cage for temperature recordings and the author moved all cages/handled all mice throughout all experiments.

The ambient light intensity within the colony room where the IVC experiment took place varied with distance from the overhead light sources and is reported within Chapter 3. The ambient light intensity within the holding room used to collect data for Chapters 4 and 5 was set at 200 lux and a red head torch was used to inspect or move mice under conditions of darkness (as mice cannot see in the red part of the spectrum of visible light). Light intensity in the recording light tight chamber was set at 200 lux during both LD and LL cycles.

Standard amounts of nesting material (relative to all other mice in the facility) were given to all experimental mice.

2.4 Health checking and distress scoring of mice

Mice were checked at least once daily, as required by the Animals (Scientific Procedures) Act 1986. Signs of good health in mice include; alert and inquisitive, lack of ocular or nasal discharges, glossy coat with no piloerection, normal posture (no hunching), regular frequency of drinking/urinating and eating/defaecating. Standard clinical parameters such as respiratory and heart rates are difficult to assess reliably in conscious mice and the significance of temperature assessment is discussed in Chapters 4 and 5. Efforts were made to minimise disturbance of all mice to reduce any effect of handling on the circadian rhythms of behaviour and physiology. Following surgery (Chapters 4 and 5) mice were checked twice daily; to check their abdominal and cranial surgical wounds and to assess the need for analgesic administration.

Chapter 3

Wheel running activity at different positions in an individually ventilated cage rack

Hypothesis: cage position (relative to overhead light sources) within an individually ventilated cage rack will affect the voluntary wheel running activity of singly-housed mice.

Acknowledgements: the assistance of Dr. Violetta Pilorz with the early data analysis of the Clocklab Timeseries data files is appreciated.

A Circadian Terminology and Abbreviations list can be found prior to the Table of Contents.

3.1 Introduction

3.1.1 Properties of Light

Light is the primary zeitgeber and photoentrainment forms the basis of many experiments investigating the circadian system. Light travels in waves and is part of the electromagnetic spectrum; with wavelengths between 350- 750 nm (Peirson et al., 2005, Foster et al., 2007), as shown in Figure 3.1;

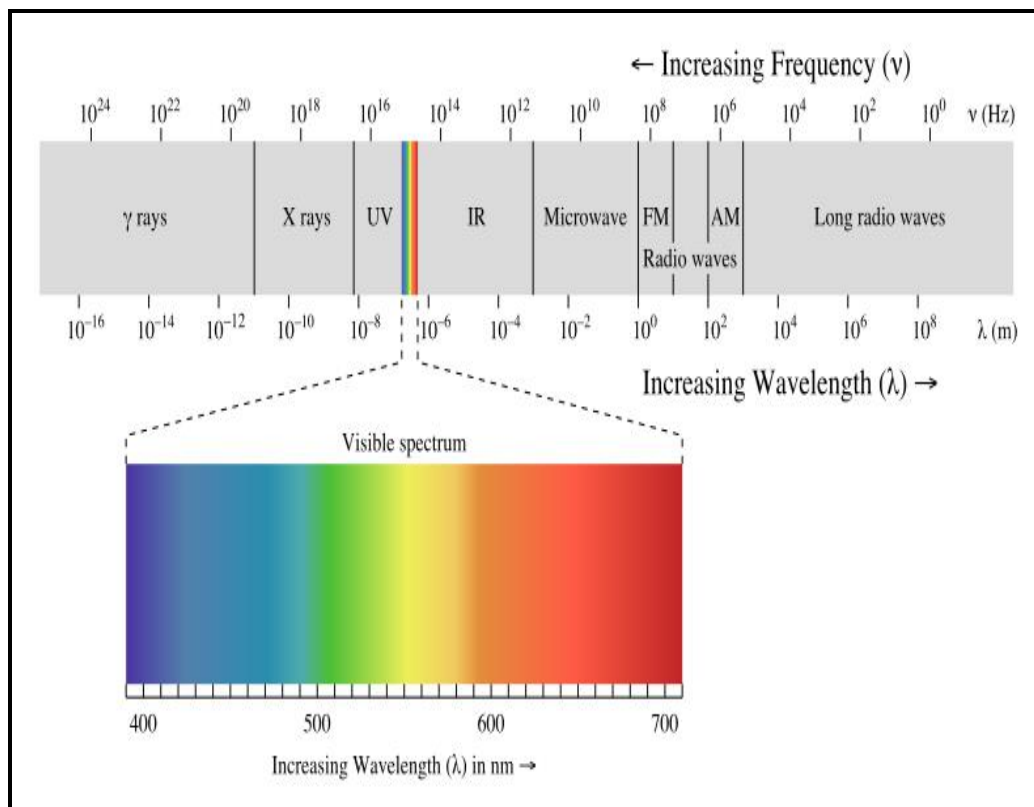


Figure 3.1 Light as part of the electromagnetic spectrum (from Peirson and Foster (2010)).

Light is polychromatic (made of many colours) and has a variable spectral quality (Lucas et al., 2014). The spectrum of natural light depends on many contributing atmospheric factors

and varies greatly but typical values of light intensity, measured in lux are 50,000-100,000 lux on a clear day, 10,000-20,000 lux on an overcast day and <1 lux under full moonlight (Münch and Bromundt, 2012). Artificial, “white” light sources also produce a broad range of wavelengths, two notable examples being incandescent lights which emit longer wavelength (red) and some infrared waves and fluorescent lights which have a strong emission peak at shorter wavelengths (blue) light (Foster et al., 2007). Light intensity can be categorised in either radiometric or photometric measurement units (Lucas et al., 2014). The former describe the absolute physical properties of light (its wavelength and energy, in watts/m²), the latter provide a relative measure of visual brightness to a human observer (in lux) (Foster et al., 2007).

3.1.2. Light and photoreception

The relative contribution of each retinal photoreceptor to circadian rhythms depends upon the duration, wavelength and intensity of ambient light (Butler and Silver, 2011). The photopigments, within the photoreceptors have discrete absorbance spectra, describing a range of wavelengths of light which elicit a biological response (Peirson et al., 2005). Currently illuminance is most commonly used method of measuring light intensity as the measuring instrument, a lux metre is widely available and inexpensive. As the spectral sensitivity of photopigments varies across species, care should be taken to apply spectral weighting to account for photoreceptor differences when using non-human subjects (Lucas et al., 2014).

Irradiance response curves (measuring the magnitude of a biological response as a function of different wavelengths of light), have been instrumental in elucidating the spectral

sensitivity of the retinal photopigments (Thompson et al., 2008) and several IRCs can be combined to generate an action spectrum (See Figure 3.2). Using relatively monochromatic light sources (limited within a narrow wavelength range) ensures accurate excitation of chosen photopigments, this can be achieved experimentally by using light emitting diode (LED) sources or by applying a filter to a polychromatic white light source (Foster et al., 2007) and confirming radiometric output values using a spectrophotometer.

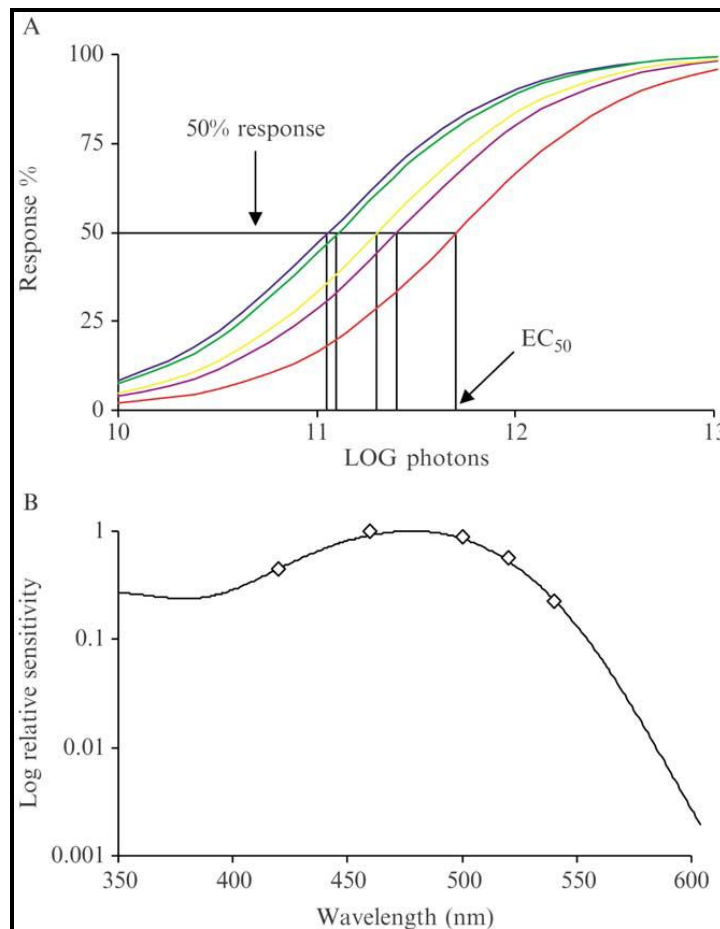


Figure 3.2 Irradiance response curve generated from five wavelengths of light (A) where the magnitude of the biological response varies with intensity (measured radiometrically in photos). The relative sensitivity is derived from the half-maximal IRC for each wavelength and plotted against wavelength to give the action spectrum (B). Figure from Foster et al. (2007).

3.1.3 Non-image forming responses relevant to locomotor activity studies

3.1.3.1 Photoentrainment

Circadian rhythms can be synchronised or entrained to the light/dark cycle, the strongest *zeitgeber*. The period of the internal rhythm is corrected for day after day, by either small or large pacemaker shifts to align it with the photoperiod. Daan (1977) postulated that the internal oscillator could either be entrained parametrically by multiple tonic accelerations or

decelerations relative to environmental light or by lesser, abrupt phasic resets at certain times of the day, such as at the light/dark transition. Recording the distribution of activity is a minimally-invasive, robust method for assessing entrainment in mammals and various parameters can be derived from recording revolutions of a running wheel placed inside the cage of mice (Jud et al., 2005). The onset of activity is useful as a phase marker (Refinetti, 2006a) and the onset phase angle is precise and has been clearly defined in several rodent species (Pohl, 1976).

Entrainment to a regular light/dark cycle occurs, provided the cycle length is reasonably comparable to internal period length, τ . Studies investigating the threshold light intensity for entrainment revealed that rods contribute to circadian entrainment during low intensity (scotopic) conditions. Ebihara et al. (1980) found that both C57BL/6 mice (with intact retinae) and C3H *rd/rd* mice (a naturally occurring mutant, deficient in rods) both entrained at a high light intensity but 70% of the *rd/rd* mice free-ran at 1 lux compared to 17% of the C57BL/6 at 0.1 lux. Melanopsin requires light of long duration and high intensity (Berson et al., 2002b, Sekaran et al., 2005, Provencio et al., 1994) but rods assist by driving photoentrainment at scotopic intensities, also signalling through cones at photopic (high intensity) levels (Altimus et al., 2010, Lall et al., 2010) allowing entrainment across various levels of environmental irradiance.

Mrosovsky (2003) also demonstrated circadian entrainment of wild type mice at light levels where the majority of *rd/rd* mice free-ran and suggests that the threshold of entrainment may be a more sensitive indicator of circadian synchronisation than the traditionally employed method, the phase shift. Butler et al. (2011) concur, as when investigating the

effects of different wavelengths of light in C57BL/6 mice, found evidence of a phase angle of entrainment at low light intensities when masking or pupillary light responses did not occur (1-2 log units lower for the respective half-maximal responses). Entrainment appears to be preserved when other, non-image forming responses to light are lost.

3.1.3.2. Masking

Light has acute effects upon locomotor activity rhythms which do not involve any input from the SCN. Masking complements clock control, allowing an animal to exploit its surroundings if conditions change abruptly and can be assessed by comparing the activity level at the corresponding time in another daily cycle when *zeitgeber* alteration did not occur (Mrosovsky, 1999). Masking is mediated primarily via the melanopsin containing- pRGCs as it occurs in mice deficient in rods and cones (Mrosovsky et al., 2001) and transgenic mice lacking melanopsin did not reduce their activity to a sustained (up to three hours) light pulse given at ZT 14 (2 hours after lights off) (Mrosovsky and Hattar, 2003). Masking is also illuminance-dependant and a threshold intensity of 1-5 lux has been quoted for C57BL/6 mice (Mrosovsky, 1994).

Classical and melanopsin pathway interactions also occur during masking responses. Positive masking (the increase in activity in response to dim light) is likely due to increased vision facilitating movement, via rod- mediated signalling, as it is absent in *rd/rdcl* mice (Mrosovsky, 1999, Thompson et al., 2008). Negative masking is mostly melanopsin-based but there is some input from the short wave sensitive (UV) cone as decompression of the irradiance range was seen in for masking responses in *rd/rdcl* mice (Thompson et al., 2008).

Redlin et al. (2005) found that *Clock* mutant mice did not show negative masking to the same degree as wild-types, despite having the same retinal composition, indicating that this gene has some effect on locomotor activity control mechanisms downstream of the SCN.

3.1.4 Effects of photoperiod on activity

The length and the nature of the photoperiod affects the activity rhythm. Laboratory experiments tend to use bright light sources, either “on” or “off” in a square waveform which bear little resemblance to natural photoperiods. Light quality changes in amount, spectral composition and direction at dawn and dusk (Foster et al., 2007, Comas and Hut, 2009) and any discrepancies between *Tau* and the photoperiod are corrected for by oscillator advances or delays during this time (Foster et al., 2007, Roenneberg and Foster, 1997). Dimming light initiates the onset of activity in nocturnal species (Pohl, 1976) and differences are apparent between animals under twilight and square wave conditions. Aschoff and Wever (1965) predicted that increased duration of twilight would advance the phase and increase the strength of the *zeitgeber*. Studies of the Syrian hamster, *Mesocricetus auratus* showed increased variability in onset times under square wave cycles (Boulos and Macchi, 2005) and entrainment did indeed improve as when, subjected to reduced and elongated photoperiods (by 2.5 hours), twilight-exposed animals stayed entrained and square wave cycle animals free-ran (Boulos et al., 1996, Boulos et al., 2002). Hamsters also delayed their activity onset by several hours when a previously established twilight phase was removed, indicating a phase shift in their activity rhythms (Boulos and Macchi, 2005). When light intensity progressively reduces over several cycles, the phase angle between activity onset and lights off becomes more positive in mice (Ebihara and

Tsuji, 1980) and C57BL/6 mice under scotopic conditions, (3 orders of magnitude below the cone pathway threshold) showed increased activity at the light/dark transition (Doyle et al., 2008). Comas et al (2009) found that extending the twilight interval to 2 hours increased the phase angle and resulted in increased variability in onset times, weakening the degree of entrainment in C57BL/6 mice. Use of constant light conditions (LL) eventually render mice completely arrhythmic, often following an initial extension in *Tau*.

3.1.5 Individually ventilated cages

Individually ventilated cages (IVCs) were established as a method of housing small laboratory animals about 20 years ago, falling between closed barrier units (where open-top or filter-top cages are used) and isolators in terms of biocontainment and biosecurity (Brandstetter et al., 2005). They are polycarbonate plastic boxes with an impermeable lid which seals the interior from the external room environment. An attached handling unit circulates air to and from each cage via individual supply and exhaust ports when cages are docked on the rack- cages can therefore be considered as separate microbiological units (Brielmeier et al., 2006, Clough et al., 1995). The incoming air passes through HEPA (high efficiency particulate air) filters, and is changed at a set frequency, resulting in standardised (temperature and relative humidity) internal conditions that should minimise variation within experimental subject animals and increase research quality and reproducibility (Höglund and Renström, 2001, Clough et al., 1995). As the animals inside are shielded from the room macroenvironment, all incoming objects such as bedding, foodstuffs and cage furniture are generally pre-sterilised by autoclaving or irradiation to prevent transfer of unwanted biological materials inside.

3.1.5.1. Advantages of IVCs

IVCs may permit increased stocking density as rodents may be stacked in vertical columns on the racks, utilising previously empty space. Separating animal and human airspaces reduces the risk of laboratory personnel developing health-threatening allergies; potent aeroallergens can arise from the proteins found in mouse urine as well as the more obvious sources such as animal hair and bedding particles (Renström et al., 2001).

Animals maintained within IVCs are protected from ambient noise levels and bright light to some degree; the light intensity inside is thought to be more evenly distributed (Clough et al., 1995). The frequent air movement results in relatively low humidity which keeps bedding substrates drier for longer, resulting in extended intervals between cage changes which is labour-saving. Before IVCs became popular, cages used to be changed several times weekly as it is known that mice prefer to nest in less-soiled areas given the choice (Godbey et al., 2011) and ammonia levels build up when cages are dirty. Forced air ventilation also reduces ammonia levels, with none being detected for several days and remaining within acceptable limits in studies of IVCs unchanged over prolonged periods of time (Corning and Lipman, 1991). Reduced frequency of changing also benefits psychological well-being as cage changes are stressful to mice, having been associated with precipitating aggression within groups (Balcombe et al., 2004) and daily changes over a two week period resulted in reduced weight gain (Beynen and van Tintelen, 1990). Rosenbaum et al. (2009) tracked measures of mouse welfare over 17 days in IVCs and found that although the cages appeared visually soiled, faecal corticosteroid levels, body mass and behaviour were all within normal limits.

The enhanced biosecurity that IVCs offer enables mice of high health status or reduced immune-competence to be kept in a relatively sterile environment. The exhaust air outlet filter can also be used for health screening purposes (detecting pathogen DNA by PCR) instead of sacrificing in-contact sentinel animals for serological testing, further reducing costs and animal numbers (Compton et al., 2004). Recycling dirty bedding from experimental animals into the cages of separately housed sentinels may also be used in IVC

systems although the success rate of disease transmission depends on the volume and frequency of transfer (Gonder and Laber, 2007).

IVCs can also be used for euthanasia using carbon dioxide gas (CO²), a common method of terminating laboratory mice. McIntyre et al. (2007) demonstrated that multiple mice could be simultaneously culled by pumping CO² through into cages docked on a rack and mice did not appear to suffer any more distress than when they were killed inside dedicated carbon dioxide chambers although rack position affects the level of CO², a dense gas per given time point inside cages. This is undoubtedly less stressful for the animals than moving them from their home cage into a novel chamber for gas delivery and equipment of this nature is now available from commercial laboratory animal equipment manufacturers (<http://www.vet-tech.co.uk/anaesthesia-supplies/co2/c02-ivc-unit.aspx>).

3.1.5.2 Disadvantages of IVCs

IVCs are more complex and require greater levels of checking and maintenance than conventional open-top cages, especially around the air inlet and outlet ports (Baumans et al., 2002, Höglund and Renström, 2001). There are some ergonomic disadvantages for animal care personnel as it's hard to see into and physically remove cages docked at the lowest and highest rack levels (Renström et al., 2001).

The forced air supply can cause noise and vibration. The average decibel level within IVCs was found to be greater than that of the macroenvironment of animal stock rooms (Perkins and Lipman, 1996). Forced ventilation can result in welfare problems as mice find drafts aversive and prefer cages where the air inlets are raised above their head level (Baumans et al., 2002). The airflow varies within a cage and mice generally choose to nest under the food hopper at the front where ventilation and ambient light levels are lowest (Kostomitsopoulos

et al., 2007). The frequency of air changes does not seem to have an effect if shelters or adequate nesting material are provided (Baumans et al., 2002, Krohn and Hansen, 2010).

Despite regular air movement, some authors found that ammonia levels can build up inside the enclosed space, resulting in damage to the mucosal lining of the respiratory tract (Divincenti Jr et al., 2012, Rosenbaum et al., 2009) although this can take several days and should be avoided with a reasonable frequency of cage changing. Size of animals, stocking density and type of bedding material used will affect the amount of ammonia generated, amongst other factors. It is difficult to record temperature, relative humidity and ammonia levels within each individual cage so many facilities often only record room macroenvironment parameters. In a 17 day study without any change of bedding materials, ammonia, relative humidity and temperature levels were higher than that of the room although did not exceed permitted levels. There are minimal escape routes for particles floating within cage air (particle mass per unit air volume depends on the level of mouse activity and the type of bedding substrate) although the natural habitat of mice suggests they have adapted to long term exposure as they have evolved to build nests from large particles (Rosenbaum et al., 2010).

Internal oxygen levels decreased from 21 to 20.5% in cages after one week with mice inside, resulting in an induced, chronic low grade hypoxia (increased levels of erythrocytes, haematocrit and haemoglobin concentration), similar to physiological changes which occur in humans at altitude or inside pressured spaces such as submarines. This coincided with an altered response to LPS injection compared to control mice housed elsewhere (York et al., 2012). Other physiological changes have been reported by David et al. (2013) where mice

suffered from chronic cold stress resulting in reduced levels of brown adipose tissue and variations in the growth of experimentally induced tumours.

Living in an IVC appears to affect the performance of mice in behavioural experiments involving tests such as the plus maze, open field, social interactions and startle response (Logge et al., 2013, Logge et al., 2014) and their use can therefore bias ongoing studies or complicate replication (Mineur and Crusio, 2009). Oliva et al. (2010) found that mice housed in ventilated cages were more aggressive and a concurrent alteration in olfactory bulb anatomy suggested that environmental changes had affected sensory input, resulting in variations in neural output. Evaluation of the reproductive performance of mice in IVCs revealed higher coefficients of variation compared to breeders housed in ventilated cabinets or open-top cages and it was proposed that breeding colonies took longer to adapt to the IVC environment than the alternative systems (Tsai et al., 2003).

3.1.6 Wheel running activity of mice

Wheel running activity has been recorded in wild, laboratory and domestic species.

A highly plastic behaviour, influenced by inherent and environmental factors, it is perceived by animals as important as it occupies a lot of the time budget (Sherwin, 1998). When mice are presented with wheels they learn to run on them rapidly, within 30 minutes (Festing and Greenwood, 1976). Wheel running studies have revealed clear differences in circadian rhythms between different strains of mice (Festing, 1977, Possidente and Stephan, 1988, Vitaterna et al., 1994, Ebihara et al., 1978). The size and shape of the wheel also has an effect with larger diameter, smooth running surfaces preferred (Banjanin and Mrosovsky, 2000).

Cardiac phenotyping studies have generated data characterising the wheel running activity of mice. Mice provided with wheels exhibit changes typical of endurance exercise; reduced body mass, increased muscle bulk and cardiac hypertrophy, with accompanying biochemical changes in myocytes (all of which are more pronounced in females than males) and increases in haematocrit and haemoglobin levels (Konhilas et al., 2004, Swallow et al., 2005, Allen et al., 2001, De Bono et al., 2006). Energy expenditure increases, resulting in a rise in food consumption (Swallow et al., 2001). Wheel running mimics normal behaviour in that it occurs mostly during darkness and appears to be a heritable trait as selective breeding for “high runner” mice resulted in a doubling of running activity after only 14 generations (Swallow et al., 2005). Total activity over 24 hours ranged between distances of 4 - 6.8 kilometres, concentrated over a 3 - 4.3 hour timeframe shortly after lights-off (Allen et al., 2001, Lapvetelainen et al., 1997). Running activity is intermittent, with short, frequent bouts of activity and mice increase the total distance covered over time by increasing their speed, not number of wheel revolutions (Girard et al., 2001, Swallow et al., 2005). Running bout durations have been described; maximum of 135 seconds, mean less than 60 seconds in *Mus domesticus* (Girard et al., 2001), and mean of 150 seconds in C57BL/6 mice (De Bono et al., 2006). Eikelboom et al. (2001) suggest that very short intervals (such as 5 seconds) should be used to evaluate wheel running activity as wheel revolution count does not equal mouse speed if the natural running bout duration is less than the bin size. Videotracking during short periods of maximal activity also showed that mice get on and off, only running actively for about 50% of the time the wheel is moving (Girard et al., 2001) and coasting also occurs where mice ride the rotating wheel without running (Koteja et al., 1999, Drickamer and Evans, 1996). When cages are set up for recording, the animal should not live within the

wheel, it should be a discrete resource, additional to the living area or revolutions will be counted wrongly as other non-locomotor behaviours are performed (Sherwin, 1998).

3.2 Methods

The general principle for this experiment was to investigate the effect of housing mice in individually ventilated cages (IVCs) on their daily locomotor activity rhythm. It was hypothesised that the vertical cage position (relative to overhead light sources) within an individually ventilated cage rack will affect the voluntary wheel running activity of singly-housed mice. Behavioural outputs such as the voluntary wheel running activity of rodents are commonly used in circadian research – using vertically-aligned wheels in conventional open-top cages while controlling the level of illuminance or light intensity across all animals. IVCs are sealed from the outside environment and the ambient temperature and relative humidity of the circulating air is controlled within narrow limits. However, the light intensity inside an IVC may vary, as it depends upon room illumination and any filtering effect of the cage wall material. IVCs are docked on cage racks in vertical columns, therefore the light intensity within varies with distance from standard overhead sources in rodent stock rooms. Cages placed higher on the rack should receive more light than those placed closer to the floor.

Under the Animals (Scientific Procedures) Act 1986, The Code of Practice for the Housing and Care of Animals used in Scientific Procedures recommends that light intensity should not exceed 350-400 lux at bench level and albino animals in particular are to be protected from high levels which may cause retinal damage (Clough, 1982, Grimm and Remé, 2013, Montalbán-Soler et al., 2012). Conversely, low levels of illuminance, or shortened photoperiods may result in poor fertility rates in breeding colonies (Amaral et al., 2014, Endo and Watanabe, 1989). The intensity, wavelength and duration of light all affect

circadian rhythms and the effect of housing mice in IVCs is of interest to both the circadian community and others using the mouse as a research model.

3.2.1 General methods

Age and sex- matched inbred strain mice (male, 8 week old, C57BL/6) were sourced from a commercial supplier (Harlan, UK) and maintained within IVCs fitted with running wheels to allow recording of activity rhythms over several days at different rack positions. Mice were given *ad-libitum* access to food (RM3(E) irradiated diet, SDS) and chlorinated water (2 x Istachlor Rapid chlorine tablets 0.35mg in 50 litres) and singly-housed to control for the effects of social interactions on locomotor activity. Relative humidity within cages varied between 45 and 52 % and temperature between 19 and 21.4°C and internal air change frequency was 12-15 times per hour. The ambient light cycle in the colony room was set at 11 hours full intensity light, 11 hours darkness and one hour dawn and dusk phases where the light intensity gradually brightened or dimmed respectively, at each end of the day (Figure 3.3).

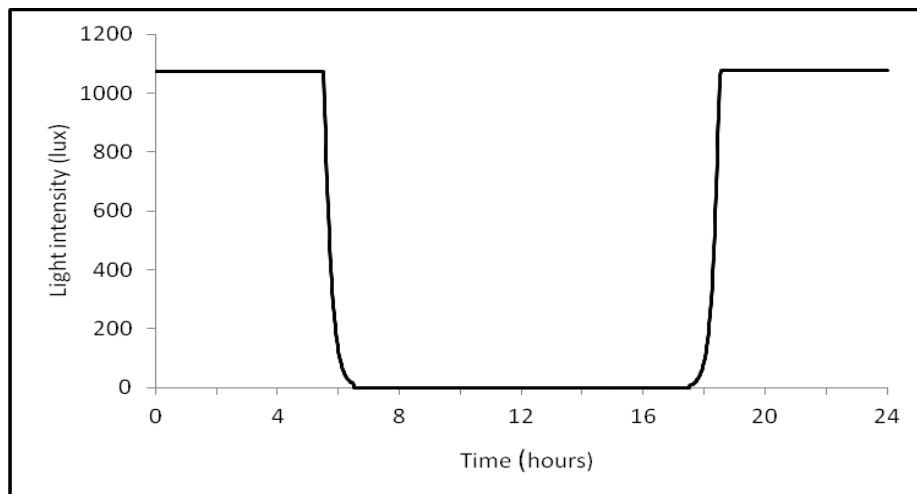


Figure 3.3 Light intensity within the colony room, measured using a TR-74Ui Illuminance UV Recorder placed on top of the cage rack for 24 hours (note that light intensity is >1000 lux at this position).

3.2.2 Husbandry and care of mice

The typical duration of an experiment was 40 days and care was taken to minimise potential stressors which might affect natural activity rhythms. The mice were handled as little as possible- visual checks were made through the transparent cage wall daily (only removing the cage from its dock if necessary) with the cage being opened briefly approximately every three days to refresh the food supply. The substrate bedding was not changed throughout the experiment, as single mice were maintained in cages which typically house 6-8 adults and require weekly changing this did not seem to result in obviously soiled bedding or adverse effects upon welfare. Other mice housed adjacent were changed weekly and as the movement of multiple cages on and off the rack results in vibration and noise, the activity data for these days was disregarded.

3.2.3 Adaptation of IVCs to include a running wheel

Mice were housed within Green Line Seal-Safe IVCs (Tecniplast, Italy).



Figure 3.4 Example of a Seal-Safe Green Line IVC rack and two views of an individually ventilated cage showing water bottle and food hopper *in-situ* (from <http://www.tecniplast.it/us/product/green-line-ivc-sealsafe-plus-mouse.html>)

Vertical space is limited in the Green Line cages compared to other models - an overhead food hopper is present at the back of the cage (adjacent to the air inlet/outlet) and a central water bottle port occupies the front half of the cage. The food hopper was removed to accommodate a fast-trac running wheel mounted on top of a mouse igloo (Lillico, U.K). Food was then provided on the cage floor in a small stainless steel bowl. Shredded cardboard nesting material (*Sizzlenest*, Datesand) was added to allow the mice to build nests within the Igloo.

The Igloo base of the running wheel was fixed to the cage floor using a custom-made grooved Perspex base plate (Mechanical Workshop, Department of Physics, University of Oxford). This base plate was secured using double-sided adhesive tape as drilling holes in an IVC would compromise its air-tight seal. The plate was positioned so that the perimeter of the fast-trac wheel passed as close as possible to the left-hand side cage wall (when viewed from above) without contact (3-5mm gap). A small circular (3x2mm) neodymium magnet (Maplin U.K.) was glued to the wheel perimeter using a two-part mixable epoxy resin adhesive (Homebase, U.K.).

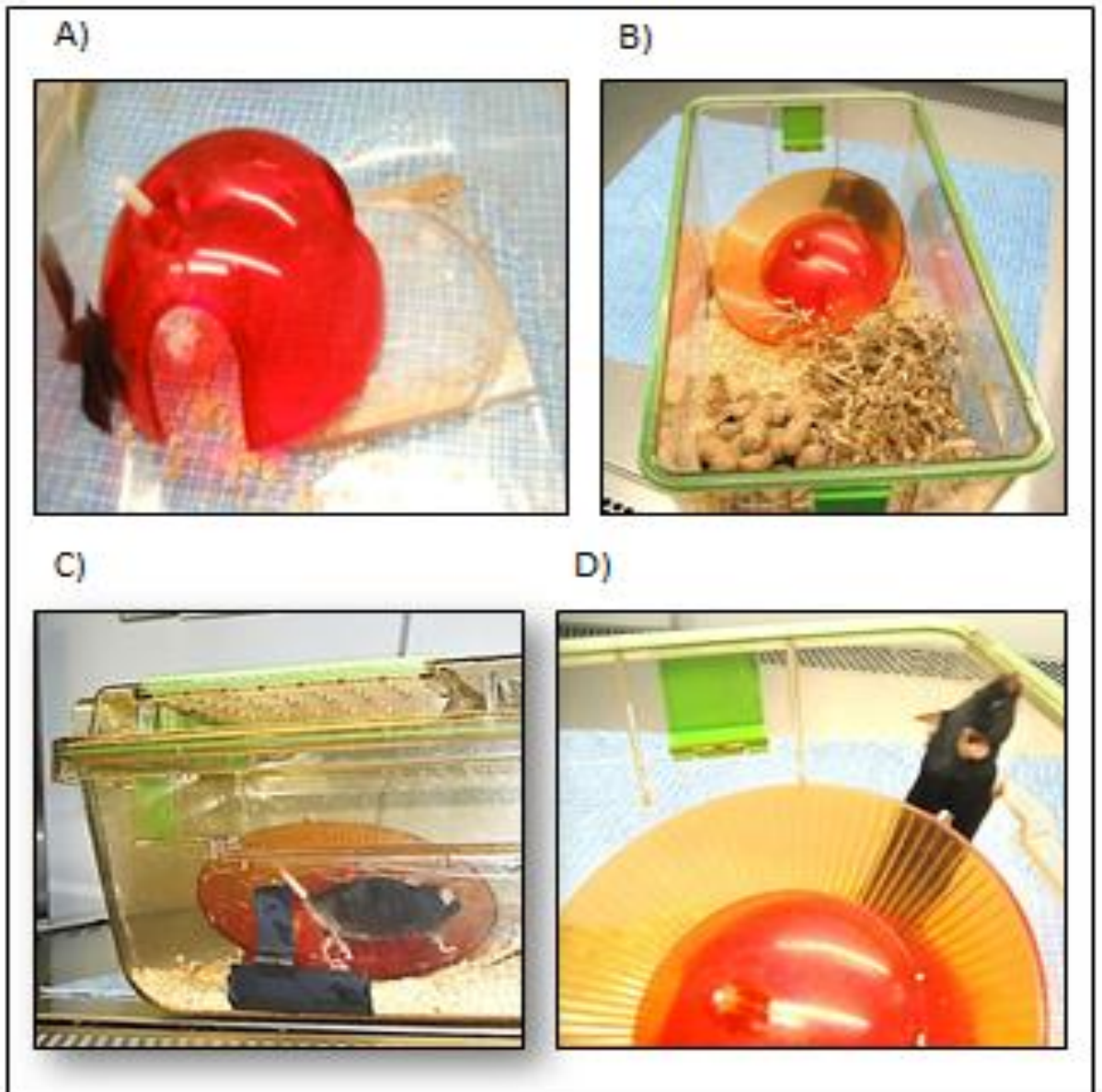


Figure 3.5 The base plate and mouse Igloo with axle for the fast-trac wheel (A), the cage set up ready for recording with food bowl placed at the front (B), mouse running on the wheel (C) and neodymium magnet attached to the wheel perimeter (D).

2.2.4 Experimental design and scheduling

Two Tecniplast Green Line Seal-Safe cage racks were present in the colony room, on which 160 cages can be docked in two formations of 8 x 10 cages either side of the central air

handling unit. The asymmetric position of overhead strip lights relative to the racks meant that illumination was not constant across each row of the racks. The presence of an animal transfer station with an inbuilt light source in one corner of the room also meant that illuminance of cages docked nearby increased during changeovers or when minor procedures were taking place (multiple times daily). Therefore, experimental mice were placed on the half rack farthest away from the transfer station. The light levels within top, middle and bottom rows of this rack were checked using a lux meter placed on the cage floor with the lid closed, range between 52 and 657 lux. The door to the colony room contained a viewing window which was covered with a red filter so light from the adjacent corridor did not get through.

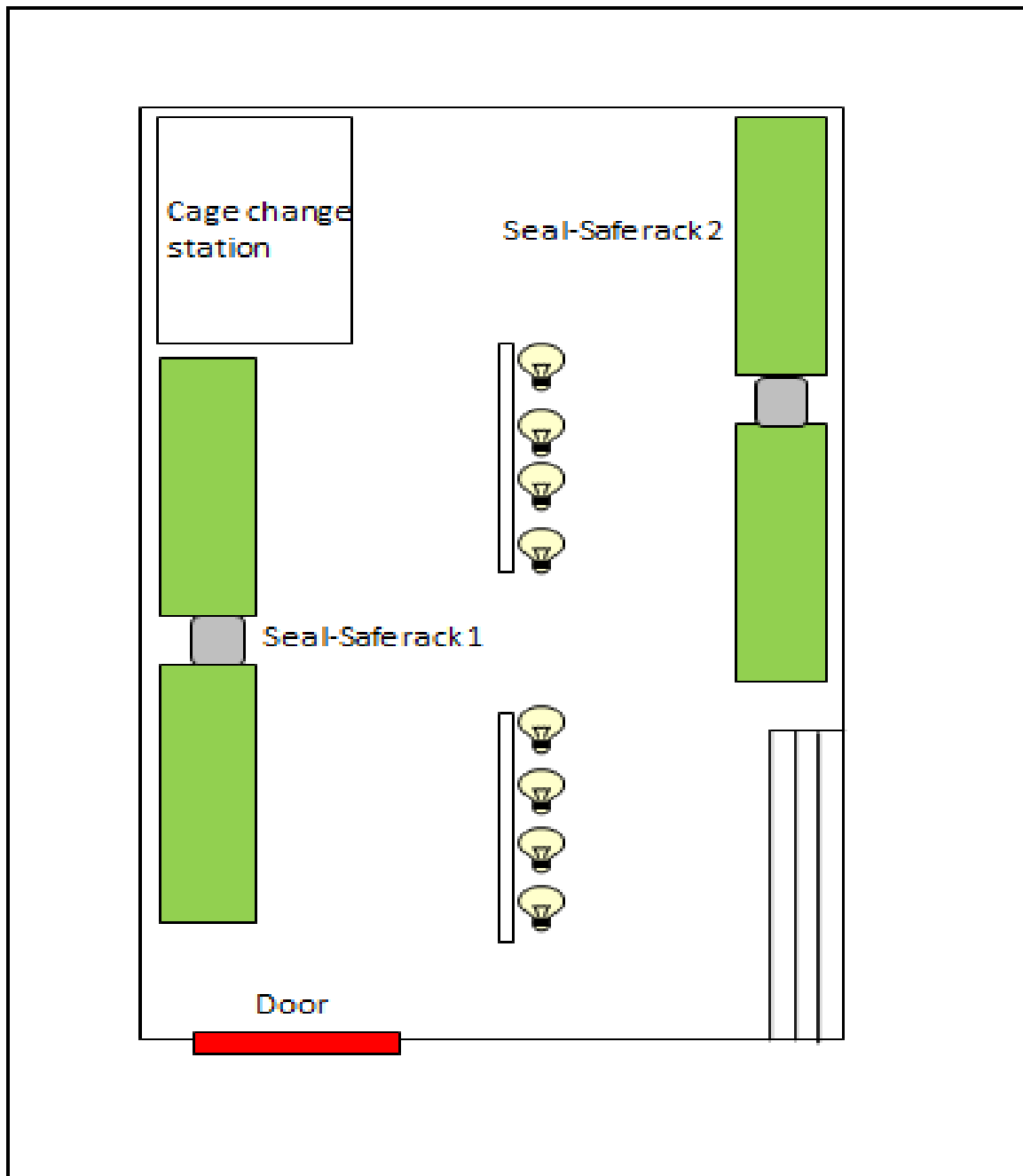


Figure 3.6 Plan of the colony room, including overhead light sources.

Columns 3 and 4 (from the end nearest the door) were chosen as they aligned approximately with the middle of the overhead strip light and their lux measurements across Rows 1, 6 and 10 (where row 1 is at the top) were the most comparable, enabling two mice to be recorded from simultaneously per vertical position.

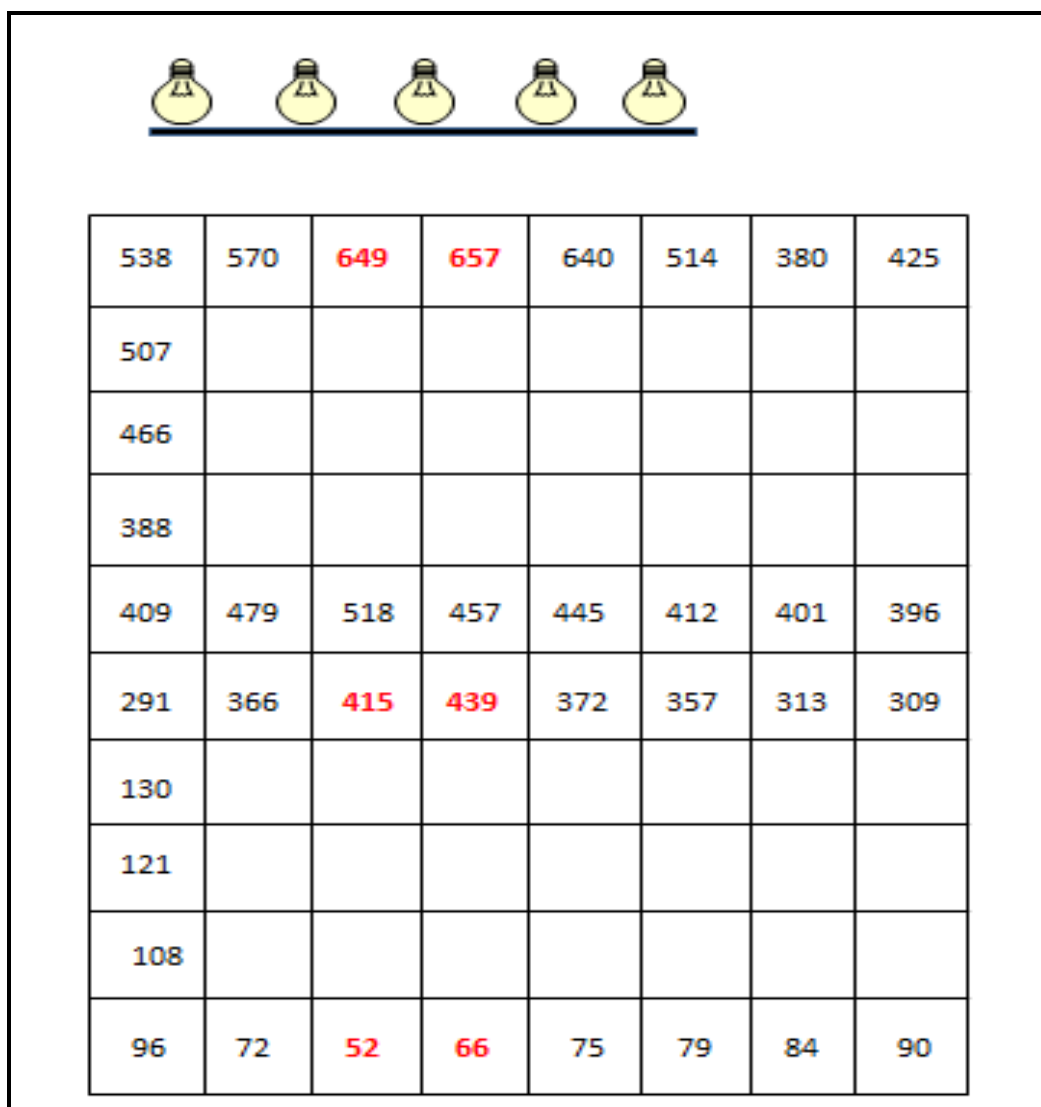


Figure 3.7 Representation of cage rack with selected experimental cages marked in red; internal light intensity (lux) marked for several cages at the top, middle, bottom and edge of rack.

There were six possible orders of rotation through rows 1 (top), 6 (middle) and 10 (bottom) as shown;

Table 3.1 Rotation patterns through top, middle and bottom cage positions on the rack.

1st position	2nd position	3rd position
Top	Middle	Bottom
Top	Bottom	Middle
Middle	Top	Bottom
Middle	Bottom	Top
Bottom	Middle	Top
Bottom	Top	Middle

A minimum of six mice were required to complete each rotation to control for increasing body size due to growth, improved fitness/propensity to run and any effect of being housed at a previous rack position. This number was increased threefold to allow for individual variation, total 18 mice, 3 per rotational order, 6 per batch (2 at the top, 2 in the middle, 2 at the bottom).

Mice were acclimatised to being singly housed for at least one week after arrival, with the Igloo, base plate and food bowl present in each cage. Running wheels were then introduced and activity counts monitored until a visually steady state was reached across all participants in an experimental batch (approximately 7 days) in the starting position. Activity was then continuously recorded for several days in different rack positions in a counterbalanced sequence as above. Each mouse spent at least 10 days in each rack

position, maximum 15 days. Variable length continuous datasets were produced for each mouse at each position, between 5 and 12 days as mice occasionally dislodged the wheels from the base plates or removed the magnets from the wheel perimeters.

Table 3.2 Summary table of mice showing order of rotation through rack (indicated vertically) and number of days analysed for each position. 22 mice ran overall as some datasets had to be discarded due to an insufficient number of days recorded.

Mouse	Position	Days analysed	Mouse	Position	Days analysed	Mouse	Position	Days analysed
3	TOP	11	6	MID	7	9	BOT	8
	MID	10		TOP	5		TOP	8
	BOT	12		BOT	5		MID	8
20	TOP	6	8	MID	8	12	BOT	8
	BOT	5		BOT	8		MID	8
	MID	5		TOP	5		TOP	8
7	TOP	8	17	MID	7	19	BOT	8
	MID	8		TOP	6		TOP	11
	BOT	8		BOT	9		MID	10
18	TOP	10	1	MID	8	21	BOT	8
	BOT	9		BOT	8		MID	6
	MID	10		TOP	12		TOP	6
14	TOP	12	22	MID	8	13	BOT	11
	MID	9		TOP	11		TOP	12
	BOT	9		BOT	9		MID	9
11	TOP	8	15	MID	11	16	BOT	5
	BOT	6		BOT	8		MID	12
	MID	8		TOP	9		TOP	5

3.2.5 Recording the activity data

Six reed switch relay cables were made by soldering twin core cables to reed switches (Electronics Workshop, Department of Physics, University of Oxford) and attached to the outside of the left hand side cage wall. Each time the wheel perimeter magnet passed the switch closed, resulting in one activity count per wheel revolution. The micro reed switches (Maplin, UK) were supported by a small piece of printed circuit board and aligned with the

wheel arc using a small suction cup and secured using electrical tape- enabling detachment each time it was necessary to take a cage off the rack. The cable lengths were tidied using cable ties and secured to the rear surface of the cage rack, ensuring that movement of all cages on and off the rack was not impeded.



Figure 3.8 Two views of the cage docked on the rack, showing suction cup and reed switch and cables.

The six relay cables were wired using block connectors (RS Components) into a plastic junction box (see Figure 3.9) which was secured onto the top of the cage rack. A light dependant resistor (LDR) (RS Components UK) on the surface of the box recorded the light cycle within the room to ensure that the centrally-programmed light cycle did not change due to timing errors or inadvertent use of an emergency override switch.

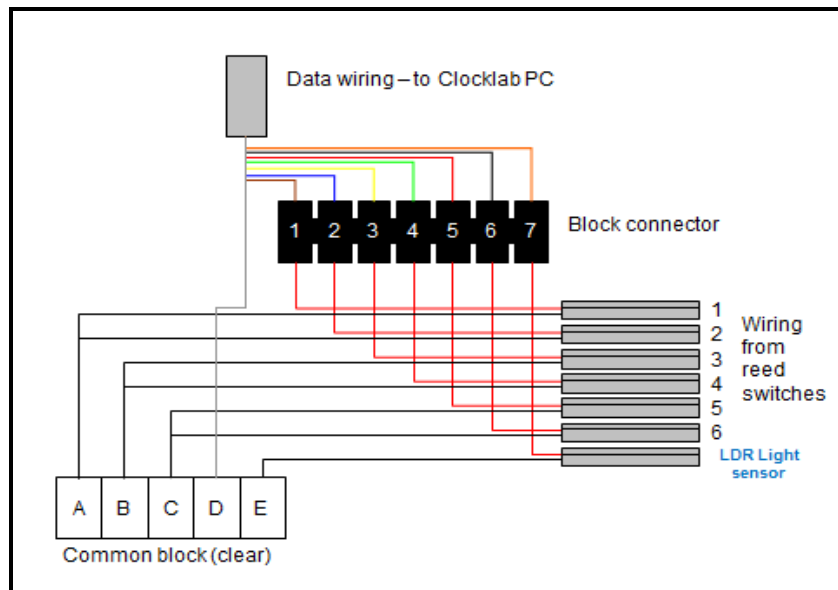


Figure 3.9 Detail of how the reed switch relays were wired inside the junction box.

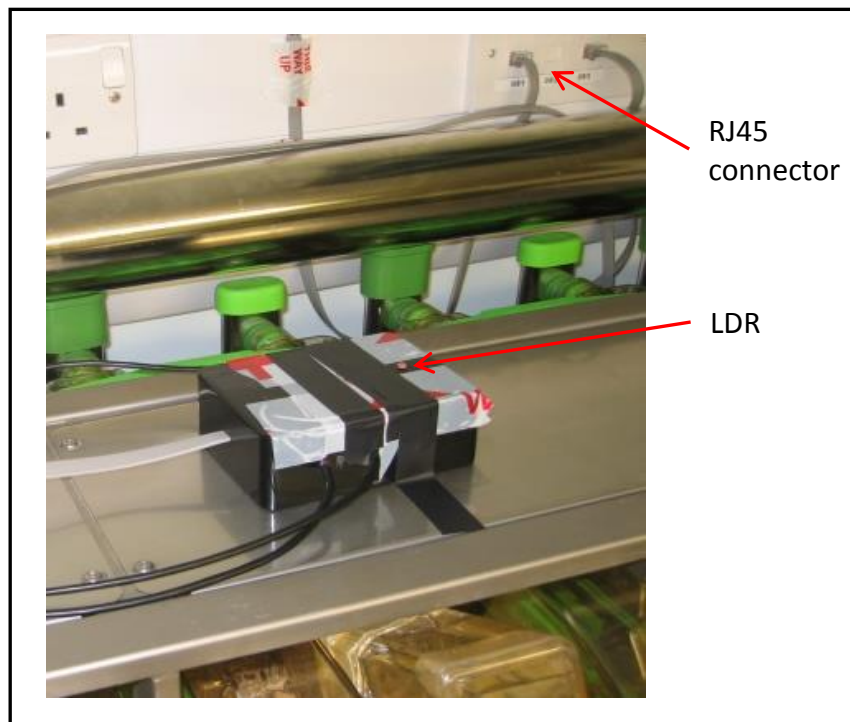


Figure 3.10 Junction box on top of cage rack containing reed relays cables wired through common blocks- reed relay cables (black), ethernet cable (grey), LDR and RJ45 connector visible.

The junction box was then connected via an RJ 45 ethernet-style connector to wiring (already present) in cable trunking at the wall/ceiling junction which linked through to a Clocklab system (Actimetrics, Wilmette, Illinois) set up in an adjacent room. Clocklab is an established circadian biology data collection and analysis package which allows simultaneous light cycle and activity recording through various types of motion sensors. Clocklab can record up to 448 activity channels via multiple 56-channel USB computer interfaces and runs under the Windows XP/7/8 operating system. The primary activity data output is an actogram which can be viewed real-time or downloaded for data extraction into a spreadsheet form using the Clocklab Analysis Toolbox for Matlab (Mathworks, Natick, Massachusetts). Activity data updated hourly onto the hard drive of the Clocklab computer and was then saved onto memory sticks at various points during the experiment for each batch of mice. This prevented data loss should the Clocklab computer crash for any reason (an external uninterruptable power supply was also used to prevent loss in the event of interruptions to mains electricity).

3.2.6 Processing the activity data

The Clocklab Toolbox was used within Matlab R2012A to produce the following outputs;

- 1) **Activity Profiles** - display average activity as a function of time (show average of activity counts per unit time over a pre-selected number of days)
- 2) **Timeseries** - display activity as a continuous function of time (show actual activity counts per unit time across the whole recording period)
- 3) **Actograms** – display activity as vertical bars within a 24 hour timeframe (show successive days vertically aligned below the first day, allowing easy identification of patterns in activity)

These data files were initially viewed as Matlab figures, which were then exported directly as jpeg (.jpg) files or extracted in a spreadsheet form and opened using Microsoft Excel.

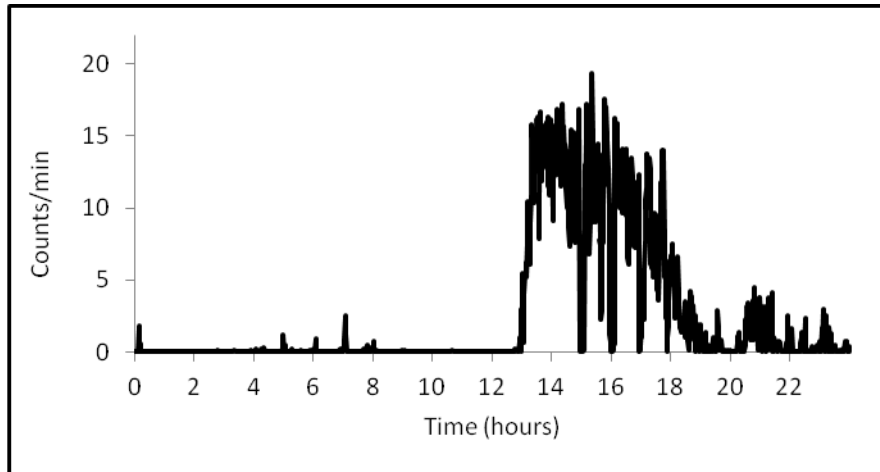


Figure 3.11 Example of an Activity Profile output plotted from downloaded data where 0 hours is the start of the light phase (ZT 0) and 13 hours is the start of the dark phase (ZT 13).

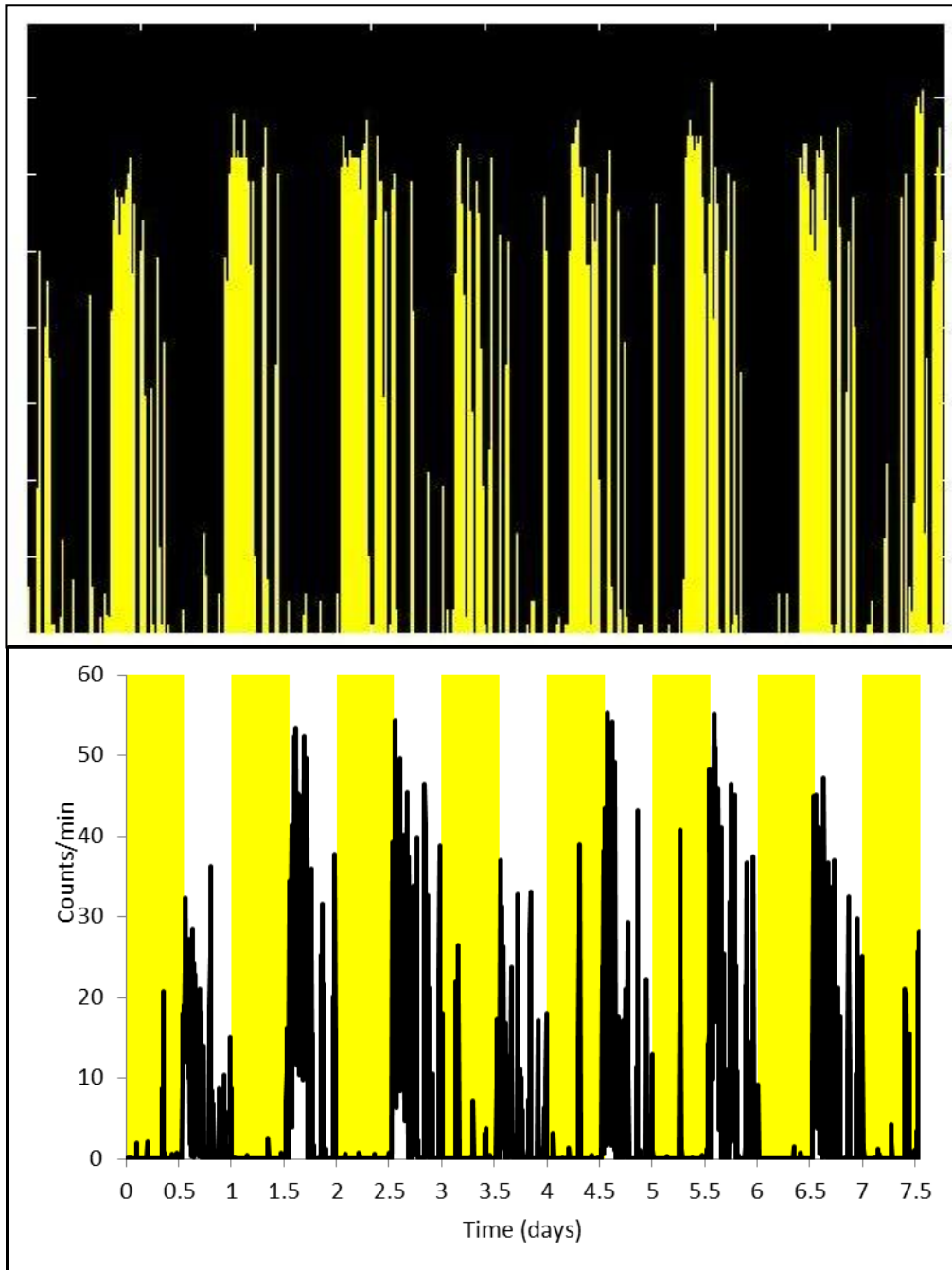


Figure 3.12 Example of a Timeseries output as a Matlab figure and plotted from downloaded data (light cycle indicated as yellow bars).

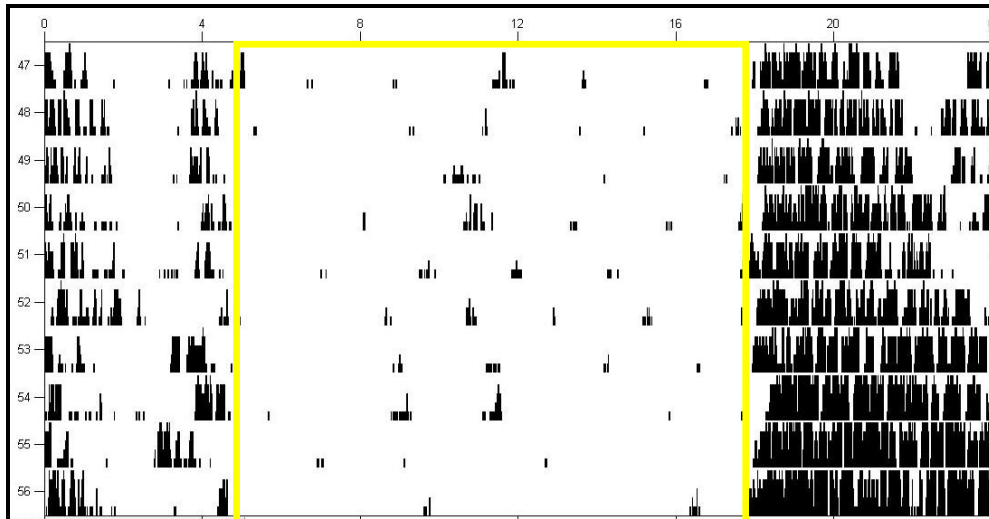


Figure 3.13 Example of an actogram output as a Matlab figure, time shown on the horizontal axis, starting and ending at midnight (0.00 hours). Successive days activity on the vertical axis (from day 47 to day 56), light (*rho*) phase from 05.00- 18.00 hours indicated in yellow.

Activity profile data can be extracted in a form where the light phase/*rho* counts and dark phase/*alpha* counts are displayed separately, by selecting the light onset and offset times within the Clocklab Toolbox. The standard error of the mean activity is also pre-calculated, enabling easy plotting of a line graph to view the average daily activity.

However, the automated division of the average activity into *alpha/rho* counts was found to be unreliable when cross-checked against the Timeseries data so the activity profile output was disregarded. The Timeseries data for each mouse in each rack position was extracted in one minute time bins (the smallest possible) for the greatest accuracy.

Timeseries data was processed by first separating it into *rho* and *alpha* counts to find activity values based on time/light status criteria from the raw data worksheet. For the *rho* phase, activity counts between 05.04-18.03 hours (or 06.04-19.03 hours depending on the date in relation to British daylight saving time) and for the *alpha* phase, activity counts between 18.04- 05.03 hours (or 19.04- 06.03 hours) were extracted- corresponding with

alpha being any time that illuminance levels were greater than zero lux, measured using a TR-74Ui Illuminance UV Recorder (T and D Corporation, sourced from LS Technology, Poole, Dorset, U.K.).

The average activity in counts per minute during an *alpha* or *rho* period across several days was then calculated and binned into hourly values. The average hourly values for each mouse at each rack position were tabulated and plotted as line graphs.

There were considerable differences in the peak activity (counts/minute) between mice (see Figure 3.14). Activity counts for each mouse at each rack position were therefore normalised as a percentage of that mouse's maximum counts across all three rack positions. This avoided mice which run further in absolute counts, introducing bias to the mean activity value per rack position (when activity counts for all mice at that position were combined) as the relative change in counts per mouse between top, middle and bottom rack positions can then be established. This normalisation does not result in any visible change to the proportions of the counts at the 3 different rack positions (see Figure 3.15).

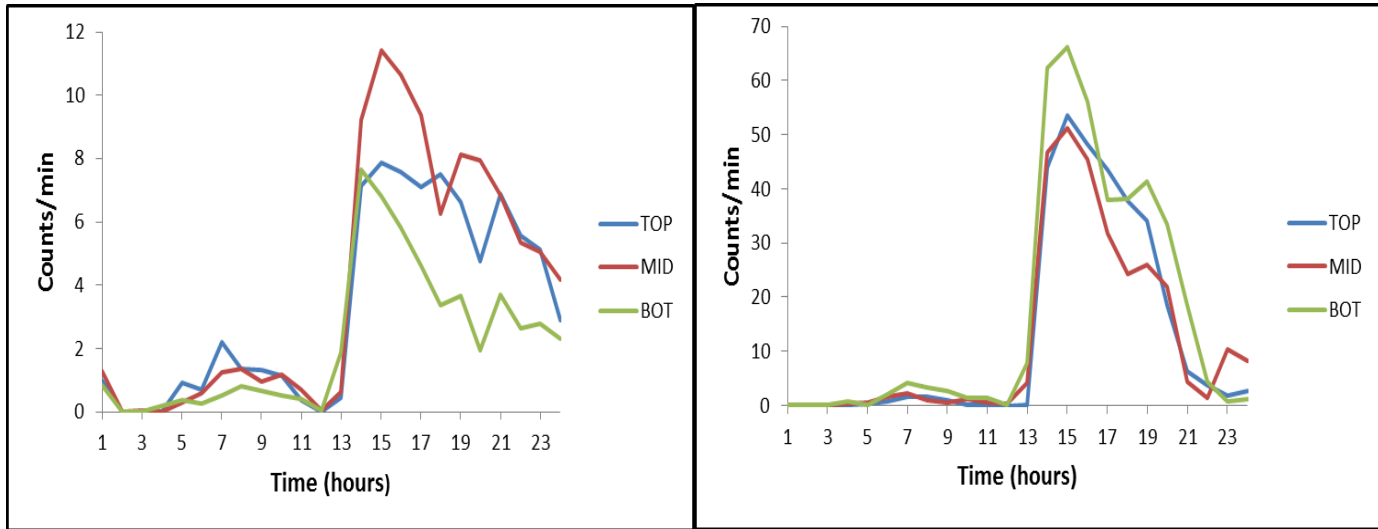


Figure 3.14 Hourly average activity plots for 2 mice, Mouse 17 (left) and Mouse 15 (right) across all 3 rack positions-plotted using raw data values (absolute counts/min). Time = 13 hours corresponds with the beginning of the dark phase. The maximum across all three positions is 11.41 counts/min for Mouse 17 and 66.17 counts/min for Mouse 15.

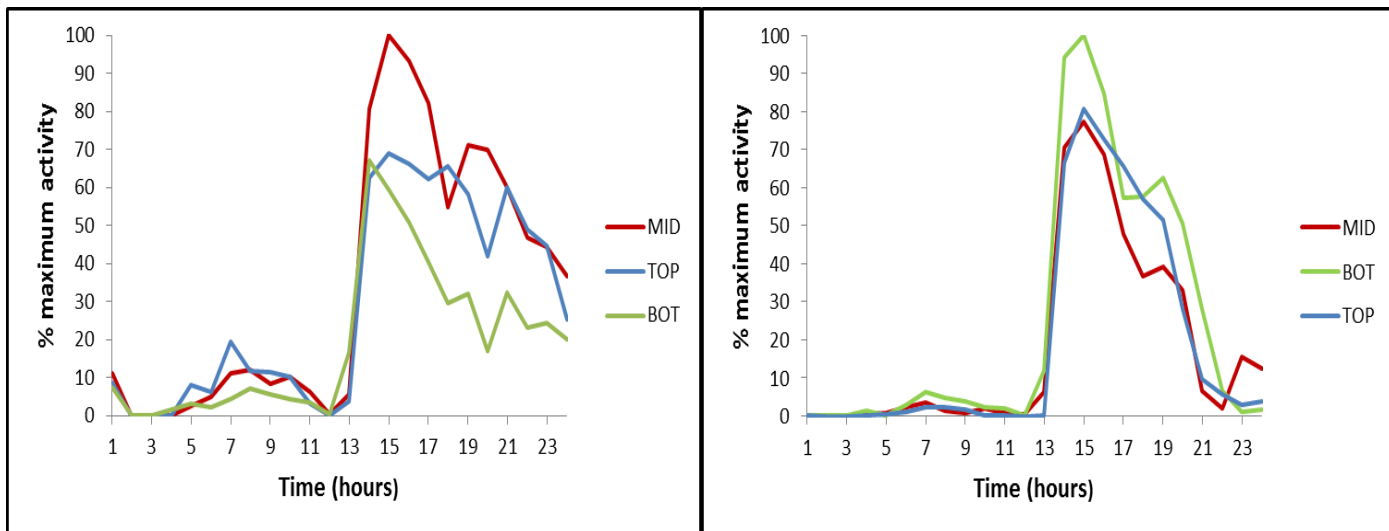


Figure 3.15 Hourly average activity plots for 2 mice, Mouse 17 (left) and Mouse 15 (right) across all 3 rack positions-plotted using activity counts data normalised as a percentage of the maximum across all 3 positions. Time= 13 hours corresponds with the beginning of the dark phase.

As mice are nocturnal and commence running just before the onset of darkness, it is likely that there is a threshold light intensity at which activity commences. Activity counts during the light to dark transition were further examined by binning data every 10 minutes during the hour before and the hour after lights off (Time= 12 – 14 hours). This data was also plotted as line graphs in both raw (absolute counts) and normalised (as a percentage of maximum counts across all three positions during this two hour timeframe) forms.

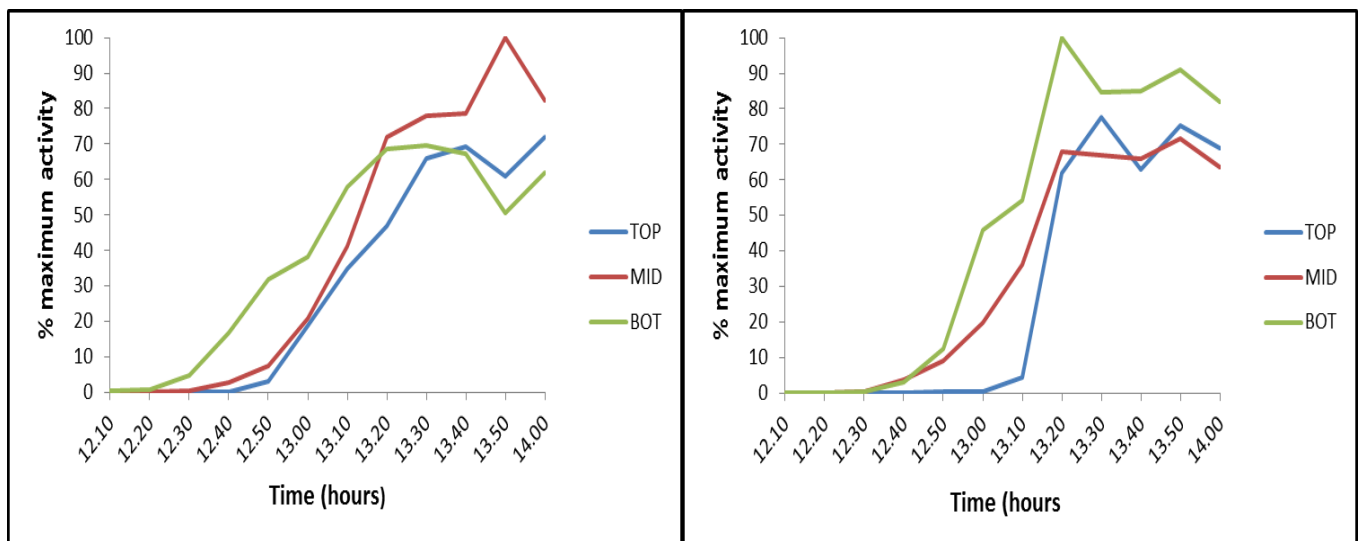


Figure 3.16 Ten minute average activity plots for 2 mice, Mouse 17 (A) and Mouse 15 (B) across all 3 rack positions during the light/dark transition-plotted using activity counts data normalised as a percentage of the maximum across all 3 positions (during the timeframe 12 - 14 hours).

Actograms for each mouse at each rack position (54 in total) were downloaded as a jpeg (.jpg) files and then saved onto Microsoft Powerpoint slides for inspection. Each actogram was checked to make sure that activity counts had been recorded each day; any “empty” or partially empty days where data were lost due to a fault in the recording set up (igloo dislodged from baseplate or magnet removed from wheel) were then omitted from the Timeseries data set and average values calculated from the addition of the days before and after to make the datasets as long as possible.

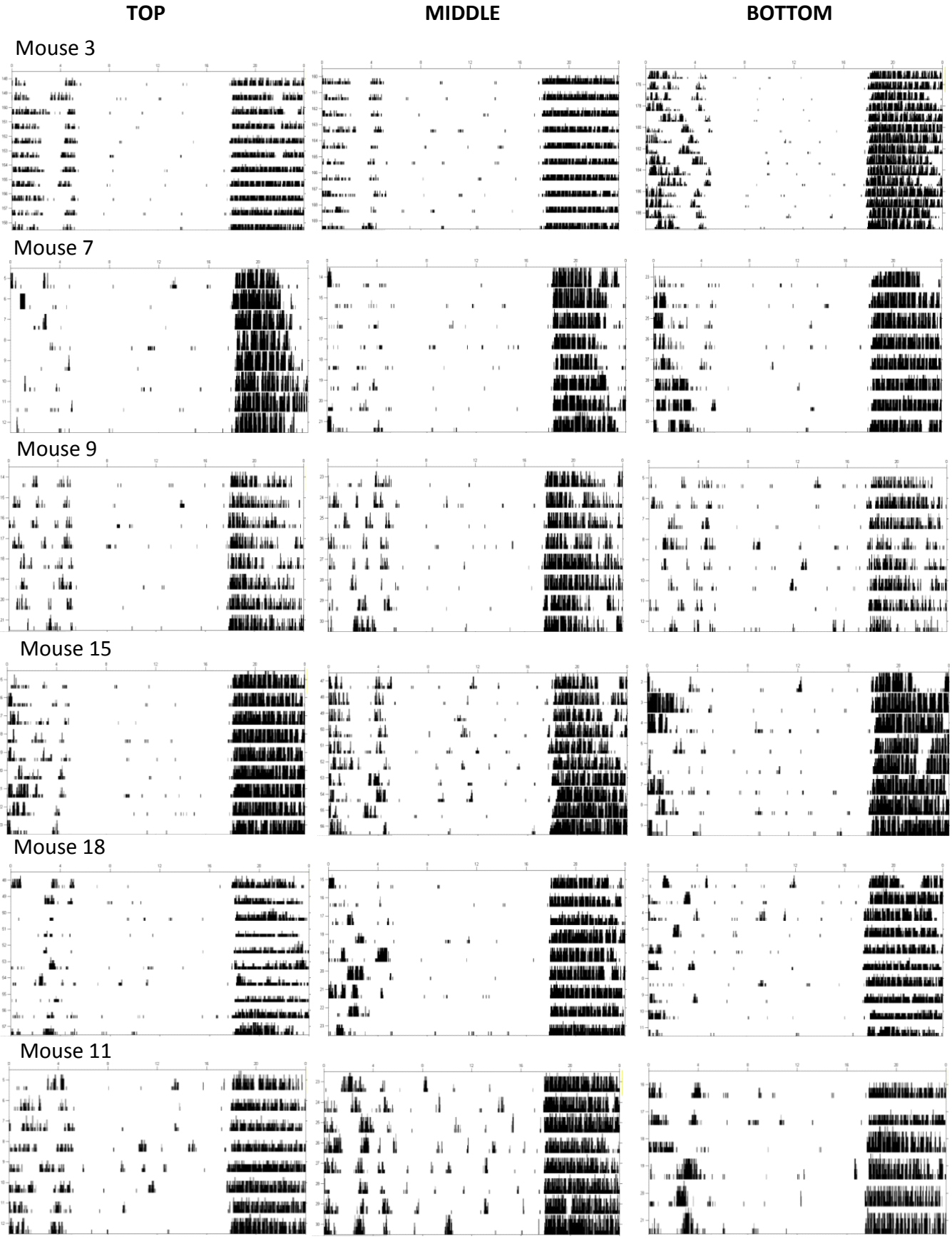


Figure 3.17 Actograms for 6 mice, from left to right, recordings from TOP, MIDDLE, BOTTOM

3.3 Statistical Analysis

Processed data from 18 mice were analysed using repeated measures ANOVA in IBM SPSS Statistics 22. As more than two experimental conditions were applied, the assumption of sphericity was checked using Mauchly's Test in SPSS. Sphericity exists when the variances of the differences between treatment levels (rack positions) are equal, indicated by a non-significant test statistic result ($p > 0.05$). When sphericity is violated, the degrees of freedom can be adjusted using the Greenhouse-Geisser or the Huynh-Feldt correction within SPSS (Field, 2009).

3.4 Results

In all plots of activity against time, Time= 0 hours is ZT 0, the beginning of the light phase, Time= 13 hours is ZT 13, the beginning of the dark phase and graphs are plotted for both raw and normalised data.

3.4.1 Average hourly activity across all rack positions

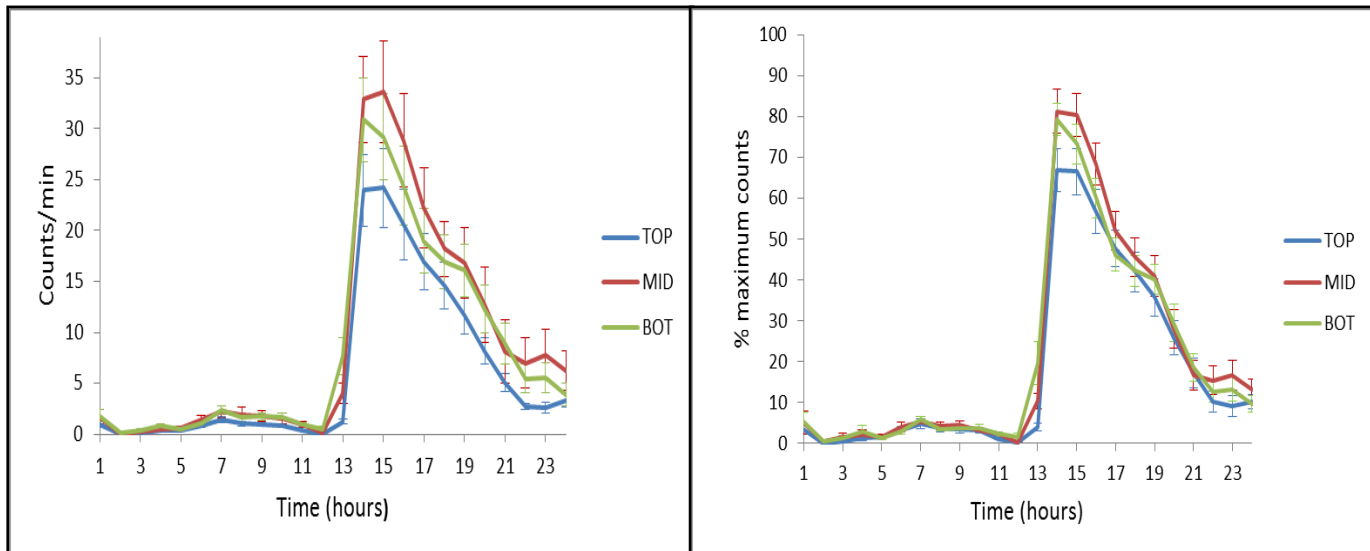


Figure 3.18 Average hourly counts of 18 mice across the three rack positions A) raw data B) data normalised as a percentage of maximum counts, with standard error of the mean (S.E.M).

The raw and normalised data plots show that almost all activity occurs during darkness and the acrophase or peak level of activity is attained quickly, with 1-2 hours of activity onset. Activity then subsides gradually towards light onset at time=24 or 0 hours (ZT 0). S.E.M. is larger for all activity recorded in the *alpha* phase, expected as activity approximates zero for the entire *rho* phase. In both plots the onset of activity at the light/dark transition appears to be synchronised but progresses most quickly for BOTTOM position mice and most slowly for TOP position mice.

3.4.2 Activity during the light phase

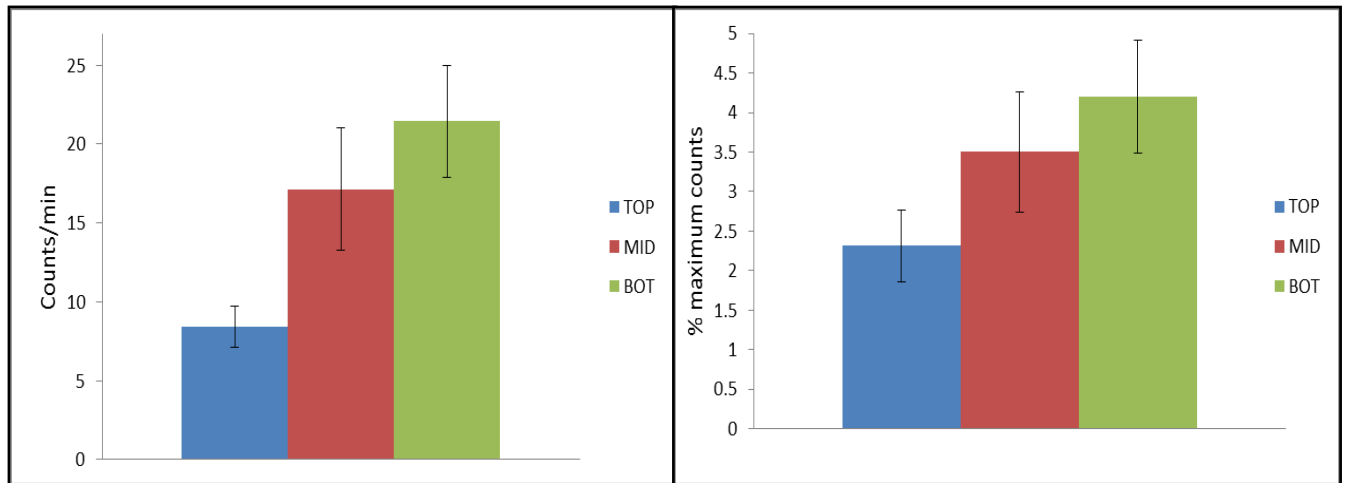


Figure 3.19 Average total activity during the light phase- raw data (left), normalised as a percentage of maximum data (right), with S.E.M.

Table 3.3 Mean light counts with standard deviation and standard error of the mean for three rack positions.

		Raw Data			Normalised Data		
Position	Number of mice	Mean counts	S.D.	S.E.M.	% Mean counts	S.D.	S.E.M.
TOP	18	8.413	5.626	1.326	2.318	1.929	0.455
MIDDLE	18	17.139	16.460	3.880	3.502	3.239	0.764
BOTTOM	18	21.451	15.059	3.549	4.201	3.040	0.717

Repeated Measures ANOVA;

Raw Data

Mauchly's statistic= 0.72 therefore sphericity assumed.

F (2, 34) = 8.27, p=0.001 (<0.05) therefore position has a significant effect on raw data activity counts during the light phase. Post-hoc contrasts between TOP, MIDDLE and BOTTOM positions with Bonferroni adjustment for multiple comparisons (p<0.05);

TOP vs. BOTTOM p=0.003, TOP vs. MIDDLE p=0.072, MIDDLE vs. BOTTOM p= 0.484 therefore light counts at the TOP are significantly different to those at the BOTTOM position (with no significant difference between TOP and MIDDLE or MIDDLE and BOTTOM).

Normalised data

Mauchly's statistic = 0.27 therefore sphericity assumed.

F (2, 34) = 4.31, p= 0.022 (<0.05) therefore position has a significant effect on normalised data activity counts during the light phase. Post-hoc contrasts between TOP, MIDDLE and BOTTOM with Bonferroni adjustment for multiple comparisons (p<0.05);

TOP vs. BOTTOM p=0.050, TOP vs. MIDDLE p=0.096, MIDDLE vs. BOTTOM p= 1.000 therefore normalised light counts at the TOP are significantly different to those at the BOTTOM position (with no significant difference between TOP and MIDDLE or MIDDLE and BOTTOM).

3.4.3 Activity during the dark phase

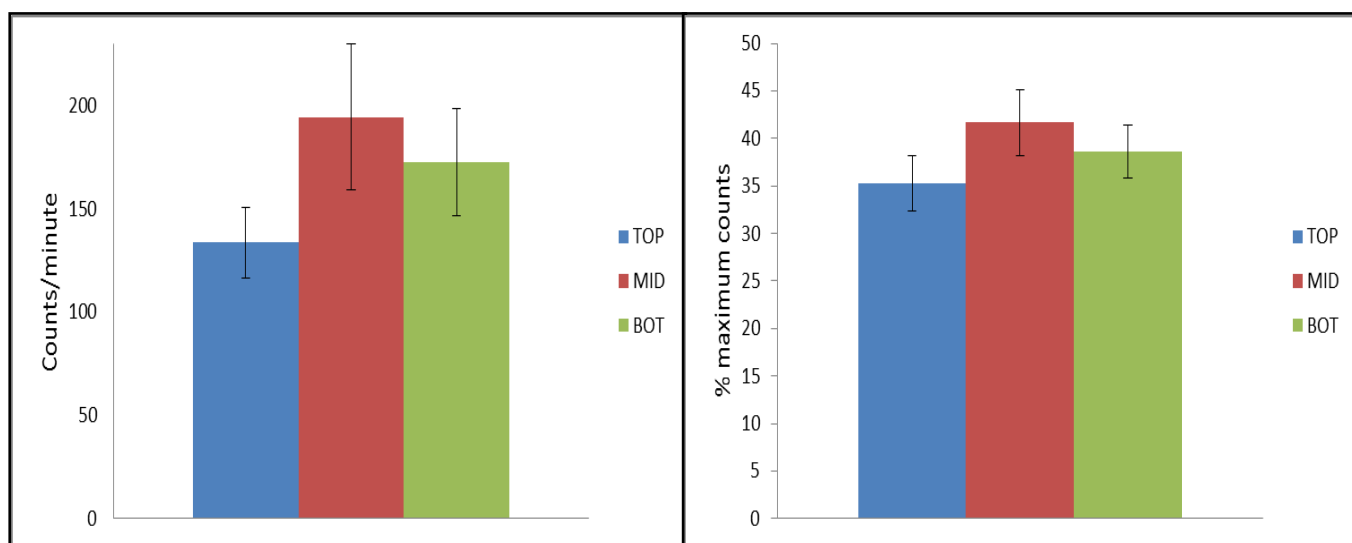


Figure 3.20 Average counts during the dark phase- raw data (left), normalised data (right), with S.E.M.

Table 3.4 Mean dark counts with S.D. and S.E.M. for mice at three rack positions.

Position	Number of mice	Raw data			Normalised data		
		Mean counts	S.D.	S.E.M.	% Mean counts	S.D.	S.E.M.
TOP	18	133.615	72.187	17.015	35.299	12.344	2.909
MIDDLE	18	194.371	149.599	35.261	41.693	14.754	3.488
BOTTOM	18	172.564	109.893	25.902	38.636		2.746

Repeated Measures ANOVA;

Raw Data

Mauchly's statistic= 0.07 therefore sphericity violated.

F (2, 34) = 2.25, p=0.124 (>0.05)

Greenhouse Geisser correction F (1.37, 23.32) = 2.225, p =0.143

Huynh Feldt correction F (1.45, 24.69) = 2.225, p=0.141

therefore position does not have a significant effect on raw data activity counts during the dark phase.

Normalised data

Mauchly's statistic = 0.184 therefore sphericity assumed.

F (2, 34) = 1.276, p= 0.292 (>0.05) therefore position does not have a significant effect on normalised data activity counts during the dark phase.

3.4.4 Activity during the light/ dark transition

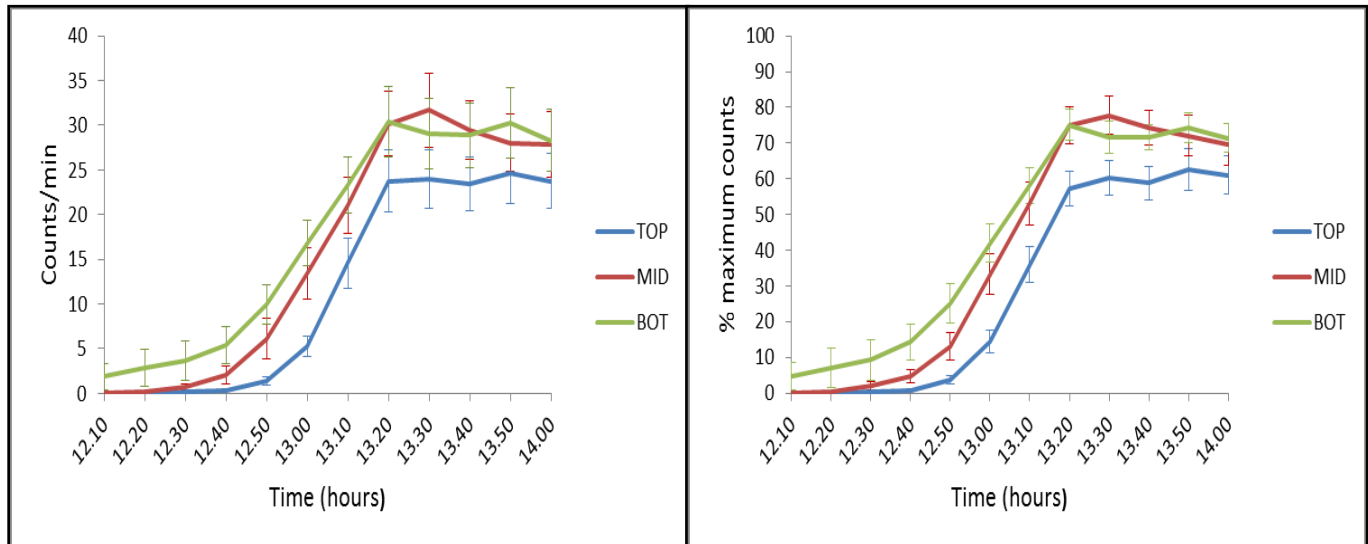


Figure 3.21 Average counts per 10 minutes at the light/dark transition (time= 12 – 14 hours) raw data (left), data normalised as a percentage of maximum counts (right) with S.E.M.

Expansion of the activity profiles in the two hours around the light/dark transition was achieved by binning the counts data every 10 minutes, instead of every hour. The advance in activity for BOTTOM position mice is clear, low levels of wheel running is already taking place at time= 12.00- 12.10 hours whereas mice at MIDDLE and TOP positions are resting. Mice across all positions seem to reach a plateau simultaneously (although this is lower for TOP position mice) and S.E.M. seems comparable throughout this 2 hour period and across TOP, MIDDLE and BOTTOM positions.

3.4.5 Activity during the hour before lights off (time = 12 -13 hours)

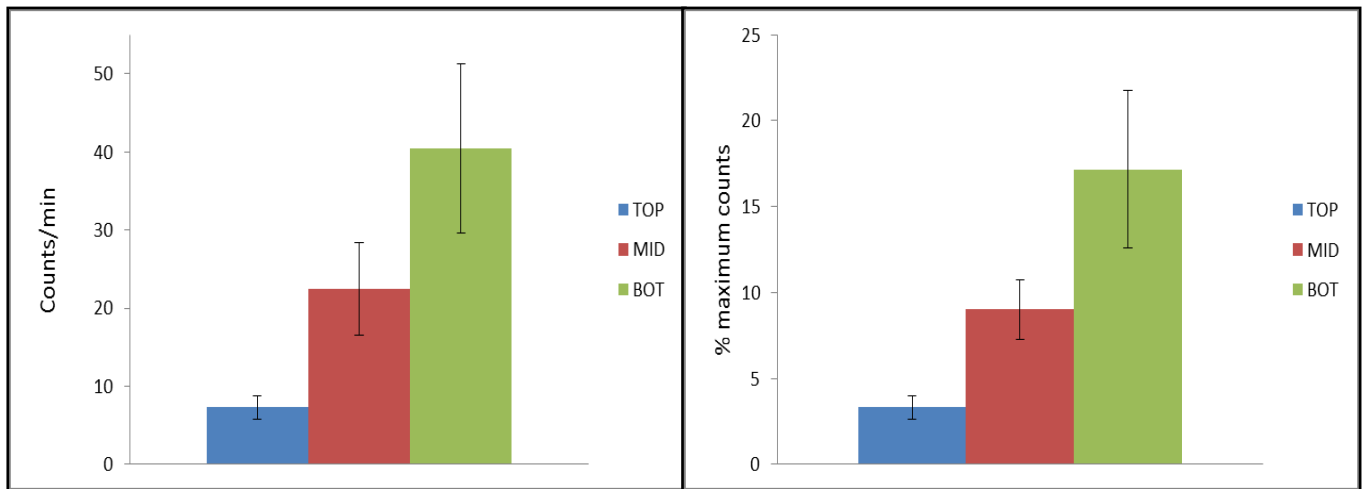


Figure 3.22 Average counts during the hour before lights off, raw data (left), data normalised as a percentage of maximum during the two hours (one hour before and one hour after) around the light dark transition (right).

Table 3.5 Mean counts during the hour before lights off, with S.D. and S.E.M. for mice at three rack positions.

Position	Number of mice	Raw data			Normalised data		
		Mean counts	S.D.	S.E.M.	% Mean counts	S.D.	S.E.M.
TOP	18	7.307	6.267	1.477	3.305	2.879	0.679
MIDDLE	18	22.476	25.308	5.965	9.015	7.293	1.719
BOTTOM	18	40.434	46.043	10.852	17.163	19.410	4.575

Repeated Measures ANOVA;

Raw Data

Mauchly's statistic= 0.03 therefore sphericity violated ($F(2, 34) = 6.33, p=0.00(<0.05)$)

Greenhouse Geisser correction $F(1.32, 22.43) = 6.33, p = 0.013$

Huynh Feldt correction $F(1.39, 23.58) = 6.33, p=0.022$

therefore position does have a significant effect on raw data activity counts during the hour before lights off. Post-hoc contrasts between TOP, MIDDLE and BOTTOM with Bonferroni adjustment for multiple comparisons, where $p < 0.05$ is significant;

TOP vs. BOTTOM $p=0.020$, TOP vs. MIDDLE $p=0.021$, MIDDLE vs. BOTTOM $p= 0.361$

therefore raw data counts at the TOP are significantly different to those at the MIDDLE and BOTTOM positions during the hour before lights off (with no significant difference between MIDDLE and BOTTOM).

Normalised data

Mauchly's statistic = 0.001 therefore sphericity violated.

($F(2, 34) = 6.713, p= 0.003 (<0.05)$)

Greenhouse Geisser correction $F(1.16, 19.74) = 6.713, p = 0.014$

Huynh Feldt correction $F(1.19, 20.29) = 6.713, p=0.014$

therefore position does have a significant effect on normalised data activity counts during the hour before lights off. Post-hoc contrasts between TOP, MIDDLE and BOTTOM with Bonferroni adjustment for multiple comparisons, where $p < 0.05$ is significant;

TOP vs. BOTTOM $p=0.022$, TOP vs. MIDDLE $p=0.004$, MIDDLE vs. BOTTOM $p= 0.270$

therefore normalised data counts at the TOP are significantly different to those at the MIDDLE and BOTTOM positions during the hour before lights off (with no significant difference between MIDDLE and BOTTOM).

3.4.6 Activity at lights off (Time = 13 hours)

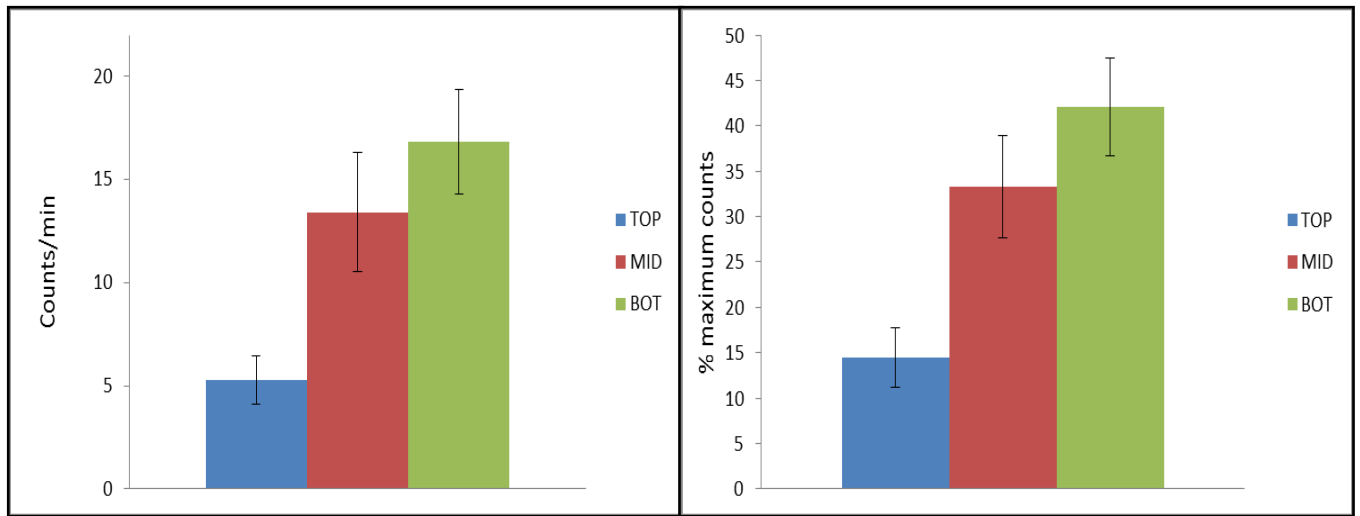


Figure 3.23 Average counts at the time of lights off, raw data (left), data normalised as a percentage of maximum during the two hours around the light dark transition (right).

Table 3.6 Mean counts at lights off with S.D. and S.E.M. for mice at three rack positions.

Position	Number of mice	Raw data			Normalised data		
		Mean counts	S.D.	S.E.M.	% Mean counts	S.D.	S.E.M.
TOP	18	5.284	4.932	1.163	14.498	13.959	3.290
MIDDLE	18	13.405	12.275	2.893	33.313	24.063	5.672
BOTTOM	18	16.817	10.745	2.532	42.053	22.925	5.403

Repeated measures ANOVA

Raw Data

Mauchly's statistic= 0.614 therefore sphericity assumed.

F (2, 34) =11.13, p<0.0005 (<0.05)

therefore position does have a significant effect on raw data activity counts at lights off.

Post-hoc contrasts between TOP, MIDDLE and BOTTOM with Bonferroni adjustment for multiple comparisons, where $p<0.05$ is significant;

TOP vs. BOTTOM $p=0.001$, TOP vs. MIDDLE $p=0.006$, MIDDLE vs. BOTTOM $p= 0.686$

therefore raw data counts at the TOP are significantly different to those at the MIDDLE and BOTTOM positions at the time of lights off (with no significant difference between the MIDDLE and BOTTOM).

Normalised data

Mauchly's statistic = 0.610 therefore sphericity assumed.

F (2, 34) = 13.65, p < 0.0005 (<0.05)

therefore position does have a significant effect on normalised data activity counts at lights off.

Post-hoc contrasts between TOP, MIDDLE and BOTTOM with Bonferroni adjustment for multiple comparisons, where $p < 0.05$ is significant;

TOP vs. BOTTOM $p=0.000$, TOP vs. MIDDLE $p=0.060$, MIDDLE vs. BOTTOM $p= 0.490$

therefore normalised data counts at the TOP are significantly different to those at the MIDDLE and BOTTOM positions at the time of lights off (with no significant difference between the MIDDLE and BOTTOM).

3.4.7 Summary of Results

Activity counts were variable within mice, so data was normalised as a percentage of maximum counts across all 3 positions. Sphericity, a test for homogeneity of variance was assessed in all datasets where Repeated Measures ANOVA was performed and results are shown in Table 3.7. For all instances where sphericity was violated, a correction of the degrees of freedom was performed.

Table 3.7 Summary table showing presence or absence of sphericity in the raw and normalised data for each statistical analysis

	Raw data	Normalised data
Activity during the light phase	sphericity assumed	sphericity assumed
Activity during the dark phase	sphericity violated	sphericity assumed
Activity during the hour before lights off	sphericity violated	sphericity violated
Activity at lights off	sphericity assumed	sphericity assumed

Rack position had a significant effect on the raw and normalised light counts, the raw and normalised counts in the hour before lights off and the raw and normalised counts at lights off, as calculated using Repeated Measures ANOVA. No effect was seen upon the raw or normalised dark counts.

Post hoc contrasts (with Bonferroni adjustment for multiple comparisons) of TOP versus MIDDLE versus BOTTOM showed that counts at the TOP were significantly different to those at the bottom during the light phase and to those at both the MIDDLE and the BOTTOM during the hour before the lights went off and at the time of lights off; these significant

differences were evident in both the raw and normalised data sets. There were no significant differences between the TOP and the MIDDLE, or the MIDDLE and the BOTTOM positions during the light phase and between the MIDDLE and the BOTTOM positions during the hour before lights off, or at the time of lights off. The average light intensities were 653, 427 and 59 lux at the TOP, MIDDLE and BOTTOM positions respectively.

Table 3.8 Summary of significant (SD) and non significant differences (NSD) between rack levels when post-hoc contrast tests were applied

	TOP vs. BOTTOM (653 vs. 59 lux)	Top vs. MIDDLE (653 vs. 427 lux)	MIDDLE vs. BOTTOM (427 vs. 59 lux)
During light phase	SD	NSD	NSD
Hour before lights off	SD	SD	NSD
At lights off	SD	SD	NSD

3.5 Discussion and Conclusion

The objective of this experiment was to study the effects of illuminance, as a consequence of cage position upon activity rhythms and entrainment in IVCs. Most modern mouse facilities use IVCs and knowing how rack position affects daily rhythms may inform husbandry routines to deliver better quality scientific data in any discipline.

3.5.1 Evaluation of methods

This experimental set-up utilised the pre-existing Clocklab activity monitoring system used for mice housed in Light Tight Cabinets in other areas of the facility. A new running wheel and switch arrangement was prepared, developed from that reported by de Bono et al. (2006); a fast-trac wheel mounted on a greased axle with an associated reed switch and odometer to record distance, time and average speed of wheel running in a cardiac phenotyping study. Festing (1976) also used a magnet-activated reed switch to record wheel running in open-top home cages, although a vertically aligned wheel suspended from the roof was used. A plastic igloo house (which doubled up as a covered nest for the mouse) was used as the base for a fast-trac wheel here, secured in place by inserting it into a grooved perspex base plate which was then glued to the cage floor.

This is likely the first study on the effect of IVC housing on circadian locomotor activity rhythms. There were several problems which limited data collection; Igloo bases were dislodged from the grooved base plates on occasion (likely due to vibrations from high running levels), wheel perimeter magnets got chewed off or became dislodged as mice moved around on the floor of the cage and food pellets accumulated under the lowest point

of the wheel, or *Sizzlenest* bedding material gathered between the wheel and the Igloo, limiting rotation. As a result, mice did not record for a consistent number of days across positions; in some instances, only a couple of continuous days' data were available and recordings from 4 of the first 18 mice had to be discarded due to intermittent recording rates. Fortunately, all mice showed running activity on the first night of wheel inclusion and none were removed from study due to lack of participation.

Three rack positions were chosen relative to the overhead light source, with experimental cages placed in three rows at the TOP, MIDDLE and BOTTOM levels. Measurement of light intensity across the rack revealed marked diversity in lux values inside cages of any given row so the two most similarly illuminated positions were chosen and the average lux values were 653, 427 and 59 lux at TOP, MIDDLE and BOTTOM levels respectively. Lux values quantify light intensity or illuminance as perceived by a human observer and use of irradiance measurements in W/m^2 is generally advised to more accurately characterise light exposure, however as this study was completed within one cage rack under one constant light source with all mice experiencing each experimental position any differences were controlled for.

The weekly cage change disrupted all mice in IVCs; abnormally elevated levels of activity were even seen before changing as a result of vibrations transmitted through the rack. Elevated activity is common after cage change and data was therefore discarded for these days. In an effort to minimise human/animal interaction these short-duration experimental cages were not changed and if they had to be opened for prolonged periods of time (i.e. to replace a dislodged magnet or Igloo) a minimally stressful method of handling the mice was used, by picking them up in plastic tunnels instead of by the tail (Hurst and West, 2010).

The specification of most IVC cages (opaque overhead filters, food hoppers and water bottle ports) meant that most of the incidental light entered the cage from the front. The cage manufacturer, Tecniplast offer some information regarding the amount of light which is transmitted through to the cage interior; in a study where incidental light intensity was 200 lux, illuminance was measured at 48 lux at the front, 14.2 lux in the middle and 10.5 lux at the back of the cage (Tecniplast FC 01 report, <http://www.tecniplast.it/en/resource-library.html?parentid=2&nodeid=15>). This gradient enables animals to select their preferred light intensity to some degree, as mice find bright light stressful (Crawley, 2008) and choose to burrow during daylight hours (Deacon, 2006) it's probable that they will habituate dimmer zones most. Only 1 of the 22 experimental mice chose to place his nest at the front of the cage, adjacent to the food bowl, all others nested inside the Igloo which is coloured red and should filter most of the incident light. Resting mice therefore needed to move to the Igloo entrance to be exposed to the ambient light within the cage and it is not known (or controlled for) how much their behaviour (time spent asleep/short bursts of activity outside the Igloo during the light phase) affected their perception of illuminance within the cage. It was not possible to set the level of illuminance inside cages so the light levels used as experimental variables were not scaled at regular intervals or orders of magnitude. Repetition of this experiment, with mice housed in conventional cages inside a light tight cabinet could remove the effect of rack vibrations, wheel robustness and the light gradient within the cage.

The C57BL/6J mouse was chosen for this experiment as it exhibits a high level of spontaneous activity compared to other inbred strains (Nikulina et al., 1991, Crabbe et al., 1999) and shows enhanced motor coordination compared to another substrain- C57BL/6N

mice (Bryant et al., 2008). Another reasonable choice would have been the C3H mouse, the background strain for the *rd/rd* and *rd/rd cl* mutants. Male C57BL/6 J mice were chosen as many circadian researchers avoid using females due to the effects of the oestrus cycle on activity rhythms (Carmichael et al., 1981) and a small pilot study conducted using 2 females prior to the main experiment did not yield successful results- these mice were appreciably smaller and lighter than age-matched male counterparts and ran so fast on these small diameter wheels that the Clocklab system was not sensitive enough to record every revolution. Marked differences in the activity patterns of C57BL/6 females and males have also been demonstrated (De Bono et al., 2006, Konhilas et al., 2004, Swallow et al., 2005, Allen et al., 2001). It was necessary to house mice singly to enable accurate recording of activity rhythms which were influenced only by environmental conditions. Mice are a social species and The Home Office Code of Practice for the Housing and Care of Animals Bred, Supplied or Used for Scientific Purposes (December 2014) permits single housing for scientific reasons but stipulates that this should be for the minimum duration necessary and that visual, auditory, olfactory or tactile contact should be maintained. As mice have low visual acuity (Chalupa and Williams, 2008) it is not known whether they could see others in adjacent cages and auditory, olfactory and tactile contact is unfortunately completely absent when IVCs are used. As there were no other regulated procedures applied to these mice the overall cost to the individual animal was hopefully relatively small.

3.5.2 Evaluation of results

The hypothesis for this experiment was that cage position (relative to overhead light sources) within an individually ventilated cage rack will affect the voluntary wheel running activity of singly-housed mice.

Total activity counts were extremely variable within (across the three rack positions) and between mice. One reason may be that, despite being a highly evolved, inbred strain the previous housing and husbandry history of these mice (when reared at the commercial breeding establishment) and other epigenetic factors such as the nutritional status of their dam or the individual mouse's position within the dominance hierarchy when group housed were unknown and may affect each mouse's propensity to wheel-run. Another reason was that the wheel axles of the igloo bases used here wore down with repeated use. Each time the cage was opened the wheel was spun by hand to check that it rotated freely. Wheels and axle rods were replaced between each group of 6 mice but a new wheel or axle was required a couple of times mid-experimental group when increased resistance was detected. It was difficult to objectively assess the degree of resistance when wheels were checked but Girard et al. (2001) managed to achieve this by measuring the deceleration rate from a set spinning speed in revolutions per minute. Variable resistance would confound any total counts data and following preliminary data analysis it became obvious that total counts within and between mice were too erratic to warrant further study. The division of activity between light (*rho*) and dark (*alpha*) phases then became relevant as a measure of entrainment (Jud 2005). Mrosovsky (2003) describes how the variations in the amount of wheel running did not affect the level of entrainment of mice and it is hoped that this was

the case, as other authors report locomotor activity as a non-photic *zeitgeber* (Hughes and Piggins, 2012, Edgar and Dement, 1991) which can alter the phase angle of entrainment (Mistlberger and Holmes, 2000), decrease *Tau* (Edgar et al., 1991) and accelerate re-entrainment to phase-shifted light cycles (Chidambaram et al., 2004). The activity counts data from each mouse were normalised as a percentage of maximum counts across all three positions to prevent the most prolific runners skewing the group mean values for each rack position. Despite this, all the results of Repeated Measures ANOVA (significant/non-significant) were the same for the raw and normalised activity counts in each analysis.

All mice entrained to the LD cycle as the levels of illuminance within cages were above threshold levels, even at the lowest rack position. Activity onsets at the beginning of the *alpha* phase appeared defined on all actograms, as shown in Figure 3.17. Butler et al. (2008) found that mice entrained to lower light intensities than elicited other non-image forming responses, indicating an enhanced efficacy of the entrainment response within the circadian system. 17% of C57BL/6 mice entrained to a light intensity of 0.1 lux (Ebihara and Tsuji, 1980) and as rods drive photoentrainment at scotopic light intensities (Altimus et al., 2010, Lall et al., 2010) it was expected that these C57BL/6 mice, with intact retinæ would show entrainment as the lowest light intensity within a given cage was 52 lux.

There was an overall experimental effect upon total activity counts between rack positions in the *rho* phase only with no significant differences seen during darkness. Post-hoc analysis showed that mice at the TOP ran less during the day than those at MIDDLE and BOTTOM positions. It was expected that reduced light intensities at lower positions (particularly at

the BOTTOM, average value 59 lux) may exert a positive masking effect, encouraging mice to be active when they would usually be resting. The absence of a significant difference between MIDDLE and BOTTOM positions suggests that high light intensities at the TOP (average intensity 653 lux) may exert a negative masking effect; mice do not sleep for prolonged periods and it is possible that sporadic short bursts of activity do occur during the light phase when they are housed in IVCs.

The phase angle of entrainment (the time difference between activity onset and lights off) varied, being more positive (starting earlier) at BOTTOM positions where the ambient light intensity was lower. This represents a positive masking effect of dimming light, enhancing locomotor activity without involving the central pacemaker. Twilight phases facilitate parametric entrainment to LD cycles by correcting any discrepancies between *Tau* and the zeitgeber (Foster et al., 2007, Pittendrigh, 1981) and the characteristic activity increase as light dims reported by Ebihara and Tsuji (1980) was evident across all mice with activity seen more than 1 hour, 30 minutes and 20 minutes before lights off at the BOTTOM, MIDDLE and TOP rack positions respectively (see Figure 3.21). Significant differences were recorded between the activity onset time of TOP and MIDDLE position mice suggesting that there could be a threshold intensity of illuminance at which locomotor activity begins. The rate of dimming of the overhead lights between CT 12 and CT 13 is not linear (see Figure 3.3) therefore measurement within the cages during the dusk phase would be necessary to confirm this.

3.5.3 Conclusion

Hypothesis: cage position (relative to overhead light sources) within an individually ventilated cage rack will affect the voluntary wheel running activity of singly-housed mice.

The results indicate that mice housed in IVCs, where the internal light intensity is between 52 and 657 lux entrain to a 13:11 LD cycle with one hour of twilight either end of the day. Total activity (wheel revolution) counts were variable within and between mice and were thought to be affected by various technical issues surrounding the running wheel used and repetition of the experiment using more robust methods would be desirable.

Activity counts during the *rho* (light) phase were reduced at the highest, most illuminated rack position and there was no effect of cage position upon activity counts during the *alpha* (dark) phase. An overall effect upon the onset of activity in relation to the time of lights off was seen, with mice placed higher on the rack starting later, although locomotor activity began before total darkness in all positions. Significant differences were found between onset times at the top and middle of the rack suggesting that a threshold intensity of illuminance may exist at which mice initiate wheel running activity.

The primary factor causing the differences in total activity during the light phase and in activity onset under dimming light is likely to be masking; producing alterations in behaviour without affecting the internal pacemaker. High light intensity negatively masks sporadic daytime activity in cages at the top of the rack and progressively dimming light during the twilight phase has a positive effect upon the initiation of activity, prior to the onset of darkness. Housing mice in IVCs under standard overhead light sources should not therefore

affect their circadian rhythms but researchers should consider the effect of cage position, as behavioural or physiological data collected around dusk may be influenced by the level of stimulation that the variable onset of activity causes. In conclusion, the position of the cage within an individually ventilated cage rack (where internal light intensities ranged from 52-657 lux) may affect the onset of activity as lights dim or the proportion of total activity which occurs during the light phase but overall effects upon circadian rhythms are negligible.

Chapter 4

Validation of infrared thermography with radiotelemetry as a method of assessing body temperature in mice

Hypothesis: Using infrared thermography/ thermal imaging to measure peripheral surface radiation is a valid method of assessing the body temperature of mice.

Hypothesis: the circadian rhythm of body temperature, as seen when mice are entrained to a regular light/dark cycle alters under conditions of constant light or constant darkness.

Acknowledgements: The contribution of Dr. Sibah Hasan for setting up the radiotelemetry system, acting as surgical assistant for the three temperature mice surgeries and for permitting the use of LD data from five EEG mice destined for another experiment is gratefully acknowledged. Dr. Eric Tam also assisted with the use of *R* to analyse period length in the datasets for the temperature mice and Dr. Carrie Potheary set up the thermal cabinet with a fan and LED lighting source.

A Circadian Terminology and Abbreviations list can be found prior to the Table of Contents

4.1 Introduction

4.1.1 Thermoregulation in mice

The mean temperature of a mouse is similar to that of an elephant but it varies more widely through the day (total range 2-4°C, up to 0.7°C difference per hour) and is more stable at night when activity levels are higher (Uchida et al., 2010, Gordon, 2012). Altering the cardiovascular response at the level of the skin is the mainstay of thermoregulation for most species but the mouse is a “metabolic specialist” which alters metabolic rate in preference to cutaneous blood flow (Phillips and Heath, 1995). In warm conditions rodents restrict their activity (negative masking of activity rhythm by heat) and spread saliva on their fur to cool by evaporation (Brown and Pham-Le, 2011). Huddling, nest-building and initiation of non-shivering thermogenesis (activation of brown adipose to produce heat) occur when cold (Harshaw and Alberts, 2012, Gaskill et al., 2013, Uchida et al., 2010).

Mice prefer warmer temperatures than they are typically kept at in laboratories (20-24°C compared to 30°C) and their thermal preferences differ depending on activity and time of day (Gaskill et al., 2012). In place preference studies mice used thermotaxis, seeking warmer areas as their first defence against cold and increased the size and complexity of the nest if this was not possible (Gaskill et al., 2011, Gaskill et al., 2012). A minimum amount of nesting material necessary for adequate nests is recognised (Gaskill et al., 2013) and the type of material provided affects body temperature (Hess et al., 2008, Gordon, 2004). Castillo et al. (2005) found that the circadian rhythms of mice that built smaller nests were more robust, possibly because they are exposed to stronger ambient temperature *zeitgeber* effects. The increased levels of activity during the dark phase assist mice in staying warm but Brown et

al. (2011) found that rats given a choice selected areas >23°C during both light and dark periods. Mice, with their high surface area to body volume ratio are at risk of hypothermia and Uchida et al. (2010) found that mice under “cold stress” at 20°C experienced changes in glucose homeostasis and also ate and drank more. Conventional laboratory environmental temperatures between 19-23°C are therefore “cold” for mice, below their lower critical temperature where metabolic rate increases above basal levels just to keep warm. This upregulation in metabolism may confound the interpretation of certain scientific studies (Gordon, 1993, Gordon et al., 2008) and it would be preferable to keep mice in their thermoneutral zone.

Hypothermia is common when mice are used as experimental disease models. Infection causes an acute phase response, with production of macrophages and neutrophils which release cytokines which travel to the brain to change the temperature set point (Olfert and Godson, 2000, Tizard, 2008). In infectious challenge or regulatory toxicity studies using rodents, an initial transient pyrexia often precedes progressive hypothermia following dosing. Temperature decline can predict impending mortality in studies of bacterial and yeast infections; mice were found to irreversibly morbid at 33°C following infection with *Candida albicans* (Warn et al., 2003) and to have a median survival time of 24 hours when temperature dropped below 36°C resulting from *Klebsiella pneumonia* infection (Kort et al., 1998). Serology sampling, to look for inflammatory markers such as acute phase proteins (Cray et al., 2009) is not practical in this small species with limited circulating volume so selecting temperature as a predictor of the humane end point reduces suffering, whilst still complying with the scientific objective of the study (Olfert and Godson, 2000, Vlach et al., 2000).

4.1.2 Methods of measuring body temperature

4.1.2.1 Contact methods

There are several ways of assessing body temperature. The standard method is by insertion of a thermometer into the rectum, to achieve a temperature approximating that of the body core. This is typical in veterinary practice although some animals are more resentful of it than others. Tympanic thermometers are successfully used in human medicine as core temperature is regarded as being close to the temperature of the hypothalamus (Sikoski et al., 2007) although two recent feline studies found that this was the most inaccurate method in comparison to rectal, axillary and oesophageal temperatures (the latter taken under anaesthesia) (Smith, 2014, Watson and Gregory, 2014). It is relatively easy to immobilise mice adequately but the associated stress is profound, causing anticipatory anxiety as habituation to protocols occurs and the pyrexia induced can persist for up to 70 minutes after the mouse is returned to its cage, likely rendering all successive measurements invalid (Poole and Stephenson, 1977). Restraint stress causes activation of the hypothalamic-pituitary-adrenal axis and of brown adipose tissue via noradrenaline release (Gordon, 1993) which will, in turn affect many other physiological and behavioural parameters. The distance of insertion of the thermometer should be standardised for valid measurements but this is difficult in mice (Miller and O'Callaghan, 1994, Kort et al., 1998) and associated with trauma and possibly sepsis (Newsom et al., 2004).

Radiotelemetry avoids the stress artefacts induced by restraint, as data can be collected remotely from freely-moving animals. It involves a sensor/transmitter unit placed within the body which sends data to a nearby receiver (Clement et al., 1989). The quality of data from unstressed animals is better (Kramer and Kinter, 2003, Kramer et al., 1998) in addition to

improving welfare around the time of sampling. The major disadvantage of radiotelemetric methods is that the animal must undergo surgery to implant the device and a post-operative recovery period must be observed for all physiological parameters to return to normal. Leon et al. (2004) found that the circadian rhythms of body temperature and activity of mice implanted with intraperitoneal transmitters were disturbed for 5 days and note that many studies using telemetry do not consider circadian rhythm recovery post-surgery. Transmitters left “floating” in the abdominal cavity may have compression effects upon behaviour or physiology for longer than the customary one week recovery period (Gordon, 2009).

Animals may be implanted without the need for surgery. Subcutaneously-injected microchips are an established method of identification and some dual function temperature sensing devices have recently come onto the veterinary market for use in the domestic species. A study of rats found that transponders left *in-situ* for one year had no effect upon body weight or food consumption and histopathological analysis of local tissues after sacrifice revealed fibroblast infiltration but no inflammatory cells (Ball et al., 1991). Hunter et al. (2014) successfully used temperature- sensing RFID transponders to track mouse welfare following experimental infection with lymphoma and Quimby et al. (2009) found good agreement between rectal and subcutaneous microchip temperatures in cats, experimentally infected with feline herpesvirus 1, in both healthy and post-infection temperature ranges. Subcutaneous transponder temperatures matched rectal temperatures better than tympanic values in a study of 13 guinea pigs (Stephens Devalle, 2005).

4.1.2.2 Non-contact methods; infrared thermography or thermal imaging

Infrared waves are part of the invisible electromagnetic spectrum. Any object (living or inert) with a temperature above 0 Kelvin (-273.15°C) emits electromagnetic radiation and measurement of the infrared fraction gives body temperature. The amount of heat a body gives off by radiation is termed its emissivity value (range between 0 and 1, where 1 is maximal, perfect emissivity, akin to that from a black body) and human skin, the thermoregulatory interface between the body core and the environment has an emissivity of 0.96-0.98 (Jones, 1998). Thermal cameras detect radiation at wavelengths of 0.8µm-1mm and an infrared thermogram is an image of temperature distribution of the body, or object surface (Ring and Ammer, 2012). Where absolute temperature values are required, the use of external reference temperature sources is important, to calibrate cameras so they can be diagnostically useful.

4.1.3 Thermal imaging in human medicine

Thermal imaging technology aids diagnosis and treatment in various areas of human medicine. Thermal imaging performed comparably with tympanic thermometry in a study to detect pyrexia associated with respiratory disease in children (Ng et al., 2005) and infrared cameras have been used for fever screening during severe acute respiratory syndrome (SARS) and the H5N1 human influenza outbreaks (Ring et al., 2010). Infrared thermography has also been used to examine the temperature of localised areas of skin; the neurological level of paralysis corresponding with a clear demarcation in skin temperature due to reduced perfusion adjacent to the spinal cord in paraplegic patients (Roehl et al., 2008).

Thermography is useful in vascular physiology studies to detect atherosclerotic plaques which are inflammatory and show as a “hot spot” (Madjiid et al., 2006) and renal blood flow

was tracked through induced ischaemia and reperfusion stages in a porcine experimental model for human kidney transplantation (Gorbach et al., 2008). The field of oncology has used thermal imaging in conjunction with ultrasound, MRI and CT scanning to delineate brain tumour margins during resection surgery (Kateb et al., 2009) and superficial assessment of malignant melanomata demonstrated deviations from normothermia in 84% of cases, with histological tumour staging correlating strongly with thermographic classification (Michel et al., 1985). Thermal imaging of the corneal surface can detect temperature changes associated with choroidal/conjunctival tumours (Wittig et al., 1992) and thermal changes were also seen in small scale studies of schizophrenic patients, where affected individuals showed increased corneal temperature which reduced following administration of anti-psychotic drugs (Shiloh et al., 2003a, Shiloh et al., 2003b). Scully et al. (2011) measured the circadian rhythms of skin temperature using infrared imaging and found that rhythms were poorly differentiated in patients on chemotherapy compared to healthy controls.

4.1.4 Thermal imaging in veterinary medicine and biomedical research

Thermal imaging has also made an impact on veterinary medicine, perhaps best known for its application to detecting the site of equine lameness (Head and Dyson, 2001) where elevated surface temperatures signal underlying inflammation or swelling. Schaefer et al. (2007, 2012) have used it to diagnose the pyrexia associated with respiratory disease in calves but it has been most frequently described in recent veterinary research articles in relation to mastitis; in dairy cattle (Polat et al., 2010), sheep (Martins et al., 2013) and camels (Samara et al., 2014) where udder skin surface temperatures correlated with somatic cell counts and the California Mastitis Test. Other studies did not find thermal

imaging useful in detecting body temperature; Ramey et al. (2011) found a poor correlation between infrared thermography of the gums and axillary skin and the rectal temperature of horses and Sikoski et al. (2007) trialled it unsuccessfully on the shoulder, face and abdomen of 51 cynomolgous macaques although it was found that shaving the hair improved the result.

Giancardo et al. (2012) showed that infrared imaging could be used to track the heat signatures of mice, where individuals can be distinguished in a group. Determination of absolute peripheral temperature was reported by Finn et al. (2011), as when investigating if transgenic mice had lower body temperatures, they found that cutaneous thermoregulation was normal and poor coat quality compared to wildtype controls was responsible for reduced heat retention. Infrared thermography compared favourably with subcutaneous transponders in an infectious disease study of mice (Warn et al., 2003) and Harshaw et al. (2012) used it to assess skin temperature and BAT activation in mouse pups at low ambient temperatures. The increased angiogenesis associated with growth of xenograft breast tumours was tracked by Song et al. (2007) and thermal imaging enabled longitudinal monitoring of tumour development and revealed a smaller secondary tumour which would have otherwise been overlooked.

4.1.5 Relationship between core and peripheral temperature in mammals

Body temperature is affected by many physiological and behavioural processes and can be used as a marker of circadian rhythmicity, health and psychological state. Systemic and localised temperature aberrations can represent infection, inflammation, vasospasm, ischaemia or neoplastic change. The body of a homeotherm can be considered as three areas, the brain, the core and the shell (the skin), the two former are maintained within

narrow limits and the shell varies depending on factors like activity, metabolic rate, local insulation and ambient conditions. When the body is warmer than the environment heat loss occurs by convection, conduction and radiation through the shell and a thermal camera will detect radiation (dry heat loss) most reliably from well vascularised, hairless areas of skin. Traditional methods attempt to estimate core body temperature by placing probes within body orifices like the rectum and the external ear canal, although a small number of authors have tracked peripheral shell temperature, as an absolute value and to establish the relationship between periphery and core. Core and skin surface temperatures of humans are known afferent inputs to the thermoregulatory system (Frank et al., 1999) and their relative cardiovascular dynamics affect sleep propensity (van den Heuvel et al., 2004, van den Heuvel et al., 2003). The temperature gradient of human skin is between is 0.2-0.5°C/mm thickness (Jones, 1998) but less is known about the skin temperature of animals. Thermal imaging shows the temperature of the epidermis (resulting from local vascular perfusion) and being non-invasive is easily applicable to many situations. Infrared emissions are often heterogenous between different body sites (Scully et al., 2011, Sikoski et al., 2007) and the circadian rhythms of the periphery may be lower, weaker or out of phase with core temperature (Piccione et al., 2013) but establishing a stable relationship between periphery and core would enable temperatures of small mammals such as mice to be assessed without stress or confounding scientific data.

4.2 Methods

The general principle for this experiment was to evaluate infrared thermography or thermal imaging as a method of assessing body temperature in freely-moving mice. Core temperature is traditionally measured using a thermometer probe inserted into a body orifice which requires restraint and interrupts normal rhythms of behaviour. Surface probes also require a degree of immobilisation, which is stressful to mice. A variety of implants may be placed inside the body, which transmit data to remote receivers to overcome this, but the invasive nature of surgical implantation compromises welfare and may affect biological rhythms post-operatively. Infrared thermography (or IRT), which measures radiant surface emissions is a non-contact method which should deliver more meaningful data. A commercially-available radiotelemetry temperature implant was placed inside the peritoneal cavity of mice and simultaneous longitudinal recording with a thermal camera allowed measurement of temperature from two body areas over several circadian cycles, under three different photoperiods. The relationship between core and peripheral body temperature was examined in 12:12 light/dark cycles and in constant light and constant darkness. Peripheral temperature was expected to be lower than core temperature and the period of both rhythms were expected to shorten (free-run) in DD and lengthen in LL. Additional data was gathered from mice carrying a similar radiotelemetry implants (also measuring electroencephalogram (EEG) via a craniotomy and electromyogram (EMG) via placement of biopotential leads in the neck muscle, in addition to temperature), also placed in the peritoneal cavity, under 12:12 LD cycles.

4.2.1 General methods

Age and sex-matched inbred strain mice (male, 12-16 weeks old, C57BL/6) were sourced from a commercial supplier (Harlan, UK) and maintained within conventional open-top cages inside light tight chambers (LTCs) to allow the light cycle to be varied from that of the stockholding room. Programmable timer plugs controlled the light cycle inside LTCs in a square wave form and the ambient light intensity was 200 lux measured at cage top level. Mice were given *ad-libitum* access to food (RM3(E) irradiated diet, SDS) and chlorinated water (2 x Istachlor Rapid chlorine tablets 0.35mg in 50 litres) and singly-housed to control effects of social interactions on body temperature. Substrate bedding material in cages was *Eco-Pure Chips 6 Premium* (Datesand) and nesting material provided was autoclaved *Sizzlenest* (Datesand). Relative humidity within the LTCs was maintained between 40 and 60 % and temperature between 19 and 21.9°C.

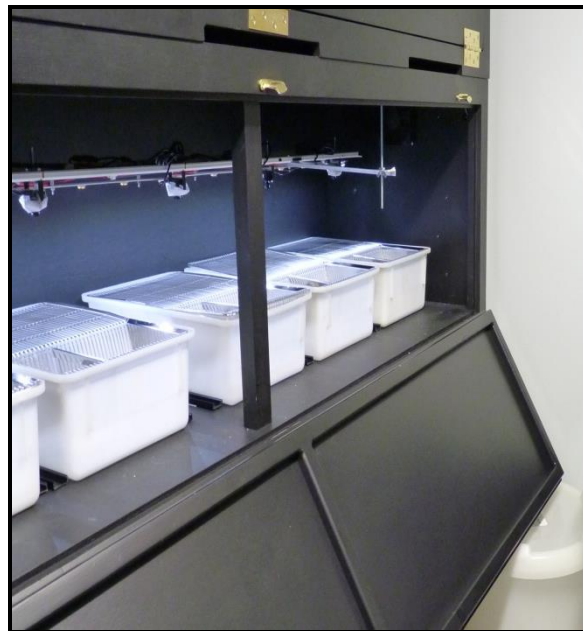


Figure 4.1 Photo of a LTC with door opened, mouse cages (unoccupied) placed under individual overhead lights.

4.2.2 Experimental design

Three “temperature” mice (M1T, M2T, M3T) were surgically implanted with TA-F10 transmitters (from Data Sciences International (DSI), St. Paul, Minnesota) and temperature was recorded under 12:12 LD, DD and LL light cycles in succession. Five “EEG” mice (M1-5 EEG) were surgically implanted with DSI F20-EET transmitters and, after short-duration recording of dual temperature rhythms under a 12:12 LD cycle were transferred to another experiment investigating sleep and cognitive behaviour under varying light cycles.

Tables 4.1 and 4.2 Duration of dual-method temperature recordings for Temperature (T) and EEG mice under different light cycles. For the Temperature mice, “Into DD” and “Into LL” refer to recordings made immediately after the light cycle was changed, i.e. recording started when changed from LD to DD and from DD to LL. DD and LL recordings are those taken at least two weeks after the transition from one light cycle to another, to allow time for any change in the temperature rhythm to stabilise.

	Time recorded in each light condition (hours)				
Mouse	12:12 LD	Into DD	DD	Into LL	LL
M1T	72	94	78	85	73
M2T	72	n/a	83	94	72
M3T	72	94	76	76	71

	Time recorded in each light condition (hours)
Mouse	12:12 LD
M1EEG	33
M2EEG	35
M3EEG	33
M4EEG	27
M5EEG	26

4.2.3 Surgical preparation of mice

4.2.3.1 Pre-surgical assessment and transmitters

All mice were health checked and weighed prior to surgery. The TA-F10 transmitter weighs 1.6g and has a capacity of 1.1cc and, as DSI recommends that mice weighing <17g are not implanted selected mice weighed between 29 and 34g at the time of surgery. This transmitter has a flat profile, no biopotential leads and a maximum of 6 months battery life. Its intended use is for collecting temperature and activity data from transgenic and knockout mice models where collection of circadian patterns or high resolution temperature changes are desired. It is magnetically actuated – turned on and off by passing a magnet adjacent to the animal’s body wall, allowing the battery to be preserved when recording is not in progress.



Figure 4.2 The Physiotel TA-F10 transmitter, image from

[http://www.datasci.com/products/implantable-telemetry/mouse-\(miniature\)/ta-f10](http://www.datasci.com/products/implantable-telemetry/mouse-(miniature)/ta-f10)

The F20-EET transmitter is designed for sleep research and other CNS applications. It weighs 3.9g and has a capacity of 1.9cc. DSI recommend a minimum animal weight of 25g and state that the battery should last for 1.5 months. Mice chosen for implantation weighed between 28 and 34g. Four biopotential leads (with an outer diameter of 0.3mm) allow recording from two biopotential channels such as EEG and EMG in addition to temperature and activity.

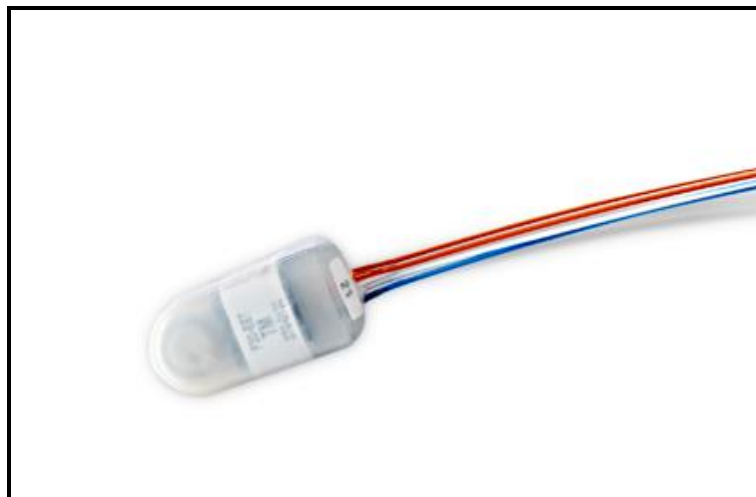


Figure 4.3 The Physiotel F20-EET transmitter, image from

[http://www.datasci.com/products/implantable-telemetry/mouse-\(miniature\)/f20-eet](http://www.datasci.com/products/implantable-telemetry/mouse-(miniature)/f20-eet)

4.2.3.2 Surgery and anaesthesia

Mice were anaesthetised with 4-5% isoflurane (*Isoflo*, Abbot Animal Health) in oxygen in an induction chamber and transferred to a face mask for maintenance once loss of righting reflex was achieved. Immediately after transfer lubricating eye drops were applied to each cornea (*Viscotears*, Alcon Laboratories) and analgesic drugs were administered by subcutaneous injection, diluted 1:10 in 0.9% saline; 0.1mg/kg buprenorphine (*Vetergesic*, Alstoe Animal Health) and 5mg/kg meloxicam (*Metacam*, Boehringer Ingelheim). Anaesthesia was maintained with 2-2.5% isoflurane in 1 litre oxygen and depth and physiological stability were monitored by counting and recording respiratory rate every 5 minutes (by the surgical assistant), alongside rectal temperature values. TA-F10 temperature implantation was relatively rapid and straightforward, surgical time < 15 minutes, F20-EET implantation was more time consuming as it was necessary to connect the biopotential leads to the cranium and neck muscles, surgical time was approximately 3-3.5 hours. Additional heating, insulation and decreases in the levels of volatile anaesthetic agent were required in the EEG cohort of mice, due to hypothermia induced by extended time under anaesthesia, this is discussed further in Chapter 5. The relevant parts of the two different procedures are described separately for clarity below.

TA-F10 Temperature mice were positioned in dorsal recumbency on a heat pad and a lubricated rectal thermometer placed and taped loosely to the tail using micropore tape. The ventral abdomen was clipped and the skin aseptically prepped using povidone iodine surgical scrub diluted 1:20 in water and then swabbed with alcohol (*Sterets Pre-injection swabs*, MidMeds). The surgeon then scrubbed hands and arms and put on sterile surgical

gloves. A non-fenestrated plastic drape (*Transdrape*, Millpledge Vet) was cut as required and placed over the mouse's abdomen.

The pedal withdrawal reflex was checked by an assistant to ensure surgical plane of anaesthesia and a midline incision was made through the skin and linea alba of the abdominal muscle layer, just longer than the TA-F10 transmitter to expose the peritoneal cavity. The transmitter (supplied ready-sterilised) was placed into the abdomen with the flat side against the viscera and 0.5mls of sterile 0.9% saline was instilled around it. The muscle layer was closed with 4/0 polyglactin 910 (*Vicryl*, Ethicon) suture with a swaged-on round-bodied needle, using simple interrupted sutures. The skin was closed using 5/0 polyglactin 910 (*Vicryl*) suture with a swaged-on reverse cutting needle, using an intradermal (buried) suture pattern. A further injection of 0.5mls 0.9% saline was administered subcutaneously to the mouse and the isoflurane anaesthetic was turned off. Mice were maintained on 100% oxygen until they showed signs of regaining their righting reflex, when they were transferred to recover in a warm chamber at 25°C. Mice were returned to the home cage once they displayed a normal level of activity in the warm chamber and post-operative temperature recording was initiated (see Chapter 5).

For the EEG mice, initial anaesthesia and analgesia and abdominal exposure were achieved in an identical manner to the Temperature mice. Following placement of the transmitter in the abdomen, the biopotential wires were passed through the abdominal muscle by first making holes using a 19 gauge needle approximately 3-4mm from one cut edge, then the muscle was closed using simple interrupted sutures. Following tunnelling of the wires under the skin to emerge on the dorsal aspect of the neck, the remainder of the surgery was executed with the mouse in ventral recumbency in a stereotaxic frame, with isoflurane and

oxygen delivered through an integrated facemask (Kopf®, David Kopf Instruments) and the head stabilised for craniotomy using Model 921 Zygoma ear cups (Kopf®). Anaesthetic maintenance, support and recovery were as for the temperature mice, although recovery took longer due to the increased surgical time. Mice were allowed at least 10 days to recover before any LD temperature recording took place.

4.2.3.3 Post-operative recovery

The home cage was adapted to allow for reduced activity and appetite immediately after surgery. Moistened food pellets were placed in shallow plastic dishes on the cage floor and strawberry jelly was also provided, as a palatable source of energy and water (mice pre-acclimatised to this, 2-3 days before surgery). Longer nozzles were placed on the water bottles to prevent mice having to rear up to drink. Analgesia (5mg/kg meloxicam diluted 1:10 in saline) was repeated 24 hours after surgery and animals were checked including inspecting their surgical wounds at least twice daily, recoveries were uneventful and no further adjustments were required.

4.2.4 Recording the temperature data

An Optris PI 160 thermal camera (<http://www.optris.com/thermal-imager-pi160>, sourced from Brian Reece Scientific Limited, Newbury, U.K) with a standard lens (61°), was used to capture surface body temperature of mice. This camera is marketed to plastic, glass, metal and surface technology industries, for continuous processes monitoring. It is USB powered and portable (dimensions 45 x 45 x 62mm) and is supplied with Microsoft Windows-compatible Optris PI Connect software for recording of temperature data, which may be as a text file, colour image or in video form. The Optris camera can track hotspots within its field of view and it was set up with a laptop computer to record live temperature data at 1

second resolution (“Time Temperature Diagram”), displaying the data in a live recording window which could be stopped and saved as necessary. Data could then be saved as .dat files and extracted into Microsoft Excel for analysis.

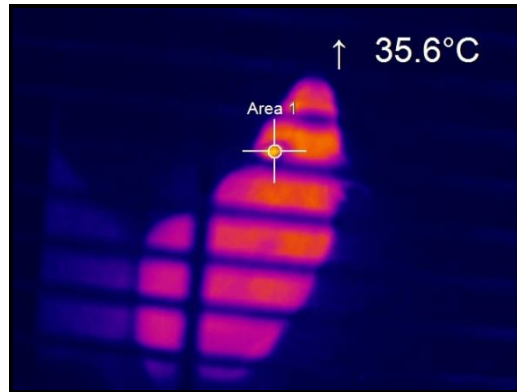


Figure 4.4 Thermal image of a mouse from above, viewed through the bars of the cage lid.

The periorbital area, Area 1 is the hotspot, measuring 35.6 °C.

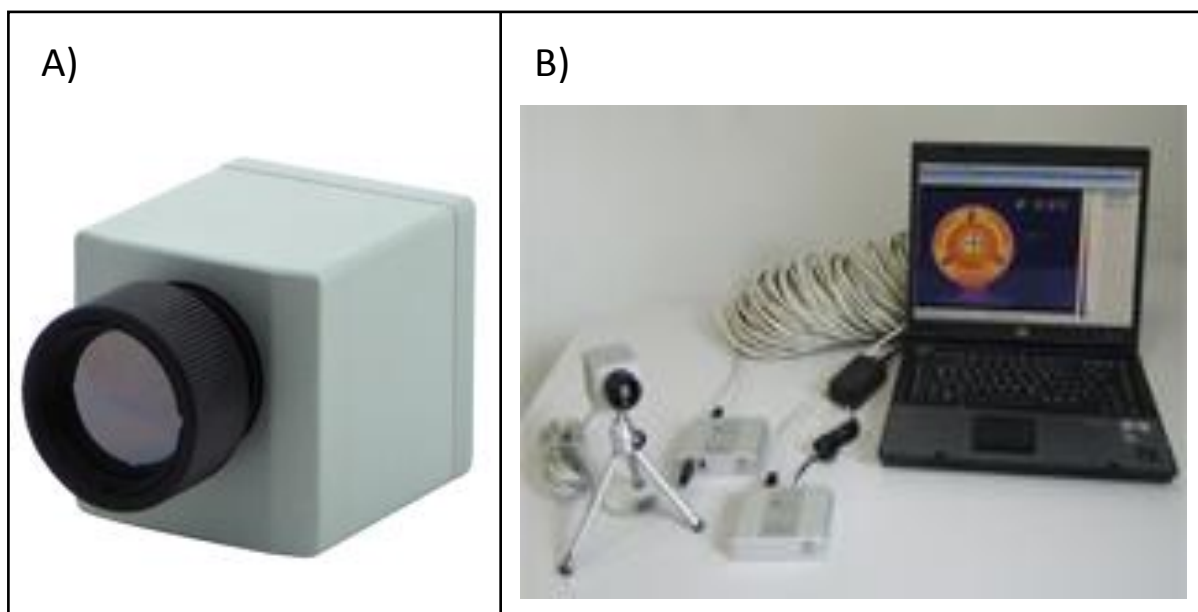


Figure 4.5 Photos of the Optris PI 160 thermal camera (A) and showing the camera linked to a laptop computer for recording (B) from <http://www.optris.com/thermal-imager-pi160>

Based on the camera's field of view, the size of cage mice were housed in, the dimensions of the DSI telemetry receiver bases and available space in the animal holding room, a customised LTC, the "thermal cabinet" was commissioned from the Mechanical Workshop, Department of Physics, University of Oxford to house the thermal camera and allow simultaneous DSI recording. The cabinet was constructed from aluminium to prevent any electrical interference from wiring around other LTCs in the room affecting the recordings. It was also anodised (made black) to prevent reflections which might increase the ambient light intensity perceived by the mice.

The thermal cabinet dimensions were 74 x 60 x 58.5cm and it incorporated an internal shelf on which it was intended a laptop could sit, two air vents on either side, both covered in cowling which housed a baffle to prevent light ingress. An electrically powered fan (Maplin, U.K.) was positioned over one of the air vents on the inside of the cabinet. Two holes at the

top of the cabinet allowed wires to pass from outside (contained inside cable glands to block light) and an overhead gantry was positioned to mount the thermal camera and L.E.D. lights. The gantry had 13cm of clearance above to accommodate the power lead on the back of the thermal camera. Larger (wider but with less vertical space) LTCs were already in use in the animal facility but these were only 45cm tall and 60cm distance between the camera and the mouse was required to view the whole cage floor area- mice were housed in these LTCs when not recording, under the same light intensity and photoperiod. Mouse cages used measured 46.5 x 28 cm and a Perspex block was placed under the food hopper during recording so the mice could not disappear from camera view at any time. Conventional wire top cage lids were used for the Temperature mice, open top (with high sides) cages were used for the EEG mice, as they progressed to a videotracking experiment where a wire cage top would have obstructed data collection.

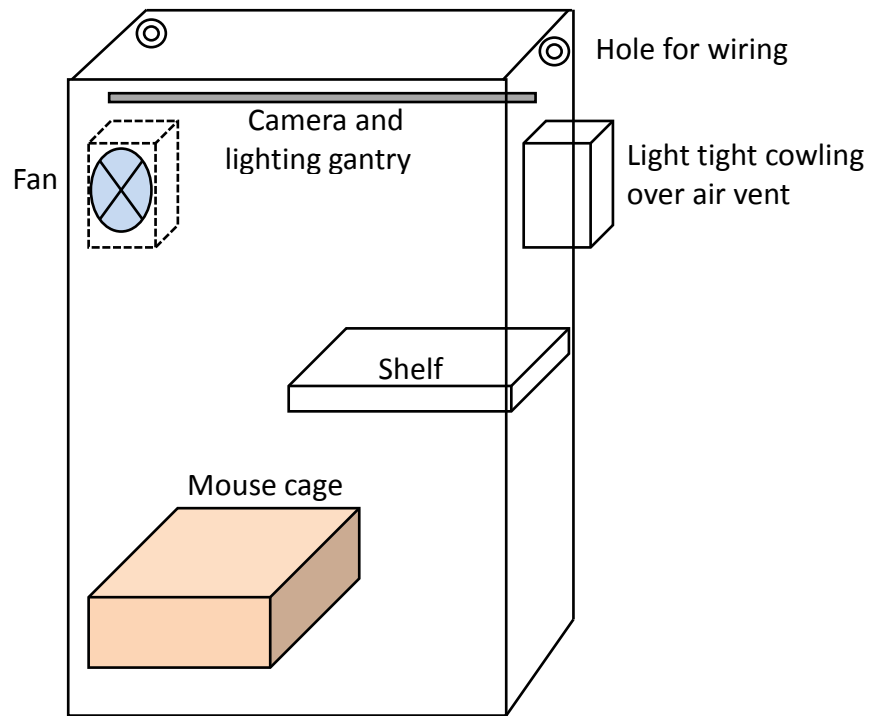


Figure 4.6 Schematic diagram of the thermal cabinet (front door missing); the mouse cage was placed on the floor on the opposite side to the shelf with the camera and lights positioned above.

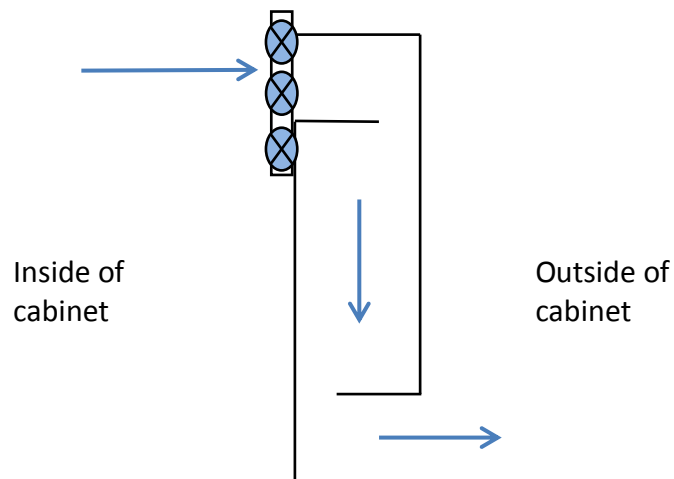


Figure 4.7 Schematic diagram of the baffle present inside the light-tight air vent cowling, a fan was placed on one cabinet wall and air was drawn through the hole in the opposite wall, across the cabinet and expelled by the fan to keep temperature and relative humidity within acceptable limits.

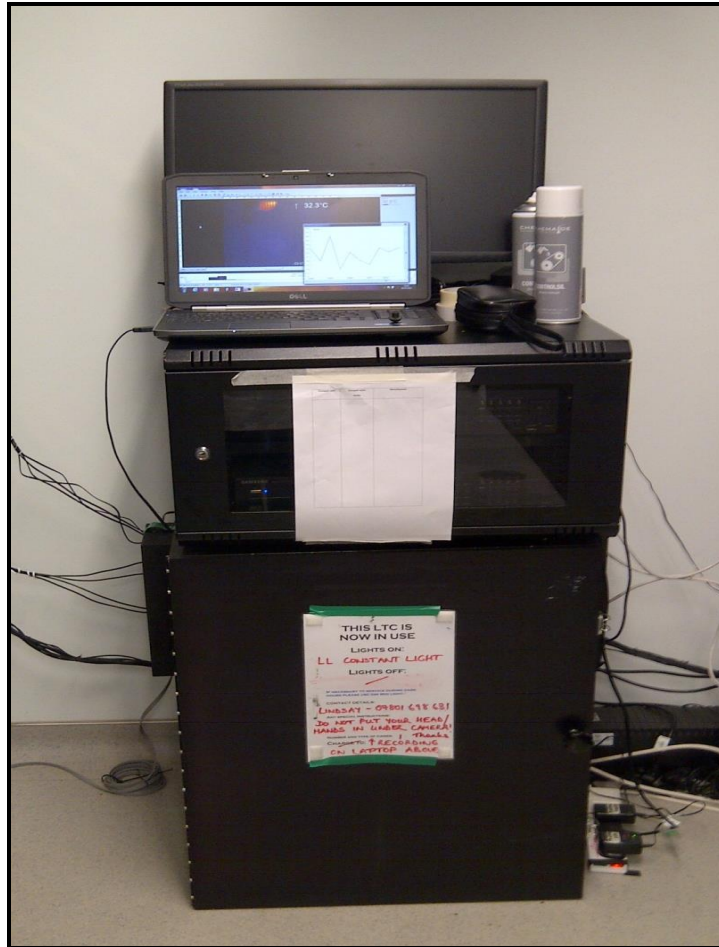


Figure 4.8 Photograph of the thermal cabinet, positioned underneath a glass-fronted cabinet housing a hard drive recorder for use in other experiments. The thermal imaging laptop was placed on top of the hard drive recorder - open thermal recording window visible on the screen. One of the thermal cabinet air vents is visible on the left hand side.

Pilot studies of the thermal camera running in an empty cabinet were conducted, to check the internal temperature when the recording laptop was placed inside, on the shelf. A rise in ambient temperature was seen during the first few hours and this was repeated and confirmed using a TR-74Ui Illuminance UV Recorder (T and D Corporation, sourced from LS Technology, Poole, Dorset, U.K.). Running the thermal camera alone over 24 hours confirmed that the source of heat was the laptop so this was positioned outside, on top of the cabinet for all live recordings.

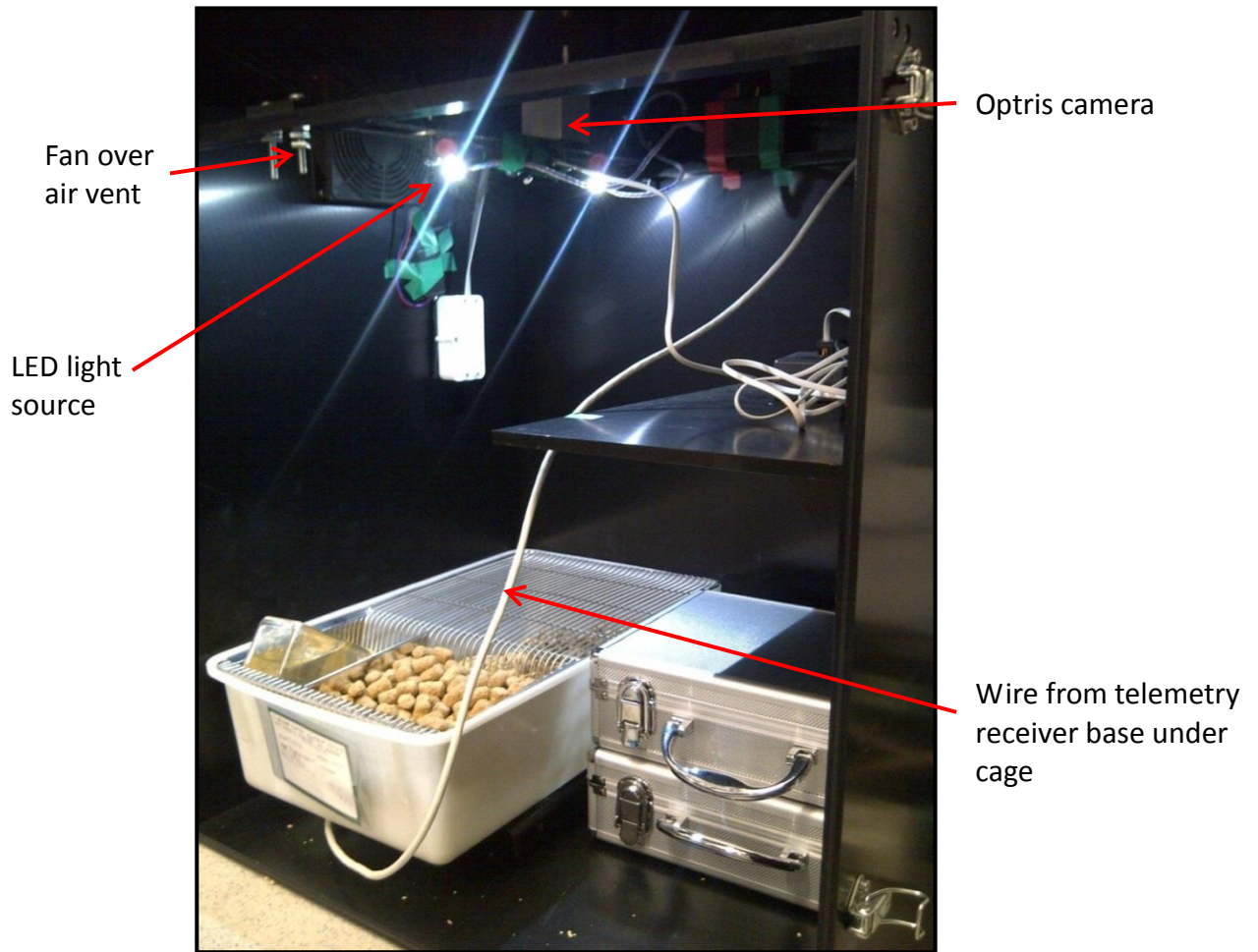


Figure 4.9 Photo of the interior of the thermal cabinet, showing position of DSI telemetry base, fan, LED lights and the Optris thermal camera. The wire top cage contains a temperature-implanted mouse.

A DSI receiver base was placed on the floor of the thermal cabinet, under the mouse's cage. This base connected to the Data Exchange Matrix box via an Ethernet cable and recorded information from the D.E.M was carried via connecting electrical wiring to a desktop computer in another room in the facility, where data automatically saved as it recorded. The transmitter inside each mouse is supplied with a unique signal to noise code and the receiver base and recording software were calibrated for these codes prior to use and storage files set up to receive the data.

Mice were transferred from standard holding LTCs into the thermal cabinet and allowed to settle for at least 10 minutes before recording started. The intraperitoneal transmitters were turned on by passing a magnet close to the mouse's abdomen, using a handheld radio switched to FM frequency background noise to confirm actuation (altered radio tone heard). The Optris Temperature Time Diagram recording window was opened simultaneously with the DSI Acquisition recording. A minimum recording duration of 3 circadian cycles was chosen as Fourier analysis of an independently-generated waveform signal with a period of 24 hours (expected entrained temperature rhythm under 12:12 LD) plus variable random noise revealed that the strongest signals occurred for datasets between 48 and 72 hours long.

4.2.5 Processing the temperature data

4.2.5.1 Peripheral temperature (Optris) data

Optris data .dat files were extracted into Microsoft Excel. As temperature had been recorded at one second resolution the files generated were very large. Raw data was first plotted to examine it visually and then it was binned by selecting the maximum value per 5 minute interval, as the thermal camera tracked the hotspots in its field of view. The "5

minute max” values were plotted and assessed to see if a sinusoidal rhythm was apparent. Finally the data was smoothed by averaging the values over one hour. There were no missing or invalid values in any of the peripheral data sets.

4.2.5.2 Core temperature (DSI) data

Data was extracted from the recording computer using DSI Dataquest ART software as text files (.txt) and opened using Microsoft Excel. The recording resolution was variable as it was not possible to select for measurements every second in some instances, when mice on other experiments were recording simultaneously (range every 1, 4 or 10 seconds). This data was also plotted in raw form and then binned as “5 minute max” values and it was noted that some erroneously high (non-physiological) and NaN (not-a-number) values were present in some data sets, especially the later ones. Filters were then applied to the data;

Filter 1- to remove non- physiological values (<34°C and > 40°C) and NaN values

Following Filter 1 the data was plotted again in “5 minute max” form and it was apparent that some high value spikes (within physiological range) were present above the trendline. Closer examination of the raw data around these points revealed that the DSI signal seemed to disappear intermittently during recording, no value was returned for variable durations of time and these lost sections of data often contained a small number of NaN and solitary temperature values which were distinctly higher than the majority of values within the time bin. Calculation of the average value of the data within the time bin returned values much lower than the maximum value calculated by the “5 minute max” function so a second filter was applied:

Filter 2- to remove values which differed from preceding and following values by $> 0.5^{\circ}\text{C}$ (this interval was selected arbitrarily as it was thought that core temperature would not change by $>0.5^{\circ}\text{C}$ over the course of 1-10 seconds, 10 seconds being the longest interval between DSI measurements). Binned core data was then smoothed over one hour as for the peripheral data. Raw, binned and smoothed data for one temperature-implanted mouse is shown in Figure 4.10;

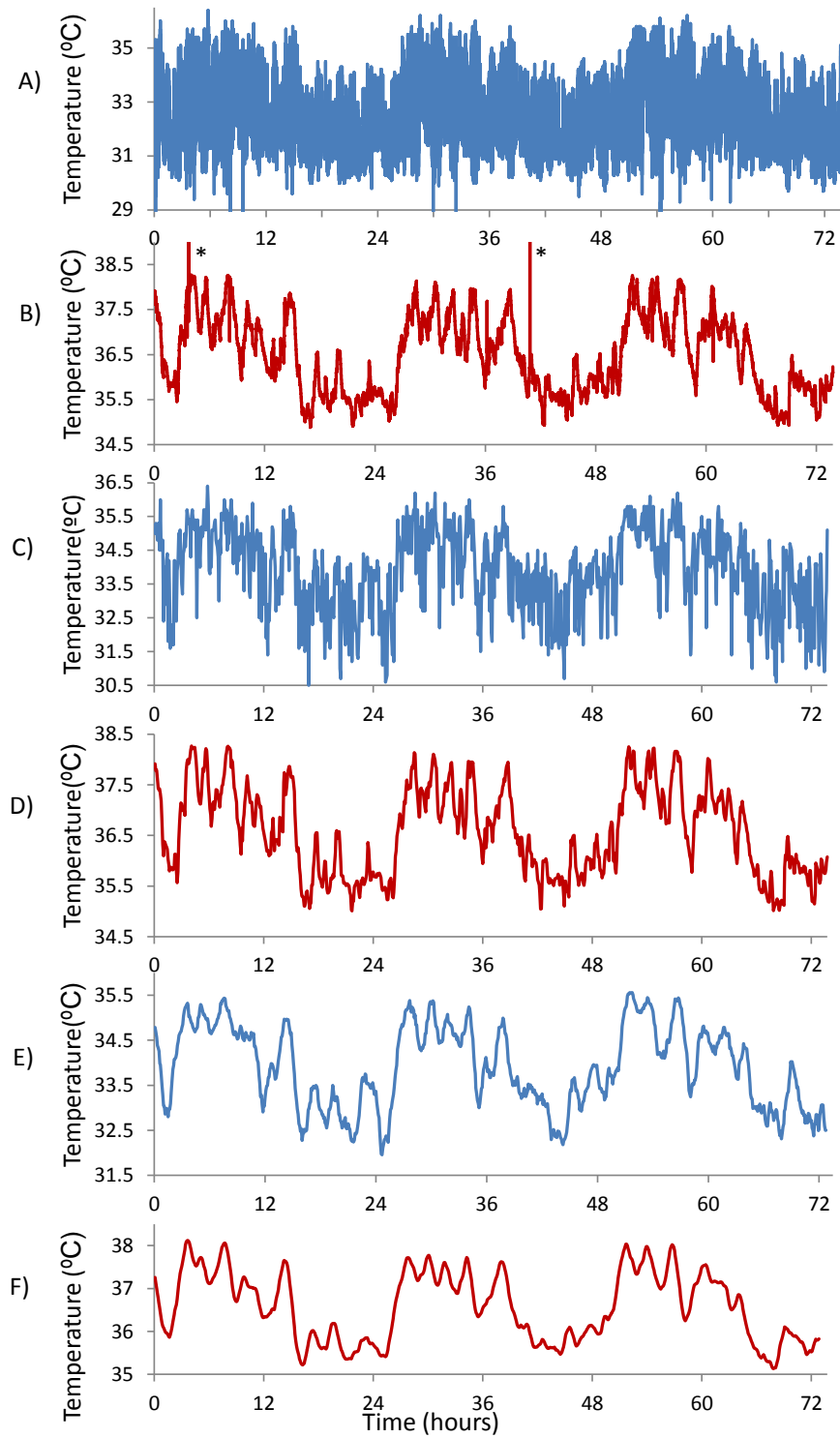


Figure 4.10. Plots of raw temperature data (A) peripheral (B) core, 5 minute max data (C) peripheral (D) core, smoothed over 1 hour data (E) peripheral (F) core for M2T under 12:12 LD cycle for 73 hours. Note the 2 spikes (*) visible in the core data in timeseries (B)

4.3 Statistical Analysis

Peripheral and core temperature data were filtered as necessary, binned as 5 minute max values and smoothed by averaging over one hour as previously described. Datasets were plotted together for preliminary visual examination, the R^2 coefficient of correlation was calculated between peripheral and core temperatures and a Bland Altman plot was generated for each mouse per light condition.

Curve fitting using non-linear regression in the statistics package *R* (freely downloadable from <http://www.r-project.org/>) was completed for the 3 Temperature mice datasets in 12:12LD, once presumed free-running in DD (at least 2 weeks post-change from LD) and when presumed arrhythmic in LL (at least 2 weeks post-change from DD) to assess period length.

4.4 Results

Results are presented for the group of 3 Temperature mice (M1T, M2T and M3T) and the 5 EEG mice (M1-5 EEG) in the following order;

4.4.1 Three Temperature mice in 12:12 LD

4.4.2 Five EEG mice in 12:12 LD

4.4.3 Three Temperature mice in transition from LD to DD

4.4.4 Three Temperature mice in DD

4.4.5 Three Temperature mice in transition from DD to LL

4.4.6 Three Temperature mice in LL

4.4.7 Temperature and Locomotor activity in Three Temperature mice

4.4.8 Cosinor analysis to assess period length for Three Temperature mice in LD, DD and LL

4.4.1 Three Temperature mice in 12:12 LD

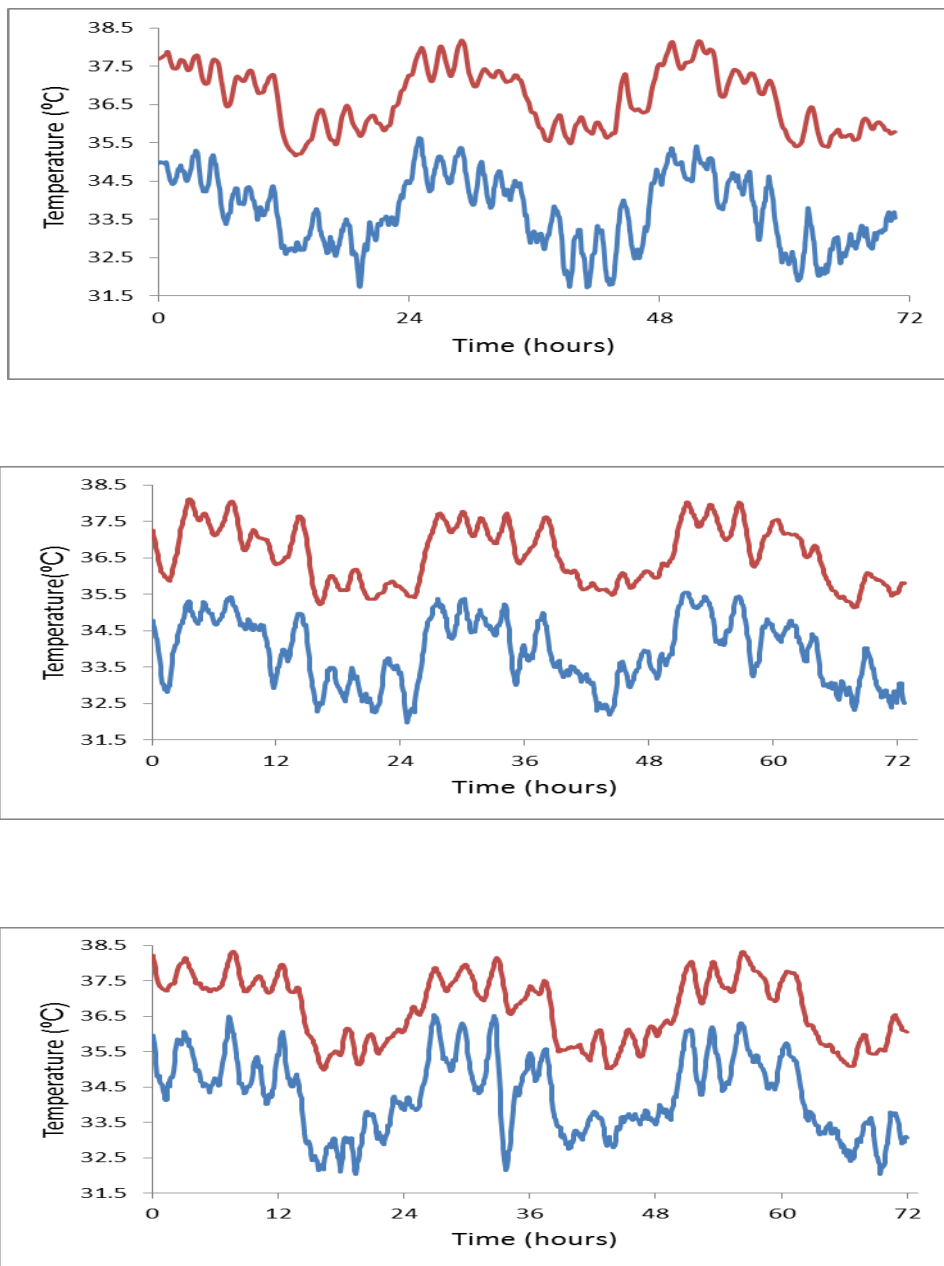


Figure 4.11 Peripheral (Optris, in blue) and core (DSI, in red) temperatures recorded over 72 hours for M1T, M2T and M3T (in vertical order).

Table 4.3 R² values for three Temperature mice in 12:12 LD.

Mouse	R ² value
M1T	0.92
M2T	0.94
M3T	0.91

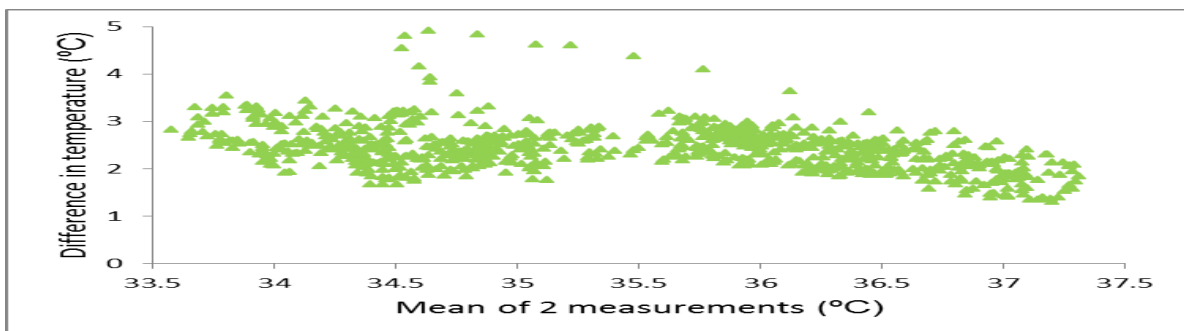
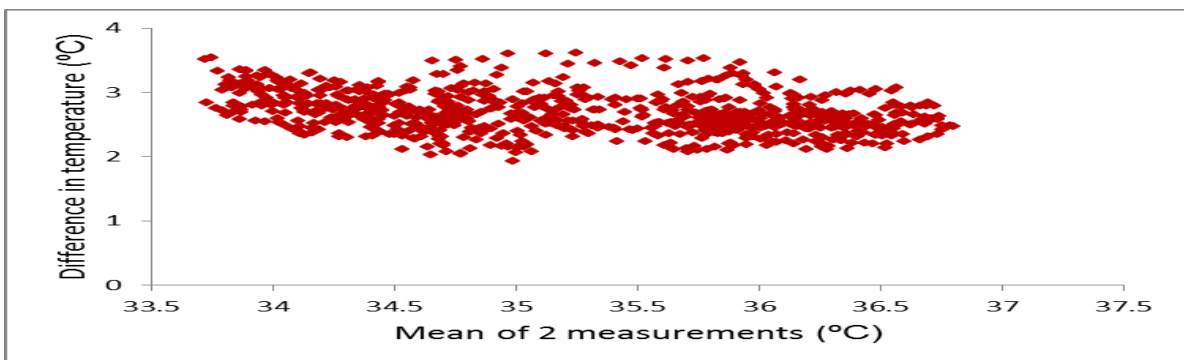
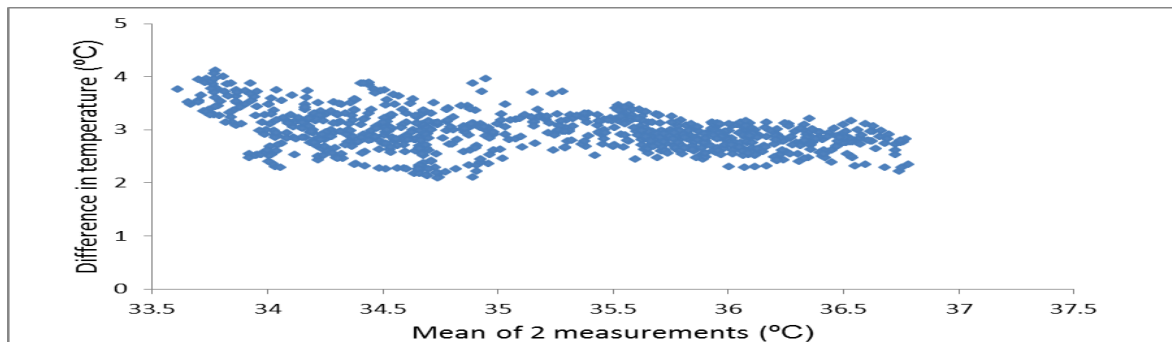


Figure 4.12 Individual Bland Altman plots for M1T, M2T and M3T in 12: 12 LD (in vertical order)

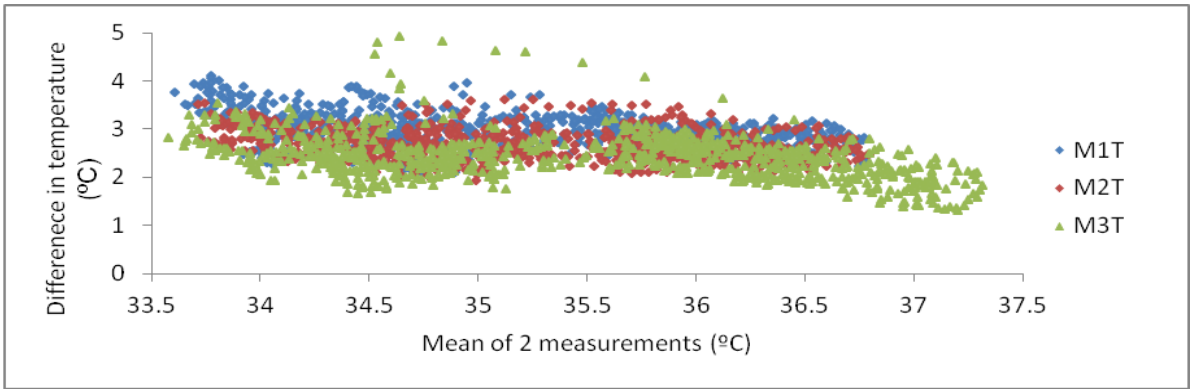


Figure 4.13 Combined Bland Altman plot for 3 temperature mice in 12:12 LD showing a visually-estimated stable relationship of 2.5-3°C between the two methods of measurement.

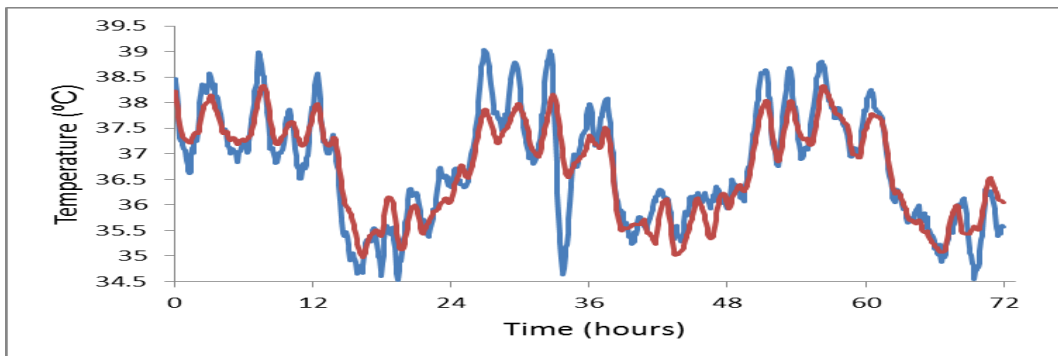
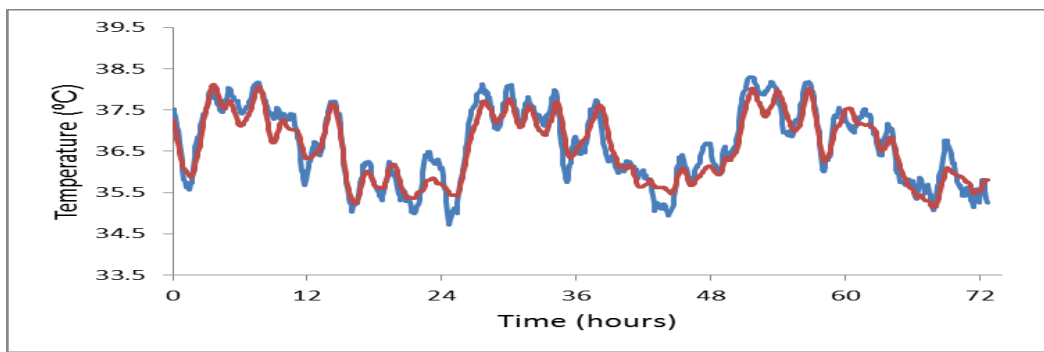
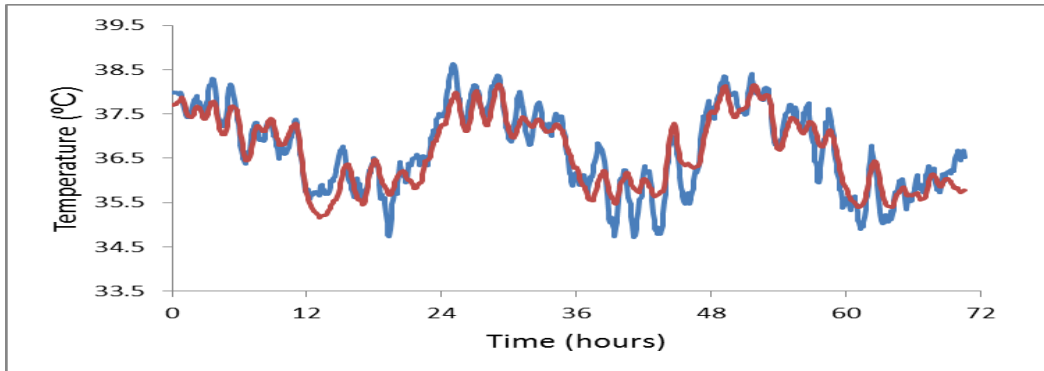


Figure 4.14 Plots of absolute core temperature values (red) and peripheral values (blue) with between 2.5-3° added, showing a strong correlation with the core temperature series; M1T (peripheral temperature plus 3°), M2T (peripheral temperature plus 2.75°) and M3T (peripheral temperature plus 2.5°) in vertical order, mice housed under 12: 12 LD cycle.

4.4.2 Five EEG mice in 12: 12 LD

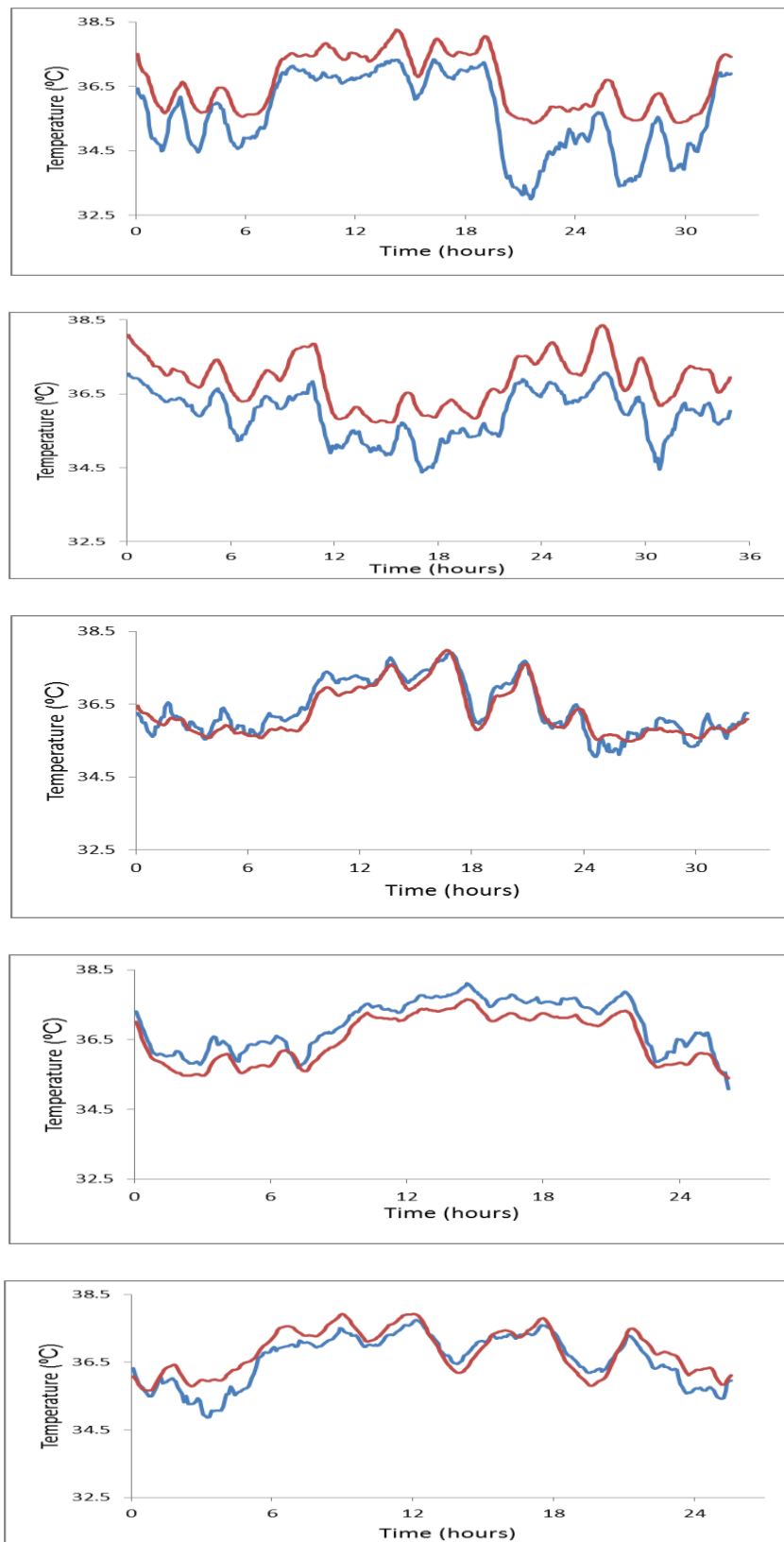


Figure 4.15 Peripheral (blue) and core (red) temperatures for M1-M5 EEG, recorded over 24-36 hours in 12:12 LD (in vertical order).

Table 4.4 R² values for five EEG mice under 12:12 LD cycle.

Mouse	R ² value
M1EEG	0.92
M2EEG	0.91
M3EEG	0.95
M4EEG	0.97
M5EEG	0.89

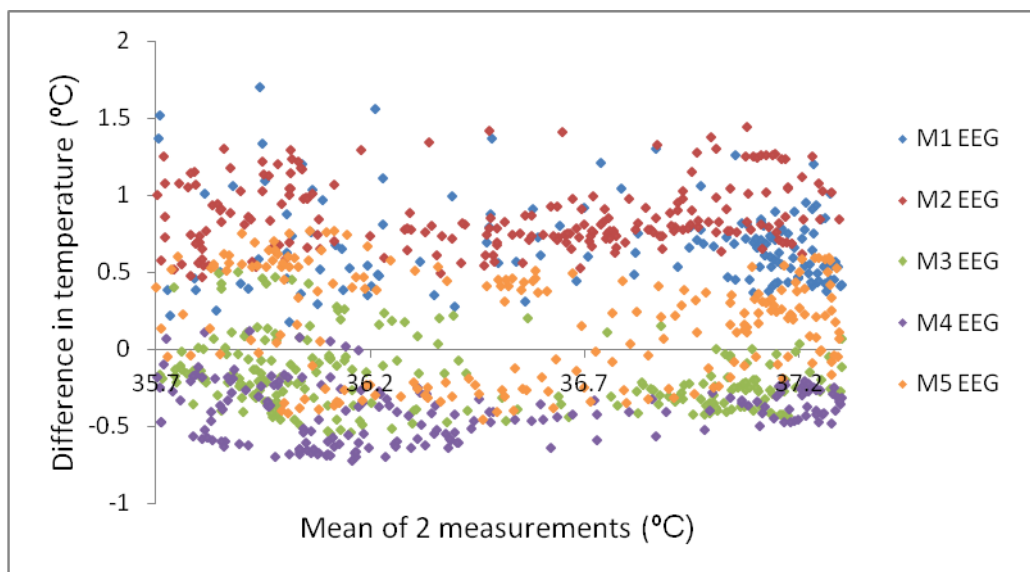


Figure 4.16 Bland Altman plot for M1-5 EEG in 5 different colours; showing a variable difference between the two methods and some mice had warmer peripheral than core temperatures (seen as negative values on the Y axis).

4.4.3 Two Temperature mice in transition from 12:12 LD to DD

(Peripheral temperature data for M2T lost due to a technical issue)

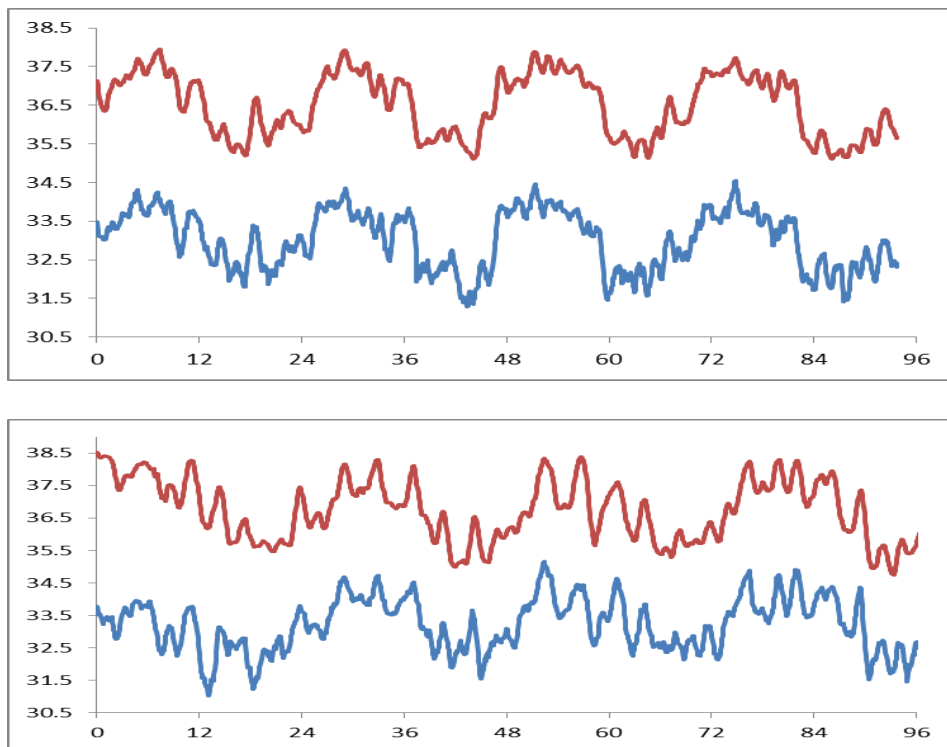


Figure 4.17 Peripheral (blue) and core (red) temperatures recorded for M1T and M3T during transition from LD to DD (in vertical order).

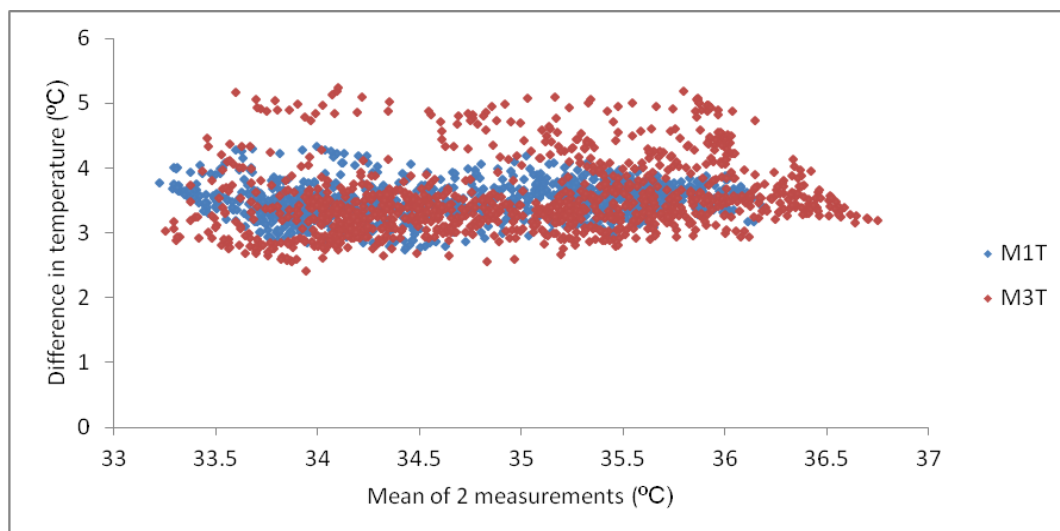


Figure 4.18 Combined Bland Altman plot for M1T and M3T in transition from LD to DD showing a stable relationship of approximately 3.5°C (as estimated by eye) between the two methods.

4.4.4 Three Temperature mice in DD

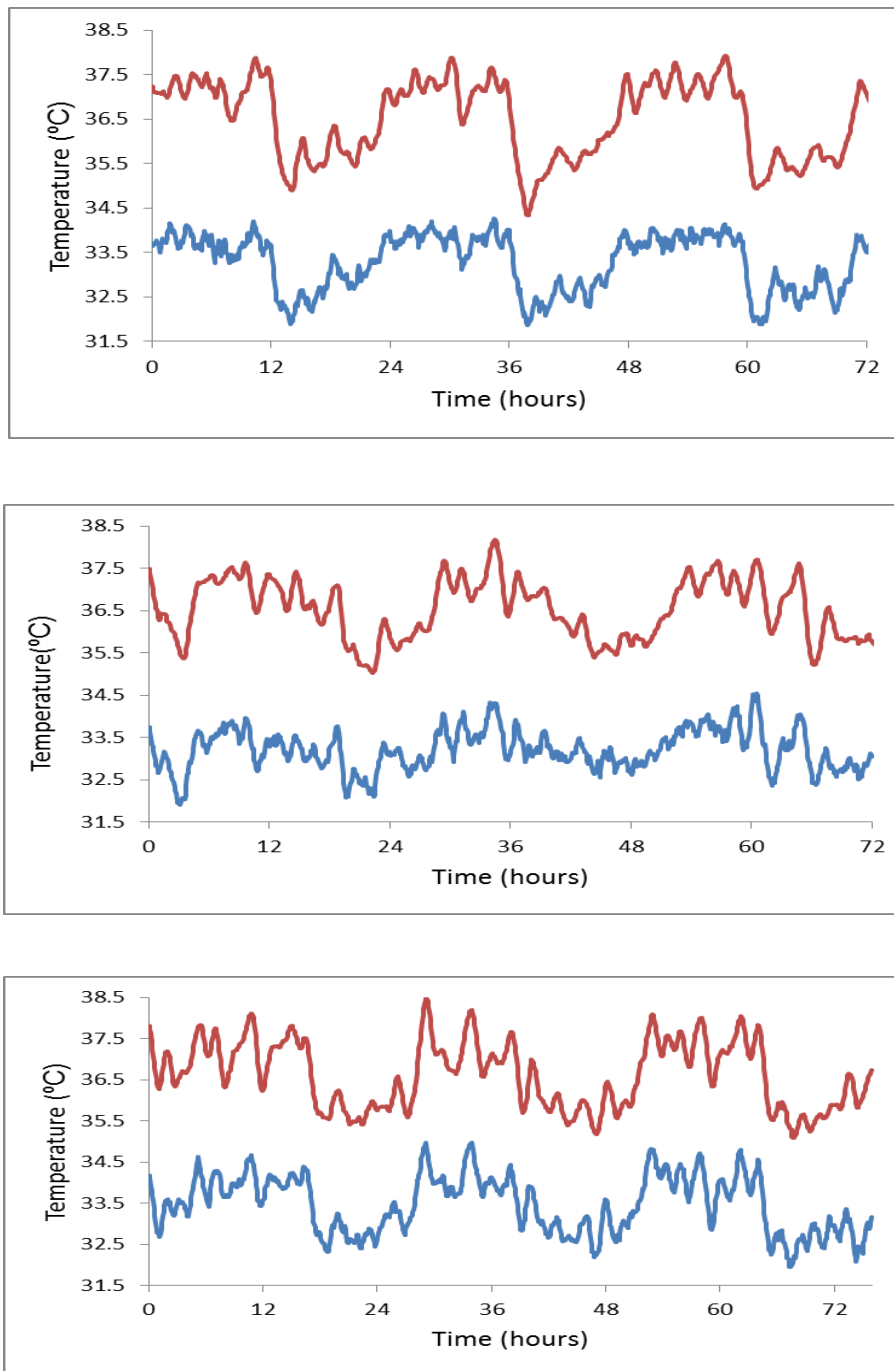


Figure 4.19 Peripheral (blue) and core (red) temperature for M1T, M2T and M3T in DD (in vertical order).

Table 4.5 R² values for 3 mice in transition to DD and when free-running in DD.

Mouse	R ² value for transition into DD	R ² value for DD
M1T	0.94	0.94
M2T	n/a	0.87
M3T	0.84	0.94

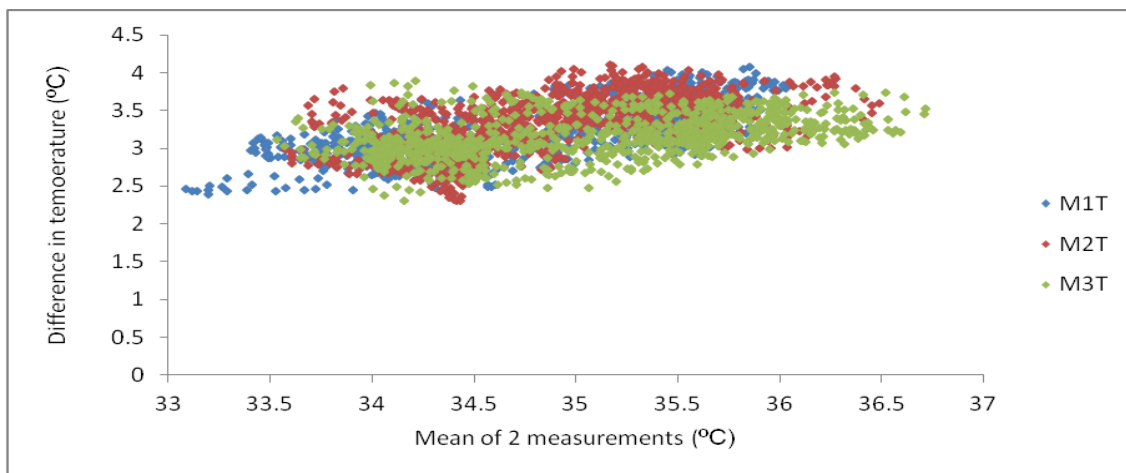


Figure 4.20 Combined Bland Altman plot for M1T, M2T and M3T in DD showing a stable relationship of 3- 3.5°C (as estimated by eye) between the two methods. The difference between the absolute values of peripheral and core temperature appears to be 0.5° greater in DD than that recorded in 12:12LD (2.5-3.0°C).

4.4.5 Three Temperature mice in transition from DD to LL

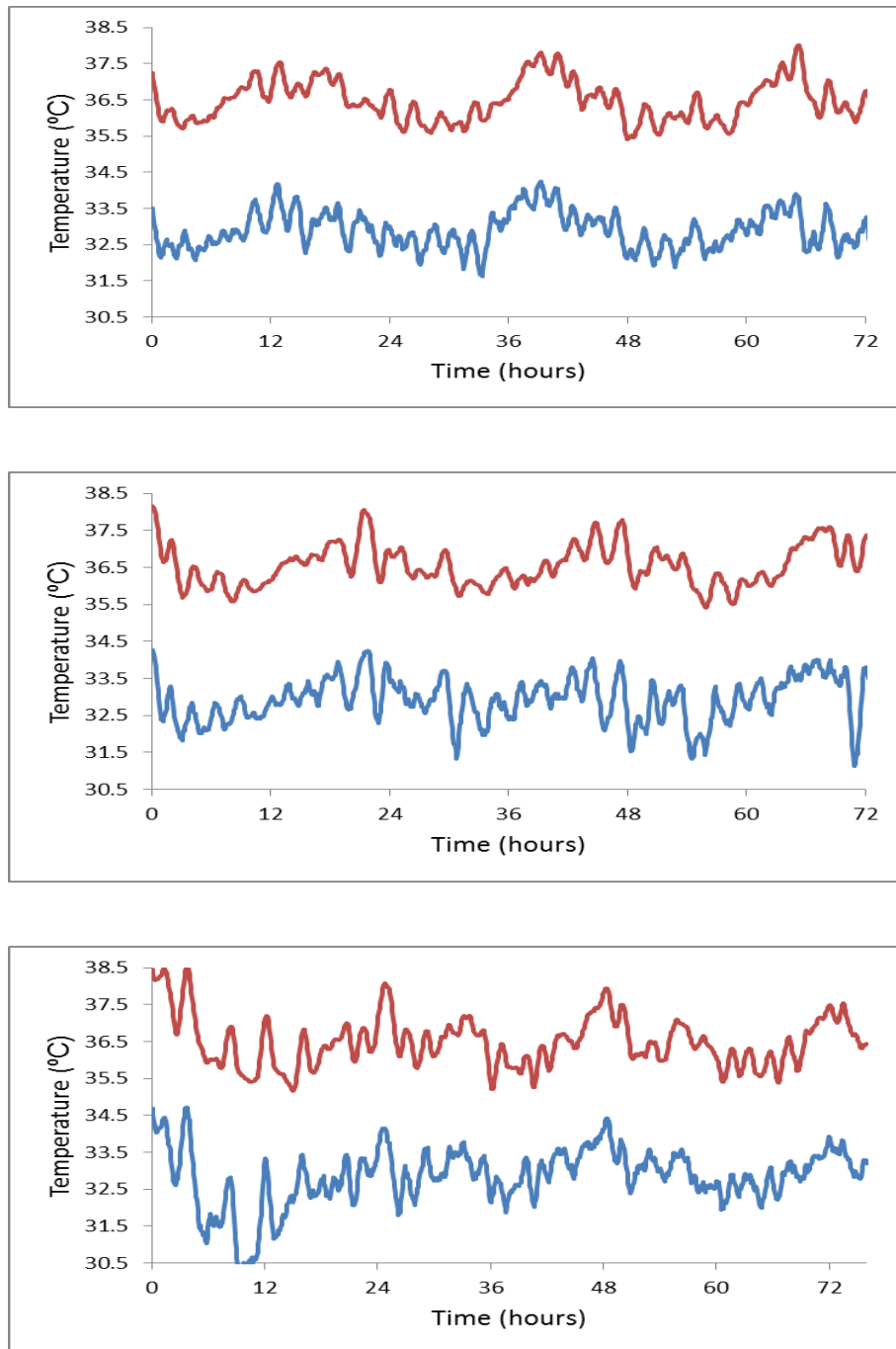


Figure 4.21 Peripheral (blue) and core (red) temperatures for M1T, M2T and M3T in transition from DD to LL (in vertical order).

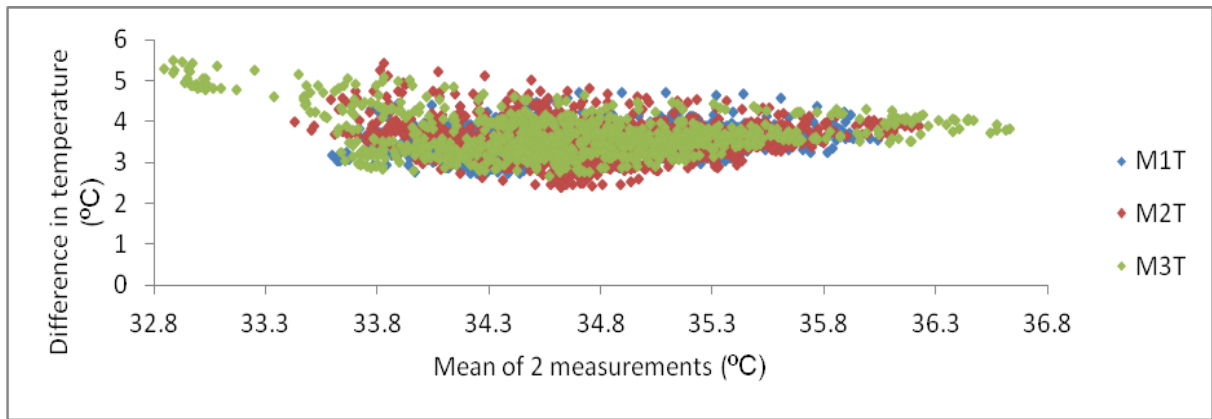


Figure 4.22 Combined Bland Altman plot for M1T, M2T and M3T in transition from DD to LL showing a stable relationship of approximately 3.5°C between the two methods (as estimated by eye). Note that the difference between peripheral and core temperatures of M3T seems to be greater, around 4°C.

4.4.6 Three temperature mice in LL

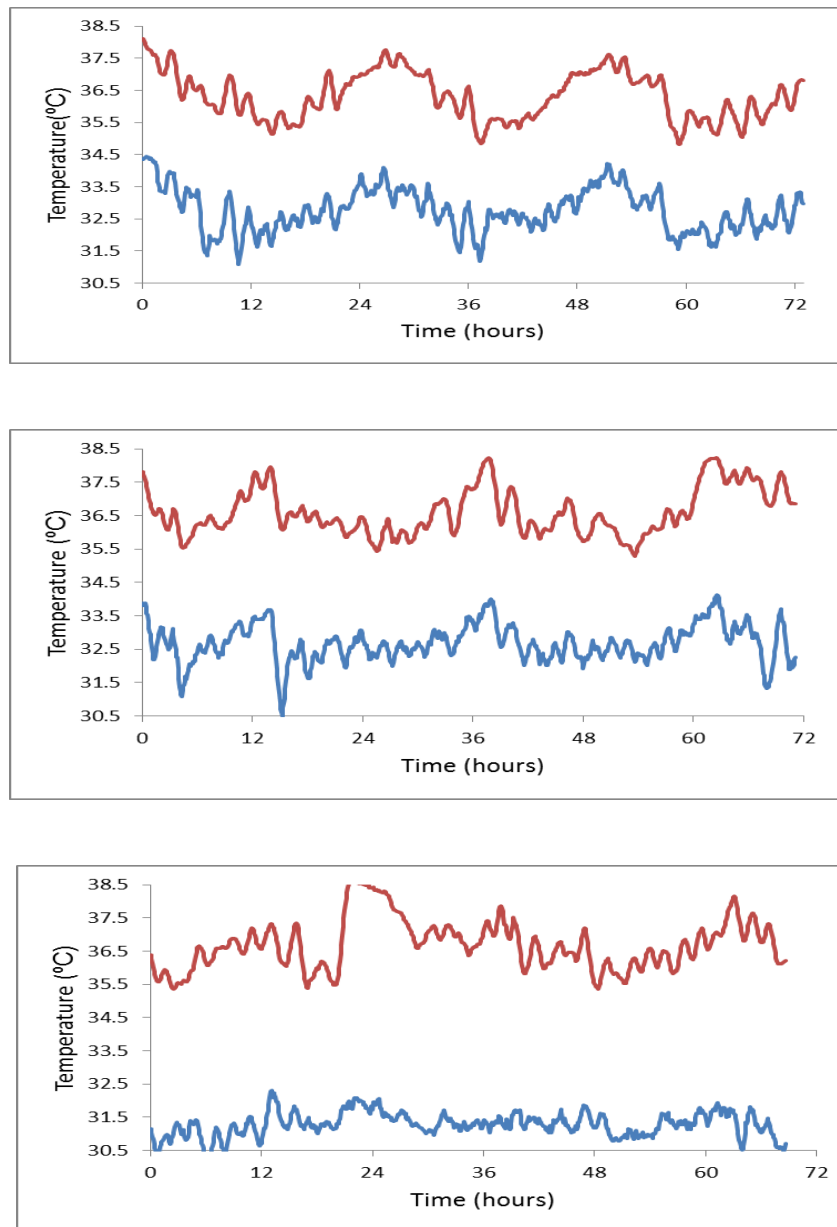


Figure 4.23 Peripheral (blue) and core (red) temperatures for M1T, M2T and M3T in LL (in vertical order). Note the larger (approximately 5°C difference) between methods for M3T and the steep rise in the DSI timeseries towards the end of the first 24 hr period. A clear circadian rhythm of temperature is most evident in M1T and hard to recognise in M3T.

Table 4.6 R² values for M1T, M2T and M3T in transition from DD to LL and in LL.

Mouse	R ² value for transition into LL	R ² value for LL
M1T	0.83	0.86
M2T	0.65	0.72
M3T	0.77	0.59

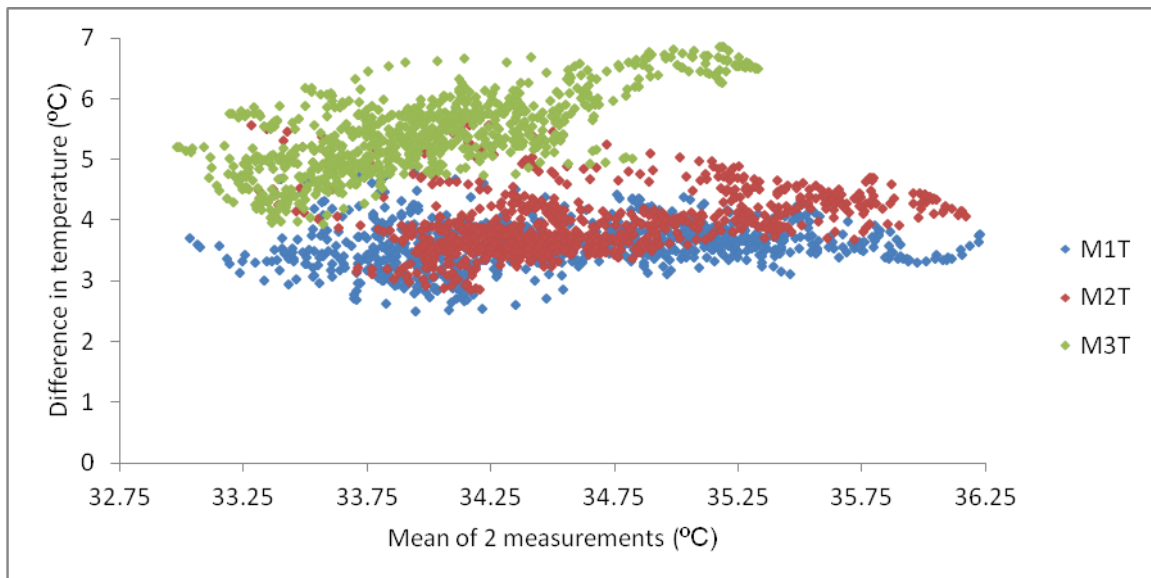


Figure 4.24 Combined Bland Altman plot for M1T, M2T and M3T in LL. A stable relationship between core and peripheral temperatures is still evident for M1T and M2T but the difference for M3T has increased to >5°C.

4.4.7 Activity and body temperature rhythms

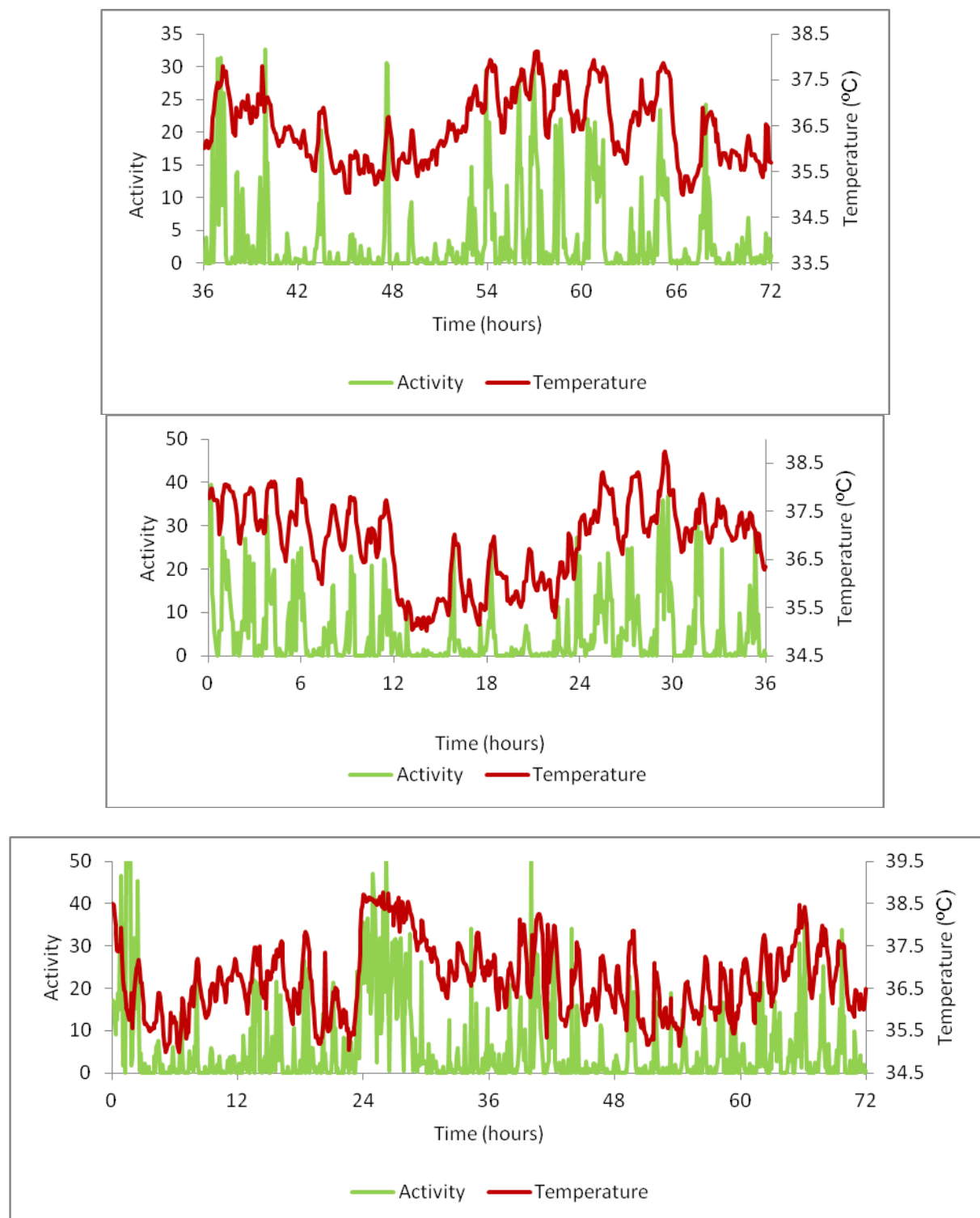


Figure 4.25 Average activity and core temperature plots for M1T in LD, M2T in DD and M3T in LL (in vertical order) showing that temperature matches activity rhythm and spikes in activity underlie ultradian rhythms in temperature- note that the steep rise just prior to 24 hours for M3T is associated with an increase in activity level.

4.4.8 Cosinor analysis for assessment of period length;

Three Temperature mice in LD, DD and LL

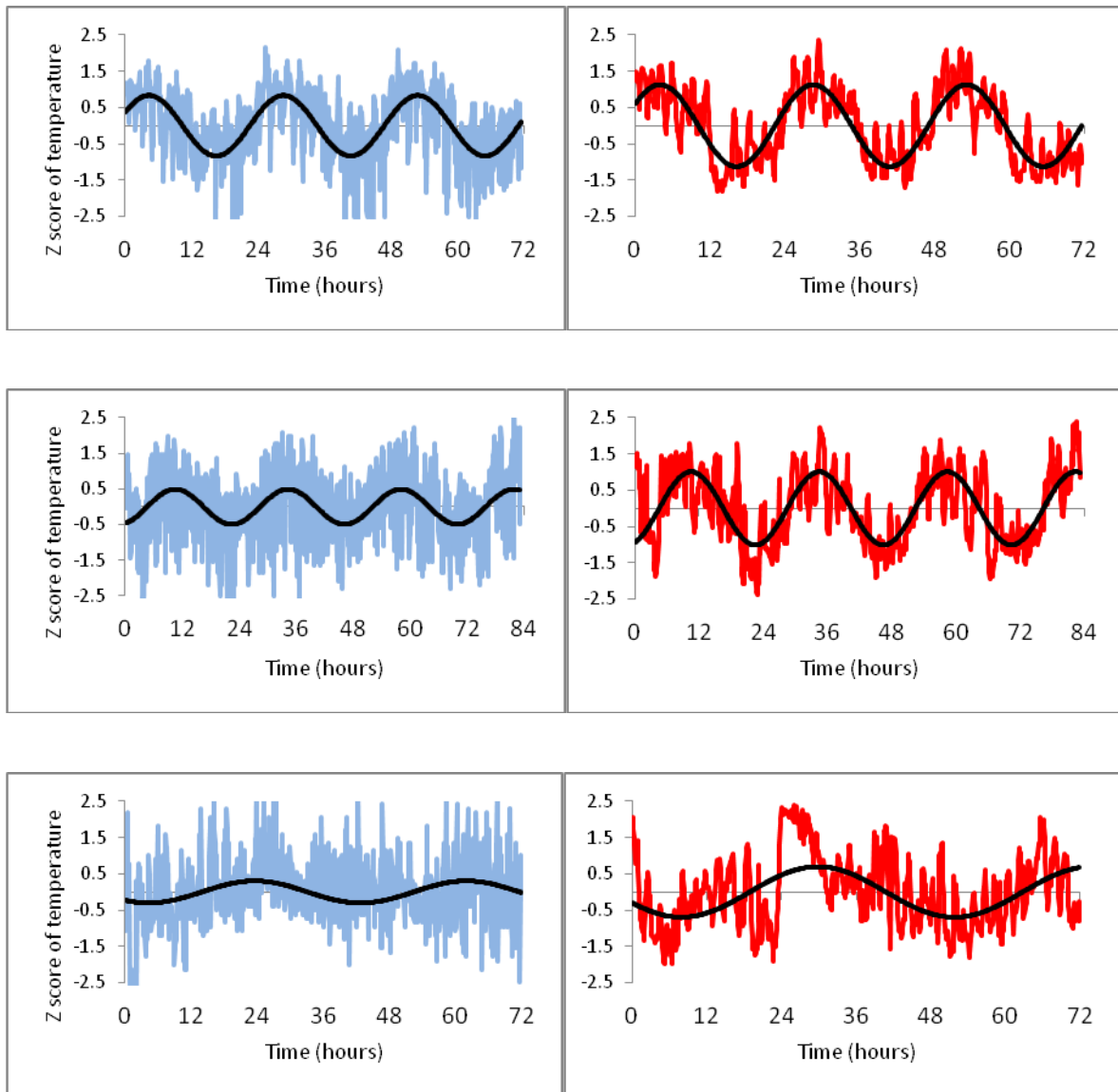


Figure 4.26 Curve fitting by non-linear regression using R (peripheral temperature plot in blue, core temperature plot in red) to determine τ in M1T in LD, M2T in DD, and M3T in LL (in vertical order); Z scores of the absolute temperature values plotted against time. Note the difference in amplitude between core and peripheral values for M1T and M2T (DSI amplitude greater) and the lack of an appreciable circadian rhythm for M3T.

Table 4.7 *Tau* values for peripheral and core temperature datasets for each Temperature mouse in LD, DD and LL. The temperature of M3T appears to be arrhythmic in LL and was therefore excluded from the average value.

Mouse	<i>Tau</i> in LD (hours)		<i>Tau</i> in DD (hours)		<i>Tau</i> in LL (hours)	
	Periphery	Core	Periphery	Core	Periphery	Core
M1T	24.28	24.57	24.48	23.92	25.48	24.97
M2T	24.68	24.69	23.79	23.95	25.41	25.54
M3T	25.07	24.68	24.31	24.38	38.45	43.88
Average of 3	24.68	24.65	24.19	24.08	25.45 (M3T excluded)	25.26 (M3T excluded)

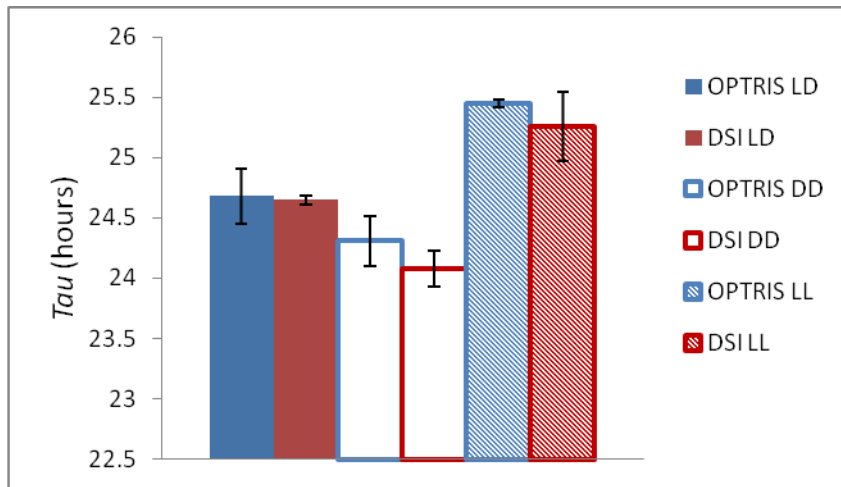


Figure 4.27 Average calculated τ values for peripheral (Optris) and core (DSI) temperatures + S.E.M. for M1T, M2T and M3T in different photoperiods (M3T excluded from LL average due to loss of temperature rhythm). Period length shortens in DD and lengthens in LL.

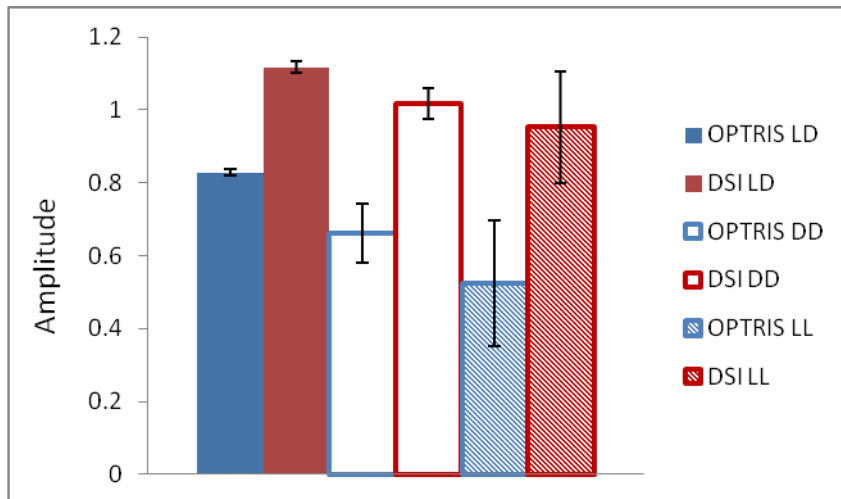


Figure 4.28 Average amplitude values for peripheral (Optris) and core (DSI) temperatures + S.E.M. for M1T, M2T and M3T in different photoperiods (M3T excluded from LL averages due to loss of temperature rhythm). Amplitude of DSI temperature rhythm is always > Optris rhythm.

4.4.9 Summary of Results

A clear circadian rhythm was visible in temperature timeseries plots for all mice in LD, by either method. Rhythms persisted in DD and for two out of three mice in LL. The daily temperature range is approximately 4°C in the periphery and 2.5°C in the core and there appears to be a relatively constant relationship between the absolute values of either method as the peaks in their rhythms are highly conserved and a linear trend can be seen in the Bland Altman (BA) scatterplots, indicating that there is no difference in the correlation at values at the extremities of the physiological range. The specific results per experimental group/light condition are discussed below;

Table 4.8 Average values per group for R² and BA temperature difference (M3T was excluded from LL calculation). BA difference was estimated by eye from the BA scatterplots.

	Temperature mice					EEG mice
	LD	Into DD	DD	Into LL	LL	LD
R² value	0.91	0.89	0.92	0.75	0.72	0.94
BA difference (°C)	2.5-3	3-3.5	3-3.5	3-3.5	3.5 (M3T = 5.5)	variable

4.4.1 and 4.4.2 Temperature and EEG mice in 12:12 LD

The average values for R² per group of mice show that there is >90% correlation between peripheral and core temperature during LD recordings. The temperature difference between methods (calculated by eye from Bland Altman plots) is a stable 2.5-3°C in

Temperature group mice (see Figure 4.11) but extremely variable in EEG mice where the peripheral temperature of some mice was greater than the core (see Figure 4.14).

4.4.3 and 4.4.4 Temperature mice in transition from LD to DD and in DD

Analysis of Temperature group mice in DD revealed that a comparable correlation persists compared to LD data but the temperature difference seen on Bland Altman plots increases slightly to 3-3.5°C (see Figure 4.18). The period length was not expected to alter within 72 hours of initiating complete darkness but it was useful to assess if the correlation between thermal camera and telemetry methods was retained in the early stages of *zeitgeber* change.

4.4.5 and 4.4.6 Temperature mice in transition from DD to LL and in LL

In both transition into and in established LL conditions the correlation coefficient decreases and Bland Altman temperature difference increases slightly to approximately 3.5°C for two mice (see Figure 4.20), and considerably more, to 5.5°C for one mouse (see Figure 4.22). The range of peripheral temperature oscillation as measured by thermal imaging appears dampened for M3T and this mouse seems to have become arrhythmic.

4.4.7 Activity and body temperature rhythms

Combined plots of temperature and activity (measured by relative displacement of the DSI transmitters over the receiver base) are shown for M1T in LD, M2T in DD and M3T in LL (Figure 4.23). Evaluation of temperature and activity plots in all mice across all light conditions show that ultradian rhythms of body temperature are determined by locomotor activity. The linear rise in core temperature just prior to 24 hours for M3T seems to be

associated with activity although the trend is not characteristic of body temperature rhythms seen previously in this mouse and cannot be explained.

4.4.8 Cosinor analysis of period length in LD, DD and LL

The period of the temperature rhythms recorded by both methods is approximately 24 hours under 12:12 LD cycle. *Tau* shortens in DD, as expected as the free-running period of C57BL/6 mice is approximately 23.7 hours in constant conditions. *Tau* increases to >25 hours in LL for M1T and M2T, also expected and one mouse (M3T) becomes arrhythmic (see Table 4.6 and Figure 4.24). Period lengthening followed by arrhythmia is a common feature of the activity rhythms of mice when housed under constant light conditions. There was a small variation in the absolute period values between the two methods and the amplitude of the temperature rhythms was always greater from the core temperature recordings (see Figure 4.26).

4.5 Discussion and Conclusion

4.5.1 Discussion of the methods

The Optris thermal camera offers a consistent method of recording peripheral temperature longitudinally in mice, a new application compared to its typical use, assessing the heat signature of inert materials in industry. The hotspot tracker seemed to capture the point of maximum temperature on the mouse's face, particularly around the eye, a well-vascularised area (see Figure 4.4). Core body temperature is traditionally measured and the coefficient of correlation between peripheral temperature data and the DSI telemetry established method of measuring core body temperature was 0.91 under standard 12:12 LD cycles. When mice were active their eyes and face were clearly visible but the typical posture adopted when nesting (tucking the head in to the chest) often obscured these from camera view. Recorded values of $<30^{\circ}\text{C}$ seen in raw data sets can likely be attributed to the mouse's face being hidden within the nest. An effort was made to provide sufficient nesting material to satisfy natural behaviour (Gaskill et al., 2013) and allow adequate insulation (particularly post-surgery) but this may have resulted in values which were not the hotspot of the animal being recorded. The calculation of the 5 minute maximum value during data processing meant that low values were not problematic. In general, the method of taking surface radiation hotspot measurements using a camera mounted above the cage works well as the face is an easily visible, well-vascularised area of the mouse. Imaging the tail has been reported for singular temperature assessments but rodents use their tail to thermoregulate via arteriovenous anastomoses (Gordon, 1993) so vascular tone to this area will be more variable than to the face.

The major flaw of the Optris software was that data were not saved automatically and some datasets were lost due to inadvertent minimising of the recording window, or closure of the laptop lid. The live image projected did allow limited welfare checks, as one on occasion the water bottle leaked and this was detected from outside the thermal cabinet as a cooler area on the cage floor. High temperatures were seen following transfer from holding LTCs to the thermal cabinet; despite retaining the mouse in its home cage and waiting for 10 minutes before recording, suggesting that stress related hyperthermia of the periphery is persistent, in concurrence with reports of the chronic nature of elevation in core temperature after restraint (Poole and Stephenson, 1977). It was not possible to start each recording at the same time in relation to the LD cycle so there may have been a temporal effect on the magnitude of the rise in temperature following moving. The core temperature rhythms recorded via DSI telemetry were much cleaner and more stable, as expected. The quality of the recordings were generally poor in the group of three Temperature mice with frequent loss of signal and return of *NaN* and non-physiological values, requiring significant filtering to extract genuine measurements. Loss of signal may occur if the mice climb on the underside of the cage lid as they increase the distance between the transmitter and the receiver base (and no loss was seen in the EEG group mice which did not have cage lids to climb on). The Bland Altman plots show that the initial temperature difference of 2.5- 3°C between methods increased over time, reaching 3-3.5°C in DD and LL recordings for two of the mice. The third mouse recorded significantly different temperatures (>5°C) towards the end and, as several months had elapsed this could be due to transmitter drift.

4.5.2 Discussion of the results

Peak values were highly conserved between peripheral and core temperature dataplots of Temperature- and EEG-implanted mice, with some variability at the lower end of the range between methods, although in general the degree of correlation was high, around 90% in LD and DD recordings. Comparison of core and peripheral temperatures during LL recordings revealed lower correlational values (average $R^2 = 0.72$) which may be due to arrhythmia (as occurred in one mouse, see below) or to a change in the temperature distribution between the core and the periphery, or to changes in transmitter performance/consistency over time as this experiment ran over several months and LL recordings were the final data collected.

Optris peripheral values were between 2.5- 4.0°C (estimated by eye from Bland Altman plots) lower than DSI core temperature in the first group of three Temperature mice. Thermography of the periphery in LD (the first light condition) revealed a 2.5- 3.0°C difference and this increased to 3.0- 3.5°C under DD conditions. There was a further increase to 3.5- 4.0°C for two of the three mice under constant light and one mouse showed a difference of >5°C (M3T, the mouse which became arrhythmic above). This experiment ran over several month's duration; several 72 hour recordings were made in each light condition and it could be repeated on a tighter timescale to see if the changes in the Bland Altman plots occurred again.

The stable relationship between methods seen in the Temperature mice did not extend to the group of five EEG mice, where the hair had been clipped for craniotomy surgery, to implant the EEG electrodes in the skull. Some mice of this group showed peripheral temperatures equalling or greater than those of the core, some were lower and in general there was no appreciable trend. The removal of hair increases the emissivity of the skin and

as this set of mice were between 10 days and 3 weeks post implantation surgery the hair had not yet grown back (and rates of regrowth vary between individuals) which may account for the differences seen. One other reason may be the configuration of the surgical implant; two small roundhead screws are inserted into the skull and covered with dental cement to secure the biopotential electrodes in place. In some mice the skin margins were apposed over the entire screw/electrode/cement assembly and in some the skin was only secured at the cranial and rostral extremities as the amount of dental cement applied was too large to achieve primary closure. The stainless steel screws, present under a thin layer of dental cement may have radiated more heat (as a result of conductance from the skull and surrounding tissues) than normal skin would have. The degree of vascularisation of the surgical wounds is also variable and depends on factors such as size of wound (number of skin vessels disrupted by incision), time elapsed since surgery and tension applied during closure. The R^2 coefficient of correlation values are high for each EEG mouse (average = 0.94) and inspection of the timeseries plots shows that the difference between thermal imaging and core telemetry methods for each animal are stable which suggests that the peripheral thermal hotspot did not change within a single mouse.

The poor reliability of the core data (compared to thermal imaging as a novel, unproven method) was disappointing and datasets required considerable filtering. The physiological range filter was chosen from viewing raw data timeseries plots for each mouse and the second filter, where values differing from their neighbours by more than 0.5°C were discounted was chosen arbitrarily, from viewing DSI temperatures taken at 1 second resolution, where the majority of adjacent values varied only by 0.01°C (over 1- 10 seconds).

Both methods indicated a clear circadian rhythm of body temperature although thermal imaging values were more labile than those of the core, as measured by DSI telemetry (amplitudes of oscillation were approximately 2.5° for the core and 4.0° for the periphery). Small radio frequency devices are available for identification of mice and some can also record temperature (see <http://www.bmds.com/products/transponders/iptt-300>). A study comparing hypothermia in rodents after dosing with infectious agents found no difference between subcutaneously or intraperitoneally- located microchips and rectal temperature (Kort et al., 1998). If subcutaneous temperature is a reliable marker of core body temperature then there is no indication to implant any device deeper in the body, improving welfare and reducing the duration and financial cost of scientific studies in which temperature data is required. Further studies using microchips could investigate the presence of temperature rhythms in subcutaneous locations, it seems probable that they exist although their amplitude is likely to be smaller, more like that of the core than the surface.

There were no commercially available methods of tracking body temperature longitudinally at the time this validation experiment started. A short pilot study was undertaken using the IPTT-300 microchip listed above, injected in the subcutaneous space of two mice. A prototype hands- free reader was trialled but did not yield any useful results. New technology is now available to do this, even in group housed animals (see <http://www.actualanalytics.com/actualhca/actualhca>) and this has further applications within circadian and behavioural research.

Body temperature has not been used extensively in murine circadian studies to date. Reasons for this include the need to place telemetric transmitters surgically (Clement et al.,

1989), or the confounds caused by the stress of restraint when collecting rectal temperature measurements (Poole and Stephenson, 1977). Tracking activity using running wheels has delivered most of the information required by circadian biologists using rodents (Verwey et al., 2013) but this has some limitations; various environmental and inherent factors influence this highly plastic behaviour which may also become self-reinforcing or addictive (Sherwin, 1998). Other methods of monitoring more “natural” behaviours are thought to be superior, such as passive infrared motion sensors within the home cage recording basal activity levels, avoiding the need for a running wheel (Pritchett et al., 2015).

It is known that body temperature of mice is tightly linked to locomotor activity (Weinert and Waterhouse, 1998), although temperature oscillations continue even if activity levels subside (Weinert et al., 2002). Peaks in activity rhythms gave rise to ultradian rhythms of body temperature in this experiment which is as reported in the literature (Aschoff, 1983). As peripheral temperature is strongly correlated with that of the core it is expected that similar results would be seen if thermal imaging of the surface hotspot replaced telemetry in these activity/ temperature studies. Temperature monitoring offers scientists a physiological marker which is unlikely to be affected by moderate fluctuations in behaviour and could be substituted for, or measured adjunctively with locomotor activity in circadian experiments. Changes in temperature rhythms may be seen when the LD cycle is altered, such as during lights pulses or the induction of phase shifts or when food is restricted and non-invasive methods of assessment permit monitoring in many different experimental situations.

The period length of the temperature rhythm, τ was examined in LD, DD and LL light cycles. Period lengths were calculated by converting temperature values into Z scores and using non-linear regression techniques in R to fit curves to the data. Refinetti (2007) suggests that Fast Fourier Transforms of the data may generate more accurate results and this method could be used in future experiments. The average τ value across three C57BL/6 mice was 24.67 hours in 12:12 LD, this decreased to 24.19 in DD; moving closer to the free-running period of the mouse, 23.7 hours as described by Arraj et al. (2006a). τ lengthened when the Temperature mice entered the LL condition with average values of 25.46 and 25.26 for peripheral and core temperatures respectively. All changes in τ noted here follow those seen in locomotor activity rhythms through LD, DD and LL conditions. Eastman and Rechtschaffen (1983) found that the body temperature rhythm of rats persisted longer than that of the sleep wake cycle in LL. Temporal deviations in surface blood flow in humans are known to affect sleep propensity (van den Heuvel et al., 2003) and longitudinal thermal imaging of sleep mutant mice may well reveal abnormalities of their peripheral temperature.

Benstaali et al. (2001) report that rhythm of temperature and locomotor activity may decouple. Arrhythmia occurred in both locomotor activity and temperature rhythms in one mouse in this study and it is possible that this was a result of being under LL conditions longer than the other two mice (as M1T and M2T were recorded before M3T, following photoperiod change in the holding LTC). It is not known if there was decoupling, or which parameter became arrhythmic first but this would be possible with continuous monitoring of mice rather than recording for 72 hour intervals. The range of oscillation or amplitude

(see Figure 1.1) was greater in LD than in DD or LL cycles for all mice, as described by Aschoff (1980).

4.5.3 Conclusion

Hypothesis: Using infrared thermography/ thermal imaging to measure peripheral surface radiation is a valid method of assessing the body temperature of mice.

Hypothesis: the circadian rhythm of body temperature, as seen when mice are entrained to a regular light/dark cycle alters under conditions of constant light or constant darkness.

This study proves that thermal imaging of the peripheral hotspot is a reliable method of assessing body temperature in mice. A stable relationship was established between peripheral and core temperature in standard LD cycles) which persisted into constant darkness, where the free-running endogenous period of peripheral temperature could be easily distinguished. Subsequent recording under constant light conditions also resulted in increases in the period length, *Tau*. Thermal hotspot tracking therefore has further potential within circadian studies where temperature rhythms can be assessed following experimental interventions or when phenotyping transgenic models. A completely non-invasive method, infrared thermography can be used without licence authority and is therefore applicable as an adjunctive measure in many animal experiments. The mouse is prone to hypothermia due to its small size and high surface area to body volume ratio and standard laboratory conditions house mice at temperatures which are comfortable for humans but fall below the murine thermoneutral zone. Body temperature is often not recorded during research studies due to the reasons outlined above, yet veterinary

assessment of mice displaying increased morbidity following procedures reveals that the majority are hypothermic and suggests that more rigorous monitoring of temperature should occur to guide interventions to improve welfare. Thermal imaging would be particularly useful in monitoring rodents recovering from anaesthesia, or in regulatory toxicology studies where temperature decline is one of the variables used to predict and apply the humane end point.

Chapter 5

Effect of implantation surgery on the post-operative core and peripheral body temperature of mice

Hypothesis: Surgery and anaesthesia disrupts the circadian rhythm of peripheral and core body temperatures

Hypothesis: The duration of surgery and anaesthesia is positively correlated with the degree of post-operative temperature disruption

This chapter is supplementary to Chapter 4 and briefly describes the post-operative changes in body temperature following anaesthesia and transmitter implantation, including a short review of the background literature.

Acknowledgements: Some data included in this chapter was collected from two cohorts of mice, surgically prepared for ECG and EEG/EMG data collection, during anaesthesia and in the immediate post-operative period. These mice were destined for use in other experiments and permission to use this data, granted by Dr. Sibah Hasan is acknowledged.

Circadian terminology is listed prior to the Table of Contents.

5.1 Introduction

Anaesthesia is a pre-requisite for carrying out painful surgical procedures on any animal. General anaesthesia should induce narcosis, muscle relaxation and analgesia (Hart, 1971) in proportions required by the procedure but may impair normal physiology in a dose-dependant manner. It is difficult to distinguish between the post-operative effects of anaesthesia and surgery but it is relatively straightforward to observe, evaluate and improve the quality of applied surgical techniques. Refining anaesthetic management is therefore vital for both the quality of the scientific data generated and the overall welfare of the animal.

5.1.1 Anaesthesia of laboratory mice

General anaesthesia of mice can be achieved using either injectable or volatile agents. Injectables are usually given intraperitoneally and provide a limited duration of anaesthesia depending on the degree of absorption from the injection site (Flecknell, 1996). A variety of drugs can be combined in many anaesthetic “cocktails”, resulting in different periods of surgical tolerance (Arras et al., 2001); short procedures may use propofol, an α -2 agonist and fentanyl for around 20 minutes of anaesthesia (Alves et al., 2009), the commonly used ketamine and α -2 agonist combination can deliver slightly longer anaesthesia (Flecknell, 1996), and neuroleptanalgesic combinations such as fentanyl and fluanisone, combined with midazolam can produce anaesthesia for over an hour (Jong et al., 2002). The placement of intraperitoneal injections may be sub-optimal (Wolfensohn and Lloyd, 2003) and if an animal is not sufficiently anaesthetised following the first injection there is no objective method of deciding how much to “top-up”, without subsequent overdosing. Volatile agents offer more predictable inductions (using an inhalation chamber) and the dose can be

easily titrated to effect, reducing the plane of anaesthesia and improving recovery quality. One disadvantage of volatiles is that procedures on the head are often hampered by the presence of a facemask during maintenance. Customised face masks have been made for stereotaxic frames to use in craniotomy procedures when repeated dosing of injectable agents to last through these typically lengthy surgeries would cause unstable anaesthesia and disrupt physiological parameters. Volatile anaesthesia is a justifiable, popular choice for long duration procedures as rodents recover faster, and fairly stable haemodynamic parameters are maintained when they are used over several hours (Szczęsny et al., 2004). Use of oxygen as the carrier gas also prevents hypoxia which is common when injectables are used alone, especially the α -2 agonists. Isoflurane has been reported as equal to sevoflurane, a newer agent, in terms of anaesthetic quality for laboratory mice (Cesarovic et al., 2010) and both are used successfully although isoflurane predominates. One undesirable effect of volatile agents is that of vasodilation which increases heat loss.

5.1.2 Thermoregulation under anaesthesia

Anaesthesia abolishes the behavioural changes which normally aid thermoregulation and as, behaviour is sustained longer than the autonomic nervous system response in conscious animals (Bicego et al., 2007), hypothermia is a frequent occurrence. The hypothalamic and thermoregulatory effector responses are also attenuated by anaesthesia and metabolic rate is reduced (Imrie and Hall, 1990). Recovering from anaesthesia with concurrent hypothermia results in hypothalamic hypersensitivity to local cooling which may lead to exaggerated thermoregulatory responses (Hammel, 1988). Anaesthetists evaluate mean temperature across two body compartments, considering that the core occupies 66% and the periphery 34% of the total at rest (Imrie and Hall, 1990). Thermoregulatory impairment

under anaesthesia results in peripheral vasodilatation, accelerating heat transfer away from the core and causing central cooling (Deakin, 1998) which contributes to postoperative morbidity. In all species, including humans, a marked drop in temperature occurs on induction and use of cold metal surgical instruments, unwarmed fluids and dry anaesthetic gases can compound the decline (Imrie and Hall, 1990). In human surgeries body temperature usually reduces by 0.5-1°C within 30 minutes (Sessler, 2008). Isoflurane anaesthesia of rats and mice without supplemental warming caused more significant mean temperature drops of 4.42 and 9.9°C respectively (Taylor, 2007). Core temperature can be measured at various sites under anaesthesia; tympanic, external auditory meatal, nasopharyngeal, oesophageal, rectal, axillary, sublingual and within the urinary bladder. All have slightly different values (Campbell, 2008) and rectal temperature is affected by heat produced from gut bacteria, faecal insulation and blood flow to hind limbs so is not always considered accurate, especially where a risk of hyperthermia exists (Imrie and Hall, 1990).

Both core and peripheral temperature should be measured perioperatively to accurately document temperature distribution (Imrie and Hall, 1990). There are limited veterinary studies within this subject area; one examined rectal, coronary band and ear base temperatures with reference to pulmonary arterial temperature, alongside cardiac output in an acute ovine trauma model and found that the core to periphery difference was unrelated to the cardiac output as severe cardiogenic shock was experimentally induced (Mansel et al., 2008). This seems unlikely and suggests that the methods of peripheral measurement were inaccurate, or not taken frequently enough. The daily rhythms of temperature in conscious ewes were measured by Piccione et al. (2013) at different

ambient temperatures and foot temperature was seen to peak three hours before rectal temperature so temporal effects may contribute to the absolute temperature difference.

5.1.2.1 Consequences of hypothermia during surgery

Perioperative hypothermia prolongs the duration of action of inhaled and intravenous anaesthetics, increases thermal discomfort once awake and is associated with delayed recovery. Increased blood loss, reduced oxygen availability to healing tissues and a raised incidence of surgical wound infections may also be seen (Reynolds et al., 2008). In humans, intraoperative core temperatures 1 to 3°C below normal are not uncommon and lead to postoperative shivering which unacceptably increases metabolic rate (Kurz, 2008). In rodents, increasing the ambient temperature to 33°C during recovery from embryo transfer procedures improved implantation rates (Bagis et al., 2004) and decreased neuronal signalling was noted following an intracerebroventricular injection study in hypothermic mice (Holscher et al., 2008). Two studies by Planel et al. (2007) and Xiao et al. (2013) found that hypothermia caused abnormal hyperphosphorylation of tau proteins in Alzheimer's disease model mice, highlighting an additional scientific requirement for normothermia during procedures.

5.1.2.2 Preventing hypothermia under anaesthesia

It is desirable to prevent hypothermia entirely by either actively or passively warming the patient under anaesthesia. In long human surgeries, or where clinical hypothermia is induced, active warming involves placing warm saline deep within the body by gastric lavage, or instillation into the bladder. Passive warming involves warming the periphery of the body by either radiant, convective or conductive methods. Forced warm air blankets are a popular choice in human and veterinary anaesthesia although they are too large to use in

rodents. Homeothermic heating blankets or pads are a good alternative with an integral thermostat which increases the pad temperature in proportion to any decreases in the animal's rectal temperature. Other low-tech but useful methods include insulation with bubblewrap or aluminium foil and "hot hands"- gloves filled with warm water, wheat bags or microwaveable discs which can be placed next to the animal. Care must be taken to avoid scalding, especially of hairless body areas such as the tails of mice. A recent addition to the veterinary and laboratory market is a heated breathing circuit for rodents (<http://www.aasmedical.co.uk/?portfolio=heated-breathing-circuit>). Caro et al. (2013) found that adding a reflective foil improved temperature maintenance of mice more than using either thermogenic gel packs or circulating warm water blankets alone. Rembert et al. (2004) assessed a forced air system, an infra-red heater and a circulating water blanket in the recovery area (not on the mouse) and found that forced air heated the microenvironment quickly and to an optimum ambient temperature. If hypothermia does occur rewarming of the patient should be carried out before recovery (Imrie and Hall, 1990). A human study compared convection and radiant methods and found that neither was superior, suggesting that continued peripheral vasoconstriction was the reason that heat did not transfer to the body core (Weyland et al., 1994). Pre-warming patients to ensure that they are above 36°C before induction minimises initial redistribution hypothermia in human patients (Torossian, 2008) and this is often done prior to blood sampling rodents to cause vasodilation and increase the chance of successful venipuncture.

5.1.3 The effect of anaesthesia and surgery on the circadian system

Gogenur et al. (2007, 2010) found that major surgery disrupted two circadian output rhythms in humans; a phase delay of melatonin secretion and an increased temperature

was seen which did not return to pre-operative levels for two days. The circadian rhythms of rodents suffer disturbances following use of injectable anaesthetics such as pentobarbitone (Ebihara et al., 1988) and propofol (Dispersyn et al., 2010). The concept of chronopharmacology, where the response varies with the phase of the cycle in which the drugs are administered is often not considered and the timing of anaesthesia and surgery in relation to the *zeitgeber* is important (Chassard and Bruguerolle, 2004). Dispersyn et al. (2008) discuss the effects of anaesthetics on circadian temporal structure, noting that maximum hypnotic effects in rodents and rabbits are during the rest phase, suggesting that this variation in potency could be due to circadian variation in the GABA receptor, the site of action of most anaesthetics. Chronopharmacology of inhalational anaesthesia was recognised many years ago when sensitivity to fluothane varied from 5 to 76% in mice, depending on the time of administration (Matthews et al., 1964). More recently, sevoflurane was seen to cause phase delays in locomotor activity and reduced *PER 2* expression levels in mice (Ohe et al., 2011) and rats (Sakamoto et al., 2005). Morphine has a greater analgesic effect during the dark phase as seen in a hot-plate test study of mice (Morris and Lutsch, 1967) and it is known that a cyclical variation of opioid receptors occurs (Chassard et al., 2007). Opioid drugs, which are used frequently for moderate to severe pain also increase body temperature as described by Adler et al. (1988). Post-surgical pain reduces activity and may even affect maintenance behaviours like eating and drinking so circadian disruption is an unfortunate, likely sequel to anaesthesia and surgery, no matter how minor the procedure.

5.2 Methods

This chapter includes supplementary temperature data collected around the time of surgical implantation of two of the three Temperature mice and the five EEG mice described in Chapter 3. In addition, data from three mice implanted with transmitters to measure electrocardiogram (ECG) is included. All mice were implanted with a radiotelemetry transmitter (measuring core temperature, with or without other parameters) inside the peritoneal cavity under identical anaesthetic protocols, although the duration and degree of surgical invasion of the three procedures differed. Rectal temperature was monitored every 5 minutes during surgery and core and peripheral temperature were recorded longitudinally using thermal imaging simultaneously with radiotelemetry upon recovery. The relative changes in core and peripheral temperature were then assessed. Poor post-operative recovery is a common problem in laboratory mice and it is thought that hypothermia compounds the effects of anaesthetic drugs and surgery-associated pain. Supplemental warming and insulation is necessary for all but the most brief procedures and body temperatures, where measured, still drop below normal physiological levels.

5.2.1 General methods

Age and sex- matched inbred strain mice (male, 8-12 weeks old, C57BL/6) were sourced from a commercial supplier (Harlan, UK) and maintained within conventional open-top cages inside light tight chambers (LTCs). Programmable timer plugs controlled the light cycle inside LTCs in a square wave form and the ambient light intensity was 200 lux measured at cage top level. Mice were given *ad-libitum* access to food (RM3(E) irradiated diet, SDS) and chlorinated water (2 x Istachlor Rapid chlorine tablets 0.35mg in 50 litres) and singly-housed to control for the effects of social interactions on body temperature. Substrate bedding

material in cages was *Eco-Pure Chips 6 Premium* (Datesand) and nesting material provided was autoclaved *Sizzlenest* (Datesand). Relative humidity within the LTCs was maintained between 40 and 60 % and temperature between 19 and 21.9°C.

5.2.2 Experimental design

Three groups of mice (Temperature, ECG, EEG) were surgically implanted with DSI transmitters (from Data Sciences International (DSI), St. Paul, Minnesota), the Temperature and EEG groups have been described previously in Chapter 4.

Table 5.1 Overview of number of mice per experimental group , type of implant and anaesthetic time.

Group	Number of mice	Type of DSI transmitter	Weight of Implant (g)	Total anaesthetic time (hours)
Temperature	2	TA-F10	1.6	0.5
ECG	3	ETA-F10	1.6	1.5
EEG	5	F20-EET	3.9	3.5

5.2.3 Surgical preparation of mice

Details for the ECG group of mice are described briefly below;

5.2.3.1 Pre-surgical assessment and transmitter detail

All mice were health checked and weighed prior to surgery. The ETA-F10 transmitter weighs 1.6g and has a capacity of 1.1cc and, as DSI recommends that mice weighing <17g are not implanted, selected mice weighed between 29 and 33g at the time of surgery. This transmitter has a flat profile and two biopotential leads (with an outer diameter of 0.3mm) and a maximum of 6 months battery life. Its intended use is for collecting heart rate and rhythm data in cardiac studies and it is magnetically actuated – turned on and off by passing a magnet adjacent to the animal’s body wall, allowing the battery to be preserved when recording is not in progress.

5.2.3.2 Surgery and anaesthesia

Mice were anaesthetised with 4-5% isoflurane (*Isoflo*, Abbot Animal Health) in oxygen in an induction chamber and transferred to a face mask for maintenance. Lubricating eye drops were applied (*Viscotears*, Alcon Laboratories) and analgesic drugs administered by subcutaneous injection, 0.1mg/kg buprenorphine (*Vetergesic*, Alstoe Animal Health) and 5mg/kg meloxicam (*Metacam*, Boehringer Ingelheim). A constant output electrical heatpad was used throughout all stages of surgery. Anaesthesia was maintained with isoflurane in 1 litre oxygen and depth and physiological stability were monitored by counting and recording respiratory rate and rectal temperature every 5 minutes. ETA- F10 implantation took approximately 70 minutes and additional heating, insulation and titration of volatile agent occurred as necessary. Implantation took place with the mouse in dorsal recumbency on a heat pad, with a lubricated rectal thermometer placed and taped loosely to the tail using micropore tape. The ventral abdomen was clipped and prepped using povidone iodine surgical scrub diluted 1:20 in water, then swabbed with alcohol (*Steret Pre-injection Swabs*, MidMeds). A non-fenestrated plastic drape (*Transdrape*, Millpledge Vet) was cut as required and placed over the mouse's abdomen. A midline incision through skin and linea alba exposed the peritoneal cavity. The transmitter was placed into the abdomen and 0.5mls of sterile 0.9% saline was instilled around it. The two biopotential leads were passed through either side of the cut muscle using a 19 gauge needle and the muscle layer was closed with 4/0 braided silk suture (*Mersilk*, Ethicon) suture in a simple interrupted pattern, anchoring the to the inside of the muscle wall. The midline incision was extended cranially and the ends of the biopotential leads were trimmed to size and sutured to the subcuticular tissues overlying the ribs (using *Mersilk*), to detect cardiac electrical signals. The skin was closed using 5/0 polyglactin 910 (*Vicryl*) suture using an intradermal suture pattern. 0.5mls 0.9%

saline was administered subcutaneously and mice were maintained on 100% oxygen until they recovered then they were transferred to recover in a warm chamber at 25°C. Mice were returned to the home cage once normal activity resumed and transferred to the thermal cabinet for immediate post-operative temperature recording.

5.2.3.3 Post-operative recovery and temperature data recording

Optris thermal camera and DSI radiotelemetry recording were as described in Chapter 4 and commenced immediately the animal left the surgical room. The home cage was adapted with soft, palatable food on the floor and a longer water bottle nozzle. Analgesia (5mg/kg injection of meloxicam) was repeated 24 hours after surgery and animals were checked twice daily. Parameters monitored were level of locomotor activity and mentation, presence of faeces on the cage floor, evidence of drinking (water bottle level reduced) or eating (reduction in amount of mashed food placed in a small dish on the cage floor), absence or presence of a hunched posture, facial grimace or piloerection, integrity of abdominal and cranial wound closures. Cages were removed from the cabinet as necessary during checking as the Optris camera would have recorded the temperature of human hands within the chamber, each check took up to 10 minutes and can be seen as prolonged low values in some datasets. Mice were not weighed during the immediate post-operative period while data was being recorded as it was thought that carrying their cages to the weighing room and removing them to place on the scales would have resulted in increased temperature due to stress (and the degree of stress imposed could not be controlled for).

5.3 Results

5.3.1 Pre-implantation baseline recordings (by Optris (peripheral temperature) method only, duration 72 hours) were obtained for the two Temperature mice, enabling direct comparison with the post-procedure recordings by peripheral and core (DSI) methods. Maintenance of rhythmicity and period length is assessed through baseline peripheral, post-op peripheral and post-op core temperature recordings.

5.3.2 Pre-operative baseline recordings were not available for the ECG and EEG groups but a lack of rhythmicity can be seen in post-operative data sets (duration 72 hours) by peripheral and core assessment methods for all these mice, for which the duration under anaesthesia was approximately 1.5 hours (ECG) and 3.5 hours (EEG). Two post-operative peripheral and core plots are shown, one from an ECG and one from an EEG mouse.

5.3.3 For all mice, a table summarising minimum rectal temperature during and at recovery from anaesthesia, peripheral and core values at the beginning of the post-op recordings (which started a maximum of 30 minutes from the end of surgery) and the midpoint (mesor) of the oscillation of temperature by each method (as judged by eye from the timeseries plots) is shown.

5.3.1 Two Temperature mice

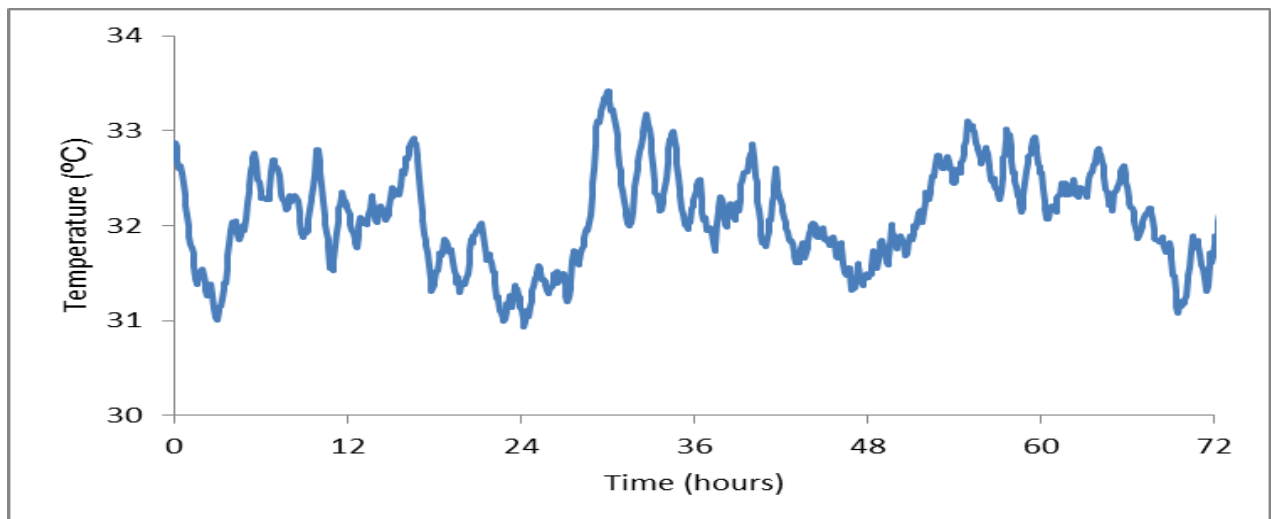
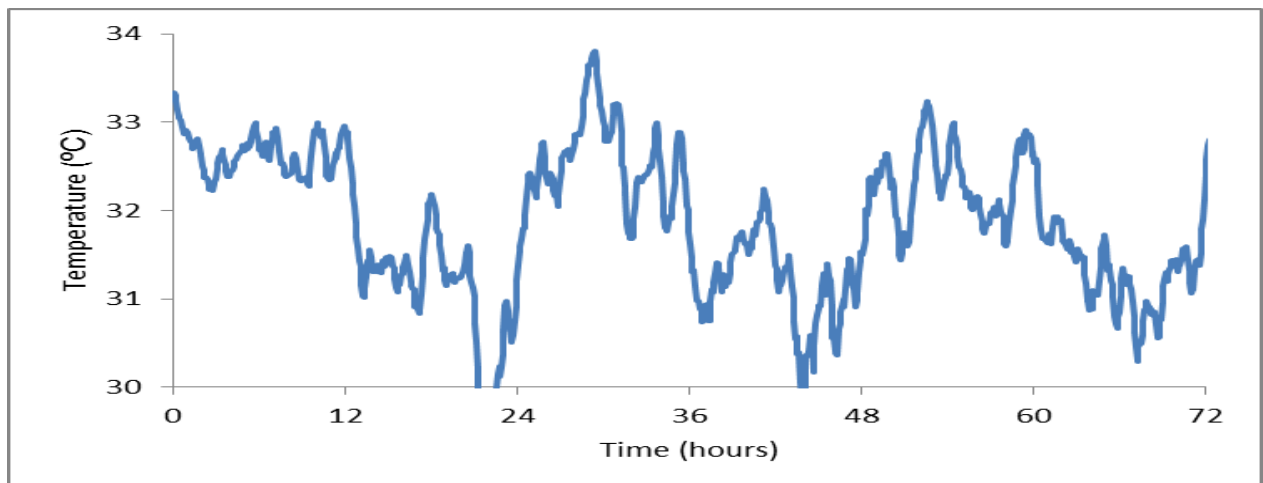


Figure 5.1 Baseline peripheral temperature recordings for M1T and M2T (in vertical order), showing an entrained rhythm under 12:12LD

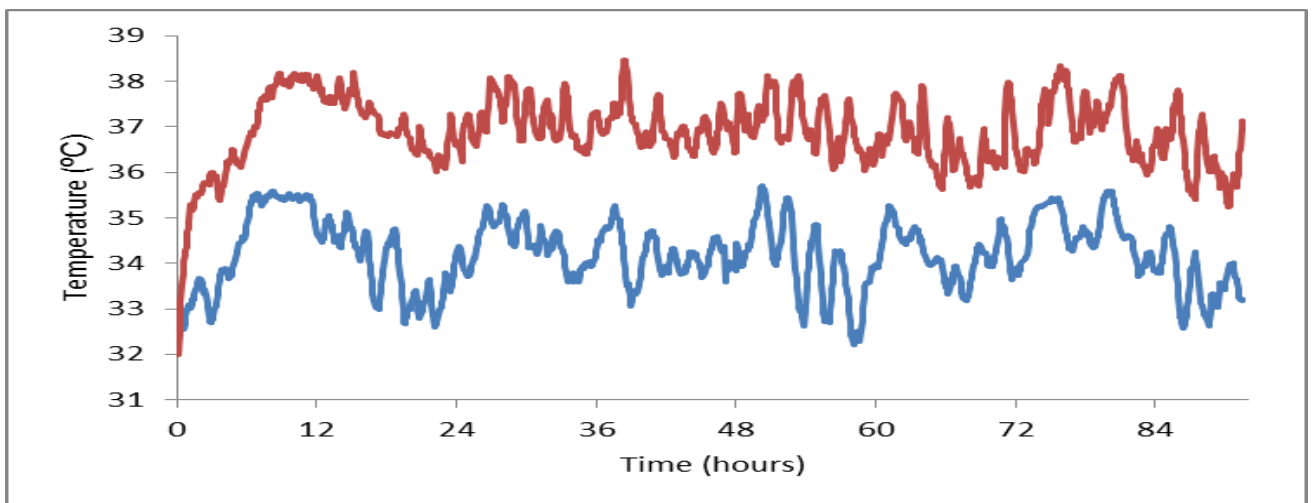
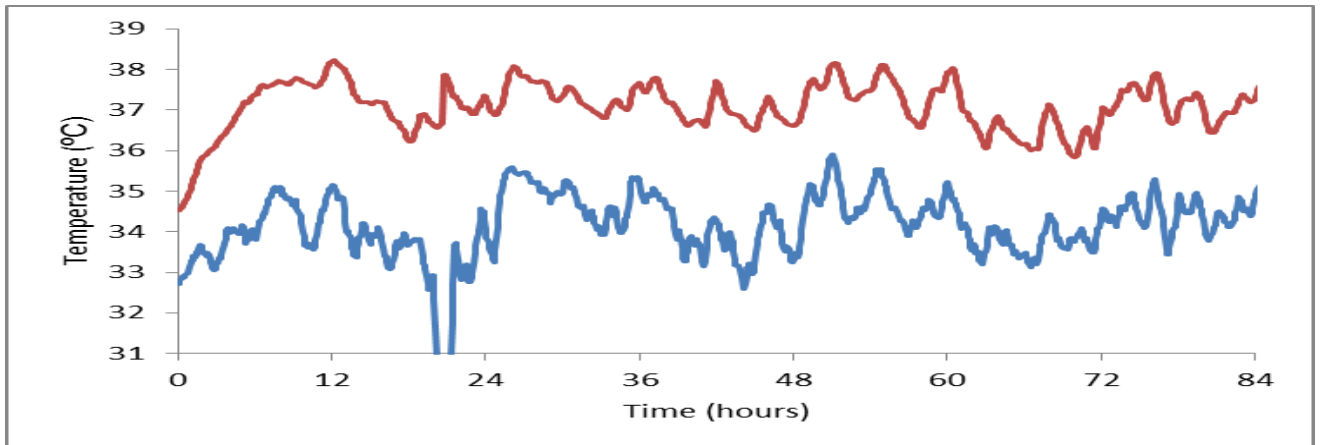


Figure 5.2 Peripheral (blue) and core (red) temperature recordings for M1T and M2T post implantation surgery (in vertical order).

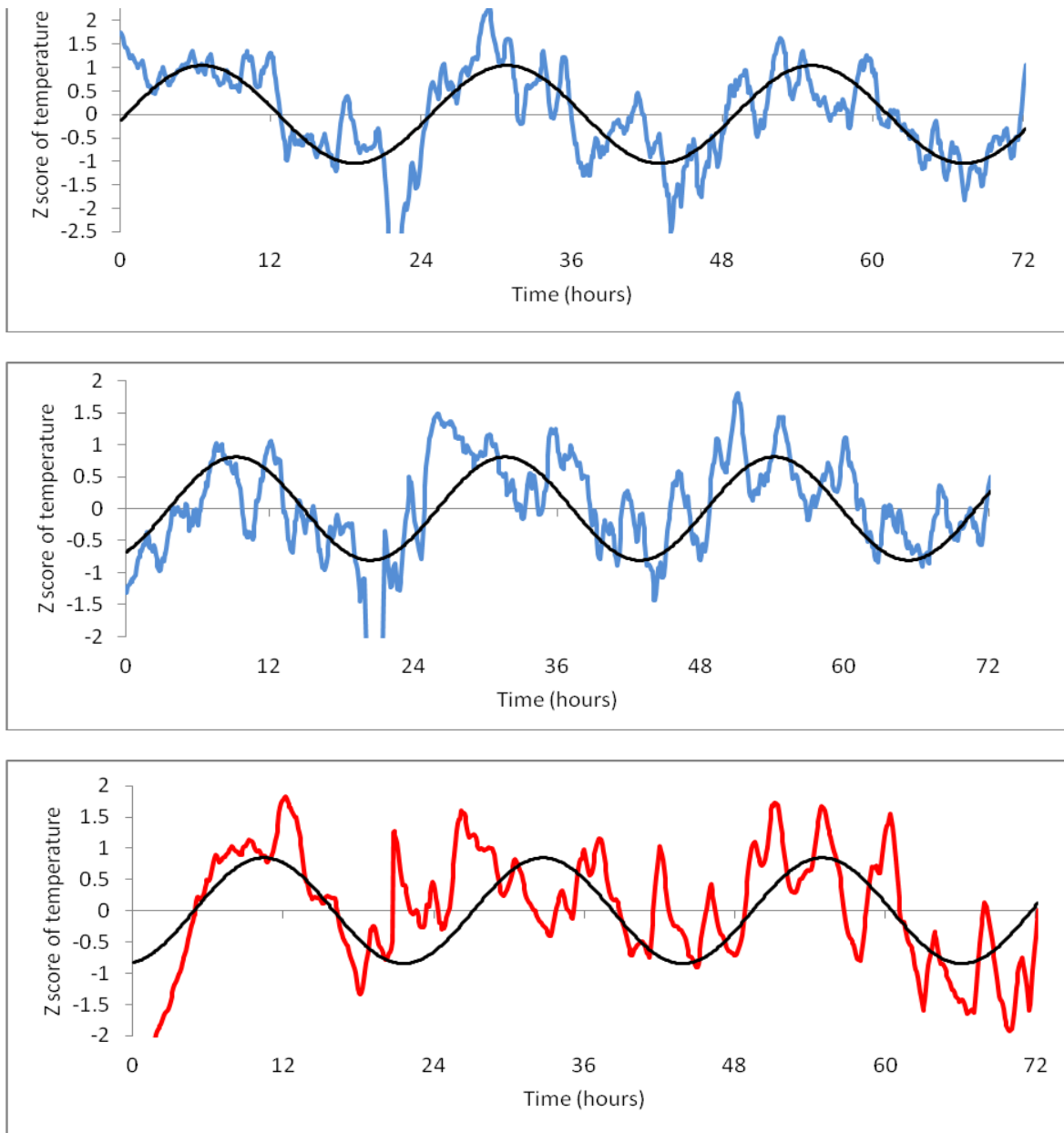


Figure 5.3 Pre-op peripheral baseline, post-op peripheral and post-op core recordings for M1T (in vertical order) with curve fitting by non-linear regression in *R*.

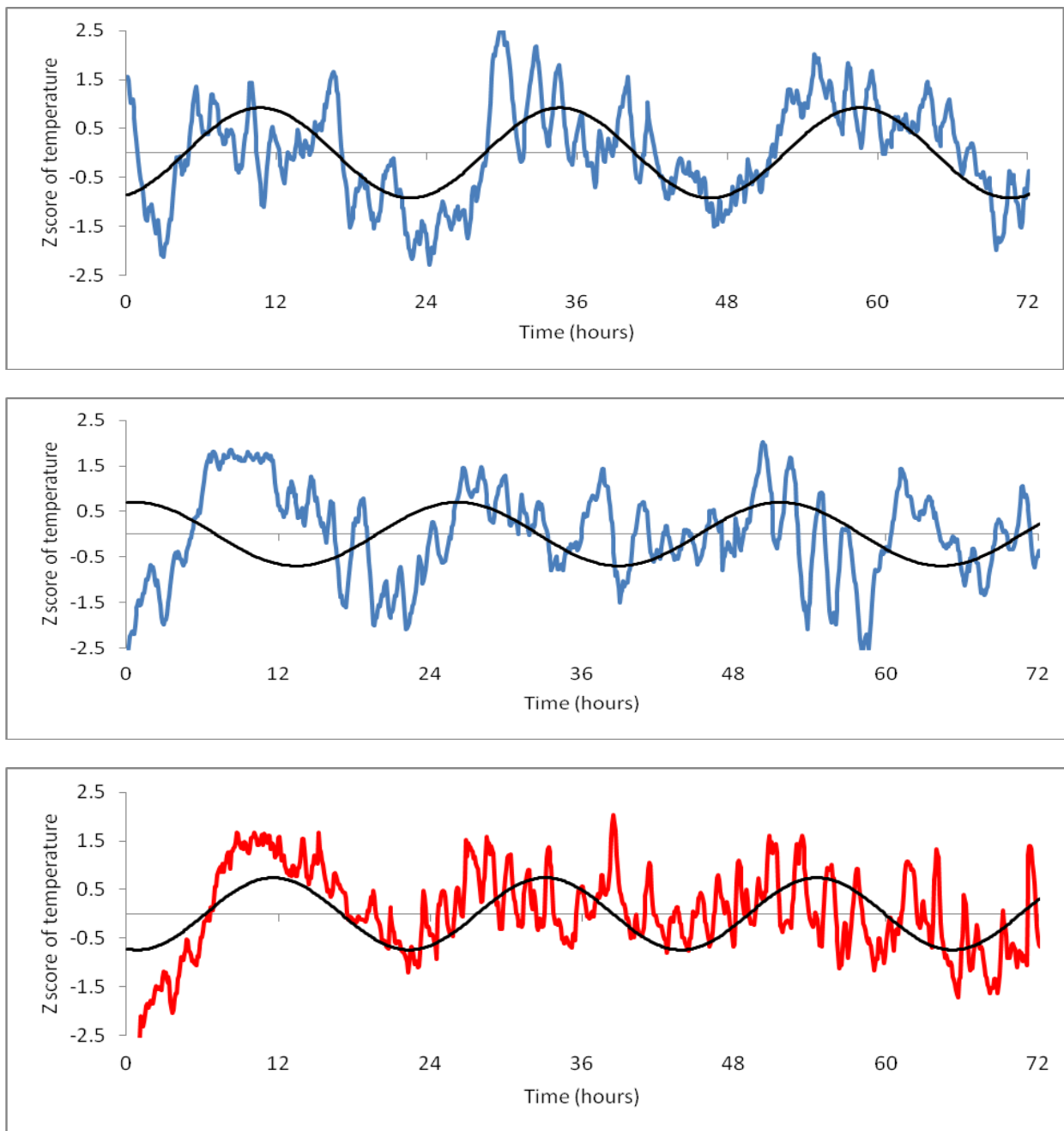


Figure 5.4 Pre-op peripheral baseline, post-op peripheral and post-op core recordings for M2T (in vertical order) with curve fitting by non-linear regression in *R*.

Table 5.2 *Tau* values for two Temperature mice through baseline and post-op recordings.

	<i>Tau</i> value (hours)		
	Baseline peripheral	Post-op peripheral	Post-op core
M1T	24.29	22.45	22.26
M2T	23.95	25.48	21.46

Tau reduces post-op for M1T, as measured by both methods. *Tau* of peripheral temperature increases for M2T and *Tau* of core temperature decreases- a poorly fitting curve for the peripheral post-op data in Figure 5.4 suggests that the *Tau* value calculated is not valid.

5.3.2 Post-operative Optris and DSI plots for ECG and EEG mice

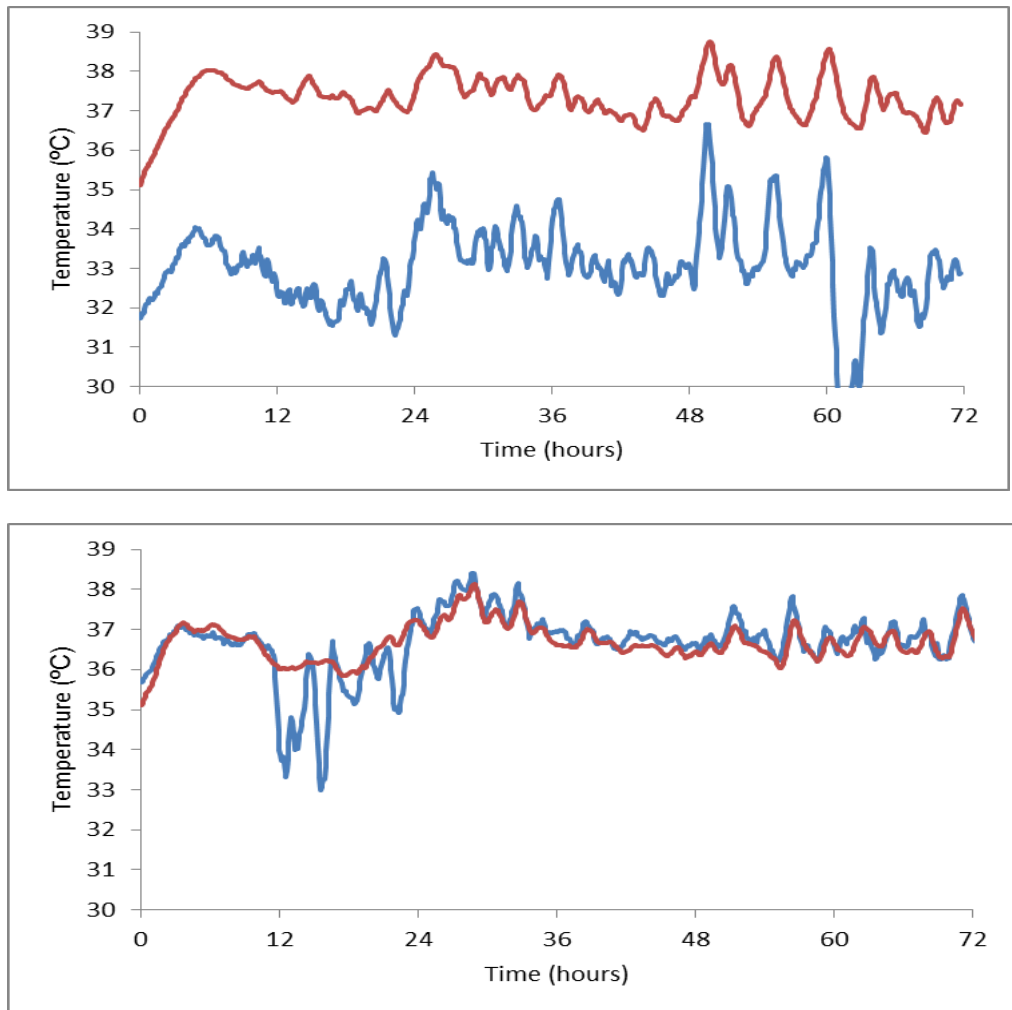


Figure 5.5 Peripheral (blue) and core (red) temperature recordings for M3ECG and M2EEG (in vertical order) showing lack of any temperature rhythm post-op. M3ECG shows an initial peripheral and central hypothermia and both areas of the body warm up at a similar rate, M2EEG shows similar absolute values for both methods of measurement apart from around 12 hours post recovery from anaesthesia when peripheral temperature drops by approximately 3 ° and core temperature is preserved around 36°C.

5.3.3 Summary of temperature variation through surgery and post-op recovery for all mice

Table 5.3 Temperature values for each mouse through the perioperative period, by rectal thermometer, Optris (peripheral) and DSI (core) temperature measurement. Mesor values are estimated by eye from the timeseries plots.

	Temperature (°C)				
	Lowest rectal value during surgery	Rectal value on recovery	DSI value start of recording	Mesor of OPTRIS recording	Mesor of DSI recording
M1T	34.8	37.2	34.4	34.0	36.75
M2T	36.0	36.8	32.0	34.0	37.0
M1ECG	34.9	36.9	35.7	34.0	37.5
M2ECG	29.9	36.5	36.5	33.0	37.25
M3ECG	30.1	36.6	35.1	33.5	37.5
M1EEG	34.2	38.6	36.8	37.0	36.75
M2EEG	32.3	36.7	35.2	34.25	36.75
M3EEG	31.7	36.9	36.0	36.75	37.25
M4EEG	30.4	36.7	35.2	37.5	37.25
M5EEG	31.7	36.7	33.3	36.25	37.0

5.3.4 Summary of results

5.3.1 Maintenance of temperature rhythm and period length after anaesthesia and surgery in M1T and M2T

A temperature rhythm is visible in the peripheral baseline recording for both mice, with *Tau* values approximately 24 hours under the 12:12 LD light cycle. Following surgery the rhythm appears weaker and *Tau* for M1T reduces (by both methods of measurement) and *Tau* for M2T increases for the peripheral recording and decreases for the core temperature recording.

5.3.2 Post-operative peripheral and core plots for ECG and EEG mice

All longer duration procedure mice were arrhythmic after surgery, by either method of assessment- M3ECG and M2EEG are shown as examples. All ECG mice show lower peripheral than core values, as seen in the Temperature cohort of mice in Chapter 4 and all EEG mice show increased peripheral temperatures, due to the shaving of hair on the head for surgery, as discussed in Chapter 4.

5.3.3 Summary of temperature variation through surgery and post-op recovery for all mice

Lowest rectal temperatures during surgery correlated with time under anaesthesia with the Temperature mice (duration of procedure 30 minutes) recording the least impairment- 34.8 and 36°C. Some ECG and EEG mice became profoundly hypothermic (29-31°C). All mice were passively rewarmed to around normothermia (37.5°C) to recover yet most became colder within the following 30 minutes (DSI core temperature values) when post-op recording started. The midpoints of the oscillation (mesor values) of the post-op temperature ranges (as judged by eye, as only the Temperature mice showed any post-op

rhythms which would justify curve- fitting analysis) were between 33-34°C for peripheral temperature in the Temperature and ECG mice and 36-37°C in the EEG mice, higher values corresponding with exposure of the skin following hair clipping on the heads of EEG mice, as discussed in Chapter 3. All core temperature mesor values were between 36.75- 37.5°C indicating a return to core normothermia despite the profound decrease in core temperature taken per rectum during the longer duration implantation procedures.

5.4 Discussion and Conclusion

5.4.1 Discussion of methods

Experimental methods have been evaluated in Chapter 4 and it only remains to discuss the management of the hypothermia seen during anaesthesia and surgery to implant these DSI transmitters. A standard flexible electrical heatpad was used for all surgeries and despite using bubblewrap insulation under the surgical drapes and applying half-filled “hot-hands” warm water gloves around the mice so as not to impede the surgeon in the EEG and ECG procedures, profound hypothermia was seen. This was concerning and reduced levels of volatile anaesthetic were required as hypothermia lowers the body’s oxygen requirement, indicating substantial physiological change. The mice were pre-warmed before recovery and their welfare was observed closely by distress scoring once recording started. Despite reaching levels at which humans have been reported to lose consciousness (Imrie and Hall 1990), all EEG and ECG mice recovered well, with no appreciable reduction in activity or appetite which was very reassuring. A recent cohort of EEG mice have been completed, not included in this thesis and use of a modern homeothermic heat pad in addition to insulation has been very successful at maintaining peri-operative normothermia. Buprenorphine was given at induction of every surgery and as ECG and EEG mice recovered later the amount of circulating drug varied so any opioid-associated increase in body temperature was not temporally controlled.

This chapter contains correlational data, collected in an *ad-hoc* manner as various mice were prepared for experiment; the number of subjects and experimental design were not planned and there are several possible confounding factors which may have affected the results. One surgeon completed the Temperature transmitter implantations and another

the EEG and ECG transmitters, which involved further positioning of biopotential electrodes elsewhere in the body and any increased weight or discomfort experienced due to these electrodes could have affected the post-op recovery of temperature rhythm. Temperature mice were implanted in the afternoon, around ZT 8 in relation to the light cycle and EEG and ECG mice were done in the morning, to allow time for post-op observations, around ZT 3. Analgesic protocols were identical between groups of mice, this was fortunate as it was expected that EEG mice would require supplemental dosing after the first day post-op. Collecting data by “piggy-backing” onto ongoing research conforms to the principles of the 3Rs but it is unfortunately not possible to control all experimental aspects, such as collecting baseline temperature data, as omitted here for the EEG and ECG groups.

5.4.2 Discussion of results

Mice undergoing short surgeries with a total anaesthetic duration of 30 minutes maintained a weaker temperature rhythm post-operatively although the period length τ , changed. Mice undergoing surgeries longer than 90 minutes suffered severe hypothermia and became arrhythmic on recovery, with no return of temperature rhythm within 72 hours, despite overall welfare status being deemed reasonable. Passive rewarming of these mice to normothermia resulted in good quality recoveries although the core temperature measured *per rectum* at the time the animal regained its righting reflex dropped 0.8-4.8°C within 30 minutes, at ambient room temperatures between 19 and 21°C. Continued environmental heating may be beneficial even if mice show a rapid return of consciousness and normal appetite and activity levels.

5.4.3 Conclusion

Hypothesis: Surgery and anaesthesia disrupts the circadian rhythm of peripheral and core body temperatures.

Hypothesis: The duration of surgery and anaesthesia is positively correlated with the degree of post-operative temperature disruption.

Hypothermia is a major obstacle facing researchers who use mice and anaesthesia-induced decreases in temperature are particularly difficult to correct as additional heat and insulation impede surgical procedures in these tiny animals. Even short procedures such as abdominal laparotomy with a total time under anaesthesia of 30 minutes affect the circadian rhythm of temperature for several days post-op. Oscillations can still be seen in data plots but they appear weaker and period length, *Tau* changes relative to baseline.

Fortunately the effects of hypothermia can be alleviated by gradually rewarming mice before recovery, over several minutes once the surgical procedure has finished. Mice recover without any apparent impairment when visual distress scoring techniques are applied. Longer duration procedures abolish circadian rhythms in both core and peripheral temperatures but visual inspection of these mice did not raise any concerns. Core temperature is preserved at the expense of peripheral temperature although in general the two methods are reasonably closely correlated during surgical recovery. Mice were passively rewarmed after surgery (until normal rectal (core) temperatures were achieved) but core temperatures recorded from indwelling implants showed that temperature decreases rapidly once the warming is discontinued. More data is required as it is not

known if avoidance of peri-operative hypothermia preserves circadian rhythms. A variety of devices exist to help prevent hypothermia and further objective studies would be beneficial to help biomedical researchers get the most out of their models.

Chapter 6 General Summary and Perspectives

The hypotheses and a summary of the results from each data chapter are described below in addition to suggestions for further development or application of the new data or techniques;

Chapter 3 Wheel running activity at different positions in an individually ventilated cage rack

Hypothesis: cage position (relative to overhead light sources) within an individually ventilated cage rack will affect the voluntary wheel running activity of singly-housed mice.

Single mice were housed at TOP, MIDDLE and BOTTOM positions on an IVC rack in a repeated measures study design, where the ambient light intensities were 653, 427 and 59 lux respectively. Locomotor activity was recorded as wheel revolutions, as an indicator of entrainment to the LD cycle and it was thought that mice kept at lower light intensities would experience a lesser degree of circadian entrainment. Mice kept at higher light intensities ran less during the *rho* (light) phase than mice at other positions but all mice entrained to the ambient light cycle, with defined onset of activity times seen on all actograms. Mice at lower rack positions began running earlier during the dusk phase as overhead lights dimmed and both the inhibition of daytime activity at the top of the rack and the early onset activity during dusk at lower levels are probably due to masking effects, which do not affect the internal clock, in the SCN. Changes in position on IVC racks should not have detrimental effect upon mice as scientific models but care should be taken to avoid taking animals off the rack for experiments during twilight periods as some will be more awake or active than others and this may affect results obtained. The hypothesis is

rejected as this information does not challenge current housing practices in mouse facilities; variation in light intensity at different levels of an IVC rack should not affect the internal clock and activity rhythms of mice.

Chapter 4 Validation of infrared thermography with radiotelemetry as a method of assessing body temperature in mice

Hypothesis: Using infrared thermography/thermal imaging to measure peripheral surface radiation is a valid method of assessing the body temperature of mice.

Hypothesis: the circadian rhythm of body temperature, as seen when mice are entrained to a regular light/dark cycle (LD) alters under conditions of constant light (LL) or constant darkness (DD).

The temperature of the body core is traditionally measured, using temporary probes or indwelling implants placed within body orifices. Thermal imaging measures surface heat emissions and hotspots occur in the most vascularised areas of the body. Tracking the peripheral hotspot of a mouse showed strong correlations with core temperature, measured using an intraperitoneal telemetric transmitter. Surface temperatures are slightly lower than the core but they display a clear oscillation of greater amplitude. Peripheral and core temperatures were recorded in mice under LD, DD and finally LL conditions. *Tau* of both temperature datasets appeared entrained to the LD cycle, shortening towards the endogenous circadian period of the mouse in DD and lengthening or becoming arrhythmic in LL. Both hypotheses are accepted.

Novel non-invasive technologies have many benefits. Licence authority is not required to use them in laboratory situations making them useful adjuncts to existing experimental

protocols and they can also be applied in field situations where animals cannot be restrained or touched. Invasive monitoring methods may confound the variables of interest; a restraint-associated pyrexia is common when mice are scruffed to insert rectal thermometers, likely rendering the results invalid. The body temperature of rodents is not commonly measured in laboratories but is of great importance, as these small animals have a high surface area to body volume ratio and are prone to heat loss, which in turn affects their general health and wellbeing. Rodents are also maintained at temperatures comfortable for human workers, below their thermoneutral zone, increasing metabolic demand to maintain normothermia. Mice increase their locomotor activity and build nests to keep warm; these behaviours are inevitably compromised if they suffer pain or distress as a result of scientific procedures applied. Any change in underlying health status is likely to reduced activity levels and therefore body temperature.

This experiment demonstrated a constant relationship between core and peripheral temperatures in clinically healthy animals. Further work could include assessments of disease models where use of infrared technology could improve detection of declining health and refine the application of the humane end point. Regulatory toxicity (safety pharmacology) protocols use rodent body temperature as an endpoint marker, generally measured using subcutaneous microchips but thermography could improve both welfare and reduce financial costs. The non-invasive nature of thermal imaging makes it useful for animals which cannot be implanted, such as neonates and for high throughput studies phenotyping transgenic animals. Thermal imaging could be useful in investigating sleep disorders, clinical conditions often characterised by temperature aberrations in human

subjects. There is also potential to it in assessing angiogenesis of surface tumours in oncology research.

Developing a method of measuring the surface hotspots of more than one animal would also open up possibilities in group experimental situations. The thermal camera used here had a large measurement range and offered fine resolution, but was relatively expensive. Less costly thermal imaging devices (perhaps those without longitudinal recording potential) could be assessed and if successful, information could be disseminated to other researchers to encourage uptake of this technology.

Chapter 5 Effect of implantation surgery on the post-operative core and peripheral body temperature of mice

Hypothesis: Surgery and anaesthesia disrupt the circadian rhythm of peripheral and core body temperatures.

Hypothesis: The duration of surgery and anaesthesia is positively correlated with the degree of post-operative temperature disruption.

Body temperature rhythms persisted following short duration surgery and anaesthesia (≤ 30 minutes) but they appeared less robust and the period length *Tau* changed, relative to baseline recordings. Longer duration procedures (≥ 90 minutes), associated with greater hypothermia under anaesthesia eliminated post-operative temperature rhythms; despite this, the quality of recoveries that mice displayed, assessed visually appeared to be satisfactory. Infrared thermography was used to obtain peripheral temperature baseline data non-invasively, then both thermography and core telemetry methods were employed simultaneously in the post-operative period. Both hypotheses are accepted.

Perioperative hypothermia is a common occurrence in small mammals and can result in increased morbidity and even loss of the animal from the study. As perioperative hypothermia is so widespread, an initial study to determine if circadian rhythm disruption occurs when body temperature is maintained within normal limits would be useful. Further work investigating increasing duration of anaesthesia and surgery would be a logical progression and collection of data from different types of surgery may reveal if increased heat loss occurs when procedures involve certain areas of the body, or varying degrees of surgical exposure. Anecdotal evidence collected during anaesthetic support for other research procedures has revealed that body temperature of mice decreases acutely at the beginning of a procedure, with losses of up to 4°C occurring during chamber induction using volatile gases such as isoflurane. Inhalational and injectable anaesthetic protocols could be compared for their propensity to affect heat loss and any supplemental heating or insulation methods employed could be objectively assessed. Some alterations/ interventions which could be addressed during volatile anaesthesia are; the induction chamber could be pre-warmed or the carrier gas could be warmed and/or humidified, adjustments could be made to the induction apparatus system to increase the rate of induction; increase % volatile agent, increase flow rate of carrier gas or reduce the size of the chamber, mice could be pre-medicated with sedative drugs to reduce the amount of volatile agent required to induce and maintain anaesthesia (as volatile agents cause vasodilation which increases heat loss). Different insulation materials, heat pads and other warming devices could be compared, the time of day that anaesthesia occurs could be varied to see if there is a temporal influence as chronopharmacology studies have indicated that drug efficacy is affected by the stage of the cycle in which they are dosed, mice themselves could be pre-warmed in a thermal cage and the absolute temperatures of any pre-warming or post-operative thermal cages could be

recorded and assessed against the degree of temperature disruption. Researchers generally allow a set number of days for post-operative recovery, before moving animals onto data collection phases of experiments. Only 72 hours of post-op data was obtained here but longer recording may have revealed the point when temperature rhythms stabilised or returned. Justifying this time point would enable workers requiring post-op data to observe adequate down-time, improving animal welfare and the quality of their results. A number of targeted adjustments to anaesthetic protocols in mice may improve thermoregulation and longitudinal temperature assessment could be combined with other non-invasive monitoring techniques to assess the impact of any new practices.

In conclusion, many physiological and behavioural parameters are measured by scientists studying biological processes at the whole animal level. Most of these outputs display circadian rhythms, regular oscillations through the light/dark cycle and high resolution and longitudinal monitoring techniques are required to identify changes accurately. Two novel methods were evaluated here; tracking locomotor activity using wheel running inside individually ventilated cages and use of thermal imaging to assess peripheral body temperature. Results showed that maintaining mice on commercially available cage racks, where the ambient light intensity with varies with distance from overhead light sources does not affect their internal body clock, although activity onset times varied due to masking effects. Thermal imaging detected clear rhythmic oscillations in surface body temperatures, enabling peripheral temperature to be used as a surrogate marker for core temperature without the need for invasive surgery or restraint to place measuring devices. Body temperature rhythms change through different light cycles in the same way that

routinely-studied locomotor rhythms do, offering an alternative method of assessing circadian status. Further use of thermal imaging in the perioperative period quantified the disruption of temperature rhythm associated with surgery and anaesthesia and could be used to refine procedural practices, improving animal welfare and scientific data quality.

Bibliography

- ABRAHAMSON, E. & MOORE, R. 2001. Suprachiasmatic nucleus in the mouse: retinal innervation, intrinsic organization and efferent projections. *Brain Research*, 916, 172-191.
- ADLER, M., GELLER, E., ROSOW, C. & COCHIN, J. 1988. The opioid system and temperature regulation. *Annual Review of Pharmacology and Toxicology*, 28, 429-449.
- ALBRECHT, U. & OSTER, H. 2001. The circadian clock and behavior. *Behavioural Brain Research*, 125, 89-91.
- ALLEN, D. L., HARRISON, B. C., MAASS, A., BELL, M. L., BYRNES, W. C. & LEINWAND, L. A. 2001. Cardiac and skeletal muscle adaptations to voluntary wheel running in the mouse. *Journal of Applied Physiology*, 90, 1900-1908.
- ALTIMUS, C., GÜLER, A., VILLA, K., MCNEILL, D., LEGATES, T. & HATTAR, S. 2008. Rods-cones and melanopsin detect light and dark to modulate sleep independent of image formation. *Proceedings of the National Academy of Sciences*, 105, 19998-20003.
- ALTIMUS, C. M., GÜLER, A. D., ALAM, N. M., ARMAN, A. C., PRUSKY, G. T., SAMPATH, A. P. & HATTAR, S. 2010. Rod photoreceptors drive circadian photoentrainment across a wide range of light intensities. *Nature Neuroscience*, 13, 1107-1112.
- ALVES, H., VALENTIM, A., OLSSON, I. & ANTUNES, L. 2009. Intraperitoneal anaesthesia with propofol, medetomidine and fentanyl in mice. *Laboratory Animals*, 43, 27-33.
- AMARAL, F. G., CASTRUCCI, A. M., CIPOLLA-NETO, J., POLETINI, M. O., MENDEZ, N., RICHTER, H. G. & SELIX, M. T. 2014. Environmental Control of Biological Rhythms: Effects on Development, Fertility and Metabolism. *Journal of Neuroendocrinology*, 26, 603-612.
- ARRAJ, M. & LEMMER, B. 2006a. Circadian rhythms in heart rate, motility, and body temperature of wild-type C57 and eNOS knock-out mice under light-dark, free-run, and after time zone transition. *Chronobiology International*, 23, 795-812.
- ARRAJ, M. & LEMMER, B. 2006b. Circadian rhythms in heart rate, motility, and body temperature of wild-type C57 and eNOS knockout mice under light/dark, free-run, and after time zone transition. *Chronobiology International*, 23, 795-812.
- ARRAS, M., AUTENRIED, P., RETTICH, A., SPAENI, D. & RÜLICHE, T. 2001. Optimization of Intraperitoneal Injection Anesthesia in Mice: Drugs, Dosages, Adverse Effects, and Anesthesia Depth. *Comparative Medicine*, 51, 443-456.
- ASCHOFF, J. 1980. The circadian rhythm of body temperature as a function of body size. In: TAYLOR, R., JOHANSEN, K. & BOLIS, L. (eds.) *Papers from the 5th International Conference on Comparative Physiology* Cambridge University Press.
- ASCHOFF, J. 1981. Thermal conductance in mammals and birds: its dependence on body size and circadian phase. *Comparative Biochemistry and Physiology Part A: Physiology*, 69, 611-619.
- ASCHOFF, J. 1983. Circadian control of body temperature. *Journal of Thermal Biology*, 8, 143-147.
- ASCHOFF, J. & VON GOETZ, C. 1988. Masking of circadian activity rhythms in hamsters by darkness. *Journal of Comparative Physiology - (A) Sensory, Neural, and Behavioral Physiology*, 162, 559-562.
- ASCHOFF, J. & WEVER, R. 1965. Circadian rhythms of finches in light-dark cycles with interposed twilights. *Comparative Biochemistry and Physiology*, 16, 507-14.

- ASHER, G. & SCHIBLER, U. 2011. Crosstalk between components of circadian and metabolic cycles in mammals. *Cell Metabolism*, 13, 125-137.
- AYDIN, C., GRACE, C. E. & GORDON, C. J. 2011. Effect of physical restraint on the limits of thermoregulation in telemetered rats. *Experimental Physiology*, 96, 1218-1227.
- BAGIS, H., ODAMAN MERCAN, H. & DINNYES, A. 2004. Exposure to warmer postoperative temperatures reduces hypothermia caused by anaesthesia and significantly increases the implantation rate of transferred embryos in the mouse. *Laboratory Animals*, 38, 50-54.
- BALCOMBE, J., BARNARD, N. & SANDUSKY, C. 2004. Laboratory routines cause animal stress. *Journal of the American Association for Laboratory Animal Science*, 43, 42-51.
- BALL, D., ARGENTIEREI, G., LIPINSKI, M., ROBISON, R., STOLL, R. & VISSCHER, G. 1991. Evaluation of a microchip implant system used for animal identification in rats. *Laboratory Animal Science*, 41, 185-186.
- BANJANIN, S. & MROSOVSKY, N. 2000. Preferences of mice, *Mus musculus*, for different types of running wheel. *Laboratory Animals*, 34, 313-318.
- BARRETT, P., SCHUSTER, C., MERCER, J. & MORGAN, P. 2003. Sensitization: a mechanism for melatonin action in the pars tuberalis. *Journal of Neuroendocrinology*, 15, 415-421.
- BARTELT, A., BRUNS, O., REIMER, R., HOHENBERG, H., ITRICH, H., PELDSCHUS, K., KAUL, M., TROMSDORF, U., WELLER, H., WAURISCH, C., EYCHMULLER, A., GORDTS, P., RINNINGER, F., BRUEGELMANN, K., FREUND, B., NIELSEN, P., MERKEL, M. & HEEREN, J. 2011. Brown adipose tissue activity controls triglyceride clearance. *Nature Medicine*, 17, 200-205.
- BASTIANINI, S., SILVANI, A., BERTEOTTI, C., MARTIRE, V. & ZOCCOLI, G. 2012. Mice show circadian rhythms of blood pressure during each wake-sleep state. *Chronobiology International*, 29, 82-86.
- BAUMANS, V., SCHLINGMANN, F., VONCK, M. & VAN LITH, H. 2002. Individually ventilated cages: beneficial for mice and men? *Journal of the American Association for Laboratory Animal Science*, 41, 13-19.
- BENLOUCIF, S., MASANA, M. & DUBOCOVICH, M. 1997a. Light-induced phase shifts of circadian activity rhythms and immediate early gene expression in the suprachiasmatic nucleus are attenuated in old C3H/HeN mice. *Brain Research*, 747, 34-42.
- BENLOUCIF, S., MASANA, M. I. & DUBOCOVICH, M. L. 1997b. Light-induced phase shifts of circadian activity rhythms and immediate early gene expression in the suprachiasmatic nucleus are attenuated in old C3H/HeN mice. *Brain Research*, 747, 34-42.
- BENSTAALI, C., MAILLOUX, A., BOGDAN, A., AUZEBY, A. & TOUITOU, Y. 2001. Circadian rhythms of body temperature and motor activity in rodents and their relationships with the light-dark cycle. *Life Sciences*, 68, 2645-56.
- BERNE, R. & LEVY, M. (eds.) 1996. *Principles of Physiology*, St Louis: Mosby.
- BERSON, D., DUNN, F. & TAKAO, M. 2002a. Phototransduction by retinal ganglion cells that set the circadian clock. *Science*, 295, 1070-1073.
- BERSON, D. M., DUNN, F. A. & TAKAO, M. 2002b. Phototransduction by Retinal Ganglion Cells That Set the Circadian Clock. *Science*, 295, 1070-1073.
- BEYNEN, A. C. & VAN TINTELEN, G. 1990. Daily change of cage depresses mass gain in mice. *Zeitschrift fur Versuchstierkunde*, 33, 106-107.

- BICEGO, K., BARROS, R. & BRANCO, L. 2007. Physiology of temperature regulation: comparative aspects. *Comparative Biochemistry and Physiology - Part A: Molecular & Integrative Physiology*, 147, 616-639.
- BITTMAN, E., DOHERTY, L., HUANG, L. & PAROSKIE, A. 2003. Period gene expression in mouse endocrine tissues. *American Journal of Physiology - Regulatory Integrative and Comparative Physiology*, 285, R561-R569.
- BORBÉLY, A. 1998. Processes underlying sleep regulation. *Hormone Research*, 49, 114-117.
- BORBÉLY, A., ACHERMANN, P., TRACHSEL, L. & TOBLER, I. 1989. Sleep initiation and initial sleep intensity: interactions of homeostatic and circadian mechanisms. *Journal of Biological Rhythms*, 4, 37-48.
- BOULOS, Z., MACCHI, M. & TERMAN, M. 1996. Twilight transitions promote circadian entrainment to lengthening light- dark cycles. *American Journal of Physiology - Regulatory Integrative and Comparative Physiology*, 271, R813-R818.
- BOULOS, Z. & MACCHI, M. M. 2005. Season- and latitude-dependent effects of simulated twilights on circadian entrainment. *Journal of Biological Rhythms*, 20, 132-144.
- BOULOS, Z., MACCHI, M. M. & TERMAN, M. 2002. Twilights Widen the Range of Photic Entrainment in Hamsters. *Journal of Biological Rhythms*, 17, 353-363.
- BOURGIN, P., HAGIWARA, G., TSAI, J., LIU, J., STEPHENSON, K., HELLER, C., O'HARA, B. & FRANKEN, P. 2008. Influence of sleep homeostasis on PER1 and PER 2 expression in the forebrain of SCN lesioned and intact mice. *Journal of Sleep Research*, 16, 445-454.
- BRANDSTETTER, H., SCHEER, M., HEINEKAMP, C., GIPPNER-STEPPERT, C., LOGE, O., RUPRECHT, L., THULL, B., WAGNER, R., WILHELM, P. & SCHEUBER, H.-P. 2005. Performance evaluation of IVC systems. *Laboratory Animals*, 39, 40-44.
- BRIELMEIER, M., MAHABIR, E., NEEDHAM, J. R., LENGGER, C., WILHELM, P. & SCHMIDT, J. 2006. Microbiological monitoring of laboratory mice and biocontainment in individually ventilated cages: a field study. *Laboratory Animals*, 40, 247-260.
- BRONSON, F. 1979. Light intensity and reproduction in wild and domestic house mice. *Biology of Reproduction*, 21, 235-239.
- BROWN, J. & PHAM-LE, N. 2011. The effect of thermopreference on circadian thermoregulation in Sprague-Dawley and Fisher 344 rats. *Journal of Thermal Biology*, 37, 309-315.
- BROWN, J. C. L. & STAPLES, J. F. 2010. Mitochondrial metabolism during fasting-induced daily torpor in mice. *Biochimica et Biophysica Acta (BBA) - Bioenergetics*, 1797, 476-486.
- BROWN, S., ZUMBRUNN, G., FLEURY-OLELA, F., PREITNER, N. & SCHIBLER, U. 2002. Rhythms of mammalian body temperature can sustain peripheral circadian clocks. *Current Biology*, 12, 1574-1583.
- BRYANT, C. D., ZHANG, N. N., SOKOLOFF, G., FANSELOW, M. S., ENNES, H. S., PALMER, A. A. & MCROBERTS, J. A. 2008. Behavioral Differences among C57BL/6 Substrains: Implications for Transgenic and Knockout Studies. *Journal of Neurogenetics*, 22, 315-331.
- BUHR, E., YOO, S. & TAKAHASHI, J. 2010. Temperature as a universal resetting cue for mammalian circadian oscillators. *Science*, 330, 379-385.
- BUTLER, M. & SILVER, R. 2011. Divergent photic thresholds in the non-image-forming visual system: entrainment, masking and pupillary light reflex. *Proceedings of the Royal Society B: Biological Sciences*, 278, 745-750.

- CAMBRAS, T., WELLER, J. R., ANGLÈS-PUJORÀS, M., LEE, M. L., CHRISTOPHER, A., DÍEZ-NOGUERA, A., KRUEGER, J. M. & DE LA IGLESIA, H. O. 2007. Circadian desynchronization of core body temperature and sleep stages in the rat. *Proceedings of the National Academy of Sciences*, 104, 7634-7639.
- CAMPBELL, I. 2008. Body temperature and its regulation. *Anaesthesia & Intensive Care Medicine*, 9, 259-263.
- CANNON, B. & NEDERGAARD, J. 2004. Brown adipose tissue: function and physiological significance. *Physiological Reviews*, 84, 277-359.
- CARMICHAEL, M. S., NELSON, R. J. & ZUCKER, I. 1981. Hamster activity and estrous cycles: Control by a single versus multiple circadian oscillator(s). *Proceedings of the National Academy of Sciences of the United States of America*, 78, 7830-7834.
- CARO, A. C., HANKENSON, F. C. & MARX, J. O. 2013. Comparison of Thermoregulatory Devices Used during Anesthesia of C57BL/6 Mice and Correlations between Body Temperature and Physiologic Parameters. *Journal of the American Association for Laboratory Animal Science*, 52, 577-583.
- CASIRAGHI, L., ODA, G., CHIESA, J., FRIESEN, W. & GOLOMBEK, D. 2012. Forced desynchronization of activity rhythms in a model of chronic jet lag in mice. *Journal of Biological Rhythms*, 27, 59-69.
- CASTANON-CERVANTES, O., WU, M., EHLEN, J., PAUL, K., GAMBLE, K., JOHNSON, R., BESING, R., MENAKER, M., GEWIRTZ, A. & DAVIDSON, A. 2010. Dysregulation of inflammatory responses by chronic circadian disruption. *Journal of Immunology*, 185, 5796-5805.
- CASTILLO, M. R., HOCHSTETLER, K. J., GREENE, D. M., FIRMIN, S. I., TAVERNIER, R. J., RAAP, D. K. & BULT-ITO, A. 2005. Circadian rhythm of core body temperature in two laboratory mouse lines. *Physiology and Behavior*, 86, 538-545.
- CESAROVIC, N., NICHOLLS, F., RETTICH, A., KRONEN, P., HÄSSIG, M., JIRKOF, P. & ARRAS, M. 2010. Isoflurane and sevoflurane provide equally effective anaesthesia in laboratory mice. *Laboratory Animals*, 44, 329-336.
- CHALLET, E., PEVET, P., VIVIEN-ROELS, B. & MALAN, A. 1997. Phase-advanced daily rhythms of melatonin, body temperature, and locomotor activity in food-restricted rats fed during daytime. *Journal of Biological Rhythms*, 12, 65-79.
- CHALUPA, L. & WILLIAMS, R. 2008. *Eye, retina and visual system of the mouse*

Massachusetts Institute of Technology Press.

- CHASSARD, D. & BRUGUEROLLE, B. 2004. Chronobiology and Anesthesia. *Anesthesiology*, 100, 413-427.
- CHASSARD, D., DUFLO, F., DE QUEIROZ SIQUEIRA, M., ALLAOUCHICHE, B. & BOSELLI, E. 2007. Chronobiology and anaesthesia. *Current Opinion in Anesthesiology*, 20, 186-190.
- CHENG, H., ALVAREZ-SAAVEDRA, M., DZIEMA, H., CHOI, Y., LI, A. & OBRIETAN, K. 2009. Segregation of expression of mPeriod gene homologs in neurons and glia: possible divergent roles of mPeriod1 and mPeriod2 in the brain. *Human Molecular Genetics*, 18, 3110-3124.
- CHIDAMBARAM, R., MARIMUTHU, G. & SHARMA, V. K. 2004. Effect of behavioural feedback on circadian clocks of the nocturnal field mouse *Mus booduga*. *Biological Rhythm Research*, 35, 213-227.

- CLEMENT, J. G., MILLS, P. & BROCKWAY, B. 1989. Use of telemetry to record body temperature and activity in mice. *Journal of Pharmacological Methods*, 21, 129-140.
- CLOUGH, G. 1982. Environmental effects on animals used in biomedical research. *Biological Reviews*, 57, 487-523.
- CLOUGH, G., WALLACE, J., GAMBLE, M. R., MERRYWEATHER, E. R. & BAILEY, E. 1995. A positive, individually ventilated caging system: a local barrier system to protect both animals and personnel. *Laboratory Animals*, 29, 139-151.
- COLWELL, C. & FOSTER, R. 1992. Photic regulation of Fos-like immunoreactivity in the suprachiasmatic nucleus of the mouse. *Journal of Comparative Neurology*, 324, 135-142.
- COMAS, M. & HUT, R. A. 2009. Twilight and Photoperiod Affect Behavioral Entrainment in the House Mouse (*Mus musculus*). *Journal of Biological Rhythms*, 24, 403-412.
- COMPTON, S. R., HOMBERGER, F. R., PATURZO, F. X. & CLARK, J. M. 2004. Efficacy of Three Microbiological Monitoring Methods in a Ventilated Cage Rack. *Comparative Medicine*, 54, 382-392.
- COOGAN, A. & WYSE, C. 2008. Neuroimmunology of the circadian clock. *Brain Research*, 1232, 104-112.
- CORNING, B. F. & LIPMAN, N. S. 1991. A comparison of rodent caging systems based on microenvironmental parameters. *Laboratory Animal Science*, 41, 498-503.
- CRABBE, J. C., WAHLSTEN, D. & DUDEK, B. C. 1999. Genetics of Mouse Behavior: Interactions with Laboratory Environment. *Science*, 284, 1670-1672.
- CRAWLEY, J. N. 2008. Behavioral Phenotyping Strategies for Mutant Mice. *Neuron*, 57, 809-818.
- CRAY, C., ZAIAS, J. & ALTMAN, N. 2009. Acute phase response in animals: a review. *Comparative Medicine*, 59, 517-526.
- DAAN, S. 1977. Tonic and phasic effects of light in the entrainment of circadian rhythms. *Annals of the New York Academy of Sciences*, Vol. 290, 51-59.
- DAAN, S. 2000. Colin Pittendrigh, Jürgen Aschoff, and the natural entrainment of circadian systems. *Journal of Biological Rhythms*, 15, 195-207.
- DAAN, S. 2010. A history of chronobiological concepts. In: ALBRECHT, U. (ed.) *The Circadian Clock*. New York: Springer.
- DAAN, S. & PITTENDRIGH, C. 1976. A functional analysis of circadian pacemakers in nocturnal rodents - II. The variability of phase response curves. *Journal of Comparative Physiology (A)*, 106, 253-266.
- DALLMANN, R., BROWN, S. A. & GACHON, F. 2014. Chronopharmacology: New insights and therapeutic implications. *Annual Review of Pharmacology and Toxicology*, 54, 339-361.
- DAVID, J. M., KNOWLES, S., LAMKIN, D. M. & STOUT, D. B. 2013. Individually Ventilated Cages Impose Cold Stress on Laboratory Mice: A Source of Systemic Experimental Variability. *Journal of the American Association for Laboratory Animal Science*, 52, 738-744.
- DE BONO, J., ADLAM, D., PATERSON, D. & CHANNON, K. 2006. Novel quantitative phenotypes of exercise training in mouse models. *American Journal of Physiology - Regulatory, Integrative and Comparative Physiology*, 290, R926-R934.
- DE GIORGI, A., MALLOZZI MENEGATTI, A., FABBIAN, F., PORTALUPPI, F. & MANFREDINI, R. 2013. Circadian rhythms and medical diseases: Does it matter when drugs are taken? *European Journal of Internal Medicine*, 24, 698-706.

- DE LA IGLESIA, H. & SCHWARTZ, W. 2002. A subpopulation of efferent neurons in the mouse suprachiasmatic nucleus is also light responsive. *Neuroreport*, 13, 857-860.
- DEACON, R. M. J. 2006. Digging and marble burying in mice: Simple methods for in vivo identification of biological impacts. *Nature Protocols*, 1, 122-124.
- DEAKIN, C. D. 1998. Changes in core temperature compartment size on induction of general anaesthesia. *British Journal of Anaesthesia*, 81, 861-864.
- DEBOER, T., VANSTEENSEL, M., DÉTÁRI, L. & MEIJER, J. 2003. Sleep states alter activity of suprachiasmatic nucleus neurons. *Nature Neuroscience*, 6, 1086-1090.
- DIJK, D. & DUFFY, J. 1999. Circadian regulation of human sleep and age-related changes in its timing, consolidation and EEG characteristics. *Annals of medicine*, 31, 130-140.
- DISPERSYN, G., PAIN, L., CHALLET, E. & TOUITOU, Y. 2008. General anesthetics effects on circadian temporal structure: an update. *Chronobiology International*, 25, 835-850.
- DISPERSYN, G., PAIN, L. & TOUITOU, Y. 2010. Propofol anaesthesia significantly alters plasma blood levels of melatonin in rats *Anaesthesiology*, 112, 333-337.
- DIVINCENTI JR, L., MOORMAN-WHITE, D., BAVLOV, N., GARNER, M. & WYATT, J. 2012. Effects of housing density on nasal pathology of breeding mice housed in individually ventilated cages. *Lab Animal*, 41, 68-76.
- DOYLE, S. E., YOSHIKAWA, T., HILLSON, H. & MENAKER, M. 2008. Retinal pathways influence temporal niche. *Proceedings of the National Academy of Sciences of the United States of America*, 105, 13133-13138.
- DRICKAMER, L. C. & EVANS, T. R. 1996. Chemosignals and activity of wild stock house mice, with a note on the use of running wheels to assess activity in rodents. *Behavioural Processes*, 36, 51-66.
- EASTMAN, C. & RECHTSCHAFFEN, A. 1983. Circadian temperature and wake rhythms of rats exposed to prolonged continuous illumination. *Physiology and Behavior*, 31, 417-27.
- EASTON, A., MEERLO, P., BERGMANN, B. & TUREK, F. 2004. The suprachiasmatic nucleus regulates sleep timing and amount in mice. *Sleep*, 27, 1307-1318.
- EBIHARA, S., GOTO, M. & OSHIMA, I. 1988. The phase-shifting effects of pentobarbital on the circadian rhythm of locomotor activity in the mouse: strain differences. *Brain Research*, 454, 404-407.
- EBIHARA, S. & TSUJI, K. 1980. Entrainment of the circadian activity rhythm to the light cycle: Effective light intensity for a Zeitgeber in the retinal degenerate C3H mouse and the normal C57BL mouse. *Physiology & Behavior*, 24, 523-527.
- EBIHARA, S., TSUJI, K. & KONDO, K. 1978. Strain differences of the mouse's free-running circadian rhythm in continuous darkness. *Physiology and Behavior*, 20, 795-799.
- EDERY, I. 2000. Circadian rhythms in a nutshell. *Physiol Genomics*, 3, 59-74.
- EDGAR, D. & DEMENT, W. 1991. Regularly scheduled voluntary exercise synchronizes the mouse circadian clock. *American Journal of Physiology - Regulatory, Integrative and Comparative Physiology*, 261, R928-R933.
- EDGAR, D., MARTIN, C. & DEMENT, W. 1991. Activity feedback to the mammalian circadian pacemaker: influence on observed measures of rhythm period length. *Journal of Biological Rhythms*, 6, 185-199.
- EIKELBOOM, R. 2001. Bins, bouts and wheel-running speed. *Animal Behaviour*, 61, 679-681.
- ENDO, A. & WATANABE, T. 1989. Effects of non-24-hour days on reproductive efficacy and embryonic development in mice. *Gamete Research*, 22, 435-441.

- FARBER, D., FLANNERY, J. & BOWES-RICKMAN, C. 1994. The rd mouse story: seventy years of research on an animal model of inherited retinal degeneration. *Progress in Retinal and Eye Research*, 13, 31-64.
- FESTING, M. 1977. Wheel activity in 26 strains of mouse. *Laboratory Animals*, 11, 257-258.
- FESTING, M. F. W. & GREENWOOD, R. 1976. Home cage wheel activity recording in mice. *Laboratory Animals*, 10, 81-85.
- FIELD, A. 2009. *Discovering Statistics using SPSS*, London, SAGE.
- FINN, R., MCLAUGHLIN, L., HUGHES, C., SONG, C., HENDERSON, C. & ROLAND WOLF, C. 2011. Cytochrome b5 null mouse: a new model for studying inherited skin disorders and the role of unsaturated fatty acids in normal homeostasis *Transgenic Research*, 20, 491-502.
- FISHER, S., GODINHO, S., POTHECARY, C., HANKINS, M., FOSTER, R. & PEIRSON, S. 2012. Rapid assessment of sleep-wake behavior in mice. *Journal of Biological Rhythms*, 27, 48-58.
- FLECKNELL, P. 1996. *Laboratory animal anaesthesia*, Cambridge, University Press.
- FOSTER, R. & PEIRSON, S. 2012. The Circadian Control of Sleep. In: KRAMER, A. & MERROW, M. (eds.) *Circadian Clocks*. in press: Springer Press.
- FOSTER, R., PROVENCIO, I., HUDSON, D., FISKE, S., GRIP, W. & MENAKER, M. 1991. Circadian photoreception in the retinally degenerate mouse (rd/rd). *Journal of Comparative Physiology A: Neuroethology, Sensory, Neural, and Behavioral Physiology*, 169, 39-50.
- FOSTER, R. G., HANKINS, M. W. & PEIRSON, S. N. 2007. Light, Photoreceptors, and Circadian Clocks. In: ROSATO, E. (ed.) *Circadian Rhythms*. Humana Press.
- FRANCIS, A. & COLEMAN, G. 1990. Ambient temperature cycles entrain the free-running circadian rhythms of the stripe-faced dunnart, *Sminthopsis macroura*. *Journal of Comparative Physiology A: Neuroethology, Sensory, Neural, and Behavioral Physiology*, 167, 357-362.
- FRANK, S., RAJA, S., BULCAO, C. & GOLDSTEIN, D. 1999. Relative contribution of core and cutaneous temperatures to thermal comfort and autonomic responses in humans. *Journal of Applied Physiology*, 86, 1588-1593.
- FRANKEN, P. & DIJK, D. 2009. Circadian clock genes and sleep homeostasis. *European Journal of Neuroscience*, 29, 1820-1829.
- FRANKEN, P., MALAFOSSSE, A. & TAFTI, M. 1998. Genetic variation in EEG activity during sleep in inbred mice. *American Journal of Physiology - Regulatory, Integrative and Comparative Physiology*, 275, R1127-R1137.
- FRANKEN, P., THOMASON, R., HELLER, H. C. & O'HARA, B. 2007. A non-circadian role for clock-genes in sleep homeostasis: a strain comparison. *BMC Neuroscience*, 8, 87.
- FRANKS, N. & ZECHARIA, A. 2011. Sleep and general anesthesia. *Canadian Journal of Anesthesia / Journal canadien d'anesthésie*, 58, 139-148.
- FREEDMAN, M., LUCAS, R., SONI, B., VON SCHANTZ, M., MUÑOZ, M., DAVID-GRAY, Z. & FOSTER, R. 1999. Regulation of mammalian circadian behavior by non-rod, non-cone, ocular photoreceptors. *Science*, 284, 502-504.
- FROY, O. 2011. The circadian clock and metabolism. *Clinical Science*, 120, 65-72.
- FULLER, C. A., LYDIC, R. & SULZMAN, F. M. 1981. Circadian rhythm of body temperature persists after suprachiasmatic lesions in the squirrel monkey. *American Journal of Physiology - Regulatory Integrative and Comparative Physiology*, 10, 385-391.

- GALLEGO, M. & VIRSHUP, D. 2007. Post-translational modifications regulate the ticking of the circadian clock. *Nature Reviews Molecular Cell Biology*, 8, 139-148.
- GASKILL, B., GORDON, C., PAJOR, E., LUCAS, J., DAVIS, J. & GARNER, J. 2012. Heat or insulation: behavioral titration of mouse preference for warmth or access to a nest. *PLoS ONE*, 7, e32799.
- GASKILL, B., ROHR, S., PAJOR, E., LUCAS, J. & GARNER, J. 2011. Working with what you've got: changes in thermal preference and behavior in mice with or without nesting material. *Journal of Thermal Biology*, 36, 193-199.
- GASKILL, B. N., GORDON, C. J., PAJOR, E. A., LUCAS, J. R., DAVIS, J. K. & GARNER, J. P. 2013. Impact of nesting material on mouse body temperature and physiology. *Physiology & Behavior*, 110-111, 87-95.
- GEISER, F. 2004. Metabolic rate and body temperature reduction during hibernation and daily torpor. *Annual Review of Physiology*, 66, 239-274.
- GEKAKIS, N., STAKNIS, D., NGUYEN, H., DAVIS, F., WILSBACNER, L., KING, D., TAKAHASHI, J. & WEITZ, C. 1998. Role of the CLOCK protein in the mammalian circadian mechanism. *Science*, 280, 1564-1569.
- GERASHCHENKO, D. & SHIROMANI, P. 2004. Different neuronal phenotypes in the lateral hypothalamus and their role in sleep and wakefulness. *Molecular Neurobiology*, 29, 41-59.
- GERHART-HINES, Z., FENG, D., EMMETT, M. J., EVERETT, L. J., LORO, E., BRIGGS, E. R., BUGGE, A., HOU, C., FERRARA, C., SEALE, P., PRYMA, D. A., KHURANA, T. S. & LAZAR, M. A. 2013. The nuclear receptor Rev-erb alpha controls circadian thermogenic plasticity. *Nature*, 503, 410-413.
- GIANCARDO, L., SONA, D., SCHEGGIA, D., PAPALEO, F. & MURINO, V. Year. Segmentation and tracking of multiple interacting mice by temperature and shape information. *In: Proceedings - International Conference on Pattern Recognition, 2012.* 2520-2523.
- GIRARD, I., MCALEER, M. W., RHODES, J. S. & GARLAND, T. 2001. Selection for high voluntary wheel-running increases speed and intermittency in house mice (*Mus domesticus*). *Journal of Experimental Biology*, 204, 4311-4320.
- GODBEY, T., GRAY, G. & JEFFERY, D. 2011. Cage-change interval preference in mice. *Lab Animal*, 40, 225-230.
- GOGENUR, I. 2010. Post-operative circadian disturbances. *Danish Medical Bulletin*, 57, 1-20.
- GÖGENUR, I., OCAK, U., ALTUNPINAR, Ö., MIDDLETON, B., SKENE, D. & ROSENBERG, J. 2007. Disturbances in Melatonin, Cortisol and Core Body Temperature Rhythms after Major Surgery. *World Journal of Surgery*, 31, 290-298.
- GONDER, J. C. & LABER, K. 2007. A renewed look at laboratory rodent housing and management. *ILAR Journal*, 48, 29-36.
- GORBACH, A., WANG, H., DHANANI, N., GAGE, F., PINTO, P., SMITH, P., KIRK, A. & ELSTER, E. 2008. Assessment of critical renal ischemia with real-time infrared imaging. *Journal of Surgical Research*, 149, 310-318.
- GORDON, C. 1993. *Temperature regulation in laboratory rodents*, New York, Cambridge University Press.
- GORDON, C. 2004. Effect of cage bedding on temperature regulation and metabolism of group-housed female mice. *Comparative Medicine*, 54, 63-68.
- GORDON, C. 2009. Quantifying the instability of core temperature in rodents. *Journal of Thermal Biology*, 34, 213-219.

- GORDON, C. 2012. The mouse: an “average” homeotherm. *Journal of Thermal Biology*, 37, 286-290.
- GORDON, C. J., SPENCER, P. J., HOTCHKISS, J., MILLER, D. B., HINDERLITER, P. M. & PAULUHN, J. 2008. Thermoregulation and its influence on toxicity assessment. *Toxicology*, 244, 87-97.
- GOTO, M. & EBIHARA, S. 1990. The influence of different light intensities on pineal melatonin content in the retinal degenerate C3H mouse and the normal CBA mouse. *Neuroscience Letters*, 108, 267-272.
- GRIMM, C. & REMÉ, C. E. 2013. Light Damage as a Model of Retinal Degeneration. *Methods in Molecular Biology*, 935, 87-97.
- GÜLER, A., ECKER, J., LALL, G., HAQ, S., ALTIMUS, C., LIAO, H., BARNARD, A., CAHILL, H., BADEA, T., ZHAO, H., HANKINS, M., BERSON, D., LUCAS, R., YAU, K. & HATTAR, S. 2008. Melanopsin cells are the principal conduits for rod-cone input to non-image-forming vision. *Nature*, 453, 102-105.
- HAIM, A. & IZHAKI, I. 1993. The ecological significance of resting metabolic rate and non-shivering thermogenesis for rodents. *Journal of Thermal Biology*, 18, 71-81.
- HAIM, A. & ZISAPEL, N. 1995. Oxygen consumption and body temperature rhythms in the golden spiny mouse: responses to changes in day length. *Physiology & Behavior*, 58, 775-778.
- HAMMEL, H. T. 1988. Anesthetics and Body Temperature Regulation. *Anesthesiology*, 68, 833-835.
- HANKINS, M., PEIRSON, S. & FOSTER, R. 2008. Melanopsin: an exciting photopigment. *Trends in Neurosciences*, 31, 27-36.
- HARPER, D. G., TORNATZKY, W. & MICZEK, K. A. 1996. Stress induced disorganization of circadian and ultradian rhythms: Comparisons of effects of surgery and social stress. *Physiology & Behavior*, 59, 409-419.
- HARSHAW, C. & ALBERTS, J. R. 2012. Group and individual regulation of physiology and behavior: a behavioral, thermographic, and acoustic study of mouse development. *Physiology & Behavior*, 106, 670-82.
- HART, R. 1971. The triad concept in veterinary anaesthesia. *Veterinary Anaesthesia and Analgesia*, 2, 14-22.
- HASSELBERG, M., MCMAHON, J. & PARKER, K. 2013. The validity, reliability, and utility of the iButton® for measurement of body temperature circadian rhythms in sleep/wake research. *Sleep Medicine*, 14, 5-11.
- HATTAR, S., LUCAS, R., MROSOVSKY, N., THOMPSON, S., DOUGLAS, R., HANKINS, M., LEM, J., BIEL, M., HOFMANN, F., FOSTER, R. & YAU, K. 2003. Melanopsin and rod-cone photoreceptive systems account for all major accessory visual functions in mice. *Nature*, 424, 76-81.
- HEAD, M. J. & DYSON, S. 2001. Talking the temperature of Equine Thermography. *The Veterinary Journal*, 162, 166-167.
- HESS, S. E., ROHR, S., DUFOUR, B. D., GASKILL, B. N., PAJOR, E. A. & GARNER, J. P. 2008. Home Improvement: C57BL/6J Mice Given More Naturalistic Nesting Materials Build Better Nests. *Journal of the American Association for Laboratory Animal Science*, 47, 25-31.
- HÖGLUND, A. U. & RENSTRÖM, A. 2001. Evaluation of individually ventilated cage systems for laboratory rodents: cage environment and animal health aspects. *Laboratory Animals*, 35, 51-57.

- HOLSCHER, C., VAN AALTEN, L. & SUTHERLAND, C. 2008. Anaesthesia generates neuronal insulin resistance by inducing hypothermia. *BMC Neuroscience*, 9, 100.
- HOLZBERG, D. & ALBRECHT, U. 2003. The circadian clock: a manager of biochemical processes within the organism. *Journal of Neuroendocrinology*, 15, 339-343.
- HUBER, R., DEBOER, T. & TOBLER, I. 2000. Effects of sleep deprivation on sleep and sleep EEG in three mouse strains: empirical data and simulations. *Brain Research*, 857, 8-19.
- HUGHES, A. T. L. & PIGGINS, H. D. 2012. Feedback actions of locomotor activity to the circadian clock. *Progress in Brain Research*, 199, 305-336.
- HUNTER, J. E., BUTTERWORTH, J., PERKINS, N. D., BATESON, M. & RICHARDSON, C. A. 2014. Using body temperature, food and water consumption as biomarkers of disease progression in mice with E[μ]-myc lymphoma. *British Journal of Cancer*, 110, 928-934.
- HURST, J. & WEST, R. 2010. Taming anxiety in laboratory mice. *Nature Methods*, 7, 825-826.
- IMRIE, M. M. & HALL, G. M. 1990. Body temperature and anaesthesia. *British Journal of Anaesthesia*, 64, 346-354.
- ISHIDA, A., MUTOH, T., UEYAMA, T., BANDO, H., MASUBUCHI, S., NAKAHARA, D., TSUJIMOTO, G. & OKAMURA, H. 2005. Light activates the adrenal gland: timing of gene expression and glucocorticoid release. *Cell Metabolism*, 2, 297-307.
- JENSEN, T., KIERSGAARD, M., SØRENSEN, D. & MIKKELSEN, L. 2013. Fasting of mice: a review. *Laboratory Animals*, 47, 225-240.
- JEON, C. J., STRETTOI, E. & MASLAND, R. H. 1998. The major cell populations of the mouse retina. *Journal of Neuroscience*, 18, 8936-8946.
- JONES, B. 1998. A reappraisal of the use of infrared thermal image analysis in medicine. *IEEE Transactions on Medical Imaging*, 17, 1019-1027.
- JONG, W. M. C., ZUURBIER, C. J., DE WINTER, R. J., VAN DEN HEUVEL, D. A. F., REITSMA, P. H., TEN CATE, H. & INCE, C. 2002. Fentanyl-fluanisone-midazolam combination results in more stable hemodynamics than does urethane- α -chloralose and 2,2,2-tribromoethanol in mice. *Contemporary Topics in Laboratory Animal Science*, 41, 28-32.
- JUD, C., SCHMUTZ, I., HAMPP, G., OSTER, H. & ALBRECHT, U. 2005. A guideline for analyzing circadian wheel-running behavior in rodents under different lighting conditions. *Biological Procedures Online*, 7, 101-116.
- KALSBECK, A., FLIERS, E., HOFMAN, M., SWAAB, D. & BUIJS, R. 2010. Vasopressin and the output of the hypothalamic biological clock. *Journal of Neuroendocrinology*, 22, 362-372.
- KALSBECK, A., VERHAGEN, L., SCHALIJ, I., FOPPEN, E., SABOUREAU, M., BOTHOREL, B., BUIJS, R. & PÉVET, P. 2008. Opposite actions of hypothalamic vasopressin on circadian corticosterone rhythm in nocturnal versus diurnal species. *European Journal of Neuroscience*, 27, 818-827.
- KATEB, B., YAMAMOTO, V., YU, C., GRUNDFEST, W. & GRUEN, J. 2009. Infrared thermal imaging: A review of the literature and case report. *NeuroImage*, 47, Supplement 2, T154-T162.
- KEENEY, A. J., HOGG, S. & MARSDEN, C. A. 2001. Alterations in core body temperature, locomotor activity, and corticosterone following acute and repeated social defeat of male NMRI mice. *Physiology & Behavior*, 74, 177-184.

- KING, D., ZHAO, Y., SANGORAM, A., WILSBACHER, L., TANAKA, M., ANTOCH, M., STEEVES, T., VITATERNA, M., KORNHAUSER, J., LOWREY, P., TUREK, F. & TAKAHASHI, J. 1997. Positional cloning of the mouse circadian Clock gene. *Cell*, 89, 641-653.
- KONDRATOV, R., KONDRATOVA, A., LEE, C., GORBACHEVA, V., CHERNOV, M. & ANTOCH, M. 2006. Post-translational regulation of circadian transcriptional CLOCK(NPAS2)/BMAL1 complex by CRYPTOCHROMES. *Cell Cycle*, 5, 890-895.
- KONHILAS, J. P., MAASS, A. H., LUCKEY, S. W., STAUFFER, B. L., OLSON, E. N. & LEINWAND, L. A. 2004. Sex modifies exercise and cardiac adaptation in mice. *American Journal of Physiology- Heart and Circulatory Physiology*, 287, H2768-H2776.
- KOPP, C., VOGEL, E., RETTORI, M., DELAGRANGE, P., GUARDIOLA-LEMAÎTRE, B. & MISLIN, R. 1998. Effects of a daylight cycle reversal on locomotor activity in several inbred strains of mice. *Physiology and Behavior*, 63, 577-585.
- KORF, H. & VON GALL, C. 2006. Mice, melatonin and the circadian system. *Molecular and Cellular Endocrinology*, 252, 57-68.
- KORNMANN, B., SCHAAD, O., BUJARD, H., TAKAHASHI, J. & SCHIBLER, U. 2007. System-driven and oscillator-dependent circadian transcription in mice with a conditionally active liver clock. *PLoS Biology*, 5, 0179-0189.
- KORT, W., HEKKING-WEIJMA, J., TENKATE, M., SORM, V. & VANSTRIK, R. 1998. A microchip implant system as a method to determine body temperature of terminally ill rats and mice. *Laboratory Animals*, 32, 260-269.
- KOSTOMITSOPOULOS, N. G., PARONIS, E., ALEXAKOS, P., BALAFAS, E., VAN LOO, P. & BAUMANS, V. 2007. The Influence of the Location of a Nest Box in an Individually Ventilated Cage on the Preference of Mice to Use It. *Journal of Applied Animal Welfare Science*, 10, 111-121.
- KOTEJA, P., GARLAND JR, T., SAX, J. K., SWALLOW, J. G. & CARTER, P. A. 1999. Behaviour of house mice artificially selected for high levels of voluntary wheel running. *Animal Behaviour*, 58, 1307-1318.
- KRAMER, K. & KINTER, L. 2003. Evaluation and applications of radiotelemetry in small laboratory animals. *Physiological Genomics*, 13, 197-205.
- KRAMER, K., VOSS, H., GRIMBERGEN, J. & BAST, A. 1998. Circadian rhythms of heart rate, body temperature, and locomotor activity in freely moving mice measured with radio telemetry. *Lab Animal*, 27, 23-26.
- KROHN, T. C. & HANSEN, A. K. 2010. Mice prefer draught-free housing. *Laboratory Animals*, 44, 370-372.
- KURZ, A. 2008. Physiology of Thermoregulation. *Best Practice & Research Clinical Anaesthesiology*, 22, 627-644.
- KUSHIKATA, T., YOSHIDA, H. & HIROTA, K. 2012. Sleep in anesthesiology – what can we learn about anesthesia from studying sleep? *Trends in Anaesthesia and Critical Care*, 2, 30-35.
- LALL, G. S., REVELL, V. L., MOMIJI, H., AL ENEZI, J., ALTIMUS, C. M., GÜLER, A. D., AGUILAR, C., CAMERON, M. A., ALLENDER, S., HANKINS, M. W. & LUCAS, R. J. 2010. Distinct Contributions of Rod, Cone, and Melanopsin Photoreceptors to Encoding Irradiance. *Neuron*, 66, 417-428.
- LAPOSKY, A., EASTON, A., DUGOVIC, C., WALISSER, J., BRADFIELD, C. & TUREK, F. 2005. Deletion of the mammalian circadian clock gene BMAL1/Mop3 alters baseline sleep architecture and the response to sleep deprivation. *Sleep*, 28, 395-409.

- LAPVETELAINEN, T., TIIHONEN, A., KOSKELA, P., NEVALAINEN, T., LINDBLOM, J., KIRALY, K., HALONEN, P. & HEIMINEN, H. J. 1997. Training a large number of laboratory mice using running wheels and analyzing running behavior by use of a computer-assisted system. *Laboratory Animal Science*, 47, 172-179.
- LEE, C., ETCHEGARAY, J., CAGAMPANG, F., LOUDON, A. & REPERT, S. 2001. Posttranslational mechanisms regulate the mammalian circadian clock. *Cell*, 107, 855-867.
- LEMMER, B. 2007. Circadian rhythm regulations of the cardiovascular system in rats and mice. *IEEE Engineering in Medicine and Biology Magazine*, 26, 30-32.
- LEON, L., WALKER, L., DUBOSE, D. & STEPHENSON, L. 2004. Biotelemetry transmitter implantation in rodents: impact on growth and circadian rhythms. *American Journal of Physiology - Regulatory, Integrative and Comparative Physiology*, 286, R967-R974.
- LEON, L. R. 2002. Cytokine regulation of fever: studies using gene knockout mice. *Journal of Applied Physiology*, 92, 2648-2655.
- LI, J., HU, W., BOEHMER, L., CHENG, M., LEE, A., JILEK, A., SIEGEL, J. & ZHOU, Q. 2006. Attenuated circadian rhythms in mice lacking the Prokineticin 2 gene. *Journal of Neuroscience*, 26, 11615-11623.
- LIGHTMAN, S. 2008. The neuroendocrinology of stress: a never ending story. *Journal of Neuroendocrinology*, 20, 880-884.
- LOGGE, W., KINGHAM, J. & KARL, T. 2013. Behavioural consequences of IVC cages on male and female C57BL/6J mice. *Neuroscience*, 237, 285-293.
- LOGGE, W., KINGHAM, J. & KARL, T. 2014. Do individually ventilated cage systems generate a problem for genetic mouse model research? *Genes, Brain and Behavior*, 13, 713-720.
- LUCAS, R., DOUGLAS, R. & FOSTER, R. 2001a. Characterization of an ocular photopigment capable of driving pupillary constriction in mice. *Nature Neuroscience*, 4, 621-626.
- LUCAS, R., FREEDMAN, M., LUPI, D., MUNOZ, M., DAVID-GRAY, Z. & FOSTER, R. 2001b. Identifying the photoreceptive inputs to the mammalian circadian system using transgenic and retinally degenerate mice. *Behavioural Brain Research*, 125, 97-102.
- LUCAS, R., HATTAR, S., TAKAO, M., BERSON, D., FOSTER, R. & YAU, K. 2003. Diminished pupillary light reflex at high irradiances in melanopsin-knockout mice. *Science*, 299, 245-247.
- LUCAS, R. J., PEIRSON, S. N., BERSON, D. M., BROWN, T. M., COOPER, H. M., CZEISLER, C. A., FIGUEIRO, M. G., GAMLIN, P. D., LOCKLEY, S. W., O'HAGAN, J. B., PRICE, L. L. A., PROVENCIO, I., SKENE, D. J. & BRAINARD, G. C. 2014. Measuring and using light in the melanopsin age. *Trends in Neurosciences*, 37, 1-9.
- LUPI, D., OSTER, H., THOMPSON, S. & FOSTER, R. 2008. The acute light-induction of sleep is mediated by OPN4-based photoreception. *Nature Neuroscience*, 11, 1068-1073.
- MADJIID, M., WILLERSON, J. & WARD CASSCELLS, S. 2006. Intracoronary thermography for detection of high risk vulnerable plaques. *Journal of the American College of Cardiology*, 47, C80-C85.
- MANSEL, J. C., SHAW, D. J., STRACHAN, F. A., GRAY, A. & CLUTTON, R. E. 2008. Comparison of peripheral and core temperatures in anaesthetized hypovolaemic sheep. *Veterinary Anaesthesia and Analgesia*, 35, 45-51.
- MARPEGAN, L., LEONE, M., KATZ, M., SOBRERO, P., BEKINSTEIN, T. & GOLOMBEK, D. 2009. Diurnal variation in endotoxin-induced mortality in mice: correlation with proinflammatory factors. *Chronobiology International*, 26, 1430-1442.

- MARTINS, R. F. S., DO PRADO PAIM, T., DE ABREU CARDOSO, C., STÉFANO LIMA DALLAGO, B., DE MELO, C. B., LOUVANDINI, H. & MCMANUS, C. 2013. Mastitis detection in sheep by infrared thermography. *Research in Veterinary Science*, 94, 722-724.
- MASANA, M., BENLOUCIF, S. & DUBOCOVICH, M. 1996. Light-induced c-fos mRNA expression in the suprachiasmatic nucleus and the retina of C3H/HeN mice. *Molecular Brain Research*, 42, 193-201.
- MATTHEWS, J., MARTE, E. & HALBERG, F. 1964. A circadian susceptibility-resistance cycle to fluothane in male B1 mice. *Canadian Journal of Anesthesia* 11, 280-290.
- MCGUIRE, R. A., RAND, W. M. & WURTMAN, R. J. 1973. Entrainment of the Body Temperature Rhythm in Rats: Effect of Color and Intensity of Environmental Light. *Science*, 181, 956-957.
- MCINTYRE, A. R., DRUMMOND, R. A., RIEDEL, E. R. & LIPMAN, N. S. 2007. Automated Mouse Euthanasia in an Individually Ventilated Caging System: System Development and Assessment. *Journal of the American Association for Laboratory Animal Science*, 46, 65-73.
- MEERLO, P., DE BOER, S. F., KOOLHAAS, J. M., DAAN, S. & VAN DEN HOOFDAKKER, R. H. 1996. Changes in daily rhythms of body temperature and activity after a single social defeat in rats. *Physiology & Behavior*, 59, 735-739.
- MENDOZA, J. 2007. Circadian clocks: setting time by food. *Journal of Neuroendocrinology*, 19, 127-137.
- MICHEL, U., HORNSTEIN, O. & SCHONBERGER, A. 1985. Infrared thermography in malignant melanoma: diagnostic potential and limits. *Hautarzt*, 36, 83-89.
- MILLER, D. & O'CALLAGHAN, J. 1994. Environment-, drug- and stress-induced alterations in body temperature affect the neurotoxicity of substituted amphetamines in the C57BL/6J mouse. *Journal of Pharmacology and Experimental Therapeutics*, 270, 752-760.
- MINEUR, Y. S. & CRUSIO, W. E. 2009. Behavioral effects of ventilated micro-environment housing in three inbred mouse strains. *Physiology & Behavior*, 97, 334-340.
- MISTLBERGER, R. & HOLMES, M. 2000. Behavioral feedback regulation of circadian rhythm phase angle in light-dark entrained mice. *American Journal of Physiology - Regulatory Integrative and Comparative Physiology*, 279, R813-R821.
- MISTLBERGER, R., MARCHANT, E. & SINCLAIR, S. 1996. Nonphotic phase-shifting and the motivation to run: cold exposure re-examined. *Journal of Biological Rhythms*, 11, 208-215.
- MISTLBERGER, R. & SKENE, D. 2004. Social influences on mammalian circadian rhythms: animal and human studies. *Biological Reviews of the Cambridge Philosophical Society*, 79, 533-556.
- MOBERG, G. 1987. A model for assessing the impact of behavioural stress on domestic animals. *Journal of Animal Science*, 65, 1228-1235.
- MONTALBÁN-SOLER, L., ALARCÓN-MARTÍNEZ, L., JIMÉNEZ-LÓPEZ, M., SALINAS-NAVARRO, M., GALINDO-ROMERO, C., DE SÁ, F. B., GARCÍA-AYUSO, D., AVILÉS-TRIGUEROS, M., VIDAL-SANZ, M., AGUDO-BARRIUSO, M. & VILLEGAS-PÉREZ, M. P. 2012. Retinal compensatory changes after light damage in albino mice. *Molecular Vision*, 18, 675-693.
- MOORE, R. & LENN, N. 1972. A retinohypothalamic projection in the rat. *The Journal of Comparative Neurology*, 146, 1-14.

- MORRIS, R. & LUTSCH, E. 1967. Susceptibility to morphine-induced analgesia in mice. *Nature*, 216, 494-495.
- MROSOVSKY, N. 1994. In praise of masking: behavioural responses of retinally degenerate mice to dim light. *Chronobiology International*, 11, 343-348.
- MROSOVSKY, N. 1996. Locomotor activity and non-photoc influences on circadian clocks. *Biological Reviews*, 71, 343-372.
- MROSOVSKY, N. 1999. Masking: History, definitions, and measurement. *Chronobiology International*, 16, 415-429.
- MROSOVSKY, N. 2003. Contribution of classic photoreceptors to entrainment. *Journal of Comparative Physiology A: Neuroethology, Sensory, Neural, and Behavioral Physiology*, 189, 69-73.
- MROSOVSKY, N. & HATTAR, S. 2003. Impaired Masking Responses to Light in Melanopsin-Knockout Mice. *Chronobiology International*, 20, 989-999.
- MROSOVSKY, N., LUCAS, R. & FOSTER, R. 2001. Persistence of masking responses to light in mice lacking rods and cones. *Journal of Biological Rhythms*, 16, 585-8.
- MÜNCH, M. & BROMUNDT, V. 2012. Light and chronobiology: Implications for health and disease. *Dialogues in Clinical Neuroscience*, 14, 448-453.
- MUTOH, T., SHIBATA, S., KORF, H. & OKAMURA, H. 2003. Melatonin modulates the light-induced sympathoexcitation and vagal suppression with participation of the suprachiasmatic nucleus in mice. *The Journal of Physiology*, 547, 317-332.
- NAGOSHI, E., SAINI, C., BAUER, C., LAROCHE, T., NAEF, F. & SCHIBLER, U. 2004. Circadian gene expression in individual fibroblasts: cell-autonomous and self-sustained oscillators pass time to daughter cells. *Cell*, 119, 693-705.
- NAYLOR, E., BERGMANN, B., KRAUSKI, K., ZEE, P., TAKAHASHI, J., VITATERNA, M. & TUREK, F. 2000. The circadian Clock mutation alters sleep homeostasis in the mouse. *Journal of Neuroscience*, 20, 8138-8143.
- NELSON, R. & ZUCKER, I. 1981. Absence of extraocular photoreception in diurnal and nocturnal rodents exposed to direct sunlight. *Comparative Biochemistry and Physiology - A Physiology*, 69, 145-148.
- NEWSOM, D., BOLGOS, G., COLBY, L. & NEMZEK, J. 2004. Comparison of body surface temperature measurement and conventional methods for measuring temperature in the mouse. *Journal of the American Association for Laboratory Animal Science*, 43, 13-18.
- NG, D., CHAN, C., LEE, R. & LEUNG, L. 2005. Non-contact infrared thermometry temperature measurement for screening fever in children. *Annals of Tropical Paediatrics: International Child Health*, 25, 267-275.
- NIKULINA, E., SKRINSKAYA, J. & POPOVA, N. 1991. Role of genotype and dopamine receptors in behaviour of inbred mice in a forced swimming test. *Psychopharmacology*, 105, 525-529.
- OELKRUG, R., HELDMAIER, G. & MEYER, C. W. 2011. Torpor patterns, arousal rates, and temporal organization of torpor entry in wildtype and UCP1-ablated mice. *Journal of Comparative Physiology B*, 181, 137-145.
- OHE, Y., IJIMA, N., KADOTA, K., SAKAMOTO, A. & OZAWA, H. 2011. The general anesthetic sevoflurane affects the expression of clock gene mPer2 accompanying the change of NAD⁺ level in the suprachiasmatic nucleus of mice. *Neuroscience Letters*, 490, 231-236.

- OKA, T., OKA, K. & HORI, T. 2001. Mechanisms and mediators of psychological stress-induced rise in core temperature. *Psychosomatic Medicine*, 63, 476-486.
- OLFERT, E. & GODSON, D. 2000. Humane endpoints for animals used in biomedical research and testing: humane endpoints for infectious disease animal models. *Institute for Laboratory Animal Research*, 41, 99-104.
- OLIVA, A. M., SALCEDO, E., HELLIER, J. L., LY, X., KOKA, K., TOLLIN, D. J. & RESTREPO, D. 2010. Toward a Mouse Neuroethology in the Laboratory Environment. *PLoS ONE*, 5, e11359.
- ONO, H., HOSHINO, Y., YASUO, S., WATANABE, M., NAKANE, Y., MURAI, A., EBIHARA, S., KORE, H. & YOSHIMURA, T. 2008. Involvement of thyrotropin in photoperiodic signal transduction in mice. *Proceedings of the National Academy of Sciences of the United States of America*, 105, 18238-18242.
- OSTER, H., DAMEROW, S., KIESSLING, S., JAKUBCAKOVA, V., ABRAHAM, D., TIAN, J., HOFFMANN, M. & EICHELE, G. 2006. The circadian rhythm of glucocorticoids is regulated by a gating mechanism residing in the adrenal cortical clock. *Cell Metabolism*, 4, 163-173.
- PANDA, S., ANTOCH, M., MILLER, B., SU, A., SCHOOK, A., STRAUME, M., SCHULTZ, P., KAY, S. A., TAKAHASHI, J. & HOGENESCH, J. 2002a. Coordinated transcription of key pathways in the mouse by the circadian clock. *Cell*, 109, 307-320.
- PANDA, S., SATO, T., CASTRUCCI, A., ROLLAG, M., DEGRIP, W., HOGENESCH, J., PROVENCIO, I. & KAY, S. 2002b. Melanopsin (Opn4) requirement for normal light-induced circadian phase shifting. *Science*, 298, 2213-2216.
- PANDO, M., MORSE, D., CERMAKIAN, N. & SASSONE-CORSI, P. 2002. Phenotypic rescue of a peripheral clock genetic defect via SCN hierarchical dominance. *Cell*, 110, 107-117.
- PAUL, M. J. & SCHWARTZ, W. J. 2007. On the Chronobiology of Cohabitation. *Cold Spring Harbor Symposia on Quantitative Biology*, 72, 615-621.
- PEIRSON, S., BUTLER, J., DUFFIELD, G., TAKHER, S., SHARMA, P. & FOSTER, R. 2006. Comparison of clock gene expression in SCN, retina, heart, and liver of mice. *Biochemical and Biophysical Research Communications*, 351, 800-807.
- PEIRSON, S. & FOSTER, R. 2010. Non Image Forming Photoreceptors. In: ALBRECHT, U. (ed.) *The Circadian Clock*. New York: Springer.
- PEIRSON, S. N., THOMPSON, S., HANKINS, M. W. & FOSTER, R. G. 2005. Mammalian Photoentrainment: Results, Methods, and Approaches. In: MICHAEL, W. Y. (ed.) *Methods in Enzymology*. Academic Press.
- PERKINS, S. E. & LIPMAN, N. S. 1996. Evaluation of Microenvironmental Conditions and Noise Generation in Three Individually Ventilated Rodent Caging Systems and Static Isolator Cages. *Contemporary Topics in Laboratory Animal Science*, 35, 61-65.
- PHILLIPS, P. & HEATH, J. 1995. Dependency of surface temperature regulation on body size in terrestrial mammals. *Journal of Thermal Biology*, 20, 281-289.
- PICCIONE, G., GIANESELLA, M., MORGANTE, M. & REFINETTI, R. 2013. Daily rhythmicity of core and surface temperatures of sheep kept under thermoneutrality or in the cold. *Research in Veterinary Science*, 95, 261-265.
- PICK, J., CHEN, Y., MOORE, J., SUN, Y., WYNER, A., FRIEDMAN, E. & KELZ, M. 2011. Rapid eye movement sleep debt accrues in mice exposed to volatile anesthetics. *Anesthesiology*, 115, 702-712.
- PITTENDRIGH, C. 1981. Circadian systems: Entrainment In: ASCHOFF, J. (ed.) *Handbook of Behavioural Neurobiology*. New York and London: Plenum Press.

- PITTENDRIGH, C. S. & DAAN, S. 1976. A functional analysis of circadian pacemakers in nocturnal rodents - IV. Entrainment: Pacemaker as clock. *Journal of Comparative Physiology (A)*, 106, 291-331.
- PLANEL, E., RICHTER, K. E. G., NOLAN, C. E., FINLEY, J. E., LIU, L., WEN, Y., KRISHNAMURTHY, P., HERMAN, M., WANG, L., SCHACHTER, J. B., NELSON, R. B., LAU, L. F. & DUFF, K. E. 2007. Anesthesia leads to tau hyperphosphorylation through inhibition of phosphatase activity by hypothermia. *Journal of Neuroscience*, 27, 3090-3097.
- POHL, H. 1976. Proportional effect of light on entrained circadian rhythms of birds and mammals. *Journal of Comparative Physiology* 112, 103-108.
- POLAT, B., COLAK, A., CENGIZ, M., YANMAZ, L., ORAL, H., BASTAN, A., KAYA, S. & HAYIRLI, A. 2010. Sensitivity and specificity of infrared thermography in detection of subclinical mastitis in dairy cows. *Journal of Dairy Science*, 93, 3525-3532.
- POOLE, S. & STEPHENSON, J. 1977. Core temperature: some shortcomings of rectal temperature measurements. *Physiology and Behavior*, 18, 203-205.
- POSSIDENTE, B. & STEPHAN, F. K. 1988. Circadian period in mice: Analysis of genetic and maternal contributions to inbred strain differences. *Behavior Genetics*, 18, 109-117.
- PRITCHETT, D., JAGANNATH, A., BROWN, L., TAM, S., HASAN, S., GATTI, S., HARRISON, P., BANNERMAN, D., FOSTER, R. & PEIRSON, S. 2015. Deletion of Metabotropic Glutamate Receptors 2 and 3 (mGlu2 & mGlu3) in Mice Disrupts Sleep and Wheel-Running Activity, and Increases the Sensitivity of the Circadian System to Light. *PLoS ONE*, 10, e0125523.
- PROVENCIO, I., ROLLAG, M. & CASTRUCCI, A. 2002. Anatomy: photoreceptive net in the mammalian retina. *Nature*, 415, 493-493.
- PROVENCIO, I., WONG, S., LEDERMAN, A., ARGAMASO, S. & FOSTER, R. 1994. Visual and circadian responses to light in aged retinally degenerate mice. *Vision Research*, 34, 1799-1806.
- QUIMBY, J., OLEA-POPELKA, F. & LAPPIN, M. 2009. Comparison of digital rectal and microchip transponder thermometry in cats. *Journal of the American Association for Laboratory Animal Science*, 48, 402-404.
- RAMEY, D., BACHMANN, K. & LEE, M. 2011. A comparative study of non-contact infrared and digital rectal thermometer measurements of body temperature in the horse. *Journal of Equine Veterinary Science*, 31, 191-193.
- REDLIN, U., HATTAR, S. & MROSOVSKY, N. 2005. The circadian CLOCK mutant mouse: impaired masking response to light. *Journal of Comparative Physiology A: Neuroethology, Sensory, Neural, and Behavioral Physiology*, 191, 51-59.
- REFINETTI, R. 2001. Dark adaptation in the circadian system of the mouse. *Physiology and Behavior*, 74, 101-107.
- REFINETTI, R. 2006a. Analysis of circadian rhythmicity. *Circadian Physiology*. 2nd ed. Boca Raton: Taylor & Francis.
- REFINETTI, R. 2006b. Ultradian and infradian rhythms. *Circadian Physiology*. Boca Raton: Taylor & Francis.
- REFINETTI, R. 2006c. Photoc environmental mechanisms. *Circadian Physiology*. 2nd ed. Boca Raton: Taylor & Francis.
- REFINETTI, R. 2007. Procedures for numerical analysis of circadian rhythms. *Biological Rhythm Research*, 38, 275-325.
- REFINETTI, R. 2010. Entrainment of circadian rhythm by ambient temperature cycles in mice. *Journal of Biological Rhythms*, 25, 247-256.

- REFINETTI, R. & MENAKER, M. 1992. The circadian rhythm of body temperature. *Physiology and Behavior*, 51, 613-637.
- REICK, M., GARCIA, J., DUDLEY, C. & MCKNIGHT, S. 2001. NPAS2: An analog of clock operative in the mammalian forebrain. *Science*, 293, 506-509.
- REMBERT, M., SMITH, J. & HOSGOOD, G. 2004. A comparison of a forced-air warming system to traditional thermal support for rodent microenvironments. *Laboratory Animals*, 38, 55-63.
- RENSTRÖM, A., BJÖRING, G. & HÖGLUND, A. U. 2001. Evaluation of individually ventilated cage systems for laboratory rodents: occupational health aspects. *Laboratory Animals*, 35, 42-50.
- REPPERT, S. & WEAVER, D. 2002. Coordination of circadian timing in mammals. *Nature*, 418, 935-941.
- REVEL, F., GOTTOWIK, J., GATTI, S., WETTSTEIN, J. & MOREAU, J. 2009. Rodent models of insomnia: a review of experimental procedures that induce sleep disturbances. *Neuroscience & Biobehavioral Reviews*, 33, 874-899.
- REYNOLDS, L., BECKMANN, J. & KURZ, A. 2008. Perioperative complications of hypothermia. *Best Practice & Research Clinical Anaesthesiology*, 22, 645-657.
- RING, E., MCEVOY, H., JUNG, A., ZUBER, J. & MACHIN, G. 2010. New standards for devices used for the measurement of human body temperature. *Journal of Medical Engineering & Technology*, 34, 249-253.
- RING, E. F. J. & AMMER, K. 2012. Infrared thermal imaging in medicine. *Physiological Measurement*, 33, R33-R46.
- RIPPERGER, J. & BROWN, S. 2010. Transcriptional regulation of circadian clocks. In: ALBRECHT, U. (ed.) *The Circadian Clock*. New York: Springer.
- RIPPERGER, J., JUD, C. & ALBRECHT, U. 2011. The daily rhythm of mice. *FEBS Letters*, 585, 1384-1392.
- ROEHL, K., BECKER, S., FUHRMEISTER, C., TEUSCHER, N., FUTING, M. & HEILMANN, A. 2008. New, non-invasive thermographic examination of body surface temperature on tetraplegic and paraplegic patients, as a supplement to existing diagnostic measures. *Spinal Cord*, 47, 492-495.
- ROENNEBERG, T. & FOSTER, R. G. 1997. Twilight Times: Light and the Circadian System. *Photochemistry and Photobiology*, 66, 549-561.
- ROSEBOOM, P., NAMBOODIRI, M., ZIMONJIC, D., POPESCU, N., R. RODRIGUEZ, I., GASTEL, J. & KLEIN, D. 1998. Natural melatonin 'knockdown' in C57BL/6J mice: rare mechanism truncates serotonin N-acetyltransferase. *Molecular Brain Research*, 63, 189-197.
- ROSENBAUM, M. D., VANDEWOUDE, S. & JOHNSON, T. E. 2009. Effects of Cage-Change Frequency and Bedding Volume on Mice and Their Microenvironment. *Journal of the American Association for Laboratory Animal Science*, 48, 763-773.
- ROSENBAUM, M. D., VANDEWOUDE, S., VOLCKENS, J. & JOHNSON, T. 2010. Disparities in Ammonia, Temperature, Humidity, and Airborne Particulate Matter between the Micro-and Macroenvironments of Mice in Individually Ventilated Caging. *Journal of the American Association for Laboratory Animal Science*, 49, 177-183.
- RUBY, N. F., BURNS, D. E. & HELLER, H. C. 1999. Circadian Rhythms in the Suprachiasmatic Nucleus are Temperature-Compensated and Phase-Shifted by Heat Pulses In Vitro. *The Journal of Neuroscience*, 19, 8630-8636.

- SAINI, C., MORF, J., STRATMANN, M., GOS, P. & SCHIBLER, U. 2012. Simulated body temperature rhythms reveal the phase-shifting behavior and plasticity of mammalian circadian oscillators. *Genes and Development*, 26, 567-580.
- SAKAMOTO, A., IMAI, J., NISHIKAWA, A., HONMA, R., ITO, E., YANAGISAWA, Y., KAWAMURA, M., OGAWA, R. & WATANABE, S. 2005. Influence of inhalation anesthesia assessed by comprehensive gene expression profiling. *Gene*, 356, 39-48.
- SAMARA, E. M., AYADI, M. & ALJUMAAH, R. S. 2014. Feasibility of utilising an infrared-thermographic technique for early detection of subclinical mastitis in dairy camels (*Camelus dromedarius*). *Journal of Dairy Research*, 81, 38-45.
- SAPER, C., CHOU, T. & SCAMMELL, T. 2001. The sleep switch: hypothalamic control of sleep and wakefulness. *Trends in Neurosciences*, 24, 726-731.
- SATO, T., YAMADA, R., UKAI, H., BAGGS, J., MIRAGLIA, L., KOBAYASHI, T., WELSH, D., KAY, S., UEDA, H. & HOGENESCH, J. 2006. Feedback repression is required for mammalian circadian clock function. *Nature Genetics*, 38, 312-319.
- SATOH, Y., KAWAI, H., KUDO, N., KAWASHIMA, Y. & MITSUMOTO, A. 2006. Temperature rhythm re-entrains faster than locomotor rhythm after a light phase shift. *Physiology & Behavior*, 88, 404-410.
- SCHAEFER, A., COOK, N., CHURCH, J., BASARAB, J., PERRY, B., MILLER, C. & TONG, A. 2007. The use of infrared thermography as an early indicator of bovine respiratory disease complex in calves. *Research in Veterinary Science*, 83, 376 - 384.
- SCHAEFER, A. L., COOK, N. J., BENCH, C., CHABOT, J. B., COLYN, J., LIU, T., OKINE, E. K., STEWART, M. & WEBSTER, J. R. 2012. The non-invasive and automated detection of bovine respiratory disease onset in receiver calves using infrared thermography. *Research in Veterinary Science*, 93, 928-935.
- SCHIBLER, U. & BROWN, S. 2005. Enlightening the adrenal gland. *Cell Metabolism*, 2, 278-281.
- SCULLY, C., KARABOUÉ, A., LIU, W., MEYER, J., INNOMINATO, P., CHON, K., GORBACH, A. & LÉVI, F. 2011. Skin surface temperature rhythms as potential circadian biomarkers for personalized chronotherapeutics in cancer patients. *Interface Focus*, 1, 48-60.
- SEKARAN, S., LUPI, D., JONES, S. L., SHEELY, C. J., HATTAR, S., YAU, K. W., LUCAS, R. J., FOSTER, R. G. & HANKINS, M. W. 2005. Melanopsin-dependent photoreception provides earliest light detection in the mammalian retina. *Current Biology*, 15, 1099-1107.
- SEMO, M., PEIRSON, S., LUPI, D., LUCAS, R., JEFFERY, G. & FOSTER, R. 2003. Melanopsin retinal ganglion cells and the maintenance of circadian and pupillary responses to light in aged rodless/coneless (*rd/rd cl*) mice. *European Journal of Neuroscience*, 17, 1793-1801.
- SESSLER, D. I. 2008. Temperature Monitoring and Perioperative Thermoregulation. *Anesthesiology*, 109, 318-338
- SHERWIN, C. M. 1998. Voluntary wheel running: a review and novel interpretation. *Animal Behaviour*, 56, 11-27.
- SHILOH, R., BODINGER, L., KATZ, N., SIGLER, M., STRYJER, R., HERMESH, H., MUNITZ, H. & WEIZMAN, A. 2003a. Lower corneal temperature in neuroleptic-treated vs. drug-free schizophrenia patients. *Neuropsychobiology*, 48, 1-4.
- SHILOH, R., PORTUGUESE, S., BODINGER, L., KATZ, N., SIGLER, M., HERMESH, H., MUNITZ, H. & WEIZMAN, A. 2003b. Increased corneal temperature in drug-free male schizophrenia patients. *European Neuropsychopharmacology*, 13, 49-52.

- SIKOSKI, P., BANKS, M., GOULD, R., YOUNG, R., WALLACE, J. & NADER, M. 2007. Comparison of rectal and infrared thermometry for obtaining body temperature in cynomolgus macaques (*Macaca fascicularis*). *Journal of Medical Primatology*, 36, 381-384.
- SMITH, V. Year. Comparison of Axillary, Aural and Rectal Temperatures in Cats. In: BSAVA Congress, 2014 Birmingham, U.K.
- SONG, C., APPELYARD, V., MURRAY, K., FRANK, T., SIBBETT, W., CUSCHIERI, A. & THOMPSON, A. 2007. Thermographic assessment of tumor growth in mouse xenografts. *International Journal of Cancer*, 121, 1055-1058.
- STEPHENS DEVALLE, J. 2005. Comparison of tympanic, transponder, and noncontact infrared laser thermometry with rectal thermometry in Strain 13 guinea pigs (*Cavia porcellus*). *Journal of the American Association for Laboratory Animal Science*, 44, 35-38.
- STRATMANN, M. & SCHIBLER, U. 2006. Properties, entrainment, and physiological functions of mammalian peripheral oscillators. *Journal of Biological Rhythms*, 21, 494-506.
- STUDHOLME, K. M., GOMPF, H. S. & MORIN, L. P. 2013. Brief light stimulation during the mouse nocturnal activity phase simultaneously induces a decline in core temperature and locomotor activity followed by EEG-determined sleep. *American Journal of Physiology- Regulatory, Integrative, Comparative Physiology*, 304, R459-R471.
- SWALLOW, J., KOTEJA, P., CARTER, P. & GARLAND, T. 2001. Food consumption and body composition in mice selected for high wheel-running activity. *Journal of Comparative Physiology B*, 171, 651-659.
- SWALLOW, J. G., RHODES, J. S. & GARLAND, T. 2005. Phenotypic and Evolutionary Plasticity of Organ Masses in Response to Voluntary Exercise in House Mice. *Integrative and Comparative Biology*, 45, 426-437.
- SWOAP, S. J. & GUTILLA, M. J. 2009. Cardiovascular changes during daily torpor in the laboratory mouse. *American Journal of Physiology- Regulatory, Integrative and Comparative Physiology*, 297, R769-R774.
- SZCZĘSNY, G., VEIHELMANN, A., MASSBERG, S., NOLTE, D. & MESSMER, K. 2004. Long-term anaesthesia using inhalatory isoflurane in different strains of mice—the haemodynamic effects. *Laboratory Animals*, 38, 64-69.
- TAKAHASHI, J., HONG, H., KO, C. & MCDEARMON, E. 2008a. The genetics of mammalian circadian order and disorder: implications for physiology and disease. *Nature Reviews Genetics*, 9, 764-775.
- TAKAHASHI, J., PINTO, L. & VITATERNA, M. 1994. Forward and reverse genetic approaches to behavior in the mouse. *Science*, 264, 1724-1733.
- TAKAHASHI, J., SHIMOMURA, K. & KUMAR, V. 2008b. Searching for genes underlying behavior: lessons from circadian rhythms. *Science*, 322, 909-912.
- TAKEDA, N. & MAEMURA, K. 2010. Circadian clock and vascular disease. *Hypertension Research*, 33, 645-651.
- TALAN, M. I., KIROV, S. A. & KOSHELEVA, N. A. 1996. Nonshivering thermogenesis in adult and aged C57BL/6J mice housed at 22°C and at 29°C. *Experimental Gerontology*, 31, 687-698.
- TANKERSLEY, C., IRIZARRY, R., FLANDERS, S. & RABOLD, R. 2002. Selected contribution: circadian rhythm variation in activity, body temperature, and heart rate between C3H/HeJ and C57BL/6J inbred strains. *Journal of Applied Physiology*, 92, 870-877.

- TAYLOR, D. 2007. Study of two devices used to maintain normothermia in rats and mice during general anesthesia. *Journal of the American Association for Laboratory Animal Science*, 46, 37-41.
- THOMPSON, S., FOSTER, R., STONE, E., SHEFFIELD, V. & MROSOVSKY, N. 2008. Classical and melanopsin photoreception in irradiance detection: negative masking of locomotor activity by light. *The European Journal of Neuroscience*, 27, 1973-9.
- TIZARD, I. 2008. Sickness behavior, its mechanisms and significance. *Animal Health Research Reviews*, 9, 87-99.
- TOKURA, H. & ASCHOFF, J. 1983. Effects of temperature on the circadian rhythm of pig-tailed macaques *Macaca nemestrina*. *American Journal of Physiology - Regulatory, Integrative and Comparative Physiology*, 245, R800-R804.
- TORNATZKY, W. & MICZEK, K. A. 1993. Long-term impairment of autonomic circadian rhythms after brief intermittent social stress. *Physiology & Behavior*, 53, 983-993.
- TOROSSIAN, A. 2008. Thermal management during anaesthesia and thermoregulation standards for the prevention of inadvertent perioperative hypothermia. *Best Practice & Research Clinical Anaesthesiology*, 22, 659-668.
- TREJO, L. J. & CICERONE, C. M. 1984. Cells in the pretectal olivary nucleus are in the pathway for the direct light reflex of the pupil in the rat. *Brain Research*, 300, 49-62.
- TSAI, J., HANNIBAL, J., HAGIWARA, G., COLAS, D., RUPPERT, E., RUBY, N., HELLER, C., FRANKEN, P. & BOURGIN, P. 2009. Melanopsin as a sleep modulator: circadian gating of the direct effects of light on sleep and altered sleep homeostasis in *Opn4*^{-/-}-mice. *PLoS Biology*, 7, e1000125.
- TSAI, P. P., OPPERMAN, D., H.D., S., MAHLER, M. & HACKBARTH, H. 2003. The effects of different rack systems on the breeding performance of DBA/2 mice. *Laboratory Animals*, 37, 44-46.
- TSUCHIYA, Y., AKASHI, M. & NISHIDA, E. 2003. Temperature compensation and temperature resetting of circadian rhythms in mammalian cultured fibroblasts. *Genes to Cells*, 8, 713-720.
- UCHIDA, K., SHIUCHI, T., INADA, H., MINOKOSHI, Y. & TOMINAGA, M. 2010. Metabolic adaptation of mice in a cool environment. *Pflügers Archiv European Journal of Physiology*, 459, 765-774.
- VAN DEN HEUVEL, C., FERGUSON, S., DAWSON, D. & GILBERT, S. 2003. Comparison of digital infrared thermal imaging (DITI) with contact thermometry: pilot data from a sleep research laboratory. *Physiological Measurement*, 24, 717-725.
- VAN DEN HEUVEL, C., FERGUSON, S., GILBERT, S. & DAWSON, D. 2004. Thermoregulation in normal sleep and insomnia: the role of peripheral heat loss and new applications for digital thermal infrared imaging (DITI). *Journal of Thermal Biology*, 29, 457-461.
- VAN DER ZEE, E., ROMAN, V., TEN BRINKE, O. & MEERLO, P. 2005. TGF α and AVP in the mouse suprachiasmatic nucleus: anatomical relationship and daily profiles. *Brain Research*, 1054, 159-166.
- VAN GELDER, R. 2003. Making (a) sense of non-visual ocular photoreception. *Trends in Neurosciences*, 26, 458-461.
- VANSELOW, J. & KRAMER, A. 2010. Posttranslational regulation of circadian clocks. In: ALBRECHT, U. (ed.) *The Circadian Clock*. New York: Springer.
- VANSOMEREN, E. J. W. 2000. More than a marker: Interaction between the circadian regulation of temperature and sleep, age-related changes and treatment possibilities. *Chronobiology International*, 17, 313-354.

- VERWEY, M., ROBINSON, B. & AMIR, S. 2013. Recording and Analysis of Circadian Rhythms in Running-wheel Activity in Rodents. *Journal of Visualized Experiments*, 71, e50186.
- VITATERNA, M., KING, D., CHANG, A., KERNHAUSER, J., LOWREY, P., MCDONALD, J., DOVE, W., PINTO, L., TUREK, F. & TAKAHASHI, J. 1994. Mutagenesis and mapping of a mouse gene, clock, essential for circadian behavior. *Science*, 264, 719-725.
- VITATERNA, M., SELBY, C., TODO, T., NIWA, H., THOMPSON, C., FRUECHTE, E., HITOMI, K., THRESHER, R., ISHIKAWA, T., MIYAZAKI, J., TAKAHASHI, J. & SANCAR, A. 1999. Differential regulation of mammalian period genes and circadian rhythmicity by cryptochromes 1 and 2. *Proceedings of the National Academy of Sciences of the United States of America*, 96, 12114-12119.
- VIVIEN-ROELS, B., MALAN, A., RETTORI, M., DELAGRANGE, P., JEANNIOT, J. & PÉVET, P. 1998. Daily variations in pineal melatonin concentrations in inbred and outbred mice. *Journal of Biological Rhythms*, 13, 403-409.
- VLACH, K., BOLES, J. & STILES, B. 2000. Telemetric evaluation of body temperature and physical activity as predictors of mortality in a murine model of staphylococcal enterotoxic shock. *Comparative Medicine*, 50, 160-166.
- VON GALL, C., DUFFIELD, G., HASTINGS, M., KOPP, M., DEGHANI, F., KORF, H. & STEHLE, J. 1998. CREB in the mouse SCN: a molecular interface coding the phase-adjusting stimuli light, glutamate, PACAP, and melatonin for clockwork access. *Journal of Neuroscience*, 18, 10389-10397.
- VON GALL, C., GARABETTE, M., KELL, C., FRENZEL, S., DEGHANI, F., SCHUMM-DRAEGER, P., WEAVER, D., KORF, H., HASTINGS, M. & STEHLE, J. 2002. Rhythmic gene expression in pituitary depends on heterologous sensitization by the neurohormone melatonin. *Nature Neuroscience*, 5, 234-238.
- VON GALL, C., WEAVER, D., MOEK, J., JILG, A., STEHLE, J. & KORF, H. 2005. Melatonin plays a crucial role in the regulation of rhythmic clock gene expression in the mouse pars tuberalis. *Annals of the New York Academy of Sciences*, 1040, 508-511.
- WARN, P., BRAMPTON, M., SHARP, A., MORRISSEY, G., STEEL, N., DENNING, D. & PRIEST, T. 2003. Infrared body temperature measurement of mice as an early predictor of death in experimental fungal infections. *Laboratory Animals*, 37, 126-131.
- WATSON, F. & GREGORY, S. Year. Agreement of a Tympanic Membrane and Rectal Thermometer Compared to Core Oesophageal Temperature in Cats Under General Anaesthesia. *In: BSAVA Congress, 2014 Birmingham, U.K.*
- WEIERGRÄBER, M., HENRY, M., HESCHELER, J., SMYTH, N. & SCHNEIDER, T. 2005. Electroencephalographic and deep intracerebral EEG recording in mice using a telemetry system. *Brain Research Protocols*, 14, 154-164.
- WEINERT, D. & WATERHOUSE, J. 1998. Diurnally changing effects of locomotor activity on body temperature in laboratory mice. *Physiology and Behavior*, 63, 837-843.
- WEINERT, D. & WATERHOUSE, J. 2007. The circadian rhythm of core temperature: effects of physical activity and aging. *Physiology & Behavior*, 90, 246-256.
- WEINERT, H., WEINERT, D. & WATERHOUSE, J. 2002. The circadian activity and body temperature rhythms of mice during their last days of life. *Biological Rhythm Research*, 33, 199-212.
- WENGER, J. R. & ALKANA, R. L. 1984. Temperature dependence of ethanol depression in C57BL/6 and BALB/c mice. *Alcohol*, 1, 297-303.

- WEYLAND, W., FRITZ, U., FABIAN, S., JAEGER, H., CROZIER, T., KIEZTMANN, D. & BRAUN, U. 1994. Efficiency of warming devices in extubated postoperative patients. *Anaesthetist*, 43, 648-657.
- WINDLE, R., WOOD, S., SHANKS, N., LIGHTMAN, S. & INGRAM, C. 1998. Ultradian rhythm of basal corticosterone release in the female rat: dynamic interaction with the response to acute stress. *Endocrinology*, 139, 443-450.
- WISOR, J., O'HARA, B., TERAOKA, A., SELBY, C., KILDUFF, T., SANCAR, A., EDGAR, D. & FRANKEN, P. 2002. A role of cryptochromes in sleep regulation. *BMC Neuroscience*, 3, 1471-2202.
- WITTE, K., ENGELHARDT, S., JANSSEN, B., LOHSE, M. & LEMMER, B. 2004. Circadian and short-term regulation of blood pressure and heart rate in transgenic mice with cardiac overexpression of the β 1-adrenoceptor. *Chronobiology International*, 21, 205-216.
- WITTIG, I., KOHLMANN, H., LOMMATZSCH, P., KRUGER, L. & HEROLD, H. 1992. Static and dynamic infrared thermometry and thermography in malignant melanoma of the uvea and conjunctiva. *Klinische Monatsblätter für Augenheilkunde*, 201, 317-323.
- WOLFENSOHN, S. & LLOYD, M. 2003. *Handbook of laboratory animal management and welfare*, Oxford, Blackwell Publishing.
- WONG, K., DUNN, F., GRAHAM, D. & BERSON, D. 2007. Synaptic influences on rat ganglion-cell photoreceptors. *The Journal of Physiology*, 582, 279-296.
- XIAO, H., RUN, X., CAO, X., SU, Y., SUN, Z., TIAN, C., SUN, S. & LIANG, Z. 2013. Temperature control can abolish anesthesia-induced tau hyperphosphorylation and partly reverse anesthesia-induced cognitive impairment in old mice. *Psychiatry and Clinical Neurosciences*, 67, 493-500.
- YANG, X. 2010. A wheel of time: The circadian clock, nuclear receptors, and physiology. *Genes and Development*, 24, 741-747.
- YANG, X., DOWNES, M., YU, R., BOOKOUT, A., HE, W., STRAUME, M., MANGELSDORF, D. & EVANS, R. 2006. Nuclear receptor expression links the circadian clock to metabolism. *Cell*, 126, 801-810.
- YOO, S., YAMAZAKI, S., LOWREY, P., SHIMOMURA, K., KO, C., BUHR, E., SIEPKA, S., HONG, H., OH, W., YOO, O., MENAKER, M. & TAKAHASHI, J. 2004. PERIOD2:LUCIFERASE real-time reporting of circadian dynamics reveals persistent circadian oscillations in mouse peripheral tissues. *Proceedings of the National Academy of Sciences of the United States of America*, 101, 5339-5346.
- YORK, J. M., MCDANIEL, A. W., BLEVINS, N. A., GUILLET, R. R., ALLISON, S. O., CENGEL, K. A. & FREUND, G. G. 2012. Individually ventilated cages cause chronic low-grade hypoxia impacting mice hematologically and behaviorally. *Brain, Behavior, and Immunity*, 26, 951-958.
- ZHOU, W., LI, J.-D., HU, W.-P., CHENG, M. Y. & ZHOU, Q.-Y. 2012. Prokineticin 2 is involved in the thermoregulation and energy expenditure. *Regulatory Peptides*, 179, 84-90.
- ZISAPEL, N., TARRASCH, R. & LAUDON, M. 2005. The relationship between melatonin and cortisol rhythms: clinical implications of melatonin therapy. *Drug Development Research*, 65, 119-125.